Molecular characterization of protein translocation pores

Dissertation

for the award of the degree

“Doctor rerum naturalium” (Dr. rer. nat.)

of the Georg-August-Universität Göttingen

within the doctoral program Biomolecules: Structure-Function-Dynamics

of the Georg-August University School of Science (GAUSS)

submitted by

Mausumi Ghosh

from

Madhya Pradesh, India

Heidelberg, 2023

Thesis Advisory Committee:

Prof. Dr. Michael Meinecke
Department of Cellular Biochemistry, University Medical Center Göttingen

Prof. Dr. Claudia Steinem
Department of Organic and Biomolecular Chemistry, University of Göttingen

Dr. Alexander Stein
Group of Membrane Protein Biochemistry, Max Planck Institute for Multidisciplinary Sciences

Members of the Examination Board:

Prof. Dr. Michael Meinecke (first reviewer)
Department of Cellular Biochemistry, University Medical Center Göttingen

Prof. Dr. Claudia Steinem (second reviewer)
Department of Organic and Biomolecular Chemistry, University of Göttingen

Further members of the Examination Board:

Dr. Alexander Stein
Group of Membrane Protein Biochemistry, Max Planck Institute for Multidisciplinary Sciences

Prof. Dr. Silvio Rizzoli
Department of Neuro- and Sensory Physiology, University Medical Center, Göttingen

Prof. Dr. Ralph Kehlenbach
Department of Molecular Biology, University Medical Center Göttingen

Prof. Dr. Ricarda Richter-Dennerlein
Department of Molecular Biology, University Medical Center Göttingen

Date of oral examination: 14.12.2023

Acknowledgments

I wish to express my deepest appreciation and gratitude to the remarkable individuals and organizations who have played an essential role in the successful completion of my PhD thesis. Your unwavering support, guidance, and encouragement have been the cornerstone of this challenging journey.

First and foremost, I would like to extend my heartfelt thanks to my dedicated thesis supervisor, Prof. Dr. Michael Meinecke. Your exceptional mentorship, profound expertise, and relentless commitment to excellence have been the driving force behind my research. I am profoundly grateful for the invaluable lessons I have learned under your guidance. Thank you for the oppourtunities and believing in me with the projects.

I am very grateful to my second and third supervisors, Prof. Dr. Claudia Steinem and Dr. Alexander Stein, for their insightful guidance, constructive feedback during and beyond TAC meetings. Your collective expertise has greatly enriched the quality of my research and helped shape its direction.

I am thankful to Prof. Dr. Ralf Erdmann and Prof. Dr. Wolfgang Schliebs and their lab members Maren Reuter, Jessica Klümper, Katharina Reglinski and Rebecca Peschel for the invaluable contributions and collaborations for the PEX5 project that have enriched our work. Niels, your patient mentorship in teaching me electrophysiology has been instrumental in my research progress. I would like to extend my thanks for your significant contributions to the paper. Your insights and expertise have greatly enriched our work.

I would also like to thank Dr. Alexander Stein again and all of his lab members for the wonderful collaboration with us in the ERAD project and your valuable inputs throughout. Benjamin Gnoth, your dedication and reliability have been truly remarkable. Thank you for providing samples to us and all the hard work that goes behind.

I owe a debt of gratitude to my colleagues at BZH. I'd like to acknowledge Caro and Beyenech for their invaluable scientific inputs and thought-provoking discussions, which have been instrumental in refining my research. Barbora, whose unwavering support and insight throughout this journey have been indispensable. To Natalie, thank you for fostering a cheerful and collaborative environment in our research group and for your creative inputs. Thank you Daryna, Fereshteh and Indrani for the support i always had from you. Thank you, Tanja, for making my lab life easier and happier at Uni Göttingen and always being there to help me. Jutta, Dexin and Marina for maintaining a positive atmosphere in the lab and for being such considerate colleagues. I can’t thank you all enough for all

the professional and personal discussions we had and how beautifully it brought out a better side to me. For helping me whenever i needed it. Your positive spirit has been a source of motivation and inspiration.

I extend my heartfelt thanks to my friends, my parents and my sister for their unwavering support and understanding during the demanding phases of this journey. Your encouragement and belief in my abilities have been a constant source of strength.

Lastly, my heartfelt gratitude goes to every individual, whether directly or indirectly involved, who contributed to the completion of this thesis. Your contributions, no matter how small, have made a significant impact on this work. I dedicate this thesis to my thesis supervisors, colleagues, friends, family, and everyone who has believed in me and supported me throughout this remarkable academic journey. Thank you all for being an integral part of this significant chapter in my academic life.

List of Publications

Parts of this thesis have been previously published in the following article:

Ghosh, Mausumi*, Niels Denkert*, Maren Reuter*, Jessica Klümper, Katharina Reglinski, Rebecca Peschel, Wolfgang Schliebs, Ralf Erdmann, and Michael Meinecke. 2023. 'Dynamics of the Translocation Pore of the Human Peroxisomal Protein Import Machinery'. *Biological Chemistry* 404 (2–3): 169–78. https://doi.org/10.1515/hsz-2022-0170.

*: these authors contributed equally

The following article is not part of this thesis:

Mukherjee, Indrani*, **Mausumi Ghosh***, and Michael Meinecke. 2021. 'MICOS and the Mitochondrial Inner Membrane Morphology – When Things Get out of Shape'. *FEBS Letters* 595 (8): 1159–83. https://doi.org/10.1002/1873-3468.14089.

*: these authors contributed equally

Patron, Maria, Daryna Tarasenko, Hendrik Nolte, Lara Kroczek, **Mausumi Ghosh**, Yohsuke Ohba, Yvonne Lasarzewski, et al. 2022. 'Regulation of Mitochondrial Proteostasis by the Proton Gradient'. *The EMBO Journal* 41 (16): e110476. https://doi.org/10.15252/embj.2021110476.

List of abbreviations

pA	Pico ampere
nm	Nano meter
AAA	ATPases Associated with diverse cellular Activities
ATP	Adenosine triphosphate
CDC48	Cell division control protein 48
CMC	Critical micelle concentration
Co-IP	Co-immunoprecipitation
COPII	Coat promoter II
CPY	carboxypeptidase Y
CTD	C-terminal domain
CUE	Coupling of ubiquitin to ER degradation
Der1	Degradation in the Endoplasmic Reticulum
DM	n-Decyl ß-maltoside
DMSO	Dimethyl sulfoxide
DOPE	1,2-dioleoyl-sn-glycero-3-Phosphoethanolamine
DOPS	1,2-dioleoyl-sn-glycero-3-phospho-L-serine
DTT	dithiothreitol
DUB	Deubiquitinating enzyme
EM	Electron microscopy
ER	Endoplasmic reticulum
ERAD	ER-associated protein degradation
ERQC	ER quality control
GT	Glucosyltransferase
GTP	Guanosine-5'-triphosphate
HECT	Homologous to E6-AP Carboxyl Terminus
HMGR	3-hydroxy-3-methylglutaryl-coenzyme A reductase
Hrd1	Hydroxymethyl glutaryl-coenzyme A reductase degradation protein 1
Hsps	Heat shock proteins
IRD	infantile Refsum disease
kD	Kilo Dalton
LUVs	Large unilamellar vesicles
MD	Molecular dynamics
Mns1	Mannosidase I
MRH	Mannose-6-phosphate receptor homology
NALD	new born adrenoleukodystrophy
NTD	N-terminal domain
OST	Oligosaccharyl transferase complex

PBDs	peroxisome biogenesis disorders
PDI/PDIA	Protein disulphide isomerase
PEX	Peroxins
PEX5L	Peroxin 5 long isoform
PEX5S	Peroxin 5 short isoform
PLB	Planar lipid bilayer
POPC	1-palmitoyl-2-oleoyl-glycero-3-Phosphocholine
PTS	peroxisomal targeting signal
RBR	Ring-Between-Ring
RING	Really Interesting New Gene
SH3	Src homology 3
SHP	small heterodimer partner
SLRs	SEL1-like repeats
SRP	Signal recognition particle
TEV	tobacco etch virus
TM	Transmembrane
TPA	TEV-Protein A
TPR	tetratricopeptide repeats
U7BR	Ubc7 binding region
Ub	Ubiquitin
UBDs	Ubiquitin binding domains
UBL	Ubiquitin-like
UDP	Uridine diphosphate
UN	Ufd1/Npl4
UPR	Unfolded protein response
UPS	Ubiquitin proteasome system
Usa1	U1-Snp1 Associating
VCP	Valosin-containing protein
WD	tryptophan-aspartic acid dipeptide
WXXX(F/Y)	pentapeptide motifs
Yos9	Yeast OS-9
ZS	Zellweger syndrome
ZSS	Zellweger spectrum syndrome

List of Contents

List of figures

Chapter1

Chapter2

List of tables

Chapter1

Chapter2

Abstract

Within the intricate realm of intracellular protein transport, individual organelles are reliant upon precise and dedicated protein machineries, commonly referred to as translocon, to facilitate the translocation of proteins to their destined subcellular compartments. In this thesis, we delve into the detailed examination of two unique translocation machineries: peroxisomal protein import mediated by Peroxin (PEX) proteins and the retrotranslocation of misfolded substrates through the Endoplasmic Reticulum-Associated Degradation (ERAD) pathway, in two distinct chapters. Both pathways share the fundamental characteristic of mediating the transport of folded proteins from the cytosol to the peroxisomal matrix or from the ER lumen to the cytosol, respectively. This investigation provides an insightful analysis of the electrophysiological properties inherent to both of these intricate transport mechanisms.

Chapter1: Peroxisomes, cellular organelles responsible for lipid metabolism and other critical processes, employ a unique import mechanism that involves peroxisomal translocon, particularly PEX5L. Peroxisomal matrix proteins are synthesized on cytosolic ribosomes and imported post-translationally. Sophisticated protein import systems have developed to facilitate various stages of this process. In humans, PEX5L has been identified as an indispensable component of the peroxisomal translocon. PEX5L serves as the primary receptor for recognizing cargo proteins harbouring a peroxisomal targeting signal (PTS). Cargo proteins bind to the soluble PEX5L in the cytosol, forming a cargo-receptor complex that is subsequently recruited to peroxisomal membranes. At this point, PEX5L interacts with the docking complex PEX13/PEX14, becoming a part of the peroxisomal membrane protein complex that assists in the transfer of cargos into the peroxisomal lumen through a yet unidentified mechanism. Our research reveals that complexes containing PEX5L, purified from human peroxisomal membranes, exhibit characteristics of water-filled pores when reconstituted into planar lipid membranes (PLB). The behaviour of these channels displays high variability in terms of conductance states, selectivity, and voltage and substrate dependent response. Our findings provide evidence of the existence of a PEX5L-associated pore in human peroxisomes, which can be activated by receptor-cargo complexes.

Chapter2: The ERAD process is a vital quality control mechanism within the endoplasmic reticulum (ER). It ensures the removal of misfolded proteins from the ER lumen to the cytosol. This process begins with the recognition of misfolded proteins within the ER lumen, followed by their transfer to a pivotal assembly known as the HRD complex. This HRD complex comprises essential components, named Hrd1, Der1, Usa1, and Hrd3. It plays a central role in retrotranslocating misfolded proteins from the ER membrane to the cytosol, where they undergo ubiquitination and subsequent

proteasomal degradation. The components involved in molecular mechanisms governing the HRD complex activity and the impact of auto-ubiquitination of the complex on the retrotranslocation process remain subjects of keen interest and investigation. In this thesis, we delve into key facets of HRD complex functionality and explore its electrophysiological characteristics. When the HRD complex is integrated into a lipid bilayer, it exhibits channel activity upon ubiquitination and undergoes partial channel closure upon deubiquitination. We further compare the electrophysiological characteristics of Hrd1 and the HRD complex. We observed a single reversal potential for Hrd1, whereas the HRD complex demonstrated a diverse reversal potential, underscoring the distinct behaviours of its components. Additionally, we observed that gating events in the HRD complex are distinct from those observed in Hrd1. Moreover, our study sheds light on the impact of Hrd1 and Der1 as membrane-thinning factors, causing bilayer destabilization in the planar lipid bilayer (PLB) experiments. This study also hints at the possibility of other components, primarily Hrd1 and Der1, playing a direct role in the retrotranslocation process other than Hrd1 alone.

Chapter 1

Dynamics of the peroxisomal protein import pore in humans

1.1 Introduction to Peroxisomes

Peroxisomes are ubiquitous, single membrane organelles with a protein-rich matrix that are found in the cytoplasm of eukaryotic cells (De Duve and Baudhuin 1966; Hruban et al. 1972). These organelles play a crucial role in numerous cellular catabolic and anabolic processes. The primary catabolic mechanisms occurring in peroxisomes involve the alpha- and beta-oxidation of fatty acids as well as the detoxification of glyoxylate. On the other hand, the main anabolic reactions taking place in peroxisomes encompass the biosynthesis of ether phospholipids, bile acids, and docosahexaenoic acid (DHA). Furthermore, peroxisomes have a role in the metabolic processes of oxygen, reactive oxygen species, and reactive nitrogen species, which are partially interconnected with other peroxisomal metabolic pathways (P. B. Lazarow 1995; Waterham, Ferdinandusse, and Wanders 2016). Functional peroxisomes play a crucial role in the growth of yeast cells on oleic acid or methanol as carbon sources. In contrast to mitochondria, nuclei, and chloroplasts, peroxisomes are devoid of DNA (van den Bosch et al. 1992). Consequently, nuclear genes are responsible for encoding all of their proteins, which are synthesized in the cytoplasm and have to be imported post-translationally. (Lazarow and Fujiki 1985). Peroxisomes in humans possess more than 50 distinct enzyme activities, primarily facilitated by specific peroxisomal proteins. Biochemically, peroxisomes contain a distinct set of proteins, including one or more H_2O_2-generating FAD-dependent oxidases and the prototypical H_2O_2-degrading catalase and peroxidases. However, a subset of these enzymes is also found in other subcellular compartments such as mitochondria and the cytosol (Wanders and Waterham 2006). The localization of peroxisomal enzymes is predominantly observed within the matrix, while the peroxisomal membrane harbors proteins that participate in a wide range of other functions, such as sorting matrix and membrane proteins, organelle motility and fission. Peroxisomal proteins are folded in the cytosol with the help of chaperones and must be precisely targeted and translocated into the peroxisomes in order to maintain the organelle's functionality.

1.1.1 Peroxisome biogenesis and peroxisome biogenesis disorders (PBDs)

Peroxisomal membrane proteins have the ability to directly localize to the peroxisomal membrane immediately following their production which facilitates the rapid proliferation of peroxisomes in response to the metabolic demands of the cell (Kim 2017). There are two existing pathways for peroxisome biogenesis. According to the first pathway, peroxisomes undergo proliferation through the process of growth and division of pre-existing organelles similar to the semi-autonomous organelles of an endosymbiont origin like mitochondria and chloroplasts. The process of peroxisome division consists of three consecutive stages: peroxisome extension, membrane constriction, and peroxisome fission. The second pathway suggests that peroxisomes are formed de novo from the endoplasmic reticulum (ER) (Agrawal and Subramani 2016). Proteins involved in the peroxisome biogenesis are known as peroxins and are encoded by PEX genes. The peroxisome biogenesis factors include all the proteins involved in peroxisomal matrix protein import, peroxisome membrane assembly and proliferation (Distel et al. 1996). At the moment, there are 37 known PEX genes which are numbered in the order they were found, with 13 PEX genes in humans (Jansen et al. 2021). Mutations in multiple PEX genes in humans have been associated with PBDs, a group of disorders that impact brain development and can lead to premature mortality (Waterham, Ferdinandusse, and Wanders 2016). The PBDs encompass a collection of genetically diverse disorders that are transmitted in an autosomal recessive manner. These disorders are characterized by a widespread impairment in peroxisome functionality. The predominant cause of PBDs is the presence of biallelic mutations in any of the 13 distinct human PEX genes (Waterham, Ferdinandusse, and Wanders 2016; Wanders et al. 2023). Zellweger spectrum syndrome (ZSS) was one of the first PBDs discovered to be caused by defects in PEX genes, and leads to abnormalities in lipid metabolism causing developmental malformations (Goldfischer et al. 1973; Heymans et al. 1983; Steinberg et al. 2006). The ZSSs encompass several conditions that have been previously documented, including cerebro-hepato-renal syndrome or Zellweger syndrome (ZS), new born adrenoleukodystrophy (NALD), infantile Refsum disease (IRD), and Heimler syndrome (Wanders et al. 2023). Peroxisomes are also essential in plants as they play a crucial role in embryogenesis and subsequent seedling germination and the absence of peroxisomes in plants can lead to deadly phenotypes (Kaur, Reumann, and Hu 2009). Hence, conducting comprehensive research on peroxisome biogenesis and the associated diseases holds significant importance.

1.1.2 Peroxisomes import machinery in mammals

The process of protein import into peroxisomes is a complex and highly regulated mechanism that encompasses several consecutive stages. Proteins destined for the peroxisomal matrix are encoded by nuclear genes, produced on cytosolic ribosomes, and subsequently transported to the peroxisomes via peroxisomal membrane proteins. The import process of proteins into peroxisomes can be categorized into five distinct stages based on the dynamics of the import receptors (Figure 1.1). These stages include: (1) recognition of cargo in the cytosol, (2) docking of the receptor/cargo complex at the peroxisomal membrane, (3) translocation of cargo across the membrane, (4) release of cargo into the peroxisomal matrix, and (5) recycling of the receptors (Hasan, Platta, and Erdmann 2013) .

Matrix proteins are recognized in the cytosol by cytosolic receptors, based on the presence of a peroxisomal targeting signal (PTS). These cytosolic receptors are discussed in section 1.1.2.1. These receptor/cargo complexes then attach to the peroxisomal membrane through a docking complex (Reguenga et al. 2001; Barros-Barbosa et al. 2019; J.-Y. Wang et al. 2019). The docking complex is accompanied by a subcomplex consisting of three conserved really interesting gene (RING) domain proteins, namely PEX2, PEX10, and PEX12, which possess E3 ligase activity. Together, the docking and RING subcomplexes form the importomer complex (Meinecke et al. 2010a; Rayapuram and Subramani 2006; Feng, Skowyra, and Rapoport 2022). The receptor/cargo complexes originating from the cytosol engage in interactions with the docking subcomplex, thereafter undergoing translocation into the peroxisomal matrix. Upon arrival, these complexes proceed to release their respective cargos within the peroxisome matrix. Subsequently, the receptors, together with the co-receptors where relevant, undergo recycling from the peroxisomes to the cytosol in order to initiate another cycle of import. This recycling process is facilitated by a set of components collectively referred to as the exportomer (Nuttall, Motley, and Hettema 2014; Platta, Hagen, and Erdmann 2013). The detailed process of protein import will be described below in a step wise manner.

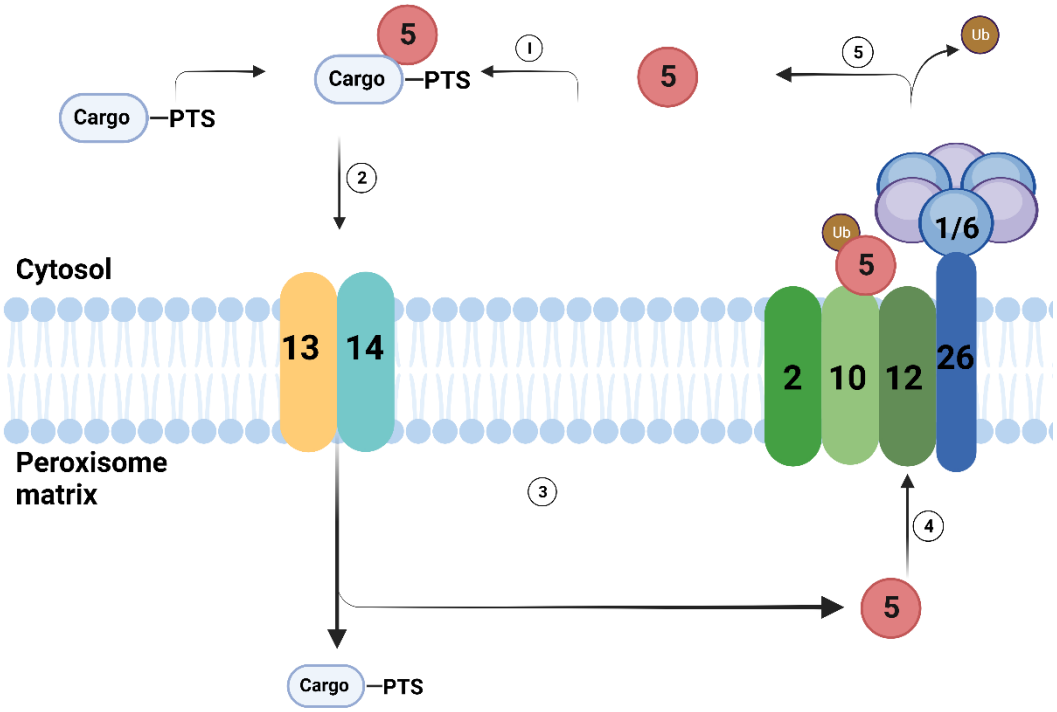

Figure 1.1 Illustration of peroxisomal matrix protein import receptor cycle. The formation of the PEX5-cargo complex occurs within the cytosol (1), after which it subsequently attaches to the peroxisomal membrane (2). This attachment facilitates the transport of cargo across the peroxisomal membrane, ultimately leading to its release into the matrix of the organelle (3). PEX5 undergoes monoubiquitination, which is essential for the subsequent interaction between PEX5 and the ubiquitin ligase PEX2/PEX10/PEX12 (4). Subsequently monoubiquitinated PEX5 is extracted into the cytosol by ATPase complex PEX1/PEX6 and its membrane anchor PEX26 (5), then the deubiquitination of PEX5 leads to unbound PEX5, which has the ability to initiate a subsequent cycle of protein import. Numbers indicate the PEX proteins. To simplify only PEX5 receptor is presented in the illustration as an example of a receptor. Created using Biorender.com

1.1.2.1 The recognition of cargo in the cytosol

The identification and sorting of peroxisomal proteins are significantly influenced by the specific PTS included in their amino acid sequences. The majority of proteins found in the peroxisomal matrix possess a C-terminal tripeptide motif known as PTS1, which is characterized by a consensus sequence of (S/A/C)-(K/R/H)-(L/M). A smaller group of matrix proteins has an N-terminal octapeptide motif called PTS2, which is characterized by a consensus sequence of (R/K)-(L/I/V)-$(X)_5$-(Q/H)-L/I/V) (Subramani 1992; Paul B. Lazarow 2006). In both yeast and humans, these sequences are recognized by distinct receptors, namely PEX5 for PTS1 and PEX7 for PTS2 (Walter and Erdmann 2019). The receptors mentioned, such as PEX5, can function independently or in conjunction with co-receptors, such as PEX7-PEX5L in mammals, Pex7-Pex18 or Pex7-Pex20 in S. cerevisiae and P. pastoris, respectively. Another peroxin, Pex9, is a Pex5-related protein identified in yeast and recognizes a

restricted set of PTS1 cargos, including malate synthase 1 and 2, as well as glutathione transferase. Consequently, Pex9 can be regarded as a PTS receptor that operates under certain physiological conditions (Farré et al. 2019). The soluble peroxisomal import receptors undergo a cyclic process of translocation between the cytosol and the peroxisomal matrix (Hasan, Platta, and Erdmann 2013).

1.1.2.1.1 PEX5

In yeast, plants and mammals, PEX5 is the primary cytosolic soluble receptor that binds to PTS1 cargos in the cytoplasm and imports peroxisomal matrix proteins into the peroxisomal lumen. The PEX5 protein exhibits a comprehensive structural arrangement, featuring an intrinsically disordered N terminal domain (NTD) that constitutes fifty percent of the protein's composition. At its C-terminus, it possesses a compact tetratricopeptide repeats (TPR) domain responsible for the recognition of PTS1 cargo proteins (Carvalho, Goder, and Rapoport 2006; Neuhaus et al. 2014; W. A. Stanley et al. 2006). PEX5 contains eight TPR repeats, which are organized in a sequential manner, with seven repetitions located in the C-terminal portion of the protein and one repeat present in the N-terminal region. TPRs consist of approximately 34 amino acids and are believed to possess the ability to create intertwined helices, facilitating interactions between proteins (Goebl and Yanagida 1991; Lamb, Tugendreich, and Hieter 1995; Zeytuni and Zarivach 2012). The two TPR triplets (TPR1-3, TPR5-7) are arranged in a circular configuration which constitutes the PTS1 binding groove and facilitates the binding of peroxisomal matrix enzymes. The cryo-EM structures of cargo bound PEX5 show that the two triplets are connected through the non-canonical TPR4, which is partially folded (Stanley et al. 2006; Gatto et al. 2000). Additionally, the N-terminal region of PEX5 exhibits several pentapeptide repetitions in the form of WXXX(F/Y). Di-aromatic pentapeptide motifs may be observed in the N-terminal regions of all PEX5 orthologs, however they may vary in terms of quantity and arrangement. There are seven of such motifs in human PEX5 (Otera et al. 2002).

In mammals, the cytosolic receptor PEX5 exists in two different isoforms PEX5S or PEX5L through alternative splicing and is responsible for the binding of newly produced proteins in the cytosol. (Braverman et al. 1998). PEX5S is the short isoform which consists of 602 amino acids and only binds to PTS1 cargos while PEX5L is the long isoform and binds to both PTS1 and PTS2 cargos (Braverman et al. 1998) (Figure 1.2). The C-terminal TPR region of PEX5 exhibits binding affinity towards PTS1 cargos with two triplets of TPR repeats (Harper, Berg, and Gould 2003; Gatto et al. 2000). Domain mapping of PEX5 shows that PEX5L contains an insert of 37 amino acids long that is positioned between amino acids 214 and 215 of PEX5S and amino acids 299–639 are involved in PTS1 recognition while amino acids from 1-214 in PTS2 cargo recognition. For PTS2 cargo recognition, PEX5L appears to interact with

PEX7, the PTS2 co-receptor, with amino acids 191–222 (Dodt et al. 2001). Domain structure of both PEX5S and PEX5L are illustrated in Figure 1.3A.

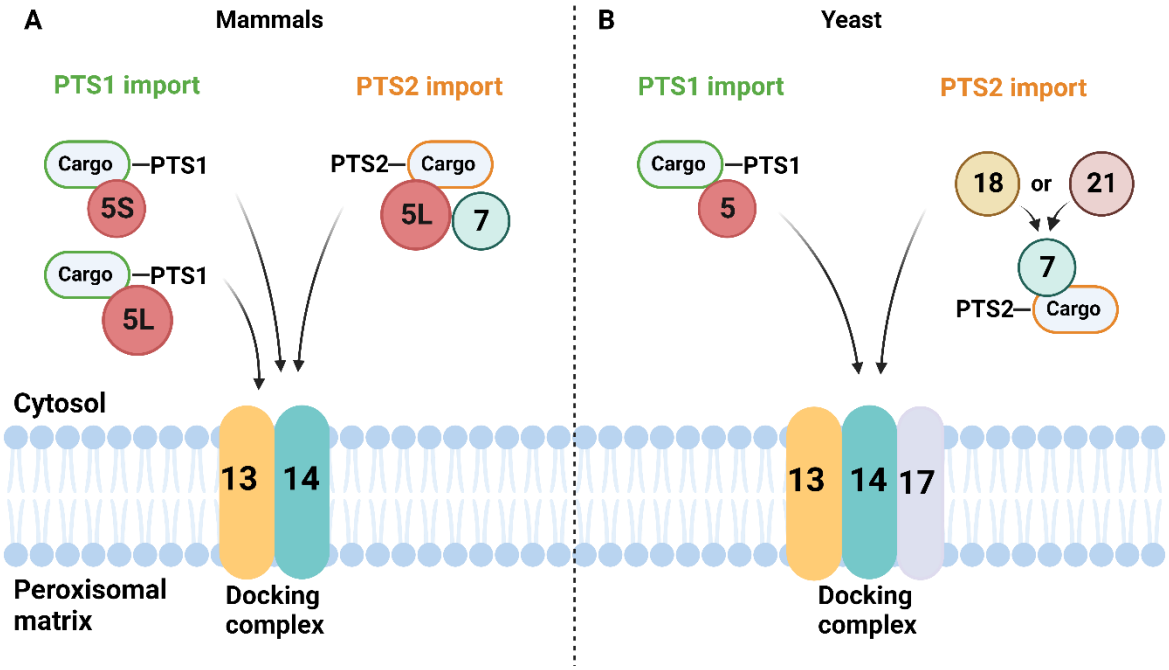

Figure 1.2 Peroxisomal import receptors and membrane docking complexes. (A) In mammals and (B) yeast. Schematic structures of the principal constituents of the yeast and mammalian import receptor and membrane docking complexes associated with the PTS1 and PTS2 import pathways. In contrast to yeast (B), mammalian cells (A) possess a minimum of two splice variants of PEX5, namely PEX5S (S representing short) and HsPex5L (L representing long). PEX5L functions as a co-receptor with PEX7 in the peroxisomal targeting signal 2 (PTS2) pathway, which is analogous to the role of ScPex18p and ScPex21p in yeast. The process of cargo-receptor complex binding to peroxisomal membrane is aided by the docking complex, which is composed of Pex14 and Pex13 in mammals, and Pex13, Pex14, and Pex17 in yeast. Created using Biorender.com

1.1.2.1.2 PEX7

The PTS2 receptor PEX7 belongs to the family of seven-bladed cone shaped tryptophan-aspartic acid dipeptide (WD)-40 repeat proteins (Figure 1.3A), which share a characteristic shape and are known to associate with members of TPR family (van der Voorn and Ploegh 1992; Kunze et al. 2011). PEX7 interacts with PEX5L to be directed to the peroxisomal membrane which is exerted by co-receptors (Otera et al. 2000; Kunze et al. 2015). In mammals and plants, PEX5 serves as a co-receptor while in yeast, Pex18 or Pex21 function as co-receptors (Figure 1.2) (Edward Purdue, Yang, and Lazarow 1998; Woodward and Bartel 2005). These co-receptors share a conserved PEX7 binding domain. In a structural model of PEX7, it is observed that two glutamate residues (Glu-113, Glu-200), which are conserved throughout evolution, constitute the binding groove. Substituting these residues with

neutral amino acids hinders the binding of cargo molecules. Conversely, a third glutamate residue (Glu-287), which is also conserved, is located in close proximity to the binding groove. However, mutating this residue does not impede the binding of cargo molecules (Kunze et al. 2011). The aforementioned hypothesis about the interaction between human PEX7 and its cargo has been supported by the elucidation of the three-dimensional structure of yeast Pex7 in complex with a PTS2 cargo protein (Pan, Nakatsu, and Kato 2013). A modified variant of the mammalian two-hybrid test showed that binding affinity between cargo and PEX5L is significantly enhanced when the co-receptor PEX7 is present (Kunze et al. 2015). This suggest that PEX7 serves as a link between cargo proteins containing a PTS2 signal and co-receptor proteins, such as PEX5L, which mediate protein transport. PEX7 is also known to be involved in PBDs. Individuals with a mutation in the PEX7 gene exhibit symptoms of rhizomelic chondrodysplasia punctata type 1 (RCDP1), characterized by various clinical manifestations including proximal limb shortening and abnormal calcification patterns in the cartilage (Braverman et al. 1998). RCDP1 patients with mutations in PEX7 show defects in PTS2 cargo import but still have normal PTS1 protein import, and shows metabolic and developmental abnormalities that involve PTS2 enzymes (Dodt et al. 2001).

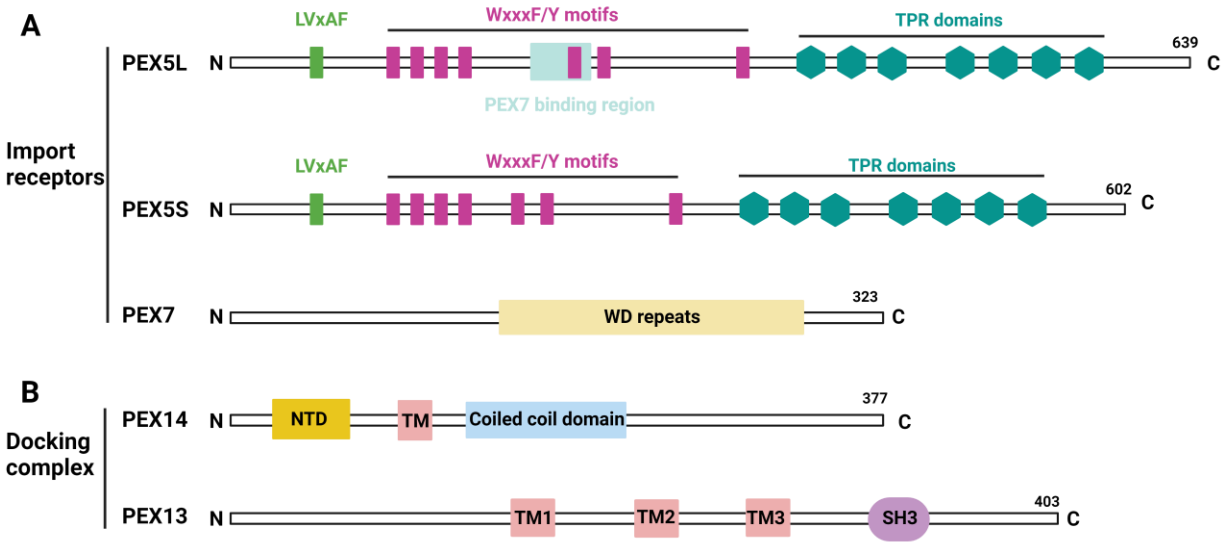

Figure 1.3 Domain structure of human PEX proteins. (A) Import receptors PEX5L, PEX5S and PEX7 (B) Docking complex PEX14 and PEX13. Their features are marked. Numbers indicate amino acid position. Tetratricopeptide repeats (TPR), pentapeptide motifs (WxxxF/FxxxW), N-terminal domain (NTD), transmembrane domain (TM), tryptophan-aspartic acid (W-D) dipeptide, Src homology domain (SH3). Created using Biorender.com

1.1.2.1.3 The oligomeric state of cargo proteins

A remarkable characteristic of peroxisomes is the ability to import proteins in a completely folded state, and even in an oligomeric and co-factor bound condition (Hasan, Platta, and Erdmann 2013; Meinecke, Bartsch, and Wagner 2016; Walter and Erdmann 2019). Transport of such large cargos has been shown by import of gold particle of size up to 9 nm (Walton, Hill, and Subramani 1995). Another group demonstrated transport of artificial DNA and large polysaccharides up to 12.5 nm when bound to PTS-proteins by the peroxisomal importomer showing the pore's flexibility for the oligomeric substrates (J. Yang, Pieuchot, and Jedd 2018).

Several studies indicated that oligomeric proteins are the substrates for protein import into the peroxisomes. In one study, pulse-chase investigations conducted on yeast have provided evidence indicating that two peroxisomal matrix enzymes, alcohol oxidase and acyl-CoA oxidase, undergo oligomerization in the cytosol before being imported (M. Q. Stewart et al. 2001; Titorenko et al. 2002). Multiple studies have demonstrated that co-expression of two proteins within a cell leads to the localization of a portion of the second protein to the peroxisome when the first protein contains a single PTS (McNew and Goodman 1994; Glover, Andrews, and Rachubinski 1994; X. Yang, Purdue, and Lazarow 2001; Islinger et al. 2009; Otera and Fujiki 2012). However, these studies focused on proteins that were overexpressed, either using recombinant genes with strong promoters or by growing yeasts in special media that induce peroxisome proliferation. These experimental circumstances may titrate the receptors PEX5 and PEX7 and prematurely oligomerize those proteins in the cytoplasm.

There are also studies indicating the import and preference of monomeric cargos. It has been found that PEX5, at physiological conditions binds to monomeric catalase (a homo-tetrameric protein in its native state), effectively inhibiting its tetramerization process with significant potency and this interaction is disrupted by NTD of PEX14, a component of the docking/translocation machinery (Freitas et al. 2011). In rat hepatocytes, PEX5 also binds and imports two other matrix proteins, acyl-CoA oxidase 1 (a homo-dimeric protein in its native state) and urate oxidase (a homo-tetramer protein in its native state), in their monomeric state rather than their corresponding oligomeric states (Freitas et al. 2015). In addition, cytosolic chaperone Hsp70 also binds to PEX5 independently of PTS1 and enhances PEX5-PTS1 cargo interaction and maintains solubility of the cargo proteins (Harper, Berg, and Gould 2003; Harano et al. 2001). There are numerous studies that present arguments regarding the oligomeric nature of peroxisomal matrix proteins and the results so far indicate that the substrates for transport into peroxisomes are quite diverse.

1.1.2.2 Docking of the receptor/cargo complex at the peroxisomal membrane

After the formation of the cargo-receptor complex, it is subsequently transported in close proximity to the peroxisomal membrane. At this point, the PEX5-cargo complex interacts with the docking complex located on the peroxisomal membrane, facilitating the import of cargo proteins into the peroxisomal matrix. The docking complex consist of PEX14 and PEX13 (Fransen, Terlecky, and Subramani 1998; Gould et al. 1996) (Figure 1.2). The subcellular distribution of PEX5 was predominantly observed in the cytoplasm in cell lines with a deficiency in PEX14, but it exhibited an accumulation at peroxisomal membranes in cells that overexpressed PEX14 (Otera et al. 2000; Demers et al. 2023). This suggests that the receptors bind to the peroxisomal membrane in presence of the docking complex.

1.1.2.2.1 PEX14

The PEX14 is conserved throughout all eukaryotes and comprised of 377 amino acids. It exhibits a globular unstructured NTD, succeeded by a brief hydrophobic transmembrane (TM) segment, which is then followed by a coiled coil region and an unstructured C-terminal domain (CTD) (Figure 1.3B) (Oliveira et al. 2002; Gaussmann et al. 2021). PEX14 has been seen to exist in different oligomeric states. According to an NMR investigation, even at elevated micromolar concentrations, the PEX14 protein is primarily present in a monomeric state (Neufeld et al. 2009). PEX14 from Chinese hamster ovary was also shown to homodimerize utilizing its coiled-coil domain (Itoh and Fujiki 2006). In yeast, Pex14 homooligomer is hypothesized to play a role in the formation of pore-like structures located in the peroxisomal membrane (Meinecke et al. 2010a). A crystal structure of the rat PEX14 NTD unveiled a tertiary structure characterized by a trimeric arrangement of three helices. The arrangement of the aromatic side chains of Phe52 and Phe35, which are situated in helices α2 and α3, respectively, plays a crucial role in maintaining the structural integrity of the NTD domain. This contributes to the formation of a hydrophobic surface cavity which has a potential to bind WXXX(F/Y) motifs of PEX5 (Su et al. 2009). The WXXX(F/Y) motifs at N-terminus of PEX5 are responsible for binding N-terminus of PEX14 with very high affinity (Schliebs et al. 1999; Saidowsky et al. 2001). Human PEX5 contains an additional PEX14 binding motif (LVxAF) which binds with lower affinity to the N-terminal than the Wxxx(F/Y) motifs (Neuhaus et al. 2014). In vitro studies suggest that PEX14 exhibits a stronger interaction with receptors carrying cargo, while PEX13 likely has a stronger interaction with PEX5 receptors that are devoid of cargo (Mukai and Fujiki 2006; Demers et al. 2023). The observation of this characteristic has suggested that PEX13 is may be involved in the process of PTS1 cargo-release from PEX5. It is noteworthy that the PEX5/PEX7/PTS2 cargo complex retains the ability to interact with

PEX13, indicating that the process of cargo-release for PTS1 and PTS2 proteins may exhibit dissimilar mechanisms (Mukai and Fujiki 2006).

1.1.2.2.2 PEX13

PEX13 is ~ 42–44 kDa integral membrane protein localized in the peroxisome and has been conserved throughout evolution. It encodes a 405-amino-acid product possessing a cytoplasmic Src homology 3 (SH3) domain that facilitates its interaction with PEX5 and multiple predicted TM domains located on either side of a binding site for PEX14 (Figure 1.3B) (Gould et al. 1996; Björkman, Gould, and Crane 2002). In yeast, the deletion of Pex13 leads to a decrease in peroxisome membrane associated Pex5 and causes the impairment of protein import involving both PTS1 and PTS2 cargos (Elgersma et al. 1996; R. Erdmann and Blobel 1996; Girzalsky et al. 1999). The N-terminal region of PEX13 is highly unstructured and exhibits a proline-rich stretch that often contains a KPWE motif, followed by a glycine-rich segment that contains several YG motifs (Brennand, Rigden, and Michels 2012; Gao et al. 2022). The YG domains are crucial for protein import. When all tyrosine residues in YG repeats of *Xenopus laevis* PEX13 were substituted with serine residues, then protein import was inhibited (Gao et al. 2022). The structure of the globular SH3 domain of both yeast and mammals has been studied as well. It displays mainly a β-barrel fold, as a whole, presents a region characterized by hydrophobic residues that collectively provide a pocket with an appropriate conformation to accommodate another known PXXP motif of Pex14 at the NTD. The opposing side of SH3 domain reveals an extra hydrophobic binding site that exhibits specificity towards the N-terminal WXXX(F/Y) motif of PEX5. (Pires et al. 2003; Douangamath et al. 2002; Bottger et al. 2000; Rüttermann and Gatsogiannis 2023). In a GST pull-down assay, it was demonstrated that NTD of PEX13 exhibits binding affinity towards PEX5, while the C-terminal SH3 region of PEX13 interacts with PEX14 (Otera et al. 2002). In yeast, SH3 domain alone is capable of interacting with both Pex5 and Pex14 (Bottger et al. 2000). In human fibroblast cells, PEX13 undergoes homo oligomerization via the NTD and mutation of a conserved residue of the C- terminal SH3 domain leads to defects in PTS1 cargo import, but does not inhibit interaction with PEX14. Thus, it's surprising that the SH3 domain is not important for homodimerization of PEX13 but the NTD is enough for localization of PEX13 to peroxisomes and its oligomerization (Krause et al. 2013). This observation implies that whereas PEX13 is evolutionarily conserved, its functional behaviour exhibits variations between yeast and humans. Mutations in a conserved tryptophan residue in the SH3 domain of PEX13 and deletion of the entire gene have been found in patients with ZSS, and show severe birth defects and death at an early age (Krause et al. 2006; Al-Dirbashi et al. 2009; Borgia et al. 2022). Apart from protein import, PEX13 is essential for the

process of selective autophagy, specifically in the degradation of Sindbis virus and damaged mitochondria (Lee et al. 2017).

1.1.2.3 Translocation of cargo across the membrane

After formation of the docking complex, cargo is translocated across the peroxisomal membrane. There are several theories regarding this translocation. The process by which folded proteins are transported across the membrane and the subsequent release of cargo continues to be an enigmatic phenomenon. It was first proposed that translocation occurs through internalization of the peroxisomal membrane to transport the matrix proteins. This was supported by internal peroxisomal membrane structures observed in both yeast and mammalian cells (McNew and Goodman 1994). But there was not sufficient evidence to prove this further. In another model, known as the simple shuttle model, the receptor undergoes shuttling between the cytosol and the membrane of peroxisomes. The receptor molecule interacts with cargo molecules on the peroxisomal membrane, and subsequently dissociates from the cargo molecules. PEX5 is proposed to facilitate the transportation of cargo molecules into the interior of the peroxisomal lumen as a shuttle (Kunau 2001). The validity of this hypothesis is substantiated by evidence indicating the insertion of the human PEX5 receptor's N terminus into the lumen during the import process, as well as experimental findings that propose the occurrence of yeast receptor-bound Pex7 entering the lumen to some extent (Dammai and Subramani 2001; Nair, Purdue, and Lazarow 2004). This gave rise to an alternative model known as the extended shuttle model, which suggest that the receptor enters the matrix to release the cargo. Dammai and Subramani (2001) also showed that PEX5 is necessary for PTS1 cargo import and that it enters the matrix. However, this model could not show how the cargo is released.

Later it was found that the minimal components required to translocate cargos are PEX5 and PEX14. This was suggested due to studies in yeast *Pichia pastoris* which showed that for the import of Pex8, which contains both PTSs and is also an important component of the importomer, only Pex5 and Pex14 were required instead of the whole docking complex consisting additionally of Pex13 and Pex17 (Ma et al. 2009). It was also shown that the affinity-purified Pex5/Pex14-containing subcomplex, when reconstituted into proteoliposomes and added to the bilayer, displays channel activity and leads to a pore size of 0.6 nm. When this subcomplex was preincubated with a PTS1 cargo, this lead to further expansion of the pore size up to 9 nm which would be enough to accommodate oligomeric cargos (Meinecke et al. 2010a). The principal constituents of the peroxisomal translocon were determined to be PTS1 receptor Pex5 and its counterpart Pex14 as they were in 1:1 stoichiometry, even though the other peroxins of the docking complex, Pex13 and Pex17, were present in minimal quantities during the reconstitution experiments (Meinecke et al. 2010a). The PTS2 specific pore was identified as well.

It is formed by the co-receptor Pex18 and the Pex14/Pex17-docking complex instead of the main receptor Pex7 (Montilla-Martinez et al. 2015). The outcome was not unexpected, as a chimeric protein consisting of Pex18 fused to the cargo binding CTD of Pex5, partially recovered PTS1 protein import in a *PEX5* deletion strain. This finding suggests that Pex5 and Pex18 perform comparable functions in the peroxisomal import pathway but for different PTS cargos (Schäfer et al. 2004; Walter and Erdmann 2019).

This led to the focus onto the transient pore formation model. According to this, translocation of cargo requires protein conducting channels. These channels were hypothesized to open when the PEX5-cargo complex engages with the docking complex located on the peroxisomal membrane (Ralf Erdmann and Schliebs 2005). The validity of this model was supported by demonstrating that PEX5 adopts a transmembrane topology within the peroxisomal membrane, whereby the N-terminus is oriented towards the cytoplasm (Azevedo and Schliebs 2006). However, the presence of a pore like structure in the peroxisomal membrane capable of accommodating folded proteins, including oligomeric proteins, has not been shown so far. In vitro experiments show that the peroxisomal membrane can allow free diffusion of smaller molecules up to 300-400 Da but prevents diffusion of larger molecules including cofactors like ATP, Coenzyme A and NADP/H (Vasily D. Antonenkov and Hiltunen 2012). Electrophysiological characterization of yeast Pex5 and docking complex pointed towards the possibility of pore formation by these components (Meinecke et al. 2010a; Montilla-Martinez et al. 2015). For PTS1 cargos, Pex5 was considered as the main translocon as in the yeast *Hansenula polymorpha*, the overexpression of Pex5 can partially compensate for the import defect seen in a Pex14 null mutant (Salomons et al. 2000). This was also in accordance with the observation in yeast and humans that PEX5 has intrinsic lipid binding activity and can insert into the membrane in vitro without binding to the docking complex (Kerssen et al. 2006). In schwann cells, the myelinating cells of the peripheral nervous system in mice, PEX5 knockout causes peroxisome dysfunction due to the defects in protein import and reduced compound muscle action potential due to the abnormal localization of the potassium channel protein Kv1.1 along with cerebral inflammatory demyelination (Kleinecke et al. 2017). The peroxisomal membrane exhibits permeability to solutes and is equipped with proteins that generate pores. The structural details explaining the assembly of all components specifically involved in the peroxisomal protein import are still missing and therefore identification of the main component of the translocon remains elusive.

1.1.2.4 Release of cargo into the peroxisomal matrix

After translocation of cargo, the peroxisomal translocation pore needs to be disassembled. It is necessary for the cycling import receptors to be liberated from the peroxisomal membrane and relocated to the cytosol. This enables the receptors to be once again accessible for the recognition of cargo and to commence a subsequent cycle of the peroxisomal protein import. This is crucial as the presence of a consistent pore would result in the compromise of the permeability barrier, a phenomenon that is inconsistent with the established characteristics of the peroxisomal membrane (Vasily D. Antonenkov and Hiltunen 2012; Ralf Erdmann and Schliebs 2005).

There are several theories regarding the release of cargo but it still remains the least understood aspect of the receptor import export cycle. One theory indicated that a change in pH in the peroxisomal matrix leads to the dissociation of cargo from PEX5. This was based on previous observations in the yeast, which indicate that the oligomeric forms of Pex5 undergo a transition from a tetramer/oligomer bound to cargo at a neutral pH of 7.2 to a monomer without cargo at an acidic pH of 6.0. It is known that the pH of *H. polymorpha* in the peroxisomal matrix ranges from approximately 5.8 to 6.0 (Nicolay et al. 1987; D. Wang et al. 2003; Ma et al. 2013). But mammalian peroxisomes display a pH between 6.9 to 7.1 which resembles the cytosolic pH (Jankowski et al. 2001). In an alternative aspect, it was shown in human fibroblast cells that the redox environment of peroxisomes is quite critical for the protein import and important for PTS1 cargo release (Apanasets et al. 2014). Supporting this argument, it was shown that the monoubiquitination at a conserved cysteine 11 at the NTD of PEX5 acts as a redox switch which can regulate PEX5 import activity. An oxidative environment leads to defects in monoubiquitination at the cysteine residue of PEX5 (Apanasets et al. 2014). This might release the cargo and also lead to export of the receptor back into the cytosol which is described in next section 1.1.2.5. Another theory is that binding affinity between PEX5 and cargo is decreased when it binds to the docking complex (Otera et al. 2002; Madrid et al. 2004; Ma, Agrawal, and Subramani 2011). It was also thought that the interactions between the NTD of PEX5 and the co-receptors and docking complex might change the structure of the C-terminal TPR domain from closed to open conformation, making it easier for the release of cargo (W. A. Stanley et al. 2006). The only evidence of a cargo release in the literature involves the interaction of oligomeric Pex5 with Pex8 (yeast *P. pastoris*) which facilitates the formation of importomer by binding to the docking complex. The reduction of a conserved N terminal cysteine residue of Pex5 leads to a hetero-oligomeric interaction between the N terminal of Pex5 with Pex8 and the subsequent dissociation of the PTS1 cargo (Agne et al. 2003; Ma et al. 2013). There is no direct evidence about the cargo release

in mammals as a homolog of Pex8 is not present in mammals. A significant portion of our understanding of cargo release is currently based on speculation and requires additional investigation.

1.1.2.5 Receptor recycling

In order to complete the import cycle, it is necessary for PEX5 to be transported back to the cytosol. This step requires monoubiquitination of PEX5 at the N- terminus near a conserved cysteine residue at the 11th position (W. Wang and Subramani 2017; Pedrosa et al. 2018). When the regular recycling process of PEX5 or of other receptors is hindered, the receptors undergo polyubiquitination on the lysine residues and are subsequently degraded by the proteasome. The degradation of substrates (PEX5 receptor here) by the ubiquitin proteasome system (UPS) is explained in detail in the next chapter in section 2.1.5. The process of receptor monoubiquitination and polyubiquitination is facilitated by a ubiquitin ligase (E3) complex that is conserved and embedded in the peroxisomal membrane. This complex comprises PEX2, PEX10, and PEX12, all of which contain RING finger domains (El Magraoui et al. 2012; Feng, Skowyra, and Rapoport 2022). The ubiquitin ligase complex forms a channel with its TM segments and a cytosolic tower with its ring finger domains. The diameter of the channel is 1 nm which contributes to the permeability of small molecules across peroxisomal membrane (Feng, Skowyra, and Rapoport 2022). The monoubiquitination of PEX5 at cysteine 11 requires the ring finger domain of PEX2 and members of the UbcH5a/b/c family are required as E2 enzymes (Sargent et al. 2016; Grou et al. 2008; Feng et al. 2022). The monoubiquitination can be reversed by the cytosolic deubiquitinase enzyme Ubiquitin Specific Protease 9x (USP9X) in mammals, which makes PEX5 available again for another round of import cycle (Grou et al. 2012; Francisco et al. 2014). When the receptor cannot be recycled further, then polyubiquitination of PEX5 occurs at lysine residues by combined action of the ring finger domains of PEX10 and PEX12 (Feng, Skowyra, and Rapoport 2022).

Recycling of the import receptor PEX5 requires energy, which is provided in form of ATP, to pull out PEX5 from the peroxisomal membrane. It was shown through in vitro experiments that PEX5 from rat hepatocytes integrates into the membrane in two different topologies in the absence of ATP. First, around 2 kDa of its N terminal is exposed into the cytosol with the C- terminal domain stays inside the matrix and second, both N and C- terminal are completely inside the lumen and bound to PEX14 (Gouveia et al. 2003). The first topology is the precursor of the second one which shows that the N-terminus of PEX5 protrudes outwards into the cytosol to be ubiquitinated (Gouveia et al. 2003). This is also supported by the cryo-EM structure of PEX2, PEX10, and PEX12 from thermophilic fungus *Thermothelomyces thermophilus,* that predicts that during the process of export, the N-terminal segment lacking a defined structure is expected to enter the channel pore from the luminal side. This

allows for the modification of the conserved cysteine residue through the action of ring finger domain of PEX2 (RF2) (Feng, Skowyra, and Rapoport 2022). In presence of ATP, it was observed that the PEX5 found in the second topology is released from the membrane, similar to PEX5 in endogenous rat hepatocytes that requires ATP for export (Gouveia et al. 2003).

The ubiquitin ligase complex works together with the ATPase complex to monoubiquitinate and extract the receptor to cytosol from the peroxisomal membrane to initiate a new round of protein import. There are members of the AAA+ protein family which are involved in unfolding and disassembly of proteins. AAA+ proteins have been implicated in the process of dislocating proteins in the inner mitochondrial membrane and the ER, to facilitate their subsequent proteolytic breakdown, which is described in detail in the next chapter (Ogura and Wilkinson 2001; Sauer et al. 2004). In the peroxisomes, this is accomplished by PEX1 and PEX6, which are highly conserved and the only known peroxins containing ATP-binding domains. They interact with each other in the presence of ATP to form a complex (Matsumoto, Tamura, and Fujiki 2003; W. Wang and Subramani 2017). The PEX1/PEX6 ATPase complex is anchored to the membrane by PEX26, but in yeast, this function is fulfilled by Pex15 (Matsumoto, Tamura, and Fujiki 2003; B. M. Gardner et al. 2018). Alpha fold prediction of the PEX1/PEX6 ATPase complex suggests that PEX1 and PEX6 assemble into a hexameric complex with alternative subunits of each. Both PEX1 and PEX6 possess a pair of NTDs, namely N1 and N2, as well as two ATPase domains, designated as D1 and D2. The ATPase domains undergo hexamerization, forming two ATPase rings that are stacked around a central pore and import of cargos into the matrix requires ATP hydrolysis in the D2 domain of the PEX6 (Judy, Sheedy, and Gardner 2022; Tamura et al. 2006). It is hypothesized that substrates of PEX1/PEX6 will initially interact with the NTDs and thereafter traverse the D1 central pore to interact with the D2 pore loops within the active ATPase ring. Among the various hypothesized substrate-binding domains, the PEX1 N1 domain has the highest degree of conservation, indicating its potential affinity for a universally conserved substrate (Judy, Sheedy, and Gardner 2022). Another protein Cdc48/p97, which also belongs to the AAA+ family, plays a crucial role in facilitating the degradation of misfolded polyubiquitinated substrates that are transported out of the ER through the proteasome-dependent pathway, and is discussed briefly in the next chapter in section 2.1.7 (Rabinovich et al. 2002; Jarosch et al. 2002; Bodnar and Rapoport 2017).

The malfunctioning of PEX1 and PEX6 genes are responsible for the majority of cases associated with PDBs (Ebberink et al. 2011). There are moderate to severe implications upon deletion and mutation of the ATPase complex. Mutation of any components of ATPase complex PEX1/PEX6 leads to a reduction in both the quantity and functionality of peroxisomes and causes accumulation of ubiquitinated PTS1/PTS2 receptors on the peroxisomal membrane leading to pexophagy (Law et al.

2017). Deletion of PEX1 in human cell lines leads to a decrease in PEX5 stability but surprisingly stabilizes PEX13 which is part of the docking complex (Ott et al. 2023). The PEX1/PEX6 with its membrane anchor PEX26 complex was also shown to interact with the docking complex. In rat heapatocytes, the interaction between human membrane anchor protein PEX26, and the docking protein PEX14 was observed. This interaction is disrupted by the ATPase activity of PEX1/PEX6 complex due to conformation change in PEX14 which is another suggested mechanism of cargo release (Tamura et al. 2014; 2006). The recruitment of PEX5 to the peroxisome membrane by PEX14 aligns with the idea that PEX26 plays a role in positioning PEX1/PEX6 complex in close proximity to PEX14-bound PEX5, hence facilitating the retrotranslocation of PEX5 to the cytosol (Rinaldi et al. 2017).

1.2 Aims

In yeast, Pex5 is responsible for the import of only PTS1 cargo. Pex7 is responsible for the import of PTS2 cargos with the help of its coreceptor Pex18 or Pex21. Both PTS1 and PTS2 pathways have been studied in yeast (Rüttermann and Gatsogiannis 2023; Edward Purdue, Yang, and Lazarow 1998; Mukai and Fujiki 2006). The mechanism of translocation has been discussed through biochemical and electrophysiological characterization. When Pex5 along with the docking complex, mainly Pex14, is reconstituted into LUVs and added to bilayer, it forms a small ion conducting pore which expands upon incubation with the PTS1 cargos (Meinecke et al. 2010a). Similarly, for the PTS2 pathway, when Pex18 along with the docking complex Pex14\Pex13\Pex17 is reconstituted, it leads to the formation of an ion channel which displays very dynamic behaviour upon incubation with PTS2 cargos (Montilla-Martinez et al. 2015). In humans, both PTS1 and PTS2 cargos are imported by PEX5L. The Import of PTS2 cargos requires PEX7 as co-receptor which helps to recruit them to the peroxisomal membrane. There are several differences between the coreceptor and components of the yeast and mammalian peroxisomal protein import machinery as described above. Therefore, it is important also to perform electrophysiological characterization of PEX complexes involved in protein import in human peroxisomes.

To study protein import machinery in humans, PEX5L containing complexes were purified from human peroxisomal membranes and electrophysiological characterization was performed. The interaction of PEX5L complex with the cargos were also studied to understand how it is different from the yeast peroxisomal protein translocon. The results are discussed in the next section.

We collaborated with the group of Prof. Dr. Ralf Erdmann and Prof. Dr. Wolfgang Schliebs and their students Maren Reuter, Jessica Klümper, Katharina Reglinski, Rebecca Peschel from Institute of Biochemistry and Pathobiochemistry, Ruhr University Bochum.

This methods and results section of this thesis are also part of the published manuscript.

Ghosh, M., Denkert, N., Reuter, M., Klümper, J., Reglinski, K., Peschel, R., Schliebs, W., Erdmann, R. and Meinecke, M. (2023) Dynamics of the translocation pore of the human peroxisomal protein import machinery. Biological Chemistry, Vol. 404 (Issue 2-3), pp. 169-178. https://doi.org/10.1515/hsz-2022-0170

1.3 Materials and methods

1.3.1 Materials

Table 1.1 Special consumables

Chemical	**Supplier**
Acetone >99.8% p.a.	Carl Roth GmbH & Co KG
Antipain	MP Biomedicals
Aprotinin	MP Biomedicals
Benzamidine hydrochloride	MP Biomedicals,
Bestatin	MP Biomedicals
Calbiosorb	Calbiochem
Chymostatin	MP Biomedicals
Digitonin	Merck
Dulbecco's modified eagle medium (DMEM)	Sigma Aldrich
Ethanol >99.8% p.a.	Carl Roth GmbH & Co KG
Fetal calf serum (FCS)	Sigma Aldrich
Filter supports	Avanti Polar Lipids
HEPES	Carl Roth GmbH & Co KG
Histodenz	Sigma Aldrich
l-a-phosphatidylcholine (PC)	Avanti Polar Lipids
l-a-phosphatidylethanolamine (PE)	Avanti Polar Lipids
Leupeptin	MP Biomedicals
l-glutamine	Gibco
Methanol >99.9% p.a.	Carl Roth GmbH & Co KG
n-Dodecyl-β-maltoside (DDM)	GLYCON Biochemicals
Nuclepore Track etched polcarbonate membrane	Whatman
PageRuler prestained protein ladder	Thermo Scientific, US
Penicillin	Gibco
Pepstatin	MP Biomedicals
Phenylmethylsulfonyl fluoride (PMSF)	Roche Diagnostics
Potassium chloride (KCl)	Carl Roth GmbH & Co KG
Streptomycin	Gibco

T75 flasks	Thermo Scientific
TEV protease (AcTEV™ protease)	Invitrogen
Trichloromethane/Chloroform	Carl Roth GmbH & Co KG
Triple Desk T500 flasks	Thermo Scientific

Table 1.2 Consumables for electrophysiological measurements

Chemical	**Supplier**
Dimethyl sulfoxide (DMSO)	Thermo Scientific, US
Magnetic stirrer	VWR
Micro hematocrit -capillary tubes	Th. Geyer GmbH & Co. KG
Parafilm	Bemis, US
PTFE-film	GoodFellow GmbH, DE
Silverwire 99.9% 0.5mm 25g	Carl Roth GmbH & Co KG
Thread preparations glasses 50x14mm	Schuett-biotec GmbH

Table 1.3 Software's used

Software	**Manufacturer**
Adobe Illustrator C26	Adobe Systems
Affinity designer	Serif
Origin Pro 8.5, Origin Pro 2022	OriginLab, US
pCLAMP 10.7	Molecular Devices, Inc
R3.6.1, RStudio-1.2.1335	Posit, PBC,

1.3.2 Methods

1.3.2.1 Cultivation of human FlpIn cells

The cell line was cultivated by Maren Reuter and Jessica Klümper at Institute of Biochemistry and Pathobiochemistry, Ruhr University Bochum. A FlpIn cell line expressing PEX5L-Protein A in a stable manner was generated as previously described (Bharti et al. 2011). Cells were cultivated in Dulbecco's modified eagle medium (DMEM) with high glucose, supplemented with 10% (v/v) FCS, 2 mM l-glutamine and 1% (v/v) Penicillin (10 U/ml)/Streptomycin (10 µg/ml). The cells were incubated at 37 °C in a humid atmosphere containing 8.5% CO_2. For maintenance, cells were cultivated in T75 flasks, while for complex isolations they were large scale cultivated in Triple Desk T500 flasks. After the cells attained a confluency of 90%, they were subjected to trypsinization and subsequently harvested by centrifugation at 200×g for 7 min. For each complex isolation, cells from 18 Triple Desk flasks were used. Sedimented cells were frozen in liquid nitrogen and then stored at −80 °C until further use.

1.3.2.2 Isolation of PEX5L complexes

The PEX5L complexes were isolated and analysed by Maren Reuter and Jessica Klümper at Institute of Biochemistry and Pathobiochemistry, Ruhr University Bochum and kindly provided to us for reconstitution and electrophysiological characterization. The FlpIn PEX5L-Protein A cell line was cultivated in Triple Desk flasks and harvested using the previously described method. The pellet was resuspended in a lysis buffer consisting of 0.2 M HEPES, 1 M potassium acetate, 50 mM magnesium acetate, pH 7.5. The ratio of buffer to pellet was 20 ml per 10 g. Additionally, the lysis buffer was supplemented with protease inhibitors including 8 mM Antipain, 0.3 mM Aprotinin, 1 mM Bestatin, 5 mM Leupeptin, 15 mM Pepstatin, 10 mM Chymostatin, 1 mM Phenylmethylsulfonyl fluoride (PMSF), 5 mM sodium fluoride, and 1 mM Benzamidine hydrochloride. Lysis was performed using glass beads with a diameter of 0.5 mm, with a ratio of 3 grams of beads for 1 g of cell pellet. Subsequently, the beads were separated from the lysate using centrifugation at 1500g for 5 minutes, utilizing the SX4750A rotor (Beckman Coulter), while maintaining a temperature of 4 °C. The obtained lysate underwent ultracentrifugation at 100,000g and a temperature of 4 °C for 1 hour using the SW 41 Ti rotor (Beckman Coulter). The resulting supernatant was utilized for isolating cytosolic complexes. On the other hand, the pellet was resuspended in lysis buffer for 1 hr at 4 °C, similar to the previous procedure, with the inclusion of an additional 5% glycerol and 1% digitonin. The sample was subjected to a second centrifugation at 100,000g and 4 °C for 1 hr and the resulting supernatant was utilized for the isolation of membrane protein complexes. The protein content of both supernatants was quantified, and each supernatant was incubated with IgG-Sepharose beads (13 µl per 10 mg protein)

for 18 hrs at 4 °C. The IgG-Sepharose was centrifuged at 1500 g for 5 min at 4 °C using SX4750A rotor. After centrifugation, the sedimented IgG-Sepharose was washed with a wash buffer consisting of 0.2 M HEPES, 1 M potassium acetate, 50 mM magnesium acetate, and pH 7.5. The wash buffer was supplemented with 8 mM Aprotinin, 1 mM Bestatin, 5 mM Leupeptin, 15 mM Pepstatin, and 1 mM PMSF. For membrane complexes, the wash buffer contained 0.2% digitonin, while for cytosolic complexes, no detergent was added to the wash buffer. The Sepharose that had undergone sedimentation was resuspended in less than 1 ml of the appropriate wash buffer and subsequently transferred to a centrifugation column known as "Mobicol F," which was equipped with a 35 µm filter manufactured by Mobitec. The beads were washed for ten times using the appropriate washing buffer. Each wash involved centrifugation at 100g at 4 °C for 30 s. To facilitate elution using the TEV protease, a total of 110 units of proteases were added per 100 µl of IgG-Sepharose. The mixture was then incubated for 2 hrs at 16 °C and 350 rpm. The Sepharose was subjected to centrifugation at 100g and 4 °C for 1 min, resulting in sedimentation. The resulting supernatant was collected and referred to as the eluate. The Sepharose resin underwent two washes using a volume of the corresponding wash buffer that was twice the volume of the column. The resulting washing fractions were then mixed with the eluate.

1.3.2.3 Preparation of PEX5L proteoliposomes

The PEX5L associated membrane complexes were reconstituted in liposome consisting of 70% l-a-phosphatidylcholine and 30% l-a-phosphatidylethanolamine. The lipid stocks were prepared in methanol/chloroform mixture, followed by drying under a continuous flow of nitrogen to a final concentration of 12 mM. In order to produce unilamellar vesicles, dried lipid was resolubilized in a buffer solution containing 150 mM KCl and 10 mM HEPES at a pH of 7.4. Subsequently, these resolubilized lipid films were subjected to a series of seven freeze-and-thaw cycles. The lipid vesicles that were acquired were subjected to extrusion using a polyvinylidene fluoride (PVDF) filter with a pore diameter of 200 nm. These extruded vesicles were used for protein reconstitution. In order to reconstitute PEX5L complexes, liposomes were subjected to partial solubilization using a solution containing 0.2% Digitonin, 0.5% DDM, and 3× digitonin buffer. The resulting mixture was then incubated for 5 min on ice. The purified SEC fraction of hPEX5L was introduced into solubilized liposomes and afterwards subjected to a 30-min incubation on ice, facilitating the spontaneous insertion of proteins. Then the removal of detergent from the mixture through the addition of 80 µl of Calbiosorb per 50 µl of lipids escalated the incorporation process. The Calbiosorbs were prepared by sequential washing with methanol, followed by a wash with 150 mM KCl and 10 mM HEPES buffer at pH 7.4. The sample mix was supplemented with Calbiosorb and afterwards incubated on a rotating

disc for 2 hrs at a of 4 °C. Following this incubation period, the proteoliposomes were removed from the Calbiosorb.

1.3.2.4 Liposome flotation assay and sodium carbonate extraction

In order to evaluate the co-migration of proteins with liposomes, we utilized density gradient flotation, employing non-ionic Histodenz as previously outlined in Truscott et al. (2001). By employing this methodology, it is possible to isolate membrane-unbound proteins from both liposomes and membrane-bound proteins. Liposomes, whether empty or containing incorporated protein, exhibit migration towards regions characterized by lower density, whereas protein that is not bound remains within the loading fraction. A polycarbonate test tube was used to create a stratified arrangement of proteoliposomes mixed with Histodenz. The addition of Histodenz resulted in a final concentration of 40%. Subsequently, discrete layers with concentrations of 20%, 10%, 5%, and 2.5% were sequentially added on top of the proteoliposomes base layer. Each layer consisted of 800 µl and was suspended in liposome buffer. The density gradient underwent centrifugation using a swinging bucket rotor (Optima XPN-100 with Sw60Ti rotor, 45k rpm, 4°C, 1 h). Subsequently, it was fractionated in 444.4µL increments, starting from the top and moving towards the bottom. The fractions were subjected to TCA precipitation with 10% TCA and subsequently analysed using SDS-PAGE PAGE and immunoblotting in order to observe and distinguish the protein that was either bound or unbound. For sodium carbonate extraction, proteoliposomes containing interfaces of the Histodenz layers were collected. These liposomes were then incubated with ice-cold 20 mM Na_2CO_3 for 30 mins while being kept on ice. Subsequently, the liposomes were centrifuged at 150,000g and 4 °C for a period of 30 mins. The total amount of pellets and supernatants obtained were assessed by SDS-PAGE or western blot.

1.3.2.5 Electrophysiological characterization

1.3.2.5.1 Principle of Electrophysiology

The cell membrane consists of a lipid bilayer that separates ions in the extracellular space from the charged proteins and ions in the cytoplasm. Lipid membranes are very good insulators, but cell membranes are made up of a mix of proteins and lipids. There are a lot of proteins classified as ion channels or translocon that cross the barrier and let charge move through them. The high resistance of the membrane is lowered by these proteins. For electrophysiological characterization of such proteins, biological membranes, as well as entire cells, can be simplified into an analogous circuit model like that of a leaky capacitor (Naumowicz and Figaszewski 2013). The electric equivalent circuit consist of a combination of resistors and capacitors. The circuit is composed of a series connection of

resistor R, which represents the combined resistance of the electrical setup (headstage and electrodes) and the electrolytes denoted by $R_{electrodes+electrolytes}$. Additionally, there is a parallel connection of capacitance $C_{membrane}$ and resistor $R_{membrane}$, which represent the capacitance and resistance of a lipid bilayer. Lastly, there is a resistor $R_{channel}$, which represents the resistance (inverse conductance 1/G) of a reconstituted ion channel (Figure 1.4A). The $R_{electrodes+electrolytes}$ are relatively minor compared to the $R_{channel}$ in a series connection, so it may be disregarded. On the other hand, the $R_{membrane}$ is significantly larger than the $R_{channel}$ in a parallel connection, allowing it to be discarded. Consequently, this results in a simplified circuit configuration (Figure 1.4B). The amount of current passing through a capacitor is influenced by variations in the applied potential. Consequently, immediately after establishing a constant holding potential U, the capacitor's $C_{membrane}$ conducts for a duration of several hundred milliseconds (ms) until the current decreases exponentially and approaches zero. The current, denoted as I, is traversing via the channel. This allows for the direct determination of the channel's conductance, denoted as G, by employing Ohm's first law.

$$U = R * I = \frac{I}{G} <=> G= \frac{I}{U} \quad (1)$$

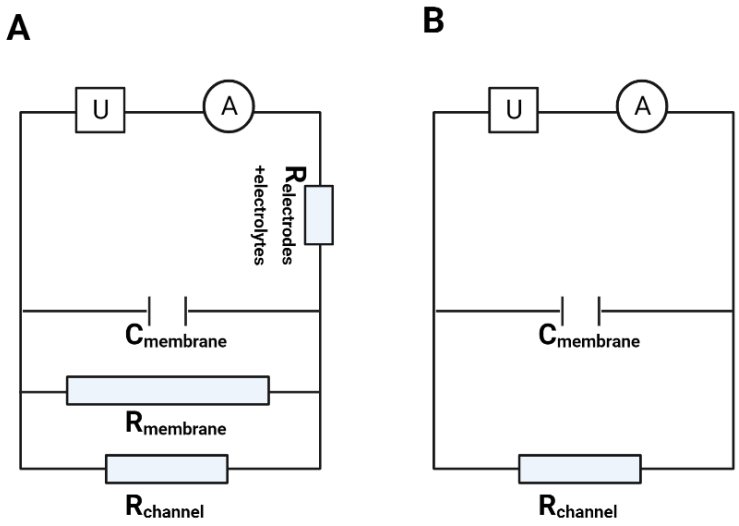

Figure 1.4 Equivalent circuit diagram of an ion channel in a biological membrane. (A) complex (B) reduced. U represents the membrane potential or voltage and A represents current generated in an electric circuit (Figure modified from Denkert 2018).

1.3.2.5.2 Assembly of the Chamber

The chambers are assembled as described in Bartsch, Harsman, and Wagner 2013. The bilayer chamber is comprised of two half teflon chambers, each containing a circular opening on its respective side. A single opening in each half-chamber was sealed using a glass plate, which was secured in place using parafilm and a tightly fitted polytetrafluoroethylene (PTFE) ring. The half chamber was initially placed inside the metal cage facing the glass outside. The chamber was coated with vacuum grease and a PTFE film with a hole of needle-tip dimensions was affixed to the other chamber within the metal cage. The aperture was formed through a meticulous process of puncturing the PTFE film with a needle and subsequently punching it with three discharges from a self-constructed spark gap. The other half of the chamber was placed into the metal cage with the glass facing outside. In this configuration, the non-glass surfaces of both half-chambers are positioned opposite to each other and securely sealed using vacuum grease and a PTFE film. The setup is then closed and tightly secured using a metal screw ring. To mix the buffer solution, magnetic stir bars measuring 2 mm in length are placed within each half-chamber. These stir bars interact with the magnetic stirrer located beneath the metal cage. Then, L-α-Phosphatidylcholine (SIV-PC) dissolved in decane (lipid concentration of 3 mg in 50 µL decane) is applied onto the PTFE film using a flexible syringe, and incubated for 20 minutes. Afterwards, 3 mL of electrophysiological buffer was added into each chamber and the bilayer was formed by pipetting up and down the buffer as described by Bartsch, Harsman, and Wagner (2013).

1.3.2.5.3 Setup and software used

Ag/AgCl electrodes were fabricated by soldering silver wire with a diameter of 1 mm to the gold connectors. The Ag electrodes can be chlorinated by immersing them in a solution of 12% NaClO for a minimum duration of 2-6 hours. The electrodes were placed within glass capillary tubes and subsequently immersed into a 2M KCl-Agar bridge. Then, Electric recordings were performed using Ag/AgCl electrodes that were connected to a CV-5-1GU headstage and afterwards to a Geneclamp 500B current amplifier (Molecular Devices, US). The currents were converted into digital format using a Digidata1440 (AD/DA) converter and recorded with a computer utilizing the software AxoScope 10.3 to record current traces at constant holding potentials or Clampex 10.3 software for recording voltage ramps. The electrode at the trans compartment was used as a reference electrode and the electrode cis compartment was connected to the ground.

1.3.2.5.4 Fusion of Proteoliposomes

Proteoliposomes were added in proximity to the bilayer within the cis compartment of the chamber using a syringe. A gradient of salt concentration was created across the membrane by placing a high

concentration of salt in the cis compartment and a low concentration of salt in the trans compartment. This gradient facilitated the fusion of proteoliposomes with the bilayer through osmotic forces (Figure 1.5) (Zimmerberg, Cohen, and Finkelstein 1980; Cohen, Niles, and Akabas 1989). Following the fusion process, the buffer present in each chamber was subjected to perfusion with a volume equivalent to 60 ml, which is equal to 20 chamber volumes. This perfusion was carried out using a standard buffer solution containing (250 mM KCl or 20 mM KCl), 10mM MOPS, pH7.0, with the aim of establishing precise salt concentrations. In order to increase fusion rates, it is possible to introduce $CaCl_2$ into the cis compartment at concentrations ranging from 10 to 20 mM.

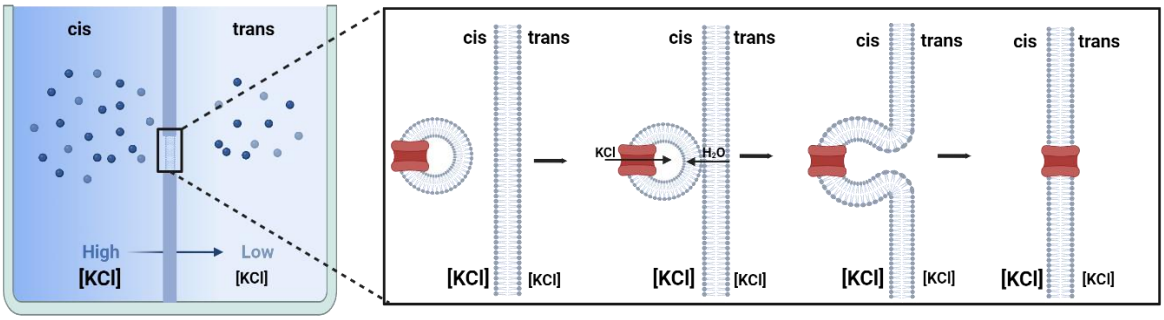

Figure 1.5 Insertion of translocon by osmotically driven fusion of proteoliposomes to the bilayer in electrophysiological setup.

1.3.2.5.5 Conductance

Fusion of an open channel on the bilayer leads to ion flux and current can be recorded with respect to the applied voltage. By applying Ohm's law (Brown and Musil 2004), the conductance of a channel at a certain voltage can be determined by dividing the recorded current by the applied voltage. This serves as an indication of the approximate size of a single pore or the collective size of multiple pores. The diameter of a cylindrical pore can be determined by Hille equation by considering a pore as a cylinder with length L, the resistivity of the buffer ρ and conductance of the channel G (Eaton 1985; Smart et al. 1997). The equation to calculate pore size is

$$d = 2 * G * \rho * \left(\frac{1}{4} + \sqrt{\frac{1}{16} + \frac{L}{G*\rho*\pi}}\right) \quad (2)$$

The value of L can vary, such as 0.5 nm for a narrow region of limited length or 5 nm for a cylindrical structure that spans over a membrane. The resistivity (ρ) of the electrophysiological buffer (250 mM

KCl, 20 mM MOPS-Tris, pH 7.0) is around 50 Ω cm. However, when electrolytes are subjected to intense electrical fields within a pore, their resistivity increases significantly. A correction factor of 5 has been calculated for such a narrow channel. The open or closed states of a particular channel can also be determined. In order to achieve this objective, the open probability (P_o) was determined by dividing the mean current (I_{mean}), which is normally measured for a minute by the maximum current, denoted as I_{max}, refers to the highest amount of electric current recorded for a pore.

$$P_o = \frac{I_{mean}}{I_{max}} \quad (3)$$

1.3.2.5.6 Reversal Potential and Ion Selectivity

The presence of an ion concentration gradient across the membrane give rise to a membrane potential. Membrane channels facilitate the movement of ions across the membrane in accordance with their respective concentration gradients, albeit at varying rates. The electrochemical membrane potential aims to achieve equilibrium in ion concentration on both sides of the membrane. The applied potential required to completely stop the net flux of ions through a membrane is termed as reversal potential. The calculation of the equilibrium potential (U_{rev}), which arises from the asymmetry caused by the transportation of a single ion species such as Na+, can be determined by using the Nernst equation.

$$U_{rev} = \frac{RT}{zF} \ln \frac{[C]_{out}}{[C]_{in}} \quad (4)$$

Where U_{rev} is the reversal potential, R is the universal gas constant (R = 8.314 J K^{-1} mol^{-1}), T is the temperature, z is valency of the respective ion, F is Faraday's constant (F = 96 485.332 C mol^{-1}) and $[C]_{out}$ and $[C]_{in}$ is ion concentration on outside and inside of the membrane respectively. Within a biological membrane, numerous ions coexist concurrently. In general, it is unlikely that there will be a voltage at which current for all ions are zero. In case there are more than one ion, we used the Goldman-Hodgkin-Katz (GHK) equation, which is derived from the Nernst-Planck equation. The resting potential, VR, is established as a voltage at which the net total of all ion currents is equal to zero. Then, determining the reversal potential relies on the concentrations of salts and the channel's relative ion

selectivity. This value can be computed by considering the ion concentrations and their permeability, utilizing the Goldman-Hodgkin-Katz equation (Goldman 1943; Hodgkin and Katz 1949).

$$U_{rev} = \frac{RT}{F} \ln \frac{\sum P_c[C]_{out} + \sum P_a[A]_{in}}{\sum P_c[C]_{in} + \sum P_a[A]_{out}} \quad (5)$$

where [C] and [A] are the concentration of cations and anions respectively and P_c or P_a are the permeability cations or anions and in and out refers to the inside and outside of the membrane respectively. In this thesis, a potassium chloride (KCl) buffer is employed, wherein the salt concentrations on the cis and trans sides of the channel are different unless specified in the experiments. The equation for determining the relative ion selectivity in this case is

$$P_K^+ : P_{Cl}^- = \frac{[Cl^-]_{trans} - \exp\left(\frac{U_{rev}F}{RT}\right) * [Cl^-]_{cis}}{\exp\left(\frac{U_{rev}F}{RT}\right) * [K^+]_{trans} - [K^+]_{cis}} \quad (6)$$

Where U_{rev} is the measured reversal potential, P_K^+ and P_{Cl}^- are the permeabilities of potassium [K^+] or chloride ions [Cl^-] with [K^+] and [Cl^-] respective ion concentrations, and cis and trans correspond to the two sides of the bilayer.

1.3.2.5.7 Data analysis

we utilized a sophisticated data analysis tool to remove potential biases associated with manual analysis of electrophysiological recordings. This tool was developed by Inder Tecuapetla-Gómez from the Institute for Mathematical Stochastics at the University of Göttingen, Germany. It is based on an estimator known as SMUCE (Stepwise Multiscale Confidence Intervals for Nonparametric Functional Estimation) and implemented in the R-package "stepR" (Hotz et al. 2013). In essence, the SMUCE method aims to recreate the original clean data by considering the estimated filter impact, so effectively eliminating the presence of white noise in the assumed pre-filtered data. Afterwards, the algorithm fits constant segments to the data that has been denoised. This reconstruction process facilitates the identification and analysis of conductance changes, dwell times, and the dynamic behaviour of translocation pores. This routine automates the detection of gating events and the calculation of dwell periods. The results of this reconstruction routine were exported in the form of

two .txt files which are the dwell time table and the list of gating events. These exported data files were further subjected to analysis using OriginPro2022.

1.4 Results

1.4.1 Purification of PEX5L-containing membrane complexes

In order to identify the pore forming activity in the human peroxisomal matrix protein import machinery, a methodology (Section 1.3.2.2) was developed to selectively isolate PEX5L as the hypothesized core element of the pore from analysis of the yeast peroxisomal translocation machinery (Meinecke et al. 2010a; Montilla-Martinez et al. 2015). The long isoform of PEX5 was selected as it is involved in both PTS1 and PTS2 import and contains a PEX7 binding site as well (Walter and Erdmann 2019; Farré et al. 2019). To achieve this objective, a FlpIn cell line was generated in which Protein A-tagged PEX5L was produced with a TEV cleavage site positioned between the tag and the protein PEX5L. Membranes were solubilized by mild digitonin treatment to maintain the integrity and interaction of integral membrane protein complexes. Then, PEX5L-complexes were purified through affinity purification using IgG Sepharose, followed by elution of the complexes by TEV protease cleavage (Figure 1.6A). SDS-PAGE analysis of the eluates from cytosolic and membrane fractions demonstrated a clear differentiation in the polypeptide composition of the PEX5L-interacting proteome (Figure 1.6B and C). The membrane-associated polypeptide with a molecular weight of 60 kDa, which is mostly related with PEX5L, probably represents PEX14. The PEX5L membrane eluate was shown to contain several membrane-bound peroxins which are known to be part of the import of cargo and export of receptors in the translocation machinery, specifically the PTS2 receptor PEX7, PEX14 with other components of docking complex PEX13, PEX12, and PEX1. To our surprise, PEX6, which is part of a functional AAA ATPase complex with PEX1, could not be detected through immunoblotting (Figure 1.6D). A number of polypeptides, approximately 80, 50, 40, and 30 kDa in size, cofractionate with the cytosolic PEX5L protein. While this study did not specifically investigate the identity of cytosolic binding partners, it is reasonable to hypothesize that these binding partners likely consist of numerous cargo proteins that have a strong affinity for the PTS1 receptor. This finding is additionally supported by immunoblotting, which reveals the interaction between catalase and the PTS1 receptor (Figure 1.6D). We also tried to detect a PTS2 protein thiolase, but couldn't detect it in the cytosolic fraction. In the membrane eluates no cargo proteins were discovered.

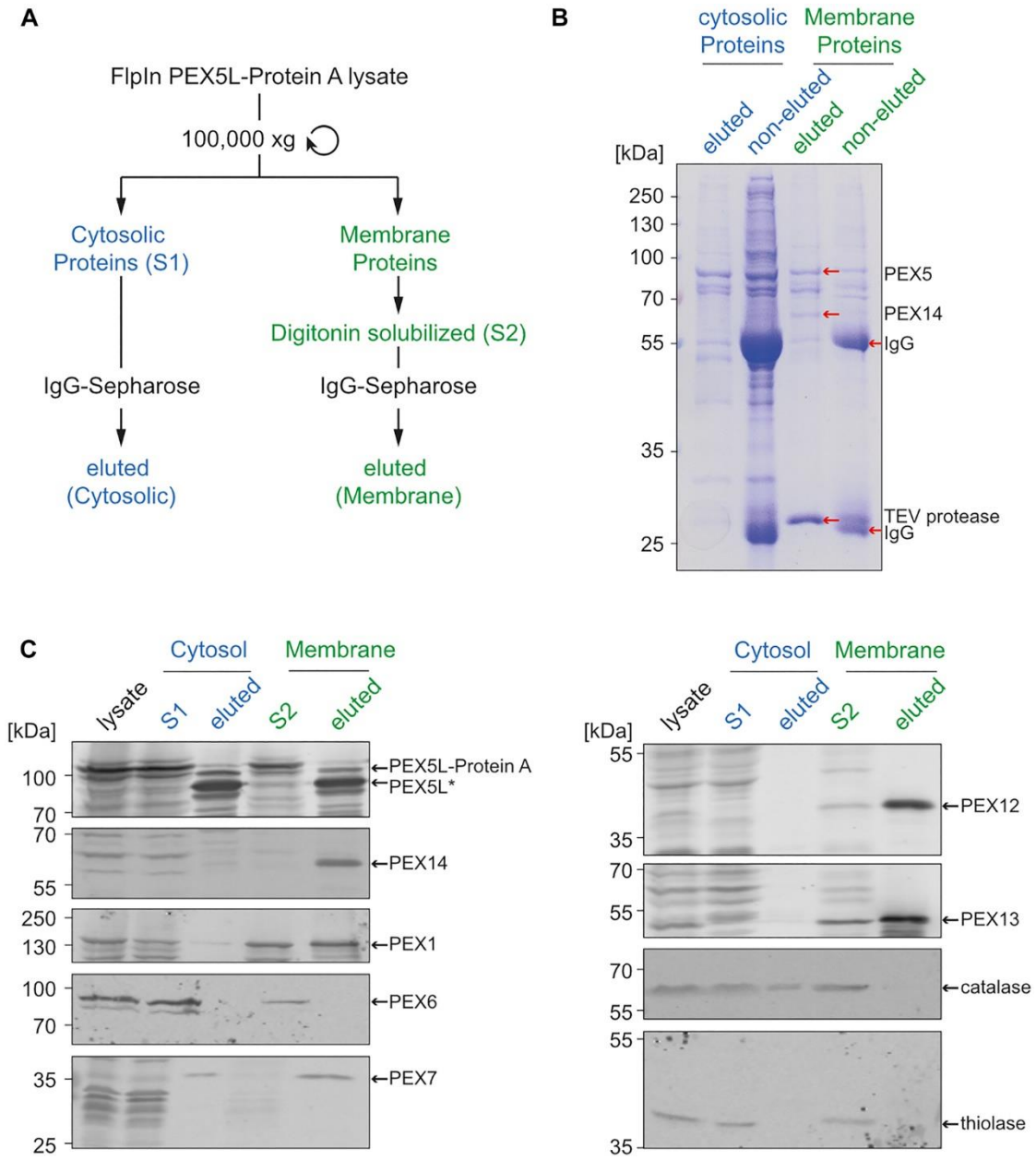

Figure 1.6 Purification of PEX5-containing membrane complexes. (A) Description of the procedure for isolating cytosolic and membrane-bound subcomplexes of the Protein A-fused PEX5L in an affinity-purification system. (B) Visualization of protein bands on SDS-PAGE stained with Colloidal Coomassie in the eluates obtained after TEV-protease treatment of cytosolic and membrane-bound PEX5L samples. To assess the efficiency of digitonin-solubilization and TEV-proteolytic cleavage, the IgG-Sepharose column material was subjected to analysis with an SDS-containing buffer to detect any remaining proteins. (C) Immunoblot assessment of the purification process, wherein lysates, input samples (S1 and S2), and the corresponding eluates were probed for the presence of peroxisomal import machinery components and matrix proteins using specific antibodies (Purification and analyses were done by Maren Reuter and Jessica Klümper, figure is from Ghosh et al. 2023)

1.4.2 Reconstitution of PEX5L eluates into liposomes

The TEV eluate obtained from solubilized membrane complexes was utilized in a mixed detergent mediated reconstitution technique to reconstitute integral membrane proteins from PEX5L eluate complexes into liposomes. The incorporation success was verified through flotation assay and carbonate extraction resistance experiments and visualized through immunoblotting (Figure 1.7A). PEX5 and PEX14 were employed as marker proteins. We observed incorporation of both PEX5 and PEX14 in the liposomes (Figure 1.7B and C).

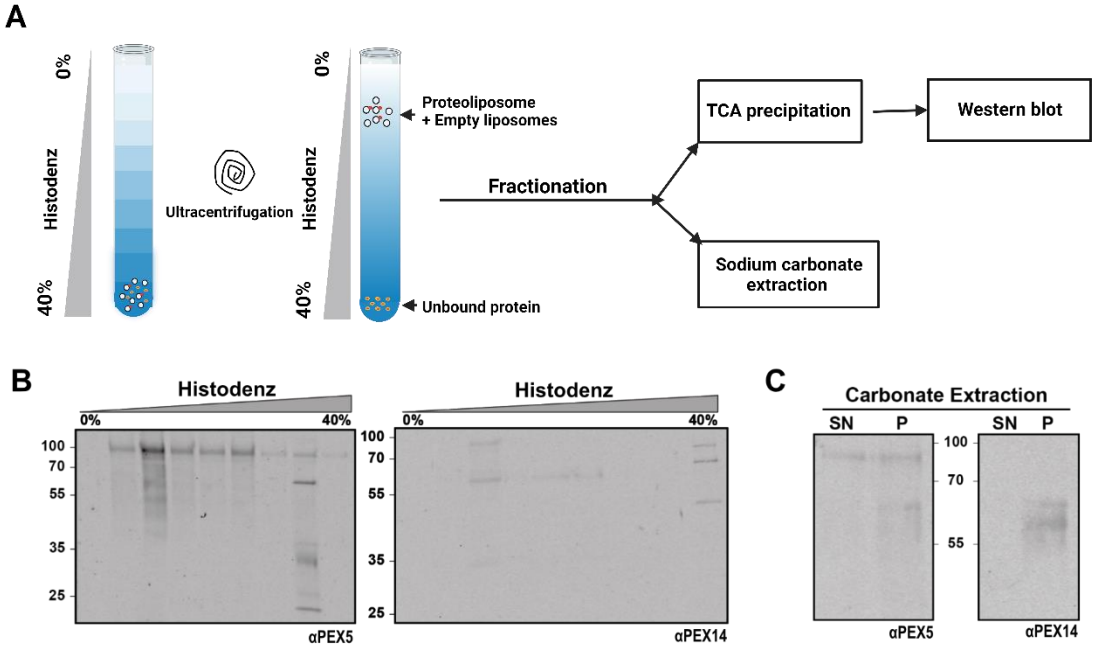

Figure 1.7 Reconstitution of affinity-purified membrane-bound subcomplexes of human Protein A-fused PEX5L into liposomes. (A) Diagram illustrating the liposome flotation assay in a histodenz gradient, followed by the analysis of the proteoliposome mixture through co-flotation and assessment of sodium carbonate resistance. Created using Biorender.com (B) Immunoblot analysis of flotation experiments against indicated antibodies. (C) Immunoblot analysis of carbonate extraction assays of PEX5 containing proteoliposomes against indicated antibodies (Figure from Ghosh et al. 2023).

1.4.3 PEX5L complex forms pore and displays yeast PTS1 pore

The pore-forming activity of proteo-liposomes containing the PEX5-complex was subsequently assessed using the PLB approach, as described in other studies (Denkert et al. 2017; Vasic et al. 2020). Electrophysiological characterization was performed together with Niels Denkert. We observed rapid fusion of ion channels upon addition of the proteoliposomes. During analyses, we found that the

electrophysiological parameters were very dynamic (Figure 1.8). The channels exhibited voltage-dependent gating, displaying a wide range of conductance states ranging from 40 to 550 pS as shown in the current trace at +60 mV and its respective conductance state histogram (Figure 1.8A and B). Under asymmetrical salt conditions (250 mM KCl, cis; 20 mM KCl, trans), voltage ramps were measured from -50 mV to +80 mV. Voltage ramp displays variable reversal potentials of +18.1 mV and +27.8 mV, that corresponds to mild ion selectivities of $P_{K^+} : P_{Cl^-}$ = 2.3:1 and 3.8:1 respectively, which showed variability in accordance with the open conformation of the channel (Figure 1.8). It is worth mentioning that previous studies have reported the presence of conductance states, dynamic gating, and mild but diverse ion selectivity in the PTS1 specific import channel found in yeast, with Pex5 and Pex14 being the central components (Meinecke et al. 2010a). In order to eliminate the possibility that the observed heterogeneity is a result of multiple channels fused together exhibiting distinct properties, we decreased the concentration of proteoliposomes prior to their fusion with the bilayer. As a result, the incidence of channel fusions was significantly lower; nonetheless, the fusions that did occur were primarily single channels.

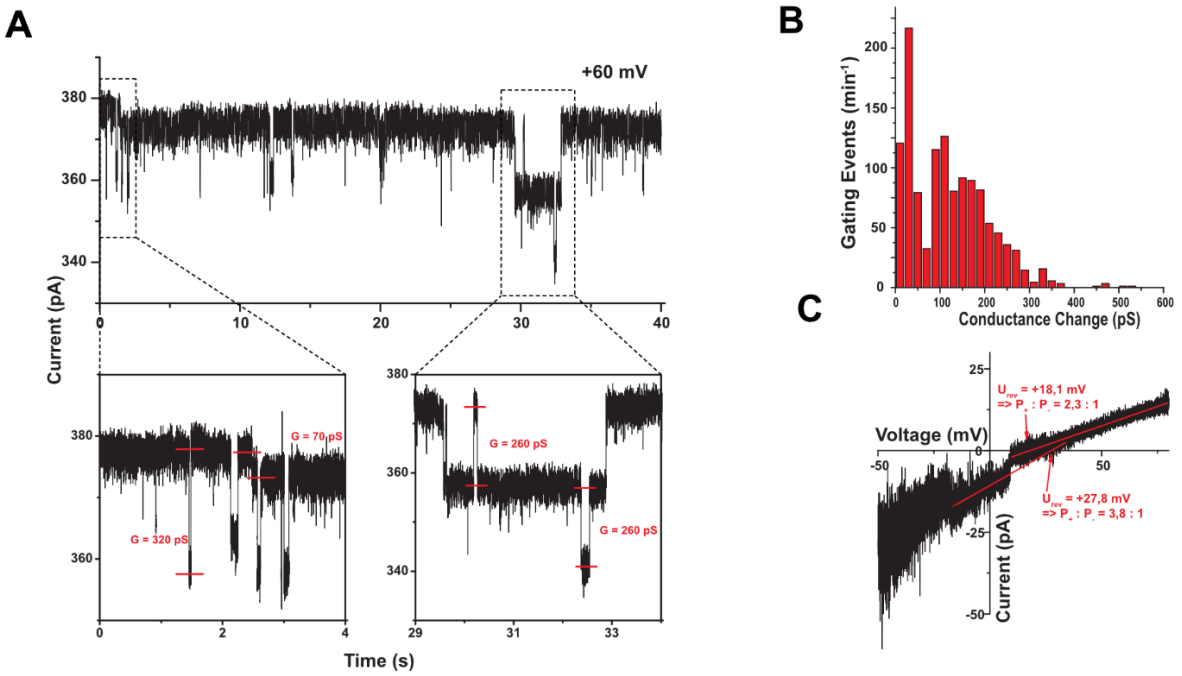

Figure 1.8 Pore forming activity of PEX5L complexes. (A) Current trace recordings of PEX5L complexes embedded in lipid bilayers in symmetric buffer conditions, at specified holding potentials (+60 mV). The zoomed-in plots reveal distinctive voltage-dependent gating events marked by changes conductance changes. (B) Histogram displaying conductance states resulting from voltage-dependent gating of PEX5L complexes, derived from current recordings at different holding potentials, and based on a minimum of three separate fusion events. (C) Current-voltage relationship for a PEX5L complexes in asymmetric buffer conditions. Linear regression analysis provides the reversal potential, which

serves as the foundation for the indicated selectivity of cations over anions, calculated using the Goldman-Hodgkin-Katz equation (Figure from Ghosh et al. 2023).

1.4.4 Low and high conductance state channel population

Through a more in-depth examination of the single-channel features, we found presence of two distinct states in our channel population which is shown in Figure 1.9. One channel population displayed very small gating events (Figure 1.9A) with relatively low conductivity of approximately 75 pS, exhibiting infrequent occurrences of higher conductance of over 400 pS which corresponds to a pore size of around 2 nm (Figure 1.9B and C). The second channel population showed gating events prominently consisting of small conductance states, but also demonstrated a higher occurrence of bigger gating events that corresponded to conductance states ranging from 400 to 900 pS which corresponds to a maximal pore size of approximately 3 nm (Figure 1.9Eand G). Both the channel population showed still mild yet changing ion selectivities (Figure 1.9D and H).

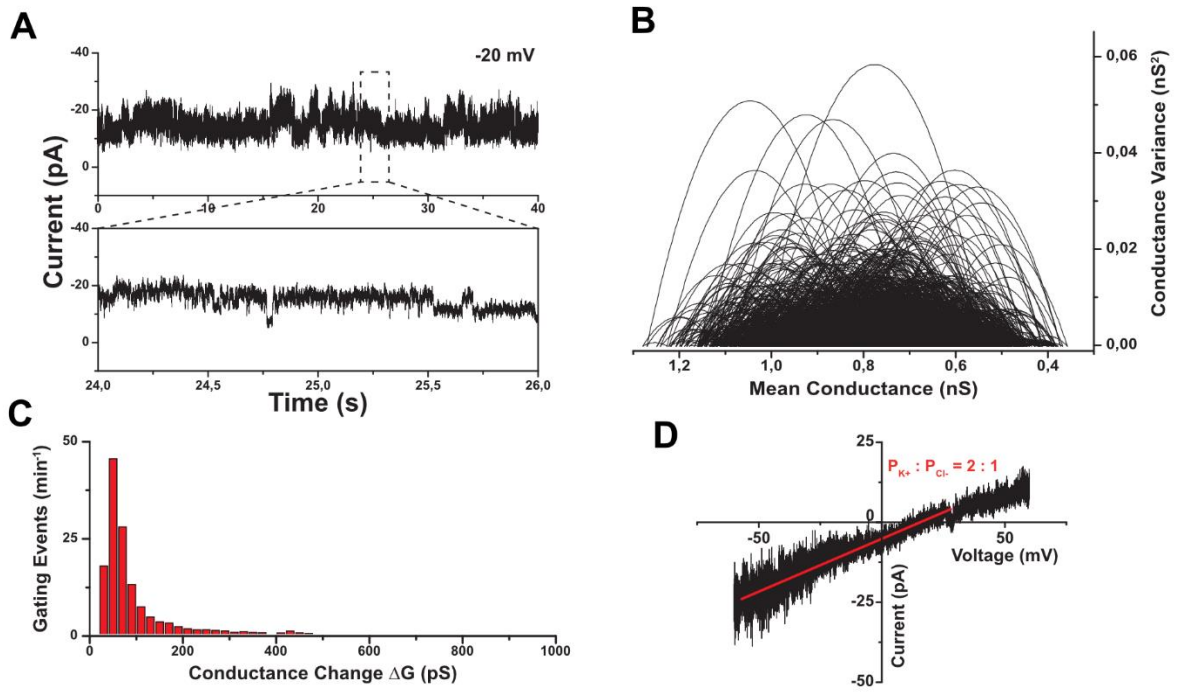

Figure 1.9 continued on next page

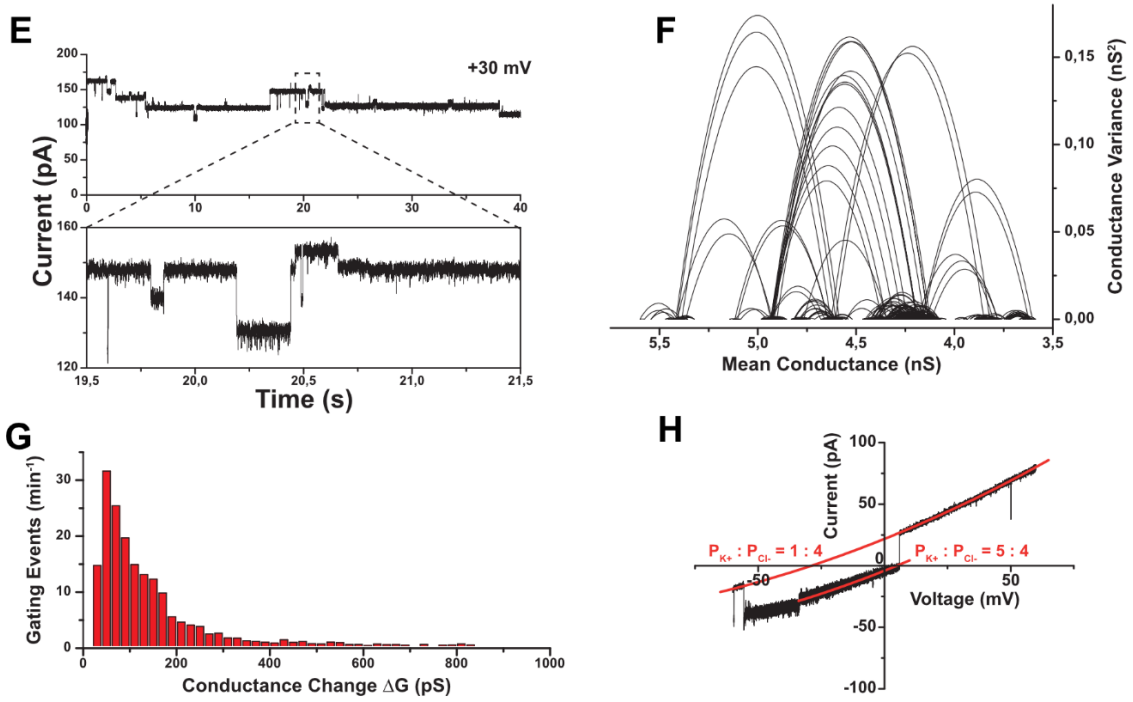

Figure 1.9 Electrophysiological characteristics of channels displaying mainly low (A-D) and high (E-H) conductance state gating. (A) Current recording of a channel primarily exhibiting low conductance state gating in symmetrical buffer conditions, at indicated holding potential. (B) Graph illustrating the relationship between mean conductance differences and their corresponding variances, derived from the current trace in (A). (C) Conductance state distribution histogram depicting voltage-dependent gating of PEX5L complexes, generated from current recordings at various holding potentials and based on at least three independent fusion events. (D) Current-voltage relationship of PEX5L complexes recorded in asymmetric buffer conditions, highlighting the indicated cation-to-anion selectivity. (E) Current trace of channel displaying predominantly small but frequent high conductance state gating under symmetrical buffer conditions, at indicated holding potential (F) Plot of mean conductance differences against their variance of the corresponding current trace (E). (G) Conductance state histogram illustrating the voltage-dependent gating of PEX5L complexes, using current recordings at different holding potentials and data from a minimum of three separate fusion events. (H) Current-voltage relationship of PEX5L complexes recorded under asymmetric buffer conditions, with the indicated cation-to-anion selectivity (Figure from Ghosh et al. 2023).

1.4.5 Cargo mediated activation of pore in PEX5L complex

In order to establish a condition where the expected import pore is in proximity with the cargo molecules, we conducted an incubation process using PEX5L complexes reconstituted in liposomes. Proteoliposomes were incubated with PEX5-PEX7-Cargo complexes, which were obtained from the soluble fractions of cell lysates that were free of membranes (Figure 1.6B, lane1-eluted). Following incubation with the soluble PEX5L-complex, the proteoliposomes were subjected to electrophysiological characterization. The measured channel parameters were found to be similar to

those previously seen for the PEX5L complexes in a condition of high conductance state (Figure 1.9). The voltage-dependent gating was shown to exhibit a distinct small conductance state of approximately 75 pS. Furthermore, bigger gating events were also seen, corresponding to conductance levels ranging from 400 to 1000 pS, which corresponds to a maximal pore size of 3.3 nm (Figure 1.10A and B). But we still observed mild ion selectivity which underwent alterations in response to gating (Figure 1.10C).

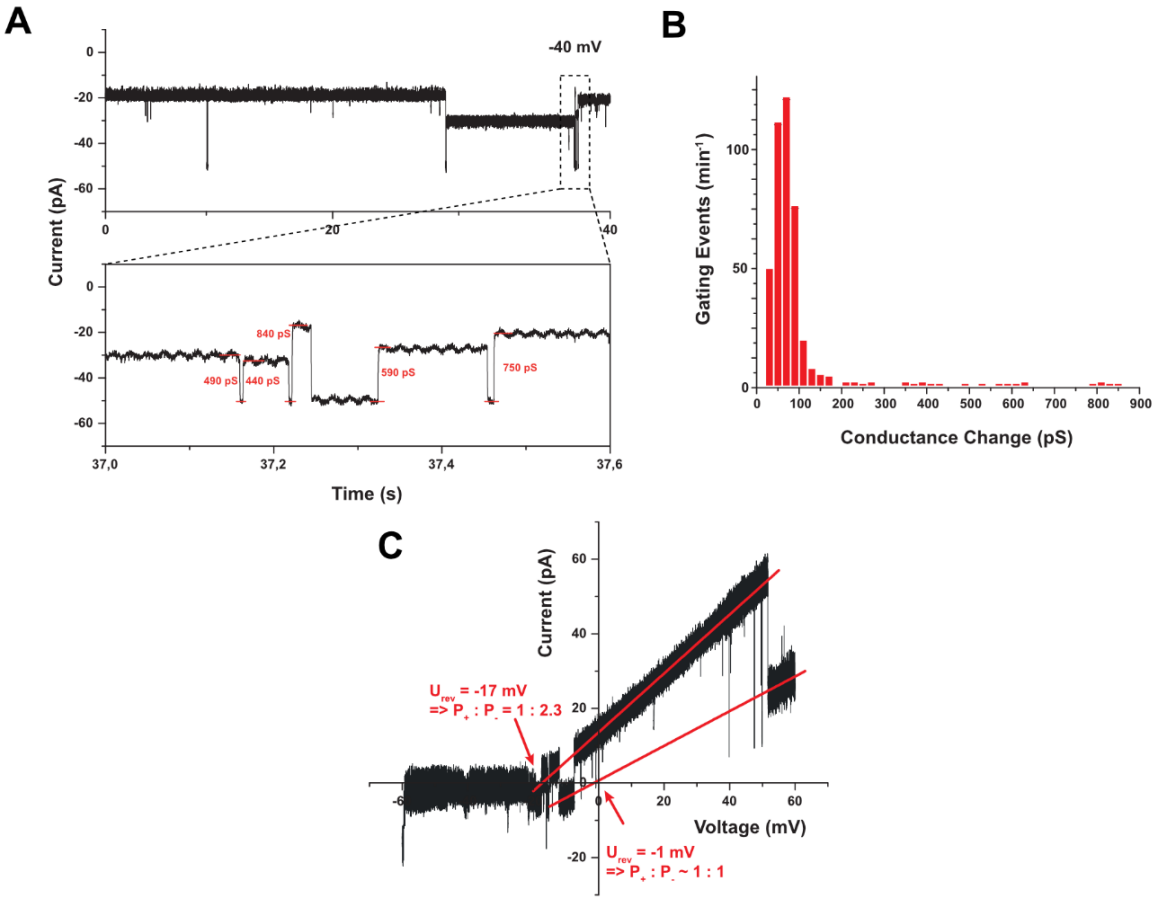

Figure 1.10 PEX5 complex activity is cargo sensitive. (A) Recorded current traces of PEX5L complexes exposed to soluble PEX5-cargo complexes fused to lipid bilayers. The measurements were conducted under symmetrical buffer conditions and at the holding potential values indicated. Zoomed-in plots reveal pronounced voltage-dependent gating events with indicated conductance state changes. (B) Histogram illustrating the distribution of conductance states resulting from the voltage-dependent gating of PEX5L complexes activated by cargo. The data is extracted from the current recordings conducted at various holding potentials and derived from a minimum of three independent fusion events. (C) Current-voltage relationship for a cargo-activated PEX5 complex under asymmetric buffer conditions. The graph highlights the indicated reversal potentials and the calculated cation-to-anion selectivity (Figure from Ghosh et al. 2023).

1.4.6 Comparison of gating events

We performed analyses of conductance state distribution histograms of PEX5L complexes, both in the absence and presence of soluble cargo containing substrates. Comparing the different conductance state histograms revealed that the addition of cargo complexes induces a shift in the complex activity towards a configuration characterized by high conductance state (Figure 1.11). We compared the relative abundance of low and high conductance state channels before and after incubation with cargo in PEX5L membrane bound complexes. As a result, following incubation with the cytosolic cargo fraction, no channel activity exhibiting just low conductance states was found (Figure 1.11B).

In order to conduct a specificity test and eliminate the possibility of nonspecific contamination occurring during the purification procedures, fusion experiments were conducted using all of the samples utilized. While membrane-integrated PEX5L complexes exhibited channel fusions in the absence and presence of soluble cargo complexes, no fusion events were detected when the eluate of a mock Protein A affinity purification was added, derived from cell lines expressing untagged wild type PEX5L (Figure 1.11C). The electrophysiological measurements were carried out under two conditions: in the absence and presence of soluble cargo, as well as when only soluble cargo complexes were used. However, no channel activity was found (Figure 1.11C). This confirmed that our previous measurements were indeed specifically detecting a human peroxisomal translocon involved in protein import rather than an unrelated contaminant. In summary, the findings indicate that the human PEX5L complexes possess the ability to generate pores. Given that the incubation of cargo complexes with membrane-integrated PEX complexes resulted in a discernible shift in activity, with only the high conductance state complex being observable, one may be inclined to hypothesize that this state signifies a conformation of the complexes that is actively involved in transport.

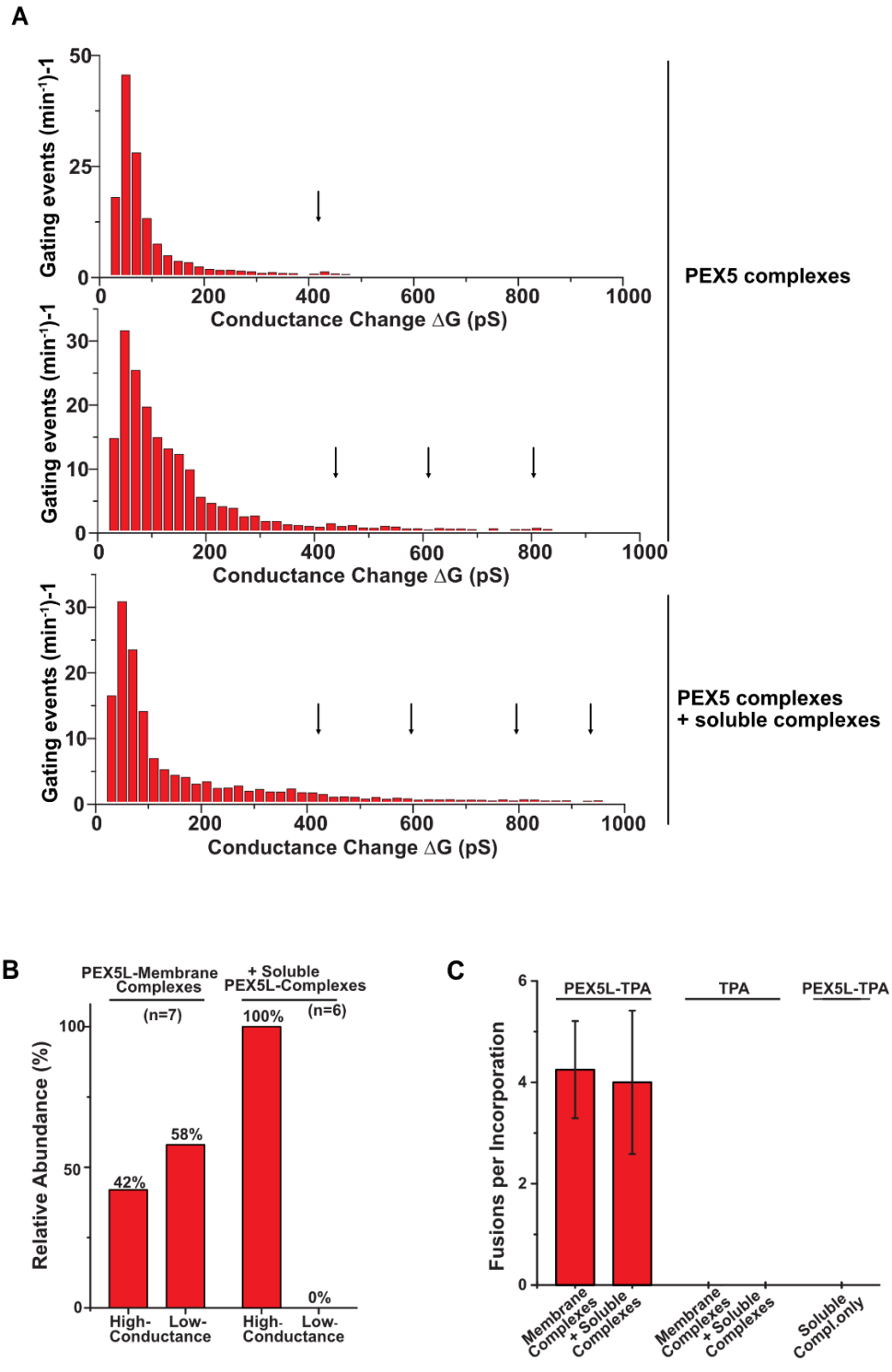

Figure 1.11 Cargo dependent changes in PEX5L activity. (A) Histograms depicting conductance states of PEX5L complexes in two sets of panels: the upper two panels represent complexes in the absence of PEX5L-cargo complexes, and the lower panel represents complexes in their presence. Arrows indicate the increasing conductance states. Conductance state data was collected from current recordings at various holding potentials and based on at least three different channel fusions. (B) Statistical representation of the relative abundance of channels displaying either predominantly small conductance states or also frequent larger conductance states, respectively. (C) Fusion rates of the specified samples, demonstrating that only PEX5L complexes purified from membranes result in channel activities (Figure from Ghosh et al. 2023).

1.5 Discussion

1.5.1 PEX5L complexes form the matrix protein transport translocon

In yeast, the components involved in the translocation of PTS1 and PTS2 cargos have been studied and the presence of a pore has been suggested through electrophysiological measurements (Meinecke et al. 2010a; Montilla-Martinez et al. 2015). In this study, we aimed to characterize the human peroxisomal translocon. PEX5 is recognized as the sole import receptor capable of translocating substrate across the peroxisomal membrane. In protein import machineries observed in other organelles, including the ER, mitochondria and chloroplasts, the recognition of cargo molecules occurs through receptors that are either constitutively associated with the target membrane or translocate from the cytosol to the cytosolic surface of the membrane (Skowyra and Rapoport 2022a).

The present investigation involved the reconstitution of affinity-purified subcomplexes of membrane-solubilized PEX5L tagged with ProteinA. These subcomplexes were then incorporated into proteoliposomes and added to PLBs for electrophysiological characterization. We observed the presence of two different channel populations, characterized by low and high conductance states. The low conductance channels are observed to have an estimated diameter of up to 2 nm and have a maximum conductance of approximately 420 pS. On the other hand, the high-conductance pores have sizes of approximately 3 nm and demonstrate a conductance of over 800 pS. This occurrence of two different conductance states for peroxisomal proteins is not unfamiliar. Electrophysiological analysis on peroxisomal membranes from both mammals and yeast also displayed the presence of two predominant channel like structures with an average conductance of 0.2 and 0.6 nS, and 1.3 and 2.5 nS in 1.0 M KCl respectively (Antonenkov et al. 2005; Grunau et al. 2009). Mammalian peroxisome channels exhibited resistance to voltage-dependent gating, indicating that they are different channel types rather than representing different conformational states of the same channel (V. D. Antonenkov et al. 2005). On the contrary to mammals, in yeast, the channel with high conductance had low cation selectivity ($P_{K^+}/P_{Cl^-} \sim 1.3$) and was stable across a broad spectrum of holding potentials (± 100 mV). However, electrophysiological properties collectively provide evidence supporting the hypothesis that the high-conductance channel is a homodimer comprising two low-conductance channels in both yeast and mammals (Grunau et al. 2009; Vasily D. Antonenkov and Hiltunen 2012). These two states might represent different stages of import. It remains uncertain whether the channels that were assessed in this study were translocon or ion channels located in the peroxisomal membrane.

1.5.2 Cargo mediated transition of PEX5L complex channel

To stimulate a cargo bound state, affinity-purified soluble PEX5L complexes derived from the cytosol were preincubated with the reconstituted membrane bound fractions which consist mainly of the docking complex PEX13/PEX14 and the receptor PEX5L. This led to the low-conductance state channels undergoing a transition to high-conductance states. These high-conductance states are characterized by an estimated maximal pore-diameters of 3.3 nm, which corresponds to around 950 pS. The observed value is significantly greater in comparison to the diameters of the protein-conducting channels found in mitochondria and chloroplasts. Specifically, the dimensions of Tom40p, Tim22p, Toc75, and Tic110 are around 2.2 nm, 1.8 nm, 1.0 nm, and 1.7 nm, respectively, which are known to transport unfolded proteins (Hill et al. 1998; Kovermann et al. 2002; Ganesan and Theg 2019). The observed high conductance state following preincubation with cytosolic PEX5L-complexes can possibly be attributed to the integration of receptor-cargo complexes into pre-established import channels located on the membrane. It is important to acknowledge, however, that even when there is no additional PEX5L-cargo present, the population of low conductance channels still exhibits an inherent capability to transition into a higher conductance state, albeit only in infrequent occurrences (Ghosh et al. 2023).

In yeast, the main conductance of PTS1 pore formed by Pex5/Pex14 complex was - 85 ± 20 pS which corresponds to a pore diameter of about 0.6 nm. Incubation of the Pex5/Pex14 complex with soluble Pex5-PTS1 cargo complex lead to high conductance gating of the translocon with a mean value of 760 ± 60 pS and maximal conductance of 1,150 pS, corresponding to a pore diameter of about 3.8 nm. The pore expanded up to 9 nm occasionally in presence of PTS1 cargo-receptor complex (Meinecke et al. 2010a). For human PEX5L complexes, we did not observe a cargo mediated expansion of the pore to that extend. The pore-diameter estimation of 3.3 nm for the human translocon is insufficient in elucidating the mechanism by which large folded and oligomeric matrix proteins are imported into peroxisomes (Montilla-Martinez et al. 2015; Walton, Hill, and Subramani 1995). One potential mechanism is that the formation of the pore occurs in response to the specific size of the substrate, resulting in broader pore openings when larger or oligomerized substrates are coupled to the import receptor similar to what has been observed for PTS1 specific pores (Meinecke et al. 2010a). The only identified PTS1 cargo in our experiments was catalase, with a diameter of 9 nm (J. Zhang et al. 1998). But we did not observe any gating events at a conductance state that could be correlated with such a larger pore size. It is possible though that the narrow range spanning from minimal to maximal, observed in the opening of the human PEX5L channel, is attributed to the distinct characteristics of

the human PEX5L protein when compared to its yeast homolog. It is important to note that our experimental approach may not fully induce the opening of this channel (Ghosh et al. 2023).

1.5.3 Minimal composition of translocon

The docking complex comprising PEX14 and PEX13 is known to be part of the peroxisomal membrane and to interact with PEX5-PTS1 cargo to translocate the cargo. According to the transient pore formation model, matrix proteins are translocated through a protein conducting channel which was shown to consist of Pex5 and Pex14 for PTS1 cargo proteins (Ralf Erdmann and Schliebs 2005; Meinecke et al. 2010a). Eluates of yeast Pex5 reconstituted in LUVs for PLB experiments contained Pex5 and Pex14 in 1:1 ratio, but it also contained Pex13/Pex17 along with other membrane bound components such as ubiquitin ligase and ATPase complex (Meinecke et al. 2010a). However, when yeast Pex5 alone, isolated from the soluble fraction was reconstituted into LUVs, no channel activity was observed, suggesting that there is no translocon formed by Pex5 alone (Meinecke et al. 2010a). It is noteworthy that the peroxisomal translocon could not be activated with a PTS1-containing synthetic peptide or full-length cargo proteins but only with Pex5 and cargo complex (Meinecke et al. 2010a). The main candidates involved in cargo translocation in humans were the receptor PEX5L and the docking complex PEX13/PEX14 (also Pex17 in yeast). Recycling of the receptor, requires it's monoubiquitination as well as the ubiquitin ligase together with the ATPase complex (Pedrosa et al. 2018; Feng et al. 2022). It is still matter of debate which component forms the main translocon of the import machinery. In the following sections, I discuss different models of cargo translocation by different components of the import machinery.

1.5.3.1 PEX5: Key Player in Peroxisomal Protein Import Dynamics

PEX5 is an important candidate to form the human translocation channel. It has been demonstrated that PEX5 is part of the peroxisomal membrane but interestingly, PEX5 does not possess any TM domain (Kunau 2001; Azevedo and Schliebs 2006; Emmanouilidis et al. 2016). In a recent study using xenopus egg extract, it was found that PEX5 adopts a TM topology and then enters the peroxisomal matrix. When it comes out, its N-terminus is facing the cytosol. The NTD of PEX14 is exposed to the matrix where it binds to the N-terminal pentapeptide motifs of PEX5 (Skowyra and Rapoport 2022a). These pentapeptide motifs of PEX5 also bind to the part of PEX13 that faces the matrix (Barros-Barbosa et al. 2019).

PEX5 is conserved in eukaryotes but there are few differences in structure and function (Jansen et al. 2021; Yu et al. 2022). The number and positions of WXXX(F/Y) motifs are not the same in PEX5

receptors across different organisms. The yeast and human PEX5 mostly differ in their unstructured N-terminus (Figure 1.12). In contrast to the yeast Pex5 protein, which possesses a single binding site for the NTD of Pex14, the human PEX5 protein is characterized by the presence of a minimum of eight binding sites for PEX14 (Neuhaus et al. 2014; Otera et al. 2000; Saidowsky et al. 2001; Gopalswamy et al. 2023). Therefore, it is possible that the size and stoichiometry of complexes formed by human PEX5 and PEX14 exhibit greater heterogeneity. It is noteworthy that the Coomassie stain of the membranous PEX5 fraction (Figure 1.6C) reveals a 1:1 stoichiometry between PEX5 and PEX14, which aligns with the molar ratio observed in the yeast translocation pore in Meinecke et al. 2010 for these two proteins. This is line with a previously proposed concept that suggest the sequential binding of individual PEX5 sites to PEX14, rather than the simultaneous binding of all eight PEX5 sites to multiple PEX14 molecules (Emmanouilidis et al. 2016; Neuhaus et al. 2014). Immunoblot analysis reveals the presence of diverse PEX5L interacting proteins in the affinity-purified human PEX5 fraction, indicating heterogeneity in human PEX5L complexes. Notably, the human whole cell lysates contain membrane-bound peroxins PEX1, considerable amounts of PEX13, and the RING-finger peroxin PEX12, which may potentially contribute or impact the pore formation (Figure 1.6C).

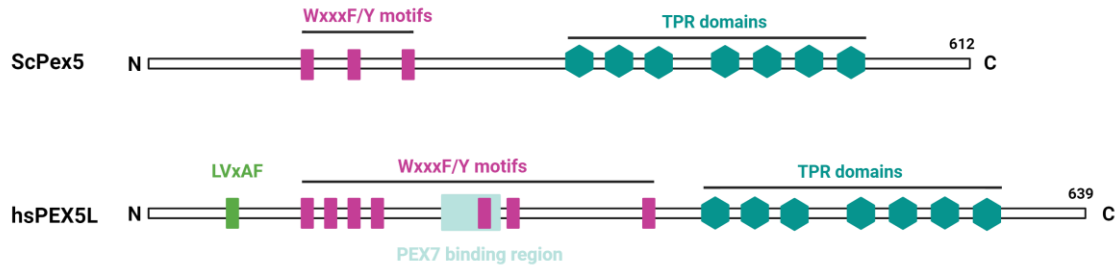

Figure 1.12 Domain structure of yeast Pex5 and human PEX5L. Yeast contains one single PTS1 receptor, namely Pex5 which contains three pentapeptide motifs (WxxxF/Y). Humans contain two isoforms of the PTS1 receptor. The long isoform PEX5L is shown here. PEX5L contains 7 WxxxF/Y motifs and one LVxAF motif at the N-terminus. Both yeast and humans contain seven tetratricopeptide (TPR) repeats which bind cargo proteins. Created using Biorender.com

PEX5L has been observed to require PEX7 in mammalian cells for trafficking PTS2 cargo across the peroxisomal membrane (Nair, Purdue, and Lazarow 2004). PEX7 was also present in the PEX5L membrane and cytosolic eluates (Figure 1.6C). Therefore, it is not out of question that the human translocon might resemble the yeast PTS2 translocation pore, which has reduced flexibility and appears to be consistently open with a diameter of approximately 4 nm (Montilla-Martinez et al. 2015). The yeast PTS2 pore consists of the coreceptor Pex18 and the docking complex Pex13/Pex14/Pex17. The PTS2 channel, upon incubation with Pex7-PTS2cargo complex, displayed an

increase in gating behaviour. The channel underwent closure in three to four recurrent current steps, which were dependent upon both the voltage and the presence of cargo. This observation demonstrates the rapidly fluctuating nature of the pore, which may be associated with specific stages of cargo transportation (Montilla-Martinez et al. 2015). This characteristic bears resemblance to some features observed in the human translocon which shows a diameter of about 3.3 nm. Human PEX5L also shows slow diffusion into the peroxisomal membrane through its N-terminus which is independent of the PTS1 cargo and PEX14 (Galiani et al. 2022). The reason for this slow diffusion was found to be a cytosolic binding partner that is exclusive to humans, although its particular identity remains unidentified (Galiani et al. 2022). PEX13 deletion strains were not checked for such diffusion.

PEX5 as a membrane shuttle

In a cell-free system based on Xenopus egg extract, Skowyra and Rapoport 2022a were able to show through protease protection assays that both N and C- terminus of PEX5 from *X. laevis* do translocate to the matrix. However, the complete translocation of PEX5 could not be verified and also how cargo would be released from the receptor in such scenario still remain mysterious. It was also shown that PEX5 accompanies cargo all the way into peroxisomes in a folded state and that the C-terminal TPR domain unfolds during retrotranslocation into the cytosol (Skowyra and Rapoport 2022a). This unfolding of the C-terminal TPR domain after translocation of matrix proteins might indicate another mechanism of cargo release. Supporting the role of human PEX5 C-terminal TPR domain, based on the structure of CTD bound to cargo proteins, it was shown that it is highly flexible and binding of high-affinity cargo proteins to the PEX5 receptor, leads to change in conformation which compactly binds PTS1 cargo-binding site down to one-third of the volume (W. A. Stanley et al. 2007; Fodor et al. 2015; Bürgi, Ekal, and Wilmanns 2021). This might indicate that in mammalian system PEX5L could act as a membrane shuttle. But how the PEX5 receptor would be released from the peroxisomal membrane to cytosol remains a mystery too.

PEX5 as a regulator

PEX5 contain seven TPR motifs (Figure 1.3). The TPR motifs have been reported in substrate binding receptor subunits of protein complexes containing protein translocation channels. Well known examples are TOM70, which tethers substrates for the TOM40 translocon complex to mitochondria and SEC72, which is involved in signal peptide recognition for the ER translocation pore Sec61 (Schlegel et al. 2007; Itskanov and Park 2019; Genge and Mokranjac 2022). The TPR motifs can also be observed in TRIP8b, a regulator of the hyperpolarization-activated cyclic nucleotide-gated (HCN) ion channel. TRIP8b binds to a C-terminal sequence motif of HCN, which bears a striking resemblance to the PTS1

pattern found in PEX5 receptor cargos. Both TRIP8b and PEX5 share a less conserved NTD and bind to PTS1 cargos in vitro (Bürgi, Ekal, and Wilmanns 2021). It could be also possible that PEX5 somehow acts as a regulator in the human translocon as it was observed for TRIP8b.

Oligomerization of PEX5L for pore formation

Oligomerization of proteins has been shown to trigger pore assembly in several toxins (Bravo et al. 2004; Mani et al. 2006; H.-Y. Kim et al. 2009; García-Sáez et al. 2011; Serra-Batiste et al. 2016). PEX5L doesn't contain any transmembrane domain (Emmanouilidis et al. 2016). The oligomerization of PEX5 has been a subject of dispute, with varying reports and conflicting findings regarding its quaternary structure. In yeast, Pex5 was shown to oligomerize (Ma et al. 2013). In *Leishmania donovani*, it was show that PEX5 exist as a tetramer and dissociates into dimer upon PTS1 cargo binding (Madrid et al. 2004). In humans, it was shown to exists as a monomer through sedimentation assays and X-ray scattering experiments (Costa-Rodrigues et al. 2005; Shiozawa et al. 2009). Fluorescence correlation spectroscopy (FCS) measurements of PEX5L did not show any homo oligomerization (Galiani et al. 2022). Most of these data are based on arrangement of PEX5 in the cytosol but not in the membrane. Therefore, it can only be speculated that it probably oligomerizes to form a pore and more interaction studies are required to clarify the arrangement of human PEX5L in the peroxisomal membrane to investigate if it is a major factor of the pore forming unit.

1.5.3.2 The Dynamics of the docking Complex in PEX5L Mediated Import

1.5.3.2.1 PEX14 as part of the translocon

Due to the 1:1 stoichiometric ratio of PEX5:PEX14 observed, PEX14 appeared to be one of the main candidates involved in the translocation of peroxisomal matrix proteins along with PEX5L. PEX14 possesses one TM domain containing AXXXA and GXXXG motifs which are known to facilitate helix-to-helix interactions and thus oligomerization of membrane proteins (Kleiger et al. 2002). It was also suggested that these motifs, along with the coiled coil domain, form a homodimer to facilitate the formation of pore-like structures located in the peroxisomal membrane (Itoh and Fujiki 2006; Meinecke et al. 2010a). However, such pore like structures could not be observed through cryo EM, NMR spectroscopy and alphafold predictions (Lill et al. 2020; Neufeld et al. 2009; Neuhaus et al. 2014; Rüttermann and Gatsogiannis 2023). Cryo-EM structures of yeast Pex14/Pex17 indicate that Pex14 forms homotrimers in a rod-shaped structure and Pex17-binding further stabilizes them (Lill et al. 2020). In humans, NTD of PEX14 is the sole structural area that possesses a PEX5 receptor binding site

(Oliveira et al. 2002). An NTD facing outside (N_{out}) in the cytosol and C terminal domain (CTD) facing inside (C_{in}) the peroxisomal matrix would be a structural possibility to capture cytosolic receptor PEX5 -cargo complex. This was initially suggested based on epitope labelling of both of the termini (Shimizu et al. 1999). Apart from its role in protein import into the matrix, PEX14 interacts with microtubules to facilitate motility and binds to beta-tubulin also through its NTD in the cytosol, but in this case shows a N_{in}-C_{out} topology (Bharti et al. 2011; Reuter et al. 2021). In protease protection assay performed in *X. laevis* on PEX14 revealed a similar topology where the N- terminal was facing towards the lumen (Skowyra and Rapoport 2022a). One plausible explanation could be that there may exist variations in multiple facets of the fundamental mechanisms between PEX14 in different organisms. Another potential explanation for how PEX5-cargo receptor complex binds to docking complex is that the specific NTD of PEX14, undergo temporary flipping across the membrane, effectively entrapping PEX5 in the cytosol and then pulling the receptor that is coupled to it into the lumen (Neuhaus et al. 2014; Yamashita et al. 2020).

Regarding its role in the pore formation, the yeast Pex14 complex, when extracted from cells lacking Pex5, showed no pore-forming activity indicating that Pex14 can't form a pore alone, similar to Pex5 (Meinecke et al. 2010a). Another group found that the depletion of human PEX14 led to a notable decline in PEX5 levels on the peroxisomal membrane in HeLa cells. Conversely, the Knockout of PEX13 led to an accumulation of PEX5 on the membranes of peroxisomes, providing evidence in favour of PEX14 as the main component involved in docking to peroxisomal membranes (Demers et al. 2023). Unfortunately, these studies didn't investigate further on the import activity.

Recently, a new motif at the C-terminus of human PEX14, named IPSWQI, was identified. It binds to the C- terminal TPR domain between the TPR motifs 4 and 5 of PEX5L and doesn't overlap with the PTS1 binding region. Mutation of the PEX14-IPSWQI residues to poly A leads to a defect in peroxisomal protein import. It was also shown that PEX14 binds more strongly to cargo free PEX5L, which represents a closed conformation of the TPR domain, than to cargo loaded PEX5L, which represents an open conformation of TPR domain (Emmanouilidis et al. 2023). This would also suggest the formation of a new binding interface at the peroxisomal membrane that may play a role in receptor docking, pore formation or even cargo release. This was supported by a study which demonstrated that the interaction between the NTD of PEX14 and the seventh and eighth WxxxF/Y-motifs of human PEX5 leads to the dissociation of PEX5 from catalase (Freitas et al. 2011). Nonetheless, biochemical experiments do prove that PEX14 is crucial for protein import together with PEX5, according to the pore formation model. But there are not structural evidences supporting a transient pore formation by PEX14 yet.

1.5.3.2.2 PEX13 as part of the translocon

PEX14 has traditionally been regarded a major factor for facilitating the translocation of hydrophilic proteins across the membrane (Meinecke et al. 2010a; Meinecke, Bartsch, and Wagner 2016). However, it is worth noting that the cryo EM structure of yeast Pex14 does not possess discernible characteristics that would enable the formation of an aqueous conduit for this purpose (Lill et al. 2020). Furthermore, it has been observed that PEX14 may not be essential for the process of import in certain organisms (Salomons et al. 2000). In contrast, PEX13 is a crucial component for import processes in all studied organisms (Williams and Distel 2006; Gao et al. 2022). Size-Exclusion chromatography of the yeast PTS1 and PTS2 specific translocon complexes showed that Pex13 was present in minor amounts which suggested that Pex13 is not the main constituent of pore forming complex (Meinecke et al. 2010a; Montilla-Martinez et al. 2015). Although considerable amounts of PEX13 co-immunoprecipitated with ProteinA-PEX5L complexes (Figure 1.6C), no conclusive comments can be made due to the use of a cell line overexpressing PEX5.

In contrast to the commonly held belief that mammalian PEX13 interacts with PEX14 and PEX5, it has been observed that the majority of PEX13 is not bound to PEX14 or even PEX5 (Krause et al. 2013). Previous studies in rat liver have shown that PEX13 was isolated as a substantial large molecular mass complex when peroxisomes were solubilized using digitonin. This finding strongly indicates that PEX13 is a component of a separate sub-complex, distinct from the complex that includes PEX14 and PEX5 (Reguenga et al. 2001). Despite multiple attempts including co-immunoprecipitation, direct contact between PEX5 and PEX13 could not be detected (Fransen, Terlecky, and Subramani 1998; Reguenga et al. 2001; Will et al. 1999; Krause et al. 2013). This observation prompted the hypothesis that mammalian PEX13 could potentially be a homopolymeric protein. Krause et al. 2013 showed that human PEX13 can homooligomerize and localize to the peroxisomal membrane through its NTD and it is important for PTS1 cargo import. Recently, the features associated with this homooligomerization were identified for *Xenopus laevis* PEX13. Conserved YG domains localised at the N- terminus of PEX13 form a mesh like structure by associating with each other similar to FG domains of nuclear pores proteins. This YG phase facilitates selective translocation of cargo across the peroxisomal membrane through the WXXX(F/Y) motifs of the import receptor yeast Pex5 (Gao et al. 2022; Ravindran et al. 2023). The flexible N-terminal unstructured region of yeast Pex13 shows the ability to form condensates. Photobleaching experiments of such condensates show that they can recover quickly indicating their viscoelastic structure. This suggests that the putative pore formed by Pex13 is transient (Ravindran et al. 2023). The presence of a transient pore is quite expected as any constant pore existing within yeast or human peroxisomes would facilitate the continuous release of peptides and

metabolites into the cytoplasm. On the other hand, unstructured regions of Pex14 were unable to form such spherical condensates, but instead form enlongated structures (Ravindran et al. 2023). PEX13 also showed dual topology with its NTD oriented towards the matrix or the cytosol (Ravindran et al. 2023). This implies that it can also act as a bait component for the PEX5 receptor in the cytosol and bring it inside the matrix. Supporting this hypothesis, it was recently shown that the C-terminal SH3 domain of human PEX13 binds WxxxF/Y motifs in the PEX5L NTD (Gaussmann et al. 2022). The same group also found a novel FxxxF peptide motif in the C-terminal region SH3 domain of human PEX13, whose binding has an autoinhibitory effect (Gaussmann et al. 2022).

The SH3 domain of yeast Pex13 was shown to bind to the PxxP motif of Pex14. In humans, the FxxxF motif of PEX13 binds to the PEX14 NTD (Figure 1.13) (Bottger et al. 2000; Douangamath et al. 2002; Emmanouilidis et al. 2016; Gaussmann et al. 2022). Interaction studies between the PEX14 NTD and the PEX13 FxxxF motif showed that PEX13 FxxxF (KD= 2.8 µM) exhibited two-fold more binding affinity than autoinhibited state of PEX13 SH3-CTR (KD= 5.4 µM) with PEX14 NTD. These findings suggest that the autoinhibited condition of PEX13 SH3-CTD can be easily relieved by its interaction with PEX14. PTS1 import is reduced with deletion of the internal FxxxF motif (Gaussmann et al. 2022). The binding affinities of the PEX proteins with each other also describe a model to delineate the order of their bindings. In this model, first, the WxxxF/Y motif of PEX5L binds to the NTD of PEX14 with strong affinity. This is then replaced by binding of the PEX13 FxxxF motif to the NTD PEX14 and PEX13 SH3 domain to the PEX5 NTD, which possibly requires large amounts of PEX13 due to their weak affinities for both PEX5 and PEX14 (Gaussmann et al. 2022). Supporting this, the detection of a large molecular mass complex that exclusively consists of PEX13 or PEX13/PEX14 has been reported already (Ravindran et al. 2023; Gao et al. 2022; Itoh and Fujiki 2006). Taken together, this data suggests that PEX13 could be the main pore forming component. However, it is important to note that yeast Pex13 alone was not sufficient to import PTS1 cargo but Pex5 was still required. If PEX13 does form a transient pore in the peroxisomal membrane, it might be regulated by PEX5. The investigation of the structural properties of PEX13, in conjunction with PEX5 and PEX14, has the potential to provide a resolution to this matter.

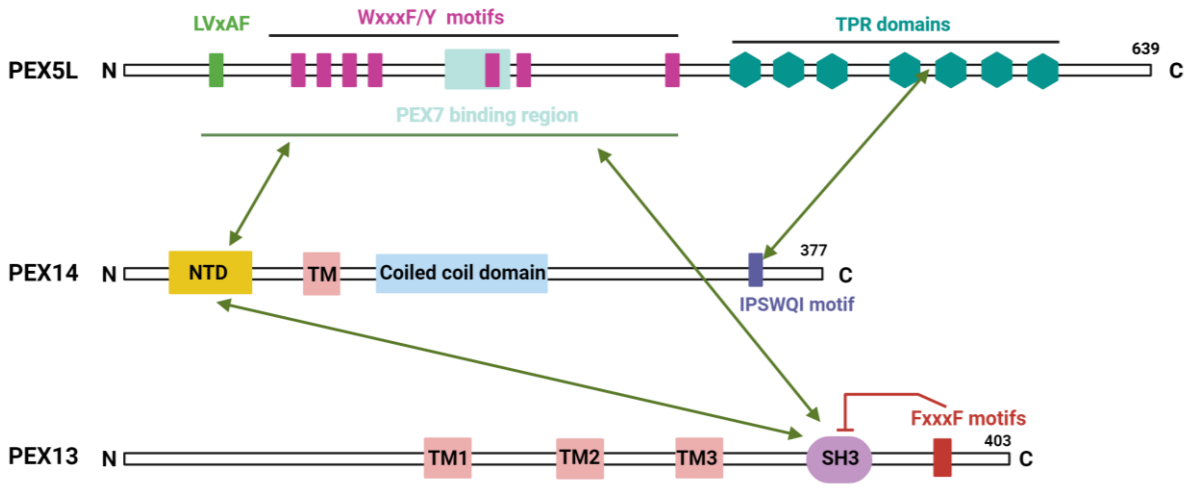

Figure 1.13 Interactions between human PEX5L, PEX14 and PEX13. The WxxxF/Y motifs of PEX5L bind to the SH3 domain of PEX13 and the NTD of PEX14. A new IPSWQI motif was found in PEX14 which binds to PEX5L between TPR motifs 4 and 5 (Emmanouilidis et al. 2023). PEX13 also binds via its SH3 domain to the NTD of PEX14. Additionally, in PEX13 a new FxxxF motifs was identified which binds to the SH3 domain of PEX13 and has an autoinhibitory effect (Gaussmann et al. 2022). Created using Biorender.com

1.5.4 Importance of the PEX1/PEX6 complex

The translocation of PEX5-cargo does not need any nucleoside triphosphate hydrolysis or a membrane potential for example, as required by mitochondrial protein transporters TIM and TOM complexes (Pedrosa et al. 2018; Truscott et al. 2001; Pitt and Buchanan 2021). Instead, it has been suggested that the driving force is generated by the strong and multivalent contacts that occur between PEX5 and PEX14 (Pedrosa et al. 2019). But the recycling and export of the receptor is energy dependent and requires ATP and the AAA ATPase complex PEX1/PEX6. In the peroxisomal membrane, PEX1 and PEX6 interact to form a complex anchored by PEX26. It was shown that the PEX1/PEX6 complex is not crucial for matrix protein import but only for export and recycling of receptors. We could not detect PEX6 but PEX1 was detected in PEX5L membrane eluate which suggests that the interaction between the two human AAA peroxins is not as stable as suggested by structural analyses and alphafold2 predictions (B. M. Gardner et al. 2018; Judy, Sheedy, and Gardner 2022). It is noteworthy that a structure for the human PEX1/PEX6 has not been reported yet. The extent of sequence similarity between human and yeast Pex1/Pex6 is notably low, with just 27% and 24% identity seen for PEX1 and PEX6, respectively. However, it is worth noting that the core ATPase domains are conserved. Alphafold2 also predicts a comparable architecture for these proteins (Judy, Sheedy, and Gardner 2022).

We speculated if there could be any change in properties of the human translocon due to absence of PEX6 as there is evidence suggesting that a defect in the ATPase complex leads to defect in protein import. Mutation in either of the two PEX1/PEX6 can be rescued partially by the overexpression of the other one. (Geisbrecht et al. 1998; Benson et al. 2021). This reduced matrix protein import was correlated with peroxisome degradation. It has been observed in fibroblast cells in patients with ZSS that mutation in PEX6 proteins exhibit decreased peroxisome numbers, enlarged peroxisomes and defects in matrix protein import (Levesque et al. 2012; Law et al. 2017). PEX6 is also not part of the minimal protein translocon machinery in peroxisomes but it is required for PEX5 receptor recycling, therefore I believe that translocon activity in vitro would not be affected drastically. The reason for absence of PEX6 should be further investigated though. In addition to PEX6, investigations have also highlighted the significance of PEX1 in the import pathway, and recycling and export of the receptor. A yeast study indicates that the deletion of *PEX1*, which inhibits pexophagy, doesn't restore protein import into peroxisomes or restore their ability to perform beta-oxidation (Mastalski, Brinkmeier, and Platta 2020). Hence, it may be inferred that Pex1 plays a significant and direct role in protein import into peroxisomes.

1.5.5 Proposed mechanism of protein import in human peroxisomes

The collective findings given in this study, in conjunction with existing knowledge in the area, enable us to put forth a streamlined mechanistic model for understanding the human translocation machinery in the import of peroxisomal matrix proteins (Figure 1.14). First, a PEX5L-cargo-coreceptor complex is formed in the cytosol. Then PEX5L with its WXXX(F/Y) motif binds to PEX14 NTD facing the cytosol. Next, there are different possibilities for formation of human translocon:

1. Our results would indicate that the pore is mainly formed by PEX5L and PEX14 (Figure 1.14, Stage 3a).

2. A transient pore could also be formed by the PEX5L, PEX14 and PEX13 and here PEX13 might play an important role to form the translocation channel by liquid-liquid phase separation of these components at the membrane (Gao et al. 2022; Ravindran et al. 2023). However, PEX5L is still crucial for cargo import together with PEX13 (Figure 1.14, Stage 3b).

The PEX14 NTD then flips towards the peroxisomal matrix and PEX5L TPR domain bound to cargo is translocated into the matrix. The cargo is then released into the matrix, probably via unfolding of the TPR domain of PEX5L. The N- terminus of PEX5L moves through the ubiquitin ligase complex consisting of PEX2, PEX10 and PEX12. PEX5L is monoubiquitinated at the N-terminal cysteine 11 and pulled out

of the peroxisomal membrane by the AAA ATPase complex PEX1/PEX6. Thus, making the receptor available for another round of the protein import cycle. The process of retrotranslocation of peroxisomal import receptors is quite similar to the ER-associated protein degradation (ERAD) mechanism. In both scenarios, substrate proteins traverse the membrane through a ubiquitin ligase with multiple spans, which leads to their ubiquitination on the cytosolic side. Following this, the proteins are removed by a AAA ATPase. More details regarding retrotranslocation in the ER will be discussed in the next chapter.

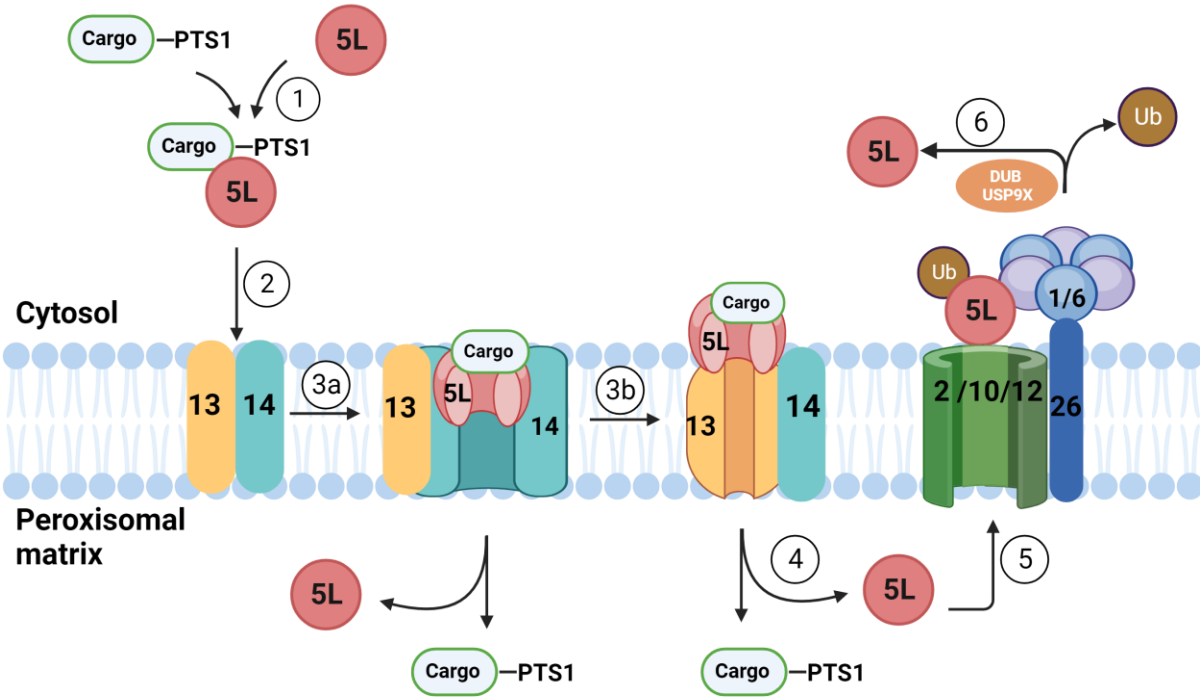

Figure 1.14 Proposed mechanism for peroxisomal PTS1 cargo import by PEX5L. PEX5L binds PTS1 cargo through its C- terminal domain (1). Receptor-cargo complex binds to the docking complex formed by PEX13 and PEX14 at the peroxisomal membrane (2). This leads to formation of a pore formed by either PEX5L/PEX14 (3a) or PEX13 (3b) through which PEX5L moves to the matrix and releases the cargo (4). Then PEX5L interacts with and is monoubiquitinated by the ubiquitin ligase channel PEX2/PEX10/PEX12 and pulled by ATP hydrolysis action of PEX1/PEX6 (5). In the cytosol, the ubiquitin molecule is removed by USP9X, freeing PEX5L for another cycle of import. Created using Biorender.com

1.6 Bibliography

Agne, Birgit, Nadja M. Meindl, Karsten Niederhoff, Henrik Einwächter, Peter Rehling, Albert Sickmann, Helmut E. Meyer, Wolfgang Girzalsky, and Wolf-H. Kunau. 2003. 'Pex8p: An Intraperoxisomal Organizer of the Peroxisomal Import Machinery'. *Molecular Cell* 11 (3): 635–46. https://doi.org/10.1016/S1097-2765(03)00062-5.

Agrawal, Gaurav, and Suresh Subramani. 2016. 'De Novo Peroxisome Biogenesis: Evolving Concepts and Conundrums'. *Biochimica et Biophysica Acta (BBA) - Molecular Cell Research*, Assembly, Maintenance and Dynamics of Peroxisomes, 1863 (5): 892–901. https://doi.org/10.1016/j.bbamcr.2015.09.014.

Al-Dirbashi, O.y., R. Shaheen, M. Al-Sayed, M. Al-Dosari, N. Makhseed, L. Abu Safieh, T. Santa, B.f. Meyer, N. Shimozawa, and F.s. Alkuraya. 2009. 'Zellweger Syndrome Caused by PEX13 Deficiency: Report of Two Novel Mutations'. *American Journal of Medical Genetics Part A* 149A (6): 1219–23. https://doi.org/10.1002/ajmg.a.32874.

Antonenkov, V. D., A. Rokka, R. T. Sormunen, R. Benz, and J. K. Hiltunen. 2005. 'Solute Traffic across Mammalian Peroxisomal Membrane--Single Channel Conductance Monitoring Reveals Pore-Forming Activities in Peroxisomes'. *Cellular and Molecular Life Sciences: CMLS* 62 (23): 2886–95. https://doi.org/10.1007/s00018-005-5233-x.

Antonenkov, Vasily D., and J. Kalervo Hiltunen. 2012. 'Transfer of Metabolites across the Peroxisomal Membrane'. *Biochimica et Biophysica Acta (BBA) - Molecular Basis of Disease*, Metabolic Functions and Biogenesis of Peroxisomes in Health and Disease, 1822 (9): 1374–86. https://doi.org/10.1016/j.bbadis.2011.12.011.

Apanasets, Oksana, Cláudia P. Grou, Paul P. Van Veldhoven, Chantal Brees, Bo Wang, Marcus Nordgren, Gabriele Dodt, Jorge E. Azevedo, and Marc Fransen. 2014. 'PEX5, the Shuttling Import Receptor for Peroxisomal Matrix Proteins, Is a Redox-Sensitive Protein'. *Traffic* 15 (1): 94–103. https://doi.org/10.1111/tra.12129.

Azevedo, Jorge E., and Wolfgang Schliebs. 2006. 'Pex14p, More than Just a Docking Protein'. *Biochimica et Biophysica Acta (BBA) - Molecular Cell Research*, Peroxisomes: Morphology, Function, Biogenesis and Disorders, 1763 (12): 1574–84. https://doi.org/10.1016/j.bbamcr.2006.09.002.

Barros-Barbosa, Aurora, Maria J. Ferreira, Tony A. Rodrigues, Ana G. Pedrosa, Cláudia P. Grou, Manuel P. Pinto, Marc Fransen, Tânia Francisco, and Jorge E. Azevedo. 2019. 'Membrane Topologies of PEX13 and PEX14 Provide New Insights on the Mechanism of Protein Import into Peroxisomes'. *The FEBS Journal* 286 (1): 205–22. https://doi.org/10.1111/febs.14697.

Bartsch, Philipp, Anke Harsman, and Richard Wagner. 2013. 'Single Channel Analysis of Membrane Proteins in Artificial Bilayer Membranes'. *Methods in Molecular Biology (Clifton, N.J.)* 1033: 345–61. https://doi.org/10.1007/978-1-62703-487-6_22.

Benson, Matthew D., Kimberly M. Papp, Geoffrey A. Casey, Alina Radziwon, Chris D. St Laurent, Lance P. Doucette, and Ian M. MacDonald. 2021. 'PEX6 Mutations in Peroxisomal Biogenesis Disorders'. *Ophthalmology Science* 1 (2): 100028. https://doi.org/10.1016/j.xops.2021.100028.

Bharti, Pratima, Wolfgang Schliebs, Tanja Schievelbusch, Alexander Neuhaus, Christine David, Klaus Kock, Christian Herrmann, et al. 2011. 'PEX14 Is Required for Microtubule-Based Peroxisome Motility in Human Cells'. *Journal of Cell Science* 124 (10): 1759–68. https://doi.org/10.1242/jcs.079368.

Björkman, Jonas, Stephen J. Gould, and Denis I. Crane. 2002. 'Pex13, the Mouse Ortholog of the Human Peroxisome Biogenesis Disorder PEX13 Gene: Gene Structure, Tissue Expression, and Localization of the Protein to Peroxisomes'. *Genomics* 79 (2): 162–68. https://doi.org/10.1006/geno.2002.6697.

Bodnar, Nicholas O., and Tom A. Rapoport. 2017. 'Molecular Mechanism of Substrate Processing by the Cdc48 ATPase Complex'. *Cell* 169 (4): 722-735.e9. https://doi.org/10.1016/j.cell.2017.04.020.

Borgia, Paola, Simona Baldassari, Nicoletta Pedemonte, Ebba Alkhunaizi, Gianluca D'Onofrio, Domenico Tortora, Elisa Calì, et al. 2022. 'Genotype-Phenotype Correlations and Disease Mechanisms in PEX13-Related Zellweger Spectrum Disorders'. *Orphanet Journal of Rare Diseases* 17 (1): 286. https://doi.org/10.1186/s13023-022-02415-5.

Bosch, H. van den, R. B. H. Schutgens, R. J. A. Wanders, and J. M. Tager. 1992. 'Biochemistry of Peroxisomes'. *Annual Review of Biochemistry* 61 (1): 157–97. https://doi.org/10.1146/annurev.bi.61.070192.001105.

Bottger, Gina, Phil Barnett, AndréT. J. Klein, Astrid Kragt, Henk F. Tabak, and Ben Distel. 2000. 'Saccharomyces Cerevisiae PTS1 Receptor Pex5p Interacts with the SH3 Domain of the Peroxisomal Membrane Protein Pex13p in an Unconventional, Non-PXXP–Related Manner'. *Molecular Biology of the Cell* 11 (11): 3963–76. https://doi.org/10.1091/mbc.11.11.3963.

Braverman, Nancy, Gabriele Dodt, Stephen J. Gould, and David Valle. 1998. 'An Isoform of Pex5p, the Human PTS1 Receptor, Is Required for the Import of PTS2 Proteins Into Peroxisomes'. *Human Molecular Genetics* 7 (8): 1195–1205. https://doi.org/10.1093/hmg/7.8.1195.

Bravo, A., I. Gómez, J. Conde, C. Muñoz-Garay, J. Sánchez, R. Miranda, M. Zhuang, S. S. Gill, and M. Soberón. 2004. 'Oligomerization Triggers Binding of a Bacillus Thuringiensis Cry1Ab Pore-Forming Toxin to Aminopeptidase N Receptor Leading to Insertion into Membrane Microdomains'. *Biochimica Et Biophysica Acta* 1667 (1): 38–46. https://doi.org/10.1016/j.bbamem.2004.08.013.

Brennand, Ana, Daniel J. Rigden, and Paul A.M. Michels. 2012. 'Trypanosomes Contain Two Highly Different Isoforms of Peroxin PEX13 Involved in Glycosome Biogenesis'. *FEBS Letters* 586 (13): 1765–71. https://doi.org/10.1016/j.febslet.2012.05.019.

Brown, P., and S.A. Musil. 2004. 'AUTOMATED DATA ACQUISITION AND PROCESSING'. In *Environmental Monitoring and Characterization*, 49–67. Elsevier. https://doi.org/10.1016/B978-012064477-3/50006-0.

Bürgi, Jérôme, Lakhan Ekal, and Matthias Wilmanns. 2021. 'Versatile Allosteric Properties in Pex5-like Tetratricopeptide Repeat Proteins to Induce Diverse Downstream Function'. *Traffic* 22 (5): 140–52. https://doi.org/10.1111/tra.12785.

Carvalho, Pedro, Veit Goder, and Tom A. Rapoport. 2006. 'Distinct Ubiquitin-Ligase Complexes Define Convergent Pathways for the Degradation of ER Proteins'. *Cell* 126 (2): 361–73. https://doi.org/10.1016/j.cell.2006.05.043.

Cohen, F S, W D Niles, and M H Akabas. 1989. 'Fusion of Phospholipid Vesicles with a Planar Membrane Depends on the Membrane Permeability of the Solute Used to Create the Osmotic Pressure.' *Journal of General Physiology* 93 (2): 201–10. https://doi.org/10.1085/jgp.93.2.201.

Costa-Rodrigues, João, Andreia F. Carvalho, Marc Fransen, Eva Hambruch, Wolfgang Schliebs, Clara Sá-Miranda, and Jorge E. Azevedo. 2005. 'Pex5p, the Peroxisomal Cycling Receptor, Is a Monomeric Non-Globular Protein'. *The Journal of Biological Chemistry* 280 (26): 24404–11. https://doi.org/10.1074/jbc.M501985200.

Dammai, Vincent, and Suresh Subramani. 2001. 'The Human Peroxisomal Targeting Signal Receptor, Pex5p, Is Translocated into the Peroxisomal Matrix and Recycled to the Cytosol'. *Cell* 105 (2): 187–96. https://doi.org/10.1016/S0092-8674(01)00310-5.

De Duve, C., and P. Baudhuin. 1966. 'Peroxisomes (Microbodies and Related Particles)'. *Physiological Reviews* 46 (2): 323–57. https://doi.org/10.1152/physrev.1966.46.2.323.

Demers, Nicholas D., Victoria Riccio, Doo Sin Jo, Sushil Bhandari, Kelsey B. Law, Weifang Liao, Choy Kim, et al. 2023. 'PEX13 Prevents Pexophagy by Regulating Ubiquitinated PEX5 and Peroxisomal ROS'. *Autophagy* 19 (6): 1781–1802. https://doi.org/10.1080/15548627.2022.2160566.

Denkert, Niels, Alexander Benjamin Schendzielorz, Mariam Barbot, Lennart Versemann, Frank Richter, Peter Rehling, and Michael Meinecke. 2017. 'Cation Selectivity of the Presequence Translocase Channel Tim23 Is Crucial for Efficient Protein Import'. Edited by Nikolaus Pfanner. *eLife* 6 (August): e28324. https://doi.org/10.7554/eLife.28324.

Denkert, Niels. 2018. 'Molecular Characterization of the Mitochondrial Presequence Translocase'. Georg-August-University Göttingen. https://doi.org/10.53846/goediss-6710.

Distel, B, R Erdmann, S J Gould, G Blobel, D I Crane, J M Cregg, G Dodt, et al. 1996. 'A Unified Nomenclature for Peroxisome Biogenesis Factors.' *Journal of Cell Biology* 135 (1): 1–3. https://doi.org/10.1083/jcb.135.1.1.

Dodt, Gabriele, Daniel Warren, Elisabeth Becker, Peter Rehling, and Stephen J. Gould. 2001. 'Domain Mapping of Human PEX5 Reveals Functional and Structural Similarities to Saccharomyces Cerevisiae Pex18p and Pex21p *'. *Journal of Biological Chemistry* 276 (45): 41769–81. https://doi.org/10.1074/jbc.M106932200.

Douangamath, Alice, Fabian V Filipp, André T.J Klein, Phil Barnett, Peijian Zou, Tineke Voorn-Brouwer, M.Cristina Vega, et al. 2002. 'Topography for Independent Binding of α-Helical and PPII-Helical Ligands to a Peroxisomal SH3 Domain'. *Molecular Cell* 10 (5): 1007–17. https://doi.org/10.1016/S1097-2765(02)00749-9.

Eaton, D.C. 1985. 'Ionic Channels of Excitable Membranes. Bertil Hille. Sunderland, Ma: Sinauer Associates, 1984'. *Journal of Neuroscience Research* 13 (4): 599–600. https://doi.org/10.1002/jnr.490130415.

Ebberink, Merel S., Petra A. W. Mooijer, Jeannette Gootjes, Janet Koster, Ronald J. A. Wanders, and Hans R. Waterham. 2011. 'Genetic Classification and Mutational Spectrum of More than 600 Patients with a Zellweger Syndrome Spectrum Disorder'. *Human Mutation* 32 (1): 59–69. https://doi.org/10.1002/humu.21388.

Edward Purdue, P., Xudong Yang, and Paul B. Lazarow. 1998. 'Pex18p and Pex21p, a Novel Pair of Related Peroxins Essential for Peroxisomal Targeting by the PTS2 Pathway'. *Journal of Cell Biology* 143 (7): 1859–69. https://doi.org/10.1083/jcb.143.7.1859.

El Magraoui, Fouzi, Bastian E. Bäumer, Harald W. Platta, Jörg S. Baumann, Wolfgang Girzalsky, and Ralf Erdmann. 2012. 'The RING-Type Ubiquitin Ligases Pex2p, Pex10p and Pex12p Form a Heteromeric Complex That Displays Enhanced Activity in an Ubiquitin Conjugating Enzyme-Selective Manner'. *The FEBS Journal* 279 (11): 2060–70. https://doi.org/10.1111/j.1742-4658.2012.08591.x.

Elgersma, Y., L. Kwast, A. Klein, T. Voorn-Brouwer, M. van den Berg, B. Metzig, T. America, H. F. Tabak, and B. Distel. 1996. 'The SH3 Domain of the Saccharomyces Cerevisiae Peroxisomal Membrane Protein Pex13p Functions as a Docking Site for Pex5p, a Mobile Receptor for the Import PTS1-Containing Proteins'. *The Journal of Cell Biology* 135 (1): 97–109. https://doi.org/10.1083/jcb.135.1.97.

Emmanouilidis, Leonidas, Mohanraj Gopalswamy, Daniel M. Passon, Matthias Wilmanns, and Michael Sattler. 2016. 'Structural Biology of the Import Pathways of Peroxisomal Matrix Proteins'. *Biochimica et Biophysica Acta (BBA) - Molecular Cell Research*, Assembly, Maintenance and Dynamics of Peroxisomes, 1863 (5): 804–13. https://doi.org/10.1016/j.bbamcr.2015.09.034.

Emmanouilidis, Leonidas, Jessica Sehr, Katharina Reglinski, Stefan Gaussmann, David Goricanec, Jonathan Kordon, Filipe Menezes, et al. 2023. 'A Novel PEX14/PEX5 Interface Links Peroxisomal Protein Import and Receptor Recycling'. Preprint. Biochemistry. https://doi.org/10.1101/2023.08.08.552478.

Erdmann, R., and G. Blobel. 1996. 'Identification of Pex13p a Peroxisomal Membrane Receptor for the PTS1 Recognition Factor'. *The Journal of Cell Biology* 135 (1): 111–21. https://doi.org/10.1083/jcb.135.1.111.

Erdmann, Ralf, and Wolfgang Schliebs. 2005. 'Peroxisomal Matrix Protein Import: The Transient Pore Model'. *Nature Reviews Molecular Cell Biology* 6 (9): 738–42. https://doi.org/10.1038/nrm1710.

Farré, Jean-Claude, Shanmuga S Mahalingam, Marco Proietto, and Suresh Subramani. 2019. 'Peroxisome Biogenesis, Membrane Contact Sites, and Quality Control'. *EMBO Reports* 20 (1): e46864. https://doi.org/10.15252/embr.201846864.

Feng, Peiqiang, Michael L. Skowyra, and Tom A. Rapoport. 2022. 'Structure and Function of the Peroxisomal Ubiquitin Ligase Complex'. *Biochemical Society Transactions* 50 (6): 1921–30. https://doi.org/10.1042/BST20221393.

Feng, Peiqiang, Xudong Wu, Satchal K. Erramilli, Joao A. Paulo, Pawel Knejski, Steven P. Gygi, Anthony A. Kossiakoff, and Tom A. Rapoport. 2022. 'A Peroxisomal Ubiquitin Ligase Complex Forms a Retrotranslocation Channel'. *Nature* 607 (7918): 374–80. https://doi.org/10.1038/s41586-022-04903-x.

Fodor, Krisztián, Janina Wolf, Katharina Reglinski, Daniel M. Passon, Ye Lou, Wolfgang Schliebs, Ralf Erdmann, and Matthias Wilmanns. 2015. 'Ligand-Induced Compaction of the PEX5 Receptor-Binding Cavity Impacts Protein Import Efficiency into Peroxisomes'. *Traffic (Copenhagen, Denmark)* 16 (1): 85–98. https://doi.org/10.1111/tra.12238.

Francisco, Tânia, Tony A. Rodrigues, Manuel P. Pinto, Andreia F. Carvalho, Jorge E. Azevedo, and Cláudia P. Grou. 2014. 'Ubiquitin in the Peroxisomal Protein Import Pathway'. *Biochimie*, Peroxisomes: biogenesis, functions and diseases, 98 (March): 29–35. https://doi.org/10.1016/j.biochi.2013.08.003.

Fransen, Marc, Stanley R. Terlecky, and Suresh Subramani. 1998. 'Identification of a Human PTS1 Receptor Docking Protein Directly Required for Peroxisomal Protein Import'. *Proceedings of the National Academy of Sciences* 95 (14): 8087–92. https://doi.org/10.1073/pnas.95.14.8087.

Freitas, Marta O., Tânia Francisco, Tony A. Rodrigues, Inês S. Alencastre, Manuel P. Pinto, Cláudia P. Grou, Andreia F. Carvalho, Marc Fransen, Clara Sá-Miranda, and Jorge E. Azevedo. 2011. 'PEX5 Protein Binds Monomeric Catalase Blocking Its Tetramerization and Releases It upon Binding the N-Terminal Domain of PEX14 *'. *Journal of Biological Chemistry* 286 (47): 40509–19. https://doi.org/10.1074/jbc.M111.287201.

Freitas, Marta O., Tânia Francisco, Tony A. Rodrigues, Celien Lismont, Pedro Domingues, Manuel P. Pinto, Cláudia P. Grou, Marc Fransen, and Jorge E. Azevedo. 2015. 'The Peroxisomal Protein Import Machinery Displays a Preference for Monomeric Substrates'. *Open Biology* 5 (4): 140236. https://doi.org/10.1098/rsob.140236.

Galiani, S., K. Reglinski, P. Carravilla, A. Barbotin, I. Urbančič, J. Ott, J. Sehr, et al. 2022. 'Diffusion and Interaction Dynamics of the Cytosolic Peroxisomal Import Receptor PEX5'. *Biophysical Reports* 2 (2): 100055. https://doi.org/10.1016/j.bpr.2022.100055.

Ganesan, Iniyan, and Steven M. Theg. 2019. 'Structural Considerations of Folded Protein Import through the Chloroplast TOC/TIC Translocons'. *FEBS Letters* 593 (6): 565–72. https://doi.org/10.1002/1873-3468.13342.

Gao, Yuan, Michael L. Skowyra, Peiqiang Feng, and Tom A. Rapoport. 2022. 'Protein Import into Peroxisomes Occurs through a Nuclear Pore–like Phase'. *Science* 378 (6625): eadf3971. https://doi.org/10.1126/science.adf3971.

García-Sáez, Ana J., Sabine B. Buschhorn, Heiko Keller, Gregor Anderluh, Kai Simons, and Petra Schwille. 2011. 'Oligomerization and Pore Formation by Equinatoxin II Inhibit Endocytosis and Lead to Plasma Membrane Reorganization'. *The Journal of Biological Chemistry* 286 (43): 37768–77. https://doi.org/10.1074/jbc.M111.281592.

Gardner, Brooke M., Dominic T. Castanzo, Saikat Chowdhury, Goran Stjepanovic, Matthew S. Stefely, James H. Hurley, Gabriel C. Lander, and Andreas Martin. 2018. 'The Peroxisomal AAA-ATPase Pex1/Pex6 Unfolds Substrates by Processive Threading'. *Nature Communications* 9 (1): 135. https://doi.org/10.1038/s41467-017-02474-4.

Gatto, Gregory J., Brian V. Geisbrecht, Stephen J. Gould, and Jeremy M. Berg. 2000. 'Peroxisomal Targeting Signal-1 Recognition by the TPR Domains of Human PEX5'. *Nature Structural Biology* 7 (12): 1091–95. https://doi.org/10.1038/81930.

Gaussmann, Stefan, Mohanraj Gopalswamy, Maike Eberhardt, Maren Reuter, Peijian Zou, Wolfgang Schliebs, Ralf Erdmann, and Michael Sattler. 2021. 'Membrane Interactions of the Peroxisomal Proteins PEX5 and PEX14'. *Frontiers in Cell and Developmental Biology* 9. https://www.frontiersin.org/articles/10.3389/fcell.2021.651449.

Gaussmann, Stefan, Julia Ott, Krzysztof M. Zak, Florent Delhommel, Grzegorz M. Popowicz, Wolfgang Schliebs, Ralf Erdmann, and Michael Sattler. 2022. 'Intramolecular Autoinhibition of Human PEX13 Modulates Peroxisomal Import'. Preprint. Biochemistry. https://doi.org/10.1101/2022.12.19.520972.

Geisbrecht, Brian V., Cynthia S. Collins, Bernadette E. Reuber, and Stephen J. Gould. 1998. 'Disruption of a PEX1–PEX6 Interaction Is the Most Common Cause of the Neurologic Disorders Zellweger Syndrome, Neonatal Adrenoleukodystrophy, and Infantile Refsum Disease'. *Proceedings of the National Academy of Sciences of the United States of America* 95 (15): 8630–35.

Genge, Marcel G., and Dejana Mokranjac. 2022. 'Coordinated Translocation of Presequence-Containing Precursor Proteins Across Two Mitochondrial Membranes: Knowns and Unknowns of How TOM and TIM23 Complexes Cooperate With Each Other'. *Frontiers in Physiology* 12. https://www.frontiersin.org/articles/10.3389/fphys.2021.806426.

Ghosh, Mausumi, Niels Denkert, Maren Reuter, Jessica Klümper, Katharina Reglinski, Rebecca Peschel, Wolfgang Schliebs, Ralf Erdmann, and Michael Meinecke. 2023. 'Dynamics of the Translocation Pore of the Human Peroxisomal Protein Import Machinery'. *Biological Chemistry* 404 (2–3): 169–78. https://doi.org/10.1515/hsz-2022-0170.

Girzalsky, W., P. Rehling, K. Stein, J. Kipper, L. Blank, W. H. Kunau, and R. Erdmann. 1999. 'Involvement of Pex13p in Pex14p Localization and Peroxisomal Targeting Signal 2-Dependent Protein Import into Peroxisomes'. *The Journal of Cell Biology* 144 (6): 1151–62. https://doi.org/10.1083/jcb.144.6.1151.

Glover, J R, D W Andrews, and R A Rachubinski. 1994. 'Saccharomyces Cerevisiae Peroxisomal Thiolase Is Imported as a Dimer.' *Proceedings of the National Academy of Sciences* 91 (22): 10541–45. https://doi.org/10.1073/pnas.91.22.10541.

Goebl, M, and M Yanagida. 1991. 'The TPR Snap Helix: A Novel Protein Repeat Motif from Mitosis to Transcription'. *Trends in Biochemical Sciences* 16 (5): 173–77. https://doi.org/10.1016/0968-0004(91)90070-c.

Goldfischer, S., C. L. Moore, A. B. Johnson, A. J. Spiro, M. P. Valsamis, H. K. Wisniewski, R. H. Ritch, W. T. Norton, I. Rapin, and L. M. Gartner. 1973. 'Peroxisomal and Mitochondrial Defects in the Cerebro-Hepato-Renal Syndrome'. *Science (New York, N.Y.)* 182 (4107): 62–64. https://doi.org/10.1126/science.182.4107.62.

Goldman, David E. 1943. 'POTENTIAL, IMPEDANCE, AND RECTIFICATION IN MEMBRANES'. *Journal of General Physiology* 27 (1): 37–60. https://doi.org/10.1085/jgp.27.1.37.

Gopalswamy, Mohanraj, Chen Zheng, Stefan Gaussmann, Hamed Kooshapur, Eva Hambruch, Wolfgang Schliebs, Ralf Erdmann, Iris Antes, and Michael Sattler. 2023. 'Distinct Conformational and Energetic Features Define the Specific Recognition of (Di)Aromatic Peptide Motifs by PEX14'. *Biological Chemistry* 404 (2–3): 179–94. https://doi.org/10.1515/hsz-2022-0177.

Gould, S. J., J. E. Kalish, J. C. Morrell, J. Bjorkman, A. J. Urquhart, and D. I. Crane. 1996. 'Pex13p Is an SH3 Protein of the Peroxisome Membrane and a Docking Factor for the Predominantly Cytoplasmic PTs1 Receptor'. *The Journal of Cell Biology* 135 (1): 85–95. https://doi.org/10.1083/jcb.135.1.85.

Gouveia, Alexandra M., Carla P. Guimarães, Márcia E. Oliveira, Carlos Reguenga, Clara Sá-Miranda, and Jorge E. Azevedo. 2003. 'Characterization of the Peroxisomal Cycling Receptor, Pex5p, Using a Cell-Free in Vitro Import System *'. *Journal of Biological Chemistry* 278 (1): 226–32. https://doi.org/10.1074/jbc.M209498200.

Grou, Cláudia P., Andreia F. Carvalho, Manuel P. Pinto, Sebastian Wiese, Heike Piechura, Helmut E. Meyer, Bettina Warscheid, Clara Sá-Miranda, and Jorge E. Azevedo. 2008. 'Members of the E2D (UbcH5) Family Mediate the Ubiquitination of the Conserved Cysteine of Pex5p, the Peroxisomal Import Receptor'. *The Journal of Biological Chemistry* 283 (21): 14190–97. https://doi.org/10.1074/jbc.M800402200.

Grou, Cláudia P., Tânia Francisco, Tony A. Rodrigues, Marta O. Freitas, Manuel P. Pinto, Andreia F. Carvalho, Pedro Domingues, et al. 2012. 'Identification of Ubiquitin-Specific Protease 9X (USP9X) as a Deubiquitinase Acting on Ubiquitin-Peroxin 5 (PEX5) Thioester Conjugate *'. *Journal of Biological Chemistry* 287 (16): 12815–27. https://doi.org/10.1074/jbc.M112.340158.

Grunau, Silke, Sabrina Mindthoff, Hanspeter Rottensteiner, Raija T. Sormunen, J. Kalervo Hiltunen, Ralf Erdmann, and Vasily D. Antonenkov. 2009. 'Channel-Forming Activities of Peroxisomal Membrane Proteins from the Yeast Saccharomyces Cerevisiae'. *The FEBS Journal* 276 (6): 1698–1708. https://doi.org/10.1111/j.1742-4658.2009.06903.x.

Harano, Tomoyuki, Shizuko Nose, Rumiko Uezu, Nobuyoshi Shimizu, and Yukio Fujiki. 2001. 'Hsp70 Regulates the Interaction between the Peroxisome Targeting Signal Type 1 (PTS1)-Receptor Pex5p and PTS1'. *Biochemical Journal* 357 (1): 157–65. https://doi.org/10.1042/bj3570157.

Harper, Courtney C., Jeremy M. Berg, and Stephen J. Gould. 2003. 'PEX5 Binds the PTS1 Independently of Hsp70 and the Peroxin PEX12*'. *Journal of Biological Chemistry* 278 (10): 7897–7901. https://doi.org/10.1074/jbc.M206651200.

Hasan, Sohel, Harald W. Platta, and Ralf Erdmann. 2013. 'Import of Proteins into the Peroxisomal Matrix'. *Frontiers in Physiology* 4 (September): 261. https://doi.org/10.3389/fphys.2013.00261.

Heymans, H. S., R. B. Schutgens, R. Tan, H. van den Bosch, and P. Borst. 1983. 'Severe Plasmalogen Deficiency in Tissues of Infants without Peroxisomes (Zellweger Syndrome)'. *Nature* 306 (5938): 69–70. https://doi.org/10.1038/306069a0.

Hill, Kerstin, Kirstin Model, Michael T. Ryan, Klaus Dietmeier, Falk Martin, Richard Wagner, and Nikolaus Pfanner. 1998. 'Tom40 Forms the Hydrophilic Channel of the Mitochondrial Import Pore for Preproteins'. *Nature* 395 (6701): 516–21. https://doi.org/10.1038/26780.

Hodgkin, A. L., and B. Katz. 1949. 'The Effect of Sodium Ions on the Electrical Activity of Giant Axon of the Squid'. *The Journal of Physiology* 108 (1): 37–77. https://doi.org/10.1113/jphysiol.1949.sp004310.

Hotz, Thomas, Ole M. Schütte, Hannes Sieling, Tatjana Polupanow, Ulf Diederichsen, Claudia Steinem, and Axel Munk. 2013. 'Idealizing Ion Channel Recordings by a Jump Segmentation Multiresolution Filter'. *IEEE Transactions on NanoBioscience* 12 (4): 376–86. https://doi.org/10.1109/TNB.2013.2284063.

Hruban, Z., E. L. Vigil, A. Slesers, and E. Hopkins. 1972. 'Microbodies: Constituent Organelles of Animal Cells'. *Laboratory Investigation; a Journal of Technical Methods and Pathology* 27 (2): 184–91.

Islinger, Markus, Ka Wan Li, Jürgen Seitz, Alfred Völkl, and Georg H. Lüers. 2009. 'Hitchhiking of Cu/Zn Superoxide Dismutase to Peroxisomes--Evidence for a Natural Piggyback Import Mechanism in Mammals'. *Traffic (Copenhagen, Denmark)* 10 (11): 1711–21. https://doi.org/10.1111/j.1600-0854.2009.00966.x.

Itoh, Ryota, and Yukio Fujiki. 2006. 'Functional Domains and Dynamic Assembly of the Peroxin Pex14p, the Entry Site of Matrix Proteins'. *The Journal of Biological Chemistry* 281 (15): 10196–205. https://doi.org/10.1074/jbc.M600158200.

Itskanov, Samuel, and Eunyong Park. 2019. 'Structure of the Posttranslational Sec Protein-Translocation Channel Complex from Yeast'. *Science* 363 (6422): 84–87. https://doi.org/10.1126/science.aav6740.

Jankowski, A., J. H. Kim, R. F. Collins, R. Daneman, P. Walton, and S. Grinstein. 2001. 'In Situ Measurements of the pH of Mammalian Peroxisomes Using the Fluorescent Protein pHluorin'. *The Journal of Biological Chemistry* 276 (52): 48748–53. https://doi.org/10.1074/jbc.M109003200.

Jansen, Renate L. M., Carlos Santana-Molina, Marco van den Noort, Damien P. Devos, and Ida J. van der Klei. 2021. 'Comparative Genomics of Peroxisome Biogenesis Proteins: Making Sense of the PEX Proteins'. *Frontiers in Cell and Developmental Biology* 9. https://www.frontiersin.org/articles/10.3389/fcell.2021.654163.

Jarosch, Ernst, Christof Taxis, Corinna Volkwein, Javier Bordallo, Daniel Finley, Dieter H. Wolf, and Thomas Sommer. 2002. 'Protein Dislocation from the ER Requires Polyubiquitination and the AAA-ATPase Cdc48'. *Nature Cell Biology* 4 (2): 134–39. https://doi.org/10.1038/ncb746.

Judy, Ryan M., Connor J. Sheedy, and Brooke M. Gardner. 2022. 'Insights into the Structure and Function of the Pex1/Pex6 AAA-ATPase in Peroxisome Homeostasis'. *Cells* 11 (13): 2067. https://doi.org/10.3390/cells11132067.

Kaur, Navneet, Sigrun Reumann, and Jianping Hu. 2009. 'Peroxisome Biogenesis and Function'. *The Arabidopsis Book / American Society of Plant Biologists* 7 (September): e0123. https://doi.org/10.1199/tab.0123.

Kerssen, Daniela, Eva Hambruch, Wibke Klaas, Harald W. Platta, Ben de Kruijff, Ralf Erdmann, Wolf-H. Kunau, and Wolfgang Schliebs. 2006. 'Membrane Association of the Cycling Peroxisome Import Receptor Pex5p *'. *Journal of Biological Chemistry* 281 (37): 27003–15. https://doi.org/10.1074/jbc.M509257200.

Kim, Hai-Young, Min-Kyu Cho, Ashutosh Kumar, Elke Maier, Carsten Siebenhaar, Stefan Becker, Claudio O. Fernandez, et al. 2009. 'Structural Properties of Pore-Forming Oligomers of α-Synuclein'. *Journal of the American Chemical Society* 131 (47): 17482–89. https://doi.org/10.1021/ja9077599.

Kim, Peter. 2017. 'Peroxisome Biogenesis: A Union between Two Organelles'. *Current Biology* 27 (7): R271–74. https://doi.org/10.1016/j.cub.2017.02.052.

Kleiger, Gary, Robert Grothe, Parag Mallick, and David Eisenberg. 2002. 'GXXXG and AXXXA: Common α-Helical Interaction Motifs in Proteins, Particularly in Extremophiles'. *Biochemistry* 41 (19): 5990–97. https://doi.org/10.1021/bi0200763.

Kleinecke, Sandra, Sarah Richert, Livia de Hoz, Britta Brügger, Theresa Kungl, Ebrahim Asadollahi, Susanne Quintes, et al. 2017. 'Peroxisomal Dysfunctions Cause Lysosomal Storage and Axonal Kv1 Channel Redistribution in Peripheral Neuropathy'. *eLife* 6 (May): e23332. https://doi.org/10.7554/eLife.23332.

Kovermann, Peter, Kaye N Truscott, Bernard Guiard, Peter Rehling, Naresh B Sepuri, Hanne Müller, Robert E Jensen, Richard Wagner, and Nikolaus Pfanner. 2002. 'Tim22, the Essential Core of the Mitochondrial Protein Insertion Complex, Forms a Voltage-Activated and Signal-Gated Channel'. *Molecular Cell* 9 (2): 363–73. https://doi.org/10.1016/S1097-2765(02)00446-X.

Krause, Cindy, Hendrik Rosewich, Melissa Thanos, and Jutta Gärtner. 2006. 'Identification of Novel Mutations in *PEX2* , *PEX6* , *PEX10* , *PEX12* , and *PEX13* in Zellweger Spectrum Patients'. *Human Mutation* 27 (11): 1157–1157. https://doi.org/10.1002/humu.9462.

Krause, Cindy, Hendrik Rosewich, Andrew Woehler, and Jutta Gärtner. 2013. 'Functional Analysis of PEX13 Mutation in a Zellweger Syndrome Spectrum Patient Reveals Novel Homooligomerization of PEX13 and Its Role in Human Peroxisome Biogenesis'. *Human Molecular Genetics* 22 (19): 3844–57. https://doi.org/10.1093/hmg/ddt238.

Kunau, Wolf-H. 2001. 'Peroxisomes: The Extended Shuttle to the Peroxisome Matrix'. *Current Biology* 11 (16): R659–62. https://doi.org/10.1016/S0960-9822(01)00386-4.

Kunze, Markus, Naila Malkani, Sebastian Maurer-Stroh, Christoph Wiesinger, Johannes A. Schmid, and Johannes Berger. 2015. 'Mechanistic Insights into PTS2-Mediated Peroxisomal Protein Import: THE CO-RECEPTOR PEX5L DRASTICALLY INCREASES THE INTERACTION STRENGTH BETWEEN THE CARGO PROTEIN AND THE RECEPTOR PEX7*'. *Journal of Biological Chemistry* 290 (8): 4928–40. https://doi.org/10.1074/jbc.M114.601575.

Kunze, Markus, Georg Neuberger, Sebastian Maurer-Stroh, Jianmin Ma, Thomas Eck, Nancy Braverman, Johannes A. Schmid, Frank Eisenhaber, and Johannes Berger. 2011. 'Structural Requirements for Interaction of Peroxisomal Targeting Signal 2 and Its Receptor PEX7'. *The Journal of Biological Chemistry* 286 (52): 45048–62. https://doi.org/10.1074/jbc.M111.301853.

Lamb, John R, Stuart Tugendreich, and Phil Hieter. 1995. 'Tetratrico Peptide Repeat Interactions: To TPR or Not to TPR?' *Trends in Biochemical Sciences* 20 (7): 257–59. https://doi.org/10.1016/S0968-0004(00)89037-4.

Law, Kelsey B., Dana Bronte-Tinkew, Erminia Di Pietro, Ann Snowden, Richard O. Jones, Ann Moser, John H. Brumell, Nancy Braverman, and Peter K. Kim. 2017. 'The Peroxisomal AAA ATPase Complex Prevents Pexophagy and Development of Peroxisome Biogenesis Disorders'. *Autophagy* 13 (5): 868–84. https://doi.org/10.1080/15548627.2017.1291470.

Lazarow, P. B. 1995. 'Peroxisome Structure, Function, and Biogenesis--Human Patients and Yeast Mutants Show Strikingly Similar Defects in Peroxisome Biogenesis'. *Journal of Neuropathology and Experimental Neurology* 54 (5): 720–25. https://doi.org/10.1097/00005072-199509000-00015.

Lazarow, P. B., and Y. Fujiki. 1985. 'Biogenesis of Peroxisomes'. *Annual Review of Cell Biology* 1 (1): 489–530. https://doi.org/10.1146/annurev.cb.01.110185.002421.

Lazarow, Paul B. 2006. 'Chapter 3.1.7. The Import Receptor Pex7p and the PTS2 Targeting Sequence'. *Biochimica et Biophysica Acta (BBA) - Molecular Cell Research*, Peroxisomes: Morphology,

Function, Biogenesis and Disorders, 1763 (12): 1599–1604. https://doi.org/10.1016/j.bbamcr.2006.08.011.

Lee, Ming Y, Rhea Sumpter Jr, Zhongju Zou, Shyam Sirasanagandla, Yongjie Wei, Prashant Mishra, Hendrik Rosewich, Denis I Crane, and Beth Levine. 2017. 'Peroxisomal Protein PEX13 Functions in Selective Autophagy'. *EMBO Reports* 18 (1): 48–60. https://doi.org/10.15252/embr.201642443.

Levesque, Sebastien, Charles Morin, Simon-Pierre Guay, Josee Villeneuve, Pascale Marquis, Wing Yan Yik, Sarn Jiralerspong, et al. 2012. 'A Founder Mutation in the PEX6 Gene Is Responsible for Increased Incidence of Zellweger Syndrome in a French Canadian Population'. *BMC Medical Genetics* 13 (1): 72. https://doi.org/10.1186/1471-2350-13-72.

Lill, Pascal, Tobias Hansen, Daniel Wendscheck, Bjoern Udo Klink, Tomasz Jeziorek, Dimitrios Vismpas, Jonas Miehling, et al. 2020. 'Towards the Molecular Architecture of the Peroxisomal Receptor Docking Complex'. *Proceedings of the National Academy of Sciences of the United States of America* 117 (52): 33216–24. https://doi.org/10.1073/pnas.2009502117.

Ma, Changle, Gaurav Agrawal, and Suresh Subramani. 2011. 'Peroxisome Assembly: Matrix and Membrane Protein Biogenesis'. *The Journal of Cell Biology* 193 (1): 7–16. https://doi.org/10.1083/jcb.201010022.

Ma, Changle, Danielle Hagstrom, Soumi Guha Polley, and Suresh Subramani. 2013. 'Redox-Regulated Cargo Binding and Release by the Peroxisomal Targeting Signal Receptor, Pex5'. *The Journal of Biological Chemistry* 288 (38): 27220–31. https://doi.org/10.1074/jbc.M113.492694.

Ma, Changle, Uwe Schumann, Naganand Rayapuram, and Suresh Subramani. 2009. 'The Peroxisomal Matrix Import of Pex8p Requires Only PTS Receptors and Pex14p'. *Molecular Biology of the Cell* 20 (16): 3680–89. https://doi.org/10.1091/mbc.e09-01-0037.

Madrid, Kleber P., Gregory De Crescenzo, Shengwu Wang, and Armando Jardim. 2004. 'Modulation of the Leishmania Donovani Peroxin 5 Quaternary Structure by Peroxisomal Targeting Signal 1 Ligands'. *Molecular and Cellular Biology* 24 (17): 7331–44. https://doi.org/10.1128/MCB.24.17.7331-7344.2004.

Mani, Rajeswari, Sarah D. Cady, Ming Tang, Alan J. Waring, Robert I. Lehrer, and Mei Hong. 2006. 'Membrane-Dependent Oligomeric Structure and Pore Formation of a β-Hairpin Antimicrobial Peptide in Lipid Bilayers from Solid-State NMR'. *Proceedings of the National Academy of Sciences* 103 (44): 16242–47. https://doi.org/10.1073/pnas.0605079103.

Mastalski, Thomas, Rebecca Brinkmeier, and Harald W. Platta. 2020. 'The Peroxisomal PTS1-Import Defect of PEX1- Deficient Cells Is Independent of Pexophagy in Saccharomyces Cerevisiae'. *International Journal of Molecular Sciences* 21 (3): 867. https://doi.org/10.3390/ijms21030867.

Matsumoto, Naomi, Shigehiko Tamura, and Yukio Fujiki. 2003. 'The Pathogenic Peroxin Pex26p Recruits the Pex1p–Pex6p AAA ATPase Complexes to Peroxisomes'. *Nature Cell Biology* 5 (5): 454–60. https://doi.org/10.1038/ncb982.

McNew, J. A., and J. M. Goodman. 1994. 'An Oligomeric Protein Is Imported into Peroxisomes in Vivo'. *The Journal of Cell Biology* 127 (5): 1245–57. https://doi.org/10.1083/jcb.127.5.1245.

Meinecke, Michael, Philipp Bartsch, and Richard Wagner. 2016. 'Peroxisomal Protein Import Pores'. *Biochimica et Biophysica Acta (BBA) - Molecular Cell Research*, Assembly, Maintenance and Dynamics of Peroxisomes, 1863 (5): 821–27. https://doi.org/10.1016/j.bbamcr.2015.10.013.

Meinecke, Michael, Christian Cizmowski, Wolfgang Schliebs, Vivien Krüger, Sabrina Beck, Richard Wagner, and Ralf Erdmann. 2010. 'The Peroxisomal Importomer Constitutes a Large and Highly Dynamic Pore'. *Nature Cell Biology* 12 (3): 273–77. https://doi.org/10.1038/ncb2027.

Montilla-Martinez, Malayko, Sabrina Beck, Jessica Klümper, Michael Meinecke, Wolfgang Schliebs, Richard Wagner, and Ralf Erdmann. 2015. 'Distinct Pores for Peroxisomal Import of PTS1 and PTS2 Proteins'. *Cell Reports* 13 (10): 2126–34. https://doi.org/10.1016/j.celrep.2015.11.016.

Mukai, Satoru, and Yukio Fujiki. 2006. 'Molecular Mechanisms of Import of Peroxisome-Targeting Signal Type 2 (PTS2) Proteins by PTS2 Receptor Pex7p and PTS1 Receptor Pex5pL *'. *Journal of Biological Chemistry* 281 (49): 37311–20. https://doi.org/10.1074/jbc.M607178200.

Nair, Devi M., P. Edward Purdue, and Paul B. Lazarow. 2004. 'Pex7p Translocates in and out of Peroxisomes in Saccharomyces Cerevisiae'. *Journal of Cell Biology* 167 (4): 599–604. https://doi.org/10.1083/jcb.200407119.

Naumowicz, Monika, and Zbigniew Artur Figaszewski. 2013. 'Pore Formation in Lipid Bilayer Membranes Made of Phosphatidylcholine and Cholesterol Followed by Means of Constant Current'. *Cell Biochemistry and Biophysics* 66 (1): 109–19. https://doi.org/10.1007/s12013-012-9459-6.

Neufeld, Christian, Fabian V Filipp, Bernd Simon, Alexander Neuhaus, Nicole Schüller, Christine David, Hamed Kooshapur, et al. 2009. 'Structural Basis for Competitive Interactions of Pex14 with the Import Receptors Pex5 and Pex19'. *The EMBO Journal* 28 (6): 745–54. https://doi.org/10.1038/emboj.2009.7.

Neuhaus, Alexander, Hamed Kooshapur, Janina Wolf, N. Helge Meyer, Tobias Madl, Jürgen Saidowsky, Eva Hambruch, et al. 2014. 'A Novel Pex14 Protein-Interacting Site of Human Pex5 Is Critical for Matrix Protein Import into Peroxisomes * ◆ '. *Journal of Biological Chemistry* 289 (1): 437–48. https://doi.org/10.1074/jbc.M113.499707.

Nicolay, K., M. Veenhuis, A. C. Douma, and W. Harder. 1987. 'A 31P NMR Study of the Internal pH of Yeast Peroxisomes'. *Archives of Microbiology* 147 (1): 37–41. https://doi.org/10.1007/BF00492902.

Nuttall, James M., Alison M. Motley, and Ewald H. Hettema. 2014. 'Deficiency of the Exportomer Components Pex1, Pex6, and Pex15 Causes Enhanced Pexophagy in Saccharomyces Cerevisiae'. *Autophagy* 10 (5): 835–45. https://doi.org/10.4161/auto.28259.

Ogura, Teru, and Anthony J. Wilkinson. 2001. 'AAA+ Superfamily ATPases: Common Structure–Diverse Function'. *Genes to Cells* 6 (7): 575–97. https://doi.org/10.1046/j.1365-2443.2001.00447.x.

Oliveira, Márcia E. M, Carlos Reguenga, Alexandra M. M Gouveia, Carla P Guimarães, Wolfgang Schliebs, Wolf-H Kunau, Manuel T Silva, Clara Sá-Miranda, and Jorge E Azevedo. 2002. 'Mammalian Pex14p: Membrane Topology and Characterisation of the Pex14p–Pex14p Interaction'. *Biochimica et Biophysica Acta (BBA) - Biomembranes* 1567 (December): 13–22. https://doi.org/10.1016/S0005-2736(02)00635-1.

Otera, Hidenori, and Yukio Fujiki. 2012. 'Pex5p Imports Folded Tetrameric Catalase by Interaction with Pex13p'. *Traffic (Copenhagen, Denmark)* 13 (10): 1364–77. https://doi.org/10.1111/j.1600-0854.2012.01391.x.

Otera, Hidenori, Tomoyuki Harano, Masanori Honsho, Kamran Ghaedi, Satoru Mukai, Atsushi Tanaka, Atsushi Kawai, Nobuhiro Shimizu, and Yukio Fujiki. 2000. 'The Mammalian Peroxin Pex5pL, the Longer Isoform of the Mobile Peroxisome Targeting Signal (PTS) Type 1 Transporter, Translocates the Pex7p·PTS2 Protein Complex into Peroxisomes via Its Initial Docking Site, Pex14p *'. *Journal of Biological Chemistry* 275 (28): 21703–14. https://doi.org/10.1074/jbc.M000720200.

Otera, Hidenori, Kiyoko Setoguchi, Maho Hamasaki, Toshitaka Kumashiro, Nobuhiro Shimizu, and Yukio Fujiki. 2002. 'Peroxisomal Targeting Signal Receptor Pex5p Interacts with Cargoes and Import Machinery Components in a Spatiotemporally Differentiated Manner: Conserved Pex5p WXXXF/Y Motifs Are Critical for Matrix Protein Import'. *Molecular and Cellular Biology* 22 (6): 1639–55. https://doi.org/10.1128/MCB.22.6.1639-1655.2002.

Ott, Julia, Jessica Sehr, Nadine Schmidt, Wolfgang Schliebs, and Ralf Erdmann. 2023. 'Comparison of Human PEX Knockout Cell Lines Suggests a Dual Role of PEX1 in Peroxisome Biogenesis'. *Biological Chemistry* 404 (2–3): 209–19. https://doi.org/10.1515/hsz-2022-0223.

Pan, Dongqing, Toru Nakatsu, and Hiroaki Kato. 2013. 'Crystal Structure of Peroxisomal Targeting Signal-2 Bound to Its Receptor Complex Pex7p-Pex21p'. *Nature Structural & Molecular Biology* 20 (8): 987–93. https://doi.org/10.1038/nsmb.2618.

Pedrosa, Ana G., Tânia Francisco, Diana Bicho, Ana F. Dias, Aurora Barros-Barbosa, Vera Hagmann, Gabriele Dodt, Tony A. Rodrigues, and Jorge E. Azevedo. 2018. 'Peroxisomal Monoubiquitinated PEX5 Interacts with the AAA ATPases PEX1 and PEX6 and Is Unfolded during Its Dislocation into the Cytosol'. *Journal of Biological Chemistry* 293 (29): 11553–63. https://doi.org/10.1074/jbc.RA118.003669.

Pedrosa, Ana G., Tânia Francisco, Maria J. Ferreira, Tony A. Rodrigues, Aurora Barros-Barbosa, and Jorge E. Azevedo. 2019. 'A Mechanistic Perspective on PEX1 and PEX6, Two AAA+ Proteins of the Peroxisomal Protein Import Machinery'. *International Journal of Molecular Sciences* 20 (21): 5246. https://doi.org/10.3390/ijms20215246.

Pires, José R., Xinji Hong, Christoph Brockmann, Rudolf Volkmer-Engert, Jens Schneider-Mergener, Hartmut Oschkinat, and Ralf Erdmann. 2003. 'The ScPex13p SH3 Domain Exposes Two Distinct Binding Sites for Pex5p and Pex14p'. *Journal of Molecular Biology* 326 (5): 1427–35. https://doi.org/10.1016/S0022-2836(03)00039-1.

Pitt, Ashley S., and Susan K. Buchanan. 2021. 'A Biochemical and Structural Understanding of TOM Complex Interactions and Implications for Human Health and Disease'. *Cells* 10 (5): 1164. https://doi.org/10.3390/cells10051164.

Platta, Harald W., Stefanie Hagen, and Ralf Erdmann. 2013. 'The Exportomer: The Peroxisomal Receptor Export Machinery'. *Cellular and Molecular Life Sciences: CMLS* 70 (8): 1393–1411. https://doi.org/10.1007/s00018-012-1136-9.

Rabinovich, Efrat, Anat Kerem, Kai-Uwe Fröhlich, Noam Diamant, and Shoshana Bar-Nun. 2002. 'AAA-ATPase P97/Cdc48p, a Cytosolic Chaperone Required for Endoplasmic Reticulum-Associated Protein Degradation'. *Molecular and Cellular Biology* 22 (2): 626–34. https://doi.org/10.1128/MCB.22.2.626-634.2002.

Ravindran, Rini, Isabel O. L. Bacellar, Xavier Castellanos-Girouard, Haytham M. Wahba, Zhenghao Zhang, James G. Omichinski, Lydia Kisley, and Stephen W. Michnick. 2023. 'Peroxisome Biogenesis Initiated by Protein Phase Separation'. *Nature* 617 (7961): 608–15. https://doi.org/10.1038/s41586-023-06044-1.

Rayapuram, Naganand, and Suresh Subramani. 2006. 'The Importomer—A Peroxisomal Membrane Complex Involved in Protein Translocation into the Peroxisome Matrix'. *Biochimica et Biophysica Acta (BBA) - Molecular Cell Research*, Peroxisomes: Morphology, Function, Biogenesis and Disorders, 1763 (12): 1613–19. https://doi.org/10.1016/j.bbamcr.2006.08.035.

Reguenga, C., M. E. Oliveira, A. M. Gouveia, C. Sá-Miranda, and J. E. Azevedo. 2001. 'Characterization of the Mammalian Peroxisomal Import Machinery: Pex2p, Pex5p, Pex12p, and Pex14p Are Subunits of the Same Protein Assembly'. *The Journal of Biological Chemistry* 276 (32): 29935–42. https://doi.org/10.1074/jbc.M104114200.

Reuter, Maren, Hamed Kooshapur, Jeff-Gordian Suda, Stefan Gaussmann, Alexander Neuhaus, Lena Brühl, Pratima Bharti, et al. 2021. 'Competitive Microtubule Binding of PEX14 Coordinates Peroxisomal Protein Import and Motility'. *Journal of Molecular Biology* 433 (5): 166765. https://doi.org/10.1016/j.jmb.2020.166765.

Rinaldi, Mauro A., Wendell A. Fleming, Kim L. Gonzalez, Jaeseok Park, Meredith J. Ventura, Ashish B. Patel, and Bonnie Bartel. 2017. 'The PEX1 ATPase Stabilizes PEX6 and Plays Essential Roles in Peroxisome Biology'. *Plant Physiology* 174 (4): 2231. https://doi.org/10.1104/pp.17.00548.

Rüttermann, Maximilian, and Christos Gatsogiannis. 2023. 'Good Things Come to Those Who Bait: The Peroxisomal Docking Complex'. *Biological Chemistry* 404 (2–3): 107–19. https://doi.org/10.1515/hsz-2022-0161.

Saidowsky, J., G. Dodt, K. Kirchberg, A. Wegner, W. Nastainczyk, W. H. Kunau, and W. Schliebs. 2001. 'The Di-Aromatic Pentapeptide Repeats of the Human Peroxisome Import Receptor PEX5 Are Separate High Affinity Binding Sites for the Peroxisomal Membrane Protein PEX14'. *The Journal of Biological Chemistry* 276 (37): 34524–29. https://doi.org/10.1074/jbc.M104647200.

Salomons, Florian A., Jan A. K. W. Kiel, Klaas Nico Faber, Marten Veenhuis, and Ida J. van der Klei. 2000. 'Overproduction of Pex5p Stimulates Import of Alcohol Oxidase and Dihydroxyacetone Synthase in a Hansenula Polymorpha pex14Null Mutant *'. *Journal of Biological Chemistry* 275 (17): 12603–11. https://doi.org/10.1074/jbc.275.17.12603.

Sargent, Graeme, Tim van Zutphen, Tatiana Shatseva, Ling Zhang, Valeria Di Giovanni, Robert Bandsma, and Peter Kijun Kim. 2016. 'PEX2 Is the E3 Ubiquitin Ligase Required for Pexophagy during Starvation'. *Journal of Cell Biology* 214 (6): 677–90. https://doi.org/10.1083/jcb.201511034.

Sauer, Robert T., Daniel N. Bolon, Briana M. Burton, Randall E. Burton, Julia M. Flynn, Robert A. Grant, Greg L. Hersch, et al. 2004. 'Sculpting the Proteome with AAA+ Proteases and Disassembly Machines'. *Cell* 119 (1): 9–18. https://doi.org/10.1016/j.cell.2004.09.020.

Schäfer, Antje, Daniela Kerssen, Marten Veenhuis, Wolf-H. Kunau, and Wolfgang Schliebs. 2004. 'Functional Similarity between the Peroxisomal PTS2 Receptor Binding Protein Pex18p and the N-Terminal Half of the PTS1 Receptor Pex5p'. *Molecular and Cellular Biology* 24 (20): 8895–8906. https://doi.org/10.1128/MCB.24.20.8895-8906.2004.

Schlegel, Thomas, Oliver Mirus, Arndt von Haeseler, and Enrico Schleiff. 2007. 'The Tetratricopeptide Repeats of Receptors Involved in Protein Translocation across Membranes'. *Molecular Biology and Evolution* 24 (12): 2763–74. https://doi.org/10.1093/molbev/msm211.

Schliebs, W., J. Saidowsky, B. Agianian, G. Dodt, F. W. Herberg, and W. H. Kunau. 1999. 'Recombinant Human Peroxisomal Targeting Signal Receptor PEX5. Structural Basis for Interaction of PEX5 with PEX14'. *The Journal of Biological Chemistry* 274 (9): 5666–73. https://doi.org/10.1074/jbc.274.9.5666.

Serra-Batiste, Montserrat, Martí Ninot-Pedrosa, Mariam Bayoumi, Margarida Gairí, Giovanni Maglia, and Natàlia Carulla. 2016. 'Aβ42 Assembles into Specific β-Barrel Pore-Forming Oligomers in Membrane-Mimicking Environments'. *Proceedings of the National Academy of Sciences* 113 (39): 10866–71. https://doi.org/10.1073/pnas.1605104113.

Shimizu, N., R. Itoh, Y. Hirono, H. Otera, K. Ghaedi, K. Tateishi, S. Tamura, et al. 1999. 'The Peroxin Pex14p. cDNA Cloning by Functional Complementation on a Chinese Hamster Ovary Cell Mutant, Characterization, and Functional Analysis'. *The Journal of Biological Chemistry* 274 (18): 12593–604. https://doi.org/10.1074/jbc.274.18.12593.

Shiozawa, Kumiko, Petr V. Konarev, Christian Neufeld, Matthias Wilmanns, and Dmitri I. Svergun. 2009. 'Solution Structure of Human Pex5.Pex14. PTS1 Protein Complexes Obtained by Small Angle X-Ray Scattering'. *The Journal of Biological Chemistry* 284 (37): 25334–42. https://doi.org/10.1074/jbc.M109.002311.

Skowyra, Michael L., and Tom A. Rapoport. 2022a. 'PEX5 Translocation into and out of Peroxisomes Drives Matrix Protein Import'. *Molecular Cell* 82 (17): 3209-3225.e7. https://doi.org/10.1016/j.molcel.2022.07.004.

Smart, O. S., J. Breed, G. R. Smith, and M. S. Sansom. 1997. 'A Novel Method for Structure-Based Prediction of Ion Channel Conductance Properties'. *Biophysical Journal* 72 (3): 1109–26. https://doi.org/10.1016/S0006-3495(97)78760-5.

Stanley, Will A., Fabian V. Filipp, Petri Kursula, Nicole Schüller, Ralf Erdmann, Wolfgang Schliebs, Michael Sattler, and Matthias Wilmanns. 2006. 'Recognition of a Functional Peroxisome Type 1 Target by the Dynamic Import Receptor Pex5p'. *Molecular Cell* 24 (5): 653–63. https://doi.org/10.1016/j.molcel.2006.10.024.

Stanley, Will A., Niko V. Pursiainen, Elspeth F. Garman, André H. Juffer, Matthias Wilmanns, and Petri Kursula. 2007. 'A Previously Unobserved Conformation for the Human Pex5p Receptor Suggests Roles for Intrinsic Flexibility and Rigid Domain Motions in Ligand Binding'. *BMC Structural Biology* 7 (April): 24. https://doi.org/10.1186/1472-6807-7-24.

Stewart, M. Q., R. D. Esposito, J. Gowani, and J. M. Goodman. 2001. 'Alcohol Oxidase and Dihydroxyacetone Synthase, the Abundant Peroxisomal Proteins of Methylotrophic Yeasts, Assemble in Different Cellular Compartments'. *Journal of Cell Science* 114 (Pt 15): 2863–68. https://doi.org/10.1242/jcs.114.15.2863.

Su, Jian-Rong, Kazuki Takeda, Shigehiko Tamura, Yukio Fujiki, and Kunio Miki. 2009. 'Crystal Structure of the Conserved N-Terminal Domain of the Peroxisomal Matrix Protein Import Receptor, Pex14p'. *Proceedings of the National Academy of Sciences* 106 (2): 417–21. https://doi.org/10.1073/pnas.0808681106.

Subramani, Suresh. 1992. 'Targeting of Proteins into the Peroxisomal Matrix'. *The Journal of Membrane Biology* 125 (2): 99–106. https://doi.org/10.1007/BF00233350.

Tamura, Shigehiko, Naomi Matsumoto, Ryota Takeba, and Yukio Fujiki. 2014. 'AAA Peroxins and Their Recruiter Pex26p Modulate the Interactions of Peroxins Involved in Peroxisomal Protein Import *'. *Journal of Biological Chemistry* 289 (35): 24336–46. https://doi.org/10.1074/jbc.M114.588038.

Tamura, Shigehiko, Shinobu Yasutake, Naomi Matsumoto, and Yukio Fujiki. 2006. 'Dynamic and Functional Assembly of the AAA Peroxins, Pex1p and Pex6p, and Their Membrane Receptor Pex26p'. *The Journal of Biological Chemistry* 281 (38): 27693–704. https://doi.org/10.1074/jbc.M605159200.

Titorenko, Vladimir I., Jean-Marc Nicaud, Huijie Wang, Honey Chan, and Richard A. Rachubinski. 2002. 'Acyl-CoA Oxidase Is Imported as a Heteropentameric, Cofactor-Containing Complex into Peroxisomes of Yarrowia Lipolytica'. *The Journal of Cell Biology* 156 (3): 481–94. https://doi.org/10.1083/jcb.200111075.

Truscott, K. N., P. Kovermann, A. Geissler, A. Merlin, M. Meijer, A. J. Driessen, J. Rassow, N. Pfanner, and R. Wagner. 2001. 'A Presequence- and Voltage-Sensitive Channel of the Mitochondrial Preprotein Translocase Formed by Tim23'. *Nature Structural Biology* 8 (12): 1074–82. https://doi.org/10.1038/nsb726.

Vasic, Vedran, Niels Denkert, Claudia C. Schmidt, Dietmar Riedel, Alexander Stein, and Michael Meinecke. 2020. 'Hrd1 Forms the Retrotranslocation Pore Regulated by Auto-Ubiquitination and Binding of Misfolded Proteins'. *Nature Cell Biology* 22 (3): 274–81. https://doi.org/10.1038/s41556-020-0473-4.

Voorn, Loesje van der, and Hidde L. Ploegh. 1992. 'The WD-40 Repeat'. *FEBS Letters* 307 (2): 131–34. https://doi.org/10.1016/0014-5793(92)80751-2.

Walter, Thomas, and Ralf Erdmann. 2019. 'Current Advances in Protein Import into Peroxisomes'. *The Protein Journal* 38 (3): 351–62. https://doi.org/10.1007/s10930-019-09835-6.

Walton, P. A., P. E. Hill, and S. Subramani. 1995. 'Import of Stably Folded Proteins into Peroxisomes'. *Molecular Biology of the Cell* 6 (6): 675–83. https://doi.org/10.1091/mbc.6.6.675.

Wanders, Ronald J. A., Myriam Baes, Daniela Ribeiro, Sacha Ferdinandusse, and Hans R. Waterham. 2023. 'The Physiological Functions of Human Peroxisomes'. *Physiological Reviews* 103 (1): 957–1024. https://doi.org/10.1152/physrev.00051.2021.

Wanders, Ronald J. A., and Hans R. Waterham. 2006. 'Biochemistry of Mammalian Peroxisomes Revisited'. *Annual Review of Biochemistry* 75: 295–332. https://doi.org/10.1146/annurev.biochem.74.082803.133329.

Wang, Dongyuan, Nina V. Visser, Marten Veenhuis, and Ida J. van der Klei. 2003. 'Physical Interactions of the Peroxisomal Targeting Signal 1 Receptor Pex5p, Studied by Fluorescence Correlation Spectroscopy*'. *Journal of Biological Chemistry* 278 (44): 43340–45. https://doi.org/10.1074/jbc.M307789200.

Wang, Jiao-Yu, Ling Li, Rong-Yao Chai, Hai-Ping Qiu, Zhen Zhang, Yan-Li Wang, Xiao-Hong Liu, Fu-Cheng Lin, and Guo-Chang Sun. 2019. 'Pex13 and Pex14, the Key Components of the Peroxisomal Docking Complex, Are Required for Peroxisome Formation, Host Infection and Pathogenicity-

Related Morphogenesis in Magnaporthe Oryzae'. *Virulence* 10 (1): 292–314. https://doi.org/10.1080/21505594.2019.1598172.

Wang, Wei, and Suresh Subramani. 2017. 'Role of PEX5 Ubiquitination in Maintaining Peroxisome Dynamics and Homeostasis'. *Cell Cycle* 16 (21): 2037–45. https://doi.org/10.1080/15384101.2017.1376149.

Waterham, Hans R., Sacha Ferdinandusse, and Ronald J. A. Wanders. 2016. 'Human Disorders of Peroxisome Metabolism and Biogenesis'. *Biochimica et Biophysica Acta (BBA) - Molecular Cell Research*, Assembly, Maintenance and Dynamics of Peroxisomes, 1863 (5): 922–33. https://doi.org/10.1016/j.bbamcr.2015.11.015.

Will, G. K., M. Soukupova, X. Hong, K. S. Erdmann, J. A. Kiel, G. Dodt, W. H. Kunau, and R. Erdmann. 1999. 'Identification and Characterization of the Human Orthologue of Yeast Pex14p'. *Molecular and Cellular Biology* 19 (3): 2265–77. https://doi.org/10.1128/MCB.19.3.2265.

Williams, Chris, and Ben Distel. 2006. 'Pex13p: Docking or Cargo Handling Protein?' *Biochimica Et Biophysica Acta* 1763 (12): 1585–91. https://doi.org/10.1016/j.bbamcr.2006.09.007.

Woodward, Andrew W., and Bonnie Bartel. 2005. 'The Arabidopsis Peroxisomal Targeting Signal Type 2 Receptor PEX7 Is Necessary for Peroxisome Function and Dependent on PEX5'. *Molecular Biology of the Cell* 16 (2): 573–83. https://doi.org/10.1091/mbc.e04-05-0422.

Yamashita, Koichiro, Shigehiko Tamura, Masanori Honsho, Hiroto Yada, Yuichi Yagita, Hidetaka Kosako, and Yukio Fujiki. 2020. 'Mitotic Phosphorylation of Pex14p Regulates Peroxisomal Import Machinery'. *Journal of Cell Biology* 219 (10): e202001003. https://doi.org/10.1083/jcb.202001003.

Yang, Jing, Laurent Pieuchot, and Gregory Jedd. 2018. 'Artificial Import Substrates Reveal an Omnivorous Peroxisomal Importomer'. *Traffic* 19 (10): 786–97. https://doi.org/10.1111/tra.12607.

Yang, X., P. E. Purdue, and P. B. Lazarow. 2001. 'Eci1p Uses a PTS1 to Enter Peroxisomes: Either Its Own or That of a Partner, Dci1p'. *European Journal of Cell Biology* 80 (2): 126–38. https://doi.org/10.1078/0171-9335-00144.

Yu, Wen-ying, Mei Lin, Hui-juan Yan, Jia-jia Wang, Sheng-min Zhang, Guo-dong Lu, Zong-hua Wang, and SHIM Won-Bo. 2022. 'The Peroxisomal Matrix Shuttling Receptor Pex5 Plays a Role in FB1 Production and Virulence in Fusarium Verticillioides'. *Journal of Integrative Agriculture* 21 (10): 2957–72. https://doi.org/10.1016/j.jia.2022.07.044.

Zeytuni, Natalie, and Raz Zarivach. 2012. 'Structural and Functional Discussion of the Tetra-Trico-Peptide Repeat, a Protein Interaction Module'. *Structure* 20 (3): 397–405. https://doi.org/10.1016/j.str.2012.01.006.

Zhang, Jingdong, Qijin Chi, Bailin Zhang, Shaojun Dong, and Erkang Wang. 1998. 'Molecular Characterization of Beef Liver Catalase by Scanning Tunneling Microscopy'. *Electroanalysis* 10 (11): 738–46. https://doi.org/10.1002/(SICI)1521-4109(199809)10:11<738

Zimmerberg, J., F. S. Cohen, and A. Finkelstein. 1980. 'Fusion of Phospholipid Vesicles with Planar Phospholipid Bilayer Membranes. I. Discharge of Vesicular Contents across the Planar Membrane'. *The Journal of General Physiology* 75 (3): 241–50. https://doi.org/10.1085/jgp.75.3.241.

Chapter 2

An Electrophysiological Exploration of the HRD Complex

2.1 Introduction

2.1.1 Translocation of Proteins Across the ER Membrane

In eukaryotic cells, many extracellular and soluble organellar proteins are synthesized on cytosolic ribosomes and translocated to the ER, where they are being folded into their tertiary or quaternary conformation before being transported to their destined organelle. Secretory and resident proteins of the plasma membrane, Golgi apparatus, lysosomes and endosomal compartment are also folded in the ER (Zimmermann et al. 2011; Rapoport, Li, and Park 2017; Sun and Brodsky 2019). ER proteins are synthesized as preproteins and are distinguished by the presence of an amino acid signal peptide. The translocation of secretory proteins synthesized on cytosolic ribosomes happens co-translationally or post-translationally at the ER through translocation machinery known as Sec61 translocon (Rapoport 2007; Zimmermann et al. 2011; Fewell and Brodsky 2013).

In the co-translational pathway, preproteins synthesized on cytosolic ribosomes require an additional signal recognition particle (SRP) which recognizes the signal peptide on the preprotein emerging from the translating ribosome. The SRP is a cytoplasmic ribonucleoprotein complex (48 kD) which has high affinity for GTP when bound to a signal peptide. Upon GTP binding, and then it is recognized by its receptor at the ER membrane. Preproteins are then translocated to the ER lumen through the Sec61 translocon and release of the preprotein into the ER lumen require under hydrolysis of GTPGTP hydrolysis. (Kalies and Hartmann 1998; Agarraberes and Dice 2001). In the post-translational pathway, fully translated preproteins associate with the chaperone Hsp70 and its co chaperone Hsp40 in the cytosol and translocate through the Sec61 translocon (Larburu et al. 2020). After the translocation of preproteins, the signal peptide is cleaved by signal peptidases for cleavable signals and then the polypeptide is folded by molecular chaperones in a thermodynamically favourable manner (Balchin, Hayer-Hartl, and Hartl 2016). Following folding and assembly, with the exception of resident ER proteins, all other proteins are transferred to the Golgi apparatus or their functional site within the secretory pathway through vesicular transport following folding and assembly.

2.1.2 Protein folding in the ER

An integrated network of molecular chaperones consisting of protein disulphide isomerase (PDI/PDIA) and the oxidizing environment of the ER lumen helps in folding of the nascent polypeptide chain by formation of disulphide bonds in the ER (Graner, Lillehei, and Katsanis 2015). N-linked glycosylation is another crucial co-translational modification which takes place in the ER, since N-linked glycoproteins account for the vast majority of secretory proteins. Glycosylation involves the attachment of the pre-assembled oligosaccharide on the polypeptide chain which can protect the polypeptide chain from aggregating and also act as a recognition signal for further post translational modifications in the Golgi apparatus (Lederkremer 2009).

2.1.3 Protein quality control in the ER

Protein folding is an energy-intensive process that requires coordination between proteins in many cellular compartments, as well as resources from several metabolic pathways. In the ER, its efficiency is extremely susceptible to changes in intracellular conditions or external stimuli. Consequently, any alterations in ER homeostasis can result in protein misfolding and an overwhelming accumulation of misfolded or unfolded proteins, a state known as ER stress (M. Wang and Kaufman 2016). This makes protein folding an error prone process and when proteins are partly folded or misfolded, hydrophobic amino acids and unstructured areas are exposed to the surrounding environment. As a result of these exposed residues, the proteins may aggregate contributing to ER stress (Balchin, Hayer-Hartl, and Hartl 2016).

Protein aggregates also impede normal cellular function causing several well-known disorders such as Alzheimer's, Parkinson's, and Huntington's illnesses, as well as prion diseases, amyloidosis, cystic fibrosis, and type 2 diabetes. Each condition is distinguished by the accumulation of misfolded proteins in different tissues, which results in distinct symptoms and organ failure (R. V. Rao and Bredesen 2004; Hartl 2017). Understanding and correcting protein misfolding are crucial areas of current investigations in the hunt for viable therapeutics for these lethal disorders.

Protein folding in the ER is a highly controlled process monitored by ER quality control (ERQC) mechanisms to prevent the accumulation of abnormal secretory and membrane proteins (Ellgaard and Helenius 2003). The cell has its own machinery to maintain protein homeostasis and to guarantee normal protein folding during ER stress, which can initiate a cascade of cellular events known as the unfolded protein response (UPR) to counteract the accumulation of unfolded protein. This adaptive response tries to restore ER function and relieve ER stress by increasing expression of chaperone

proteins to assist correct folding and by lowering overall protein production to reduce the strain on the ER (Read and Schröder 2021). In addition to its involvement in protein folding and quality control, the unfolded Protein Response (UPR) coordinates with another protein quality control mechanism known as ER-associated protein degradation (ERAD) by upregulating its components under ER stress (Tsai and Weissman 2010). ERAD is responsible for recognizing misfolded proteins in the ER membrane or lumen and extracting them in an energy-dependent manner through membrane pores for transport to cytosolic proteasomes. Protein extraction via ER membrane pores is referred to as dislocation or retrotranslocation (Hampton and Sommer 2012; Byun et al. 2014). During ER stress, the UPR increases the production of particular ERAD components, such as E3 ubiquitin ligases and the retrotranslocation machinery, to identify and retrieve misfolded proteins from the ER. These misfolded proteins are then polyubiquitinated, which targets them for proteasomal degradation (Hwang and Qi 2018). Working together, the UPR and ERAD provide a key quality control mechanism, assuring the clearance of aberrant proteins from the ER and limiting the accumulation of toxic aggregates that might impair cellular function. Under varied physiological and pathological situations, the tight control and coordination of the UPR and ERAD are critical for sustaining ER proteostasis and cellular health.

2.1.4 ERAD pathway

ERAD is an evolutionarily conserved process, through which misfolded proteins are retrotranslocated from the ER lumen to the cytosol as shown in Figure 2.1. To target misfolded proteins for degradation, the ERAD pathway includes the ubiquitin-proteasome pathway (described in section 2.1.5), which marks the substrates on the cytosolic surface of the ER by covalent attachment of polyubiquitin chains, leading to identification and degradation of the protein by the 26S proteasome. Before the protein can be degraded by the proteasome, it has to be extracted from the ER membrane. The energy for extraction of the substrate is provided by a cytosolic chaperone, the AAA ATPase known as Cdc48 in yeast, or p97 in mammals (Rabinovich et al. 2002).

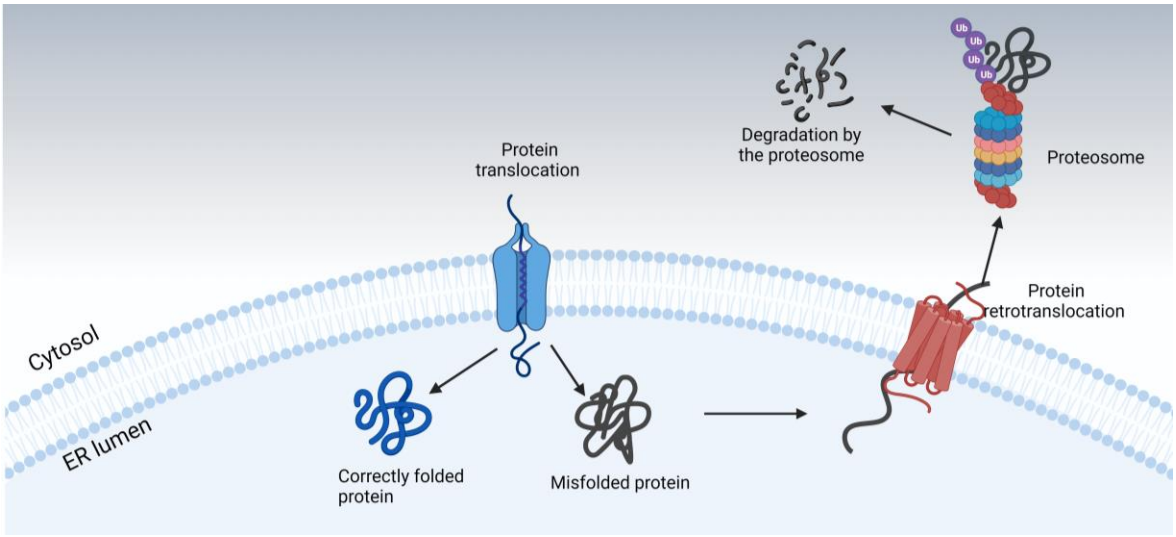

Figure 2.1 The ERAD pathway for degradation of misfolded ER proteins. The protein translocon import proteins to the ER lumen where they are folded to their native confirmation or misfolded. ERAD initiation occurs when quality control receptors recognize misfolded proteins as abnormal molecules. Terminally misfolded or unassembled proteins are sorted to an ER-membrane-associated retrotranslocation/ubiquitination complex with adaptor proteins recognizing the ERAD substrate. A translocon facilitates retrotranslocation of a protein to the cytosol, often accompanied by ubiquitination by an ER-associated E3 ubiquitin ligase. Then the ERAD substrate is extracted from the ER and prepared for proteasomal degradation in the cytosol. Created with BioRender.com

Integral membrane proteins constitute a key class of ERAD substrates with segments in the lumen and the cytosol**.** Based on the misfolded substrates, the ERAD route has been divided into three distinct pathways in yeast: ERAD-L, ERAD-M, and ERAD-C (Figure 2.2). The location of the misfolded domain inside the ER—whether in the lumen (L), within the membrane (M), or on the cytosolic side (C)—determines these routes (Huyer et al. 2004; Carvalho, Goder, and Rapoport 2006; Vembar and Brodsky 2008). ERAD-L substrates — either soluble or integral membrane proteins with misfolded protein domain in the ER lumen — interact with the Hrd1 ubiquitin ligase complex. ERAD-C substrates rely on a complex containing the Doa10 ubiquitin ligase. The ERAD-M route is far less well understood, although its substrates appear to be ubiquitylated by the HRD complex as well (Vembar and Brodsky 2008; Hampton and Sommer 2012).

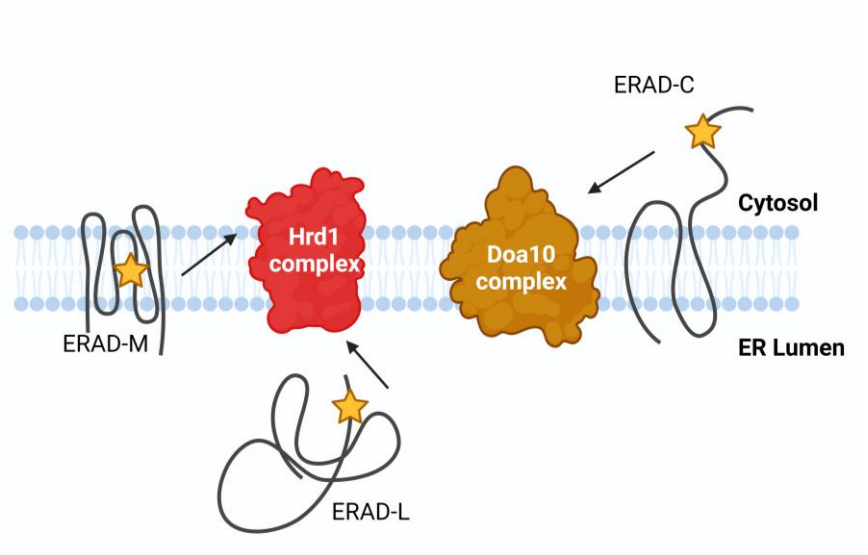

Figure 2.2: Schematic representation of the different divisions of yeast ERAD. ERAD-L encompasses substrates with defects in the luminal region, ERAD-M involves substrates with defects in the membrane region, and ERAD-C focuses on substrates with defects in the cytosolic region. The Hrd1 complex is involved in ERAD-L and ERAD-M pathways, while the Doa10 complex is specific to the ERAD-C pathway. Created with BioRender.com

2.1.5 The Ubiquitin-proteasome pathway

The ubiquitin-proteasome system is a critical intracellular protein degradation machinery that regulates many cellular activities. The process begins with the covalent attachment of ubiquitin, a small 8.6kD protein (76 amino acids), to the target protein. A cascade of enzymes, including E1 (ubiquitin-activating enzyme), E2 (ubiquitin-conjugating enzyme), and E3 (ubiquitin ligase), carry out this ubiquitination (Pickart and Eddins 2004) (Figure 2.3). Firstly, Ubiquitin is activated by an ATP-dependent process that generates a thioester bond between the active site cysteine of the E1 and the C-terminus of ubiquitin (Hershko and Ciechanover 1998). The activated ubiquitin molecule is then transferred from the E1 cystine to a cystine residue on the E2 enzyme. Then the E3 ligase binds both, the substrate protein and E2, and transfers ubiquitin from the E2 enzyme to a lysine or an N terminal methionine on the substrate. This step can be performed perpetually to generate a chain of ubiquitins (Hershko and Ciechanover 1998). Ubiquitin can be linked to polyubiquitin chains by any of its seven lysine residues (K6, K11, K27, K29, K33, K48, or K63) as well as the amino group of M1 (Akutsu, Dikic, and Bremm 2016). The K48 chains are specifically involved in proteasomal degradation. Finally, the 26S proteasome, a huge protein complex with proteolytic activity, recognizes the ubiquitinated protein. The 26S proteasome consist of a cylindrical 20S core particle that contain the proteolytic active site and a 19S regulatory particle, which sits on both ends of the core particle and consists of

base and lid subassemblies. Three ubiquitin receptors, the scaffolding protein, and six AAA+ ATPase subunits create a heterohexameric ring-shaped motor in the base subassembly which can interact with K48-linked chains and insert substrate into the core particle. The lid subassembly contains a crucial deubiquitinating enzyme (DUB) which makes ubiquitin conjugation to target substrates, a reversible process. DUBs remove the ubiquitin molecules from the substrate and split the ubiquitin chain into ubiquitin monomers in order to attach to the E1 enzymes anew (Chen et al. 2021; Snyder and Silva 2021). The proteasome then unfolds the ubiquitinated protein and degrades it into smaller peptides, releasing ubiquitin for reuse (A. L. Schwartz and Ciechanover 2009; Gong et al. 2016).

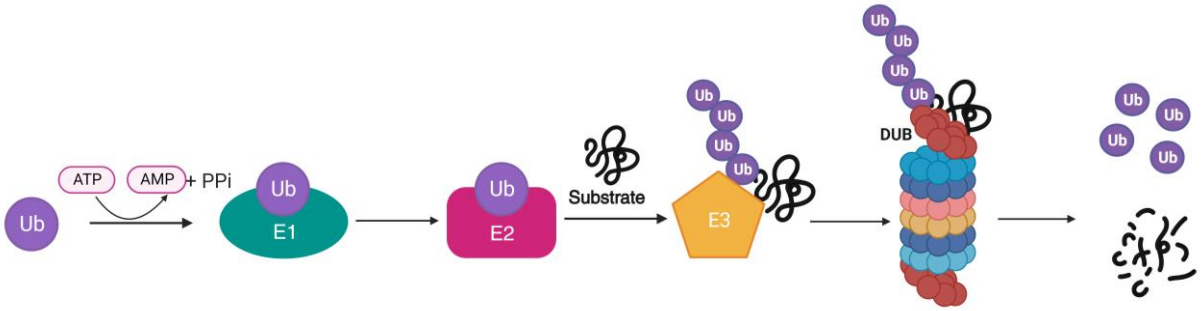

Figure 2.3 Illustration of the ubiquitin-proteasome system (UPS). Ubiquitin-activating enzyme (E1) initiates the ubiquitination process by activating ubiquitin (Ub) through an energy-driven ATP-dependent reaction. Activated ubiquitin is then transferred to the target protein by the ubiquitin-conjugating enzyme (E2) and ubiquitin ligase (E3) enzyme. Finally, protein degradation occurs through recognition by the proteasome, resulting in the breakdown of the polyubiquitinated protein into smaller peptides and amino acids. Polyubiquitin molecules are removed by deubiquitinating enzymes (DUBs) to complete the UPS cycle, ready for recycling and subsequent rounds of ubiquitination (adapted from Bachiller et al. 2020). Created with BioRender.com

E3 ligases target a wide range of substrates for ubiquitination involved in a variety of cellular activities such as signalling, DNA repair, ER stress and programmed cell death (Humphreys et al. 2021; Cabana and Lussier 2022). E3 ligases are classified into three types based on their catalytic domain: Really Interesting New Gene (RING), Homologous to E6-AP Carboxyl Terminus (HECT), or Ring-Between-Ring (RBR) (Zheng and Shabek 2017). Among these three, only the RING E3 ligase catalyses direct ubiquitin transfer from E2 to the substrate, while HECT and RBR ligases engage in the formation of a thioester intermediate by binding ubiquitin prior to the subsequent transfer of ubiquitin to the substrate. (Riley et al. 2013; George et al. 2018). It is noteworthy that in the human genome, there exist over 600 genes encoding for E3 ligases, whereas the number of genes encoding E2 enzymes is only 30-50. In yeast,

there are 12 E2s and approximately 80 E3s, which suggests the necessity of ubiquitination for a diverse array of substrates. (George et al. 2018; M. D. Stewart et al. 2016).

2.1.6 ERAD-L pathway in Saccharomyces cerevisiae

2.1.6.1 Substrate Recognition for ERAD-L

The degradation of proteins with misfolded luminal domains in yeast is primarily facilitated by the ERAD-L pathway. Within this system, a significant focus of research lies in the investigation of misfolded N-glycosylated proteins as substrates. N-linked glycosylation is an essential post-translational modification that takes place within the ER of eukaryotic cells. The process entails the incorporation of a pre-assembled oligosaccharide glucose3-mannose9-N-acetylglucosamine2-asparagine ($Glc_3Man_9GlcNAc_2$), which refers to a chain of sugar molecules. This assembly occurs onto particular asparagine residues within an N-X-S or N-X-T sequence within a protein domain that is either unfolded or flexible by the oligosaccharyl transferase complex (OST) during their import into the ER (Helenius and Aebi 2004; Breitling and Aebi 2013). The unfolded state of the protein may be facilitated by the OST complex, which associates with the Sec61 translocon on the luminal side of the ER (Chavan and Lennarz 2006). These oligosaccharides are bulky which causes a stable conformational change in structure of the substrate, bringing two free cystine side chains in close proximity with each other. This lowers the energy barrier for disulfide bond formation by the protein-oxidoreductase PDI1 for glycosylated substrates (Bakshi et al. 2022). Formation of disulfide bonds further stabilizes the substrate and effectively hinder the process of oligosaccharide addition by blocking the access of glycoenzymes or chaperone to oligosaccharides (Allen, Naim, and Bulleid 1995).

The nascent N-glycosylated protein has a three-branch structure with $Glc_3Man_9GlcNAc_2$ (Figure 2.4). The elimination of the initial two glucose residues by glucosidase I on one branch enables interactions with two ER-resident chaperone/lectin proteins, calnexin and calreticulin, which may result in protein folding (Brodsky 2012; Byun et al. 2014). The removal of third glucose by glucosidase II, results in the production of a $Man_9GlcNAc_2$ glycan and causes release from these lectins. Then the folded protein can be transported out of the ER, whereas re-attachment of this glucose by UDP-glucose and glycoprotein glucosyltransferase (GT) permits reassociation of lectins. Yeast lack GT enzymes and additional mannose trimming is required to target the substrate to ERAD. Mannosidase I (Mns1) extracts the -1,2-mannose from the B-branch of the glycan, resulting in the formation of $Man_8GlcNAc_2$ (Jakob et al. 1998). In yeast, the $Man_8GlcNAc_2$ glycan can be found on both correctly folded and

misfolded proteins that exit the ER in COPII (coat promoter II) vesicles. This suggests that Mns1 fails to distinguish between these two types of proteins (Gauss et al. 2011; Sun and Brodsky 2019). Another mannosidase, Htm1 (EDEM in mammals) generates $Man_7GlcNAc_2$ with an exposed -1,6-mannose in order to specifically generate an ERAD glycan signal (Clerc et al. 2009). The protein-oxidoreductase PDI1 is closely connected with Htm1, and Htm1 preferentially processes glycoproteins that have a prolonged engagement with PDI1 as a result of their aberrant conformation (Gauss et al. 2011; Pfeiffer et al. 2016) (Figure 2.4). Proteins try to refold until the elimination of three or four mannose residues which targets these proteins to ERAD. These misfolded glycoproteins are recognized by Yos9 lectins (OS-9 and XTP-3B in mammals). These lectins have an affinity for hydrophobic motifs and transport the substrates to Hrd3, one essential element of the HRD complex (Goot et al. 2018). Mannose-6-phosphate receptor homology (MRH) domain of Yos9 is responsible for identifying the trimmed oligosaccharide on misfolded substrate (Quan et al. 2008). Deletion of *yos9* leads to a slower degradation of several ERAD substrates (Szathmary et al. 2005; W. Kim, Spear, and Ng 2005) indicating its role in recognition of substrates. The substrate is additionally associated with the ER-luminal Hsp70 chaperone Kar2 (BiP in mammals), as well as its Hsp40 cochaperones Scj1 and Jem1 (Jakob et al. 1998; Nishikawa et al. 2001; Gauss et al. 2011). Yos9 can bind to Kar2 and contributes to the maintenance of solubility of misfolded substrates. (Denic, Quan, and Weissman 2006). Multiple attempts are made to refold proteins prior to their classification as ERAD substrates. In this thesis, we used a misfolded form of the yeast vacuolar enzyme carboxypeptidase Y (CPY), called CPY* (G225R), which is a widely accepted model substrate for ERAD-L pathway (Finger, Knop, and Wolf 1993). It was shown that CPY* remained in the ER during vacuolar trafficking, whereas correctly folded WT CPY was carried to the vacuoles via Golgi apparatus (Izawa et al. 2012). To briefly summarize, Yos9 is responsible for recognizing misfolded, glycosylated luminal proteins and localising them to the HRD complex via its interaction with Hrd3, an essential component of the HRD complex.

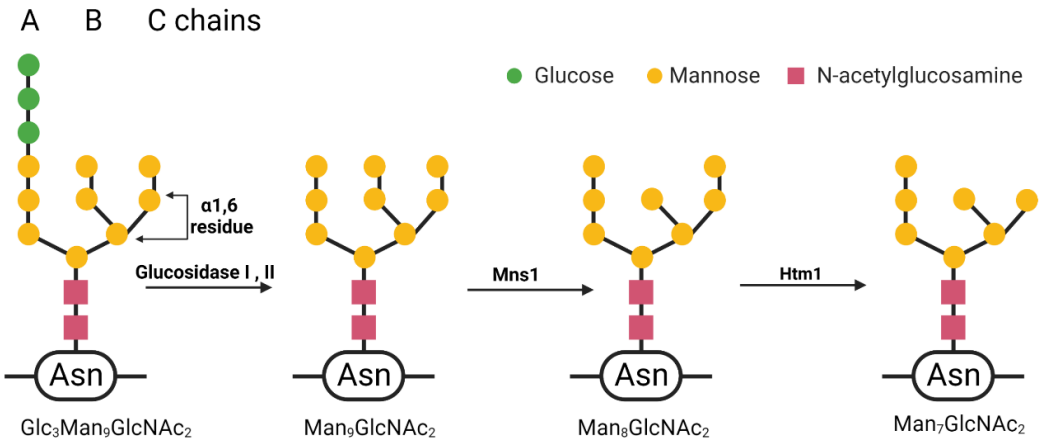

Figure 2.4 caption on the next page

Figure 2.4: Structure of N-Glycans and its processing in ER. The core N-glycan is composed of the A, B and C branches which are attached to an asparagine (Asn) residue on the misfolded substrate. First, the three terminal glucose residues in the branch A, are cleaved by glucosidases 1 and 2. Then mannose in the B branch is cleaved by Mns1, resulting in the formation of $Man_8GlcNAc_2$ glycan. Finally, the cleavage of the terminal mannose residue by Htm1 in the C branch, results in a Man_7 $GlcNAc_2$ glycan which is used as a degradation signal in ERAD for misfolded substrates (Adapted from Ninagawa, George, and Mori 2021) Created with BioRender.com

2.1.6.2 Retrotranslocation: components of HRD Complex

Once the substrate is recognized by Yos9, it is brought to the HRD complex. Here subunits of the complex engage with the substrate to dislocate it to the cytosol upon autoubiquitination of Hrd1. The substrate is then ubiquitinated on the cytosolic side which is explained in section 2.1.6.3. The HRD complex consists of the ubiquitin RING-E3 ligase Hrd1, Hrd3, Usa1, and Der1 (Vashistha et al. 2016) (Figure 2.5). In the following section the individual subunits involved in these steps and how they interact with the substrate will be introduced.

Hrd1

Hrd1 is widely recognized as an E3 ligase in the ERAD (both L and M) pathway. It's also the central component of HRD complex since requirement for the other components of ERAD-L (Hrd3, Usa1, and Der1) can be circumvented through the overexpression of Hrd1 (Carvalho, Stanley, and Rapoport 2010). Hrd1 stands for HMG-CoA Reductase Degradation as it is involved in the regulation of steroid synthesis by facilitating the degradation of HMGR (3-hydroxy-3-methylglutaryl-coenzyme A reductase), an enzyme that acts as a rate limiting enzyme in steroid biosynthesis (R. G. Gardner et al. 2000; Foresti et al. 2013; P. Wu et al. 2021). Hrd1 possesses eight transmembrane (TM) domains, with both, the N-terminal region and the C-terminus RING domain, oriented towards the cytosol. (Schoebel et al. 2017; Nakatsukasa et al. 2022). The cytosolic RING domain of Hrd1 encapsulates the active site that is responsible for ubiquitinating the substrate by facilitating the transfer of ubiquitin molecules from one or more E2 enzymes to specific misfolded substrates (Schulz et al. 2017). Hrd1 also undergoes autoubiquitination on lysine residues of its cytosolic RING domain, which triggers the retrotranslocation of a substrate's misfolded luminal domain across the membrane (Baldridge and Rapoport 2016). Hrd1 interacts with the substrate polypeptide segment in close proximity to the α1,6 mannose residue through its TM domains. Crosslinking experiments showed that the misfolded substrate exhibits a conformational change resulting in the formation of a loop structure which interacts with Der1 and Hrd1 in the ER membrane (Carvalho, Stanley, and Rapoport 2010). Hrd1 interacts with Hrd3 on its luminal side and with Usa1 on its cytosolic side, with Usa1 acting as a

mediator between Hrd1 and Der1 (Figure 2.5). Hrd1 binds to Usa1 via its N-terminal cytosolic region, while it interacts with Der1 through its C-terminal cytosolic region. (R. G. Gardner et al. 2000; Horn et al. 2009; Knop et al. 1996).

Hrd3

While Hrd1 serves as the central HRD E3 ligase, the precise function of Hrd3 has remained elusive. Both Hrd1 and Hrd3 exhibit a high degree of conservation, with Hrd1 being identified as the limiting factor in the degradation process of misfolded substrates (Bays et al. 2001; Bordallo et al. 1998; Mehnert, Sommer, and Jarosch 2014; Mehnert et al. 2015; Vashistha et al. 2016). Hrd3 is known to stabilize Hrd1 by interacting with its TM domain (R. G. Gardner et al. 2000). Hrd3 exposes a substantial domain into the ER lumen that contains a multitude of SEL1-like repeats (SLRs). These SLRs exhibit a notable level of structural resemblance to tetratricopeptide repeats (TPRs). It is widely accepted that TPRs and SLRs play a crucial role in facilitating protein-protein interactions (Dong et al. 2008). In vivo, Hrd3 displays the ability to bind misfolded proteins. Additionally, it preserves denatured proteins by maintaining them in a soluble state without folding, thereby inhibiting their aggregation (Gauss, Sommer, and Jarosch 2006; Mehnert et al. 2015). Deletion of *hrd3* results in the degradation of Hrd1 and leads to the impairment of the ligase's overall functionality (R. G. Gardner et al. 2000). Hrd3 also binds to Kar2 and Yos9, establishing a luminal surveillance complex which is responsible for the recruitment of misfolded substrates to the ERAD pathway as described under section 2.1.6.1 (Denic, Quan, and Weissman 2006; Carvalho, Goder, and Rapoport 2006).

Der1

The interaction between misfolded substrates and Hrd3 leads to close spatial association with another membrane protein of the HRD complex, Der1 (Mehnert, Sommer, and Jarosch 2014). Der1 is an integral membrane protein and member of the rhomboid superfamily which constitutes multi spanning membrane proteins that possess four to six TM helices. Both the N and C termini of Der1 are located within the cytosol. Der1 was the first protein, discovered to participate in the degradation process of soluble, misfolded substrates CPY* and PrA* (Hitt and Wolf 2004; Knop et al. 1996). It has been demonstrated in previous studies that Der1 exhibits a distinct preference for soluble ERAD substrates (Hitt and Wolf 2004). The deletion of *der1* results in heightened ER stress, which subsequently triggers the activation of the UPR and is also one of the genes that exhibit the highest level of upregulation during the UPR (Knop et al. 1996; Hitt and Wolf 2004). Der 1 can bind misfolded proteins directly but with limited capacity even in situations where the substrate receptor Hrd3 is absent. Der1 has been demonstrated to enhance the process of membrane insertion of ERAD

substrates, thereby initiating their translocation from the ER to the cytoplasm (Gauss, Sommer, and Jarosch 2006; Mehnert, Sommer, and Jarosch 2014). When Der1 itself is deleted, the model substrate CPY* remains within the ER, showing impairment of the retrotranslocation process (Mehnert, Sommer, and Jarosch 2014). In previous in vivo cross-linking experiments, Hrd1 and Der1 were found to be in a close proximity. This arrangement may facilitate the effective transfer of substrates from Hrd3 to the other subunits of HRD complex via Der1 (Mehnert, Sommer, and Jarosch 2014; Mehnert et al. 2015). Der1 is known to oligomerize via Usa1 interaction. It was shown that deletion of *usa1* leads to disassociation of Der1 oligomers. Nevertheless, the induction of UPR pathway through dithiothreitol (DTT) treatment could partially circumvent the need for Usa1-dependent oligomerization, through the overexpression of Der1 (Mehnert, Sommer, and Jarosch 2014). Function of Der1 is primarily centered around the retrotranslocation process of ERAD-L substrates.

Usa1

The role of Usa1 in facilitating the recruitment of Der1 to the E3-ligase Hrd1 has been described (Carvalho, Goder, and Rapoport 2006). Usa1 is an integral membrane protein that exposes both its N and C termini towards the cytosol. The C-terminal region of Usa1 interacts with Der1. This interaction only serves to establish a connection between Hrd1 and Der1 (Horn et al. 2009). The N-terminal region of Usa1 possesses a ubiquitin-like (UBL) domain, which appears to be involved in the degradation of Hrd1, even in absence of *hrd3* which was thought to degrade Hrd1 by destabilizing it (Carroll and Hampton 2010). The UBL domain of Usa1 was also found to ubiquitinate the model substrate CPY* (W. Kim, Spear, and Ng 2005). Usa1 is known to interact with the chaperone complex Cdc48-Ufd1-Npl4, which recognizes ubiquitinated proteins and extracts them from the ER membrane. Since, CPY* ubiquitination is unaffected in Cdc48 mutants, the association between Usa1 and Cdc48 is likely indirect and irrelevant to Usa1's function in CPY* ubiquitination (Ye, Meyer, and Rapoport 2001; Jarosch et al. 2002).

Through proteomic studies it was also found that Usa1 is a binding partner for Hrd1 (Gavin et al. 2006). Previous co-IP experiments indicated that Usa1 can lead to the oligomerization of Hrd1, which is not essential for the degradation of soluble misfolded substrates but rather important for the membrane bound substrates of ERAD (Horn et al. 2009). Recently, it has been observed through disulfide crosslinking approach in a *usa1*Δ strain, that the Hrd1–Hrd1 interaction is not dependent on either Usa1 or Der1. However, this interaction is enhanced when Ubc7, an E2 enzyme, is absent. These findings suggest that polyubiquitination is necessary for the disassembly of Hrd1 dimers (Pisa and Rapoport 2022).

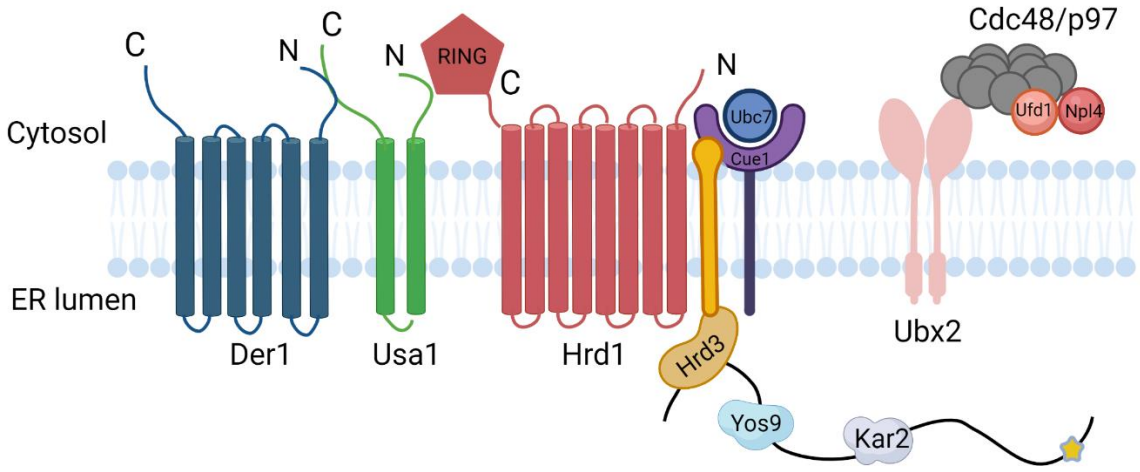

Figure 2.5: Schematic representation of the HRD1 complex. The Hrd1 E3 ligase interacts with the E2 enzyme Ubc7, facilitated by Cue1 recruitment and activation at the ER. Misfolded luminal substrates are recognised (ERAD-L) by the Yos9 lectin, the Kar2 Hsp70 protein, and Hrd3 during the ERAD process. Ubiquitination and retrotranslocation of ERAD-L substrates depends on Der1 arriving at the HRD complex together with Usa1 which mediates oligomerization of the HRD complex. Simultaneously, the Cdc48 complex is recruited to the ER via the Ubx2 adaptor protein. Once ubiquitinated, these substrates are extracted from the ER by the coordinated action of Cdc48 and the co-factors Ufd1 and Npl4 (Adapted from Zattas and Hochstrasser 2015). Created with BioRender.com

2.1.6.3 Ubiquitination

Ubiquitination of misfolded proteins is a critical step to target them for proteasomal degradation. Ubc7 (in mammals Ube2g1 and Ube2g2) is an E2 enzyme for Hrd1 E3 ligase (Xu et al. 2009). It's a soluble protein that is recruited to the membrane by interaction with Cue1, an adaptor protein (Lopata et al. 2020). Ubc7 pre-assembles longer ubiquitin chains on a cysteine in its active site that are then transferred, all together, to the target misfolded protein by the E3 ligases (Ravid and Hochstrasser 2007; Li et al. 2007). The ubiquitin chains produced by Ubc7 are K48-linked. This type of linkage specifically marks misfolded proteins for proteasomal degradation. Cue1 has a single transmembrane helix with an Ubc7 binding region domain (U7BR) that binds to Ubc7 in the cytosol and recruits it to the ER membrane (Lopata et al. 2020). The binding of U7BR domain of Cue1 to Ubc7 also promotes increased ubiquitination activity of substrates, independently of the presence of E3 ligase Hrd1 (Bazirgan and Hampton 2008). In addition to the U7BR domain, Cue1 also contains a coupling of ubiquitin to ER degradation (CUE) domain which is known to enhance the process of ubiquitination. The mechanism of how the CUE domain enhances ubiquitination is not known, but it was recently

shown that it has ubiquitin binding domains (UBDs) which can bind to both monoubiquitin as well as to polyubiquitin chains (Bagola et al. 2013; Lopata et al. 2020).

Hrd1 autoubiquitinates and can be a substrate of ERAD. A deubiquitinating enzyme Ubp1 was identified, that removes Hrd1's polyubiquitin modification and prevents Hrd1 from unregulated degradation (Peterson et al. 2019). Hrd1 autoubiquitination activates E3 ligase activity due to the UBL domain of Usa1 and autoubiquitination is inhibited by the absence of Hrd1 interacting partner Hrd3. Hrd1 can cycle through autoubiquitination and deubiquitination during ERAD because of this delicate equilibrium (Baldridge and Rapoport 2016; Peterson et al. 2019). This provides a regulatory mechanism to maintain the proper level and activity of Hrd1 within the cell.

2.1.7 Cdc8 mediated extraction of substrates

After being retrotranslocated across the ER membrane through the HRD complex and undergoing polyubiquitination on the cytosolic side of the ER, substrates are extracted by Cdc48 (Bays et al. 2001; Jarosch et al. 2002; Ye, Meyer, and Rapoport 2001). Cdc48 is a homo-hexameric AAA+ ATPase that is highly conserved. Its main function is to extract polyubiquitinated, misfolded proteins from the ER and enables their transfer to the proteasome for degradation. It facilitates the formation of adaptable initiation regions within densely packed substrates that would otherwise be resistant to interaction and degradation by the proteasome (Stolz et al. 2011; Christianson and Ye 2014; Olszewski et al. 2019). Cdc48 is composed of an N-terminal (N) domain, two consecutive AAA domains (D1 and D2) responsible for the hydrolysis of ATP connected by a brief linker, and a pliable C-terminal tail. The AAA domains are arranged in a configuration of two concentric rings encircling a central pore (Bodnar and Rapoport 2017). The Ufd1/Npl4 (UN) heterodimer serves as a cofactor for Cdc48. The UN molecule interacts with the N domain of Cdc48 and facilitates the recruitment of polyubiquitinated substrates to the Cdc48 ATPase (Ye, Meyer, and Rapoport 2003).

In an in vitro system designed to mimic ERAD processes, it was observed that a polyubiquitinated misfolded substrate could be efficiently removed from the cellular membrane by both Cdc48 and UN (Stein et al. 2014). On the contrary, Baldridge and Rapoport 2016 demonstrated in their in vitro experiments that not substrate ubiquitination but Hrd1 polyubiquitination might be enough for the retrotranslocation of substrates, supporting previous observations in mammals (Bernardi et al. 2010; X. Wang et al. 2013). Nevertheless, recent cryo-EM structures of the Cdc48 complex with Ufd1/Npl4 and a polyubiquitinated substrate show that the Cdc48 complex starts substrate processing by cleaving off a ubiquitin molecule. Then the unfolded ubiquitin molecule on the substrate binds to Npl4 and sends its N-terminal portion through both the hexameric ATPase rings. The pore loops of the

second ring form a staircase that moves the polypeptide through the core of the cavity like a conveyor belt. By making the ubiquitin chain unfold, the Cdc48 ATPase complex can deal with a wide range of substrates (Twomey et al. 2019). For substrate dissociation from Cdc48, another DUB enzyme unknown in yeast (Otu1 in mammals), binds to the N domain of Cdc48 and deubiquitinates the substrate by removing ubiquitin molecules. The substrate is released, but short ubiquitin chains are left behind (Stein et al. 2014; Bodnar and Rapoport 2017). In summary, Cdc48 unfolds and extracts the polyubiquitinated substrates from the ER membrane, followed by their complete retrotranslocation to the cytosol for subsequent degradation by proteasomes, with the energy required for this process being derived from ATP hydrolysis.

2.1.8 Proteasomal Degradation

The trimmed ubiquitinated substrates are further ubiquitinated by an additional E4 ubiquitin chain elongation factor known as Ufd2, resulting in the formation of K48-ubiquitin branches. (Liu et al. 2017)**.** After undergoing processing to achieve the optimal chain length, proteins that have been ubiquitinated are accompanied to the proteasome by soluble escort factors, namely Rad23 and Dsk2. These proteins then interact with the proteasomal receptor Rpn1, which is situated on the base of the 19s RP in the proteasome. The interaction is enhanced by the attachment of the polyubiquitin chain to the ubiquitin receptors Rpn10 and Rpn13 (Medicherla et al. 2004; I. Kim, Mi, and Rao 2004; Elsasser et al. 2002; 2004; Husnjak et al. 2008). Then the polyubiquitinated substrate is degraded by the proteasome as described in The Ubiquitin-proteasome pathway in section 2.1.5.

2.1.9 Anomalies in the retrotranslocation pathway

It has been a topic of discussion in the scientific community for a number of years as to how misfolded substrates get retrotranslocated and what could be the primary retrotranslocon in the ERAD pathway. There are several candidates for the role with one of the first ones being Sec61.

2.1.9.1 Sec61 in retrotranslocation pathway

Sec61 is the central protein translocon for ER proteins but it was also the was first candidate proposed to retrotranslocate misfolded substrates due to numerous previous observations (Xie and Ng 2010). In cell free systems, association of several ERAD substrates with Sec61 was seen and in case of mutation in Sec61, several substrates were retained in the ER, associated with PDI (Pilon, Schekman, and Römisch 1997; Pilon et al. 1998; Pauline Gillece et al. 1999). Yeast cells overexpressing the ERAD substrate CPY* had an ER protein import deficiency that was restored by increasing Sec61 expression

while overexpression of WT CPY caused no import defect, demonstrating that the protein translocation channel limits ER import if export demand of substrates is strong (Ng, Spear, and Walter 2000). The strong binding affinity of Sec61 proteoliposomes to the 19S subunit of the proteasome, demonstrates its involvement in the regulation of upstream processes related to the degradation of misfolded substrates (Kalies et al. 2005). Sec61 also interacts with Hrd1 partner Hrd3 and the model substrate CPY*. This interaction between Sec61 and CPY* only last until the substrate starts degrading on the cytosolic side of the ER and in *hrd1* deletion strain, CPY* is retained in the ER and the interaction between Hrd3, Sec61 and CPY* is enhanced, suggesting that Sec61 could be part of ERAD (Schäfer and Wolf 2009). The interaction between Sec61 and various components associated with ERAD, including Ubc6, Ubc7, Cue1, Ubx7, and Ubp1, indicates a significant physical proximity between the Sec61 channel and the ERAD machinery (Pereira et al. 2019). Furthermore, it is of importance that the interaction between Sec61 and Mpd1, a homolog of PDI and a recognized factor in ERAD, plays a significant role in the degradation process of CPY* (Pereira et al. 2019).

In another study, Sec61 could translocate antigens from the endosomal compartment to the cytosol. However, downregulation of Hrd1 also reduced the transport indicating a partial role of both Sec61 and Hrd1 (Zehner et al. 2015). In contrast, the presence of antibodies targeting Sec61 did not yield any discernible impact on the export of a soluble ERAD substrate Δgpαf, a nonglycosylated derivative of the yeast pro-α factor from mammalian ER microsomes, but Derlin-1 (mammalian homolog of Der1) antibodies did block the export (Wahlman et al. 2007). However, it is worth noting that the antibodies did exhibit a hindering effect on the export of small glycopeptides through the Sec61 channels (P. Gillece, Pilon, and Römisch 2000). Another lab showed through crosslinking experiments that Sec61 can't be the retrotranslocon as it doesn't form very strong crosslinks with the misfolded model substrate CPY*, and the crosslinks were also not dependent on the presence of other ERAD components, in contrast to those observed with Hrd1 (Carvalho, Stanley, and Rapoport 2010).

In a recent study, it was observed that yeast cells expressing Sec61, lacking the N-terminal amphipathic helix exhibited significant impairments in growth and experienced notable deficiencies in the import of proteins into the ER after translation. Additionally, yeast cells expressing Sec61 without N-terminal acetylation demonstrated an accumulation of CPY* in the ER compared to wild-type CPY. This suggests that either the post-translational import of CPY* into the ER was prolonged in this mutant or that N-terminal acetylation of Sec61 plays a role in the ERAD process (Elia et al. 2019). Altogether, the results are very inconclusive to indicate role of Sec61 as the central retrotranslocon in yeast. The precise composition of the retrotranslocation channel still remains a topic of debate within the academic community.

2.1.9.2 Der1 mediated retrotranslocation

Der1 is one of the key constituents of the HRD complex and has been postulated as a potential channel due to its characteristics as a multi-spanning membrane protein that exhibits interactions with its substrates on both sides of the ER membrane (Carvalho, Stanley, and Rapoport 2010; A. M. Stanley, Carvalho, and Rapoport 2011). The deletion of *der1* resulted in the accumulation of CPY* within the ER lumen, triggering an UPR response (Knop et al. 1996). Subsequent investigations have been conducted to ascertain its involvement in the process of retrotranslocation. Der1 binds to the ERAD misfolded substrate CPY* via its luminal loop (Mehnert, Sommer, and Jarosch 2014). Mutations in the TM domains of Der1 block the translocation of soluble misfolded substrate through the ER membrane. Photocrosslinking experiments and immunoprecipitation analyses of this ERAD mutant showed that Der1 appears to be properly integrated into the HRD complex and it still binds to the misfolded substrate CPY* via its luminal loop; however, the quantity of crosslinking products involving Hrd1, Usa1, and Hrd3 was significantly reduced, suggesting that there were moderate alterations in the structure of Der1. These changes likely impeded the degradation of substrates (Mehnert, Sommer, and Jarosch 2014). In a recent study, it was demonstrated via disulfide crosslinking experiments that the luminal loop of Der1 exhibits the ability to bind the substrate in close proximity to the glycan attachment site (Pisa and Rapoport 2022). It was also suggested that lipid thinning aids in the retrotranslocation process of luminal ERAD-L substrates (Wu et al. 2020). Der1 forms a lateral gate on the luminal side which interacts with Hrd1 to create a semi-channel that promotes lipid thinning. Molecular dynamics (MD) simulation conducted with Der1 revealed that a specific region of the protein exhibited hydrophilic properties, thereby providing evidence for its involvement in facilitating the transport of soluble membrane substrates as a "half channel" (Nejatfard et al. 2021).

However, there are doubts about Der1's function as a channel. Der1 belongs to a family of homologous pseudo rhomboid protease that exhibits a specific structural organization and a high-resolution structure of GlpG, a well-known protein from this family, does not exhibit any discernible pathway across the membrane, which could function as a channel (Y. Wang, Zhang, and Ha 2006; Z. Wu et al. 2006; Greenblatt, Olzmann, and Kopito 2011). It is crucial to note that overexpression of Der1 alone is inadequate in compensating for the loss of other components within the HRD complex, as one would anticipate if Der1 were the principal constituent of the retrotranslocon (Horn et al. 2009; Carvalho, Stanley, and Rapoport 2010). These pieces of evidence suggest that Der1 might or might not be involved in the formation of the translocon channel of the HRD ligase and it is important to note that this topic remains controversial and has not been extensively studied.

2.1.9.3 Hrd1's role in retrotranslocation

Hrd1 has emerged as the primary candidate for the formation of a retrotranslocation channel. The initial indication of Hrd1's channel formation was derived from the observation that its overexpression in yeast renders the other constituents of the HRD complex unnecessary for the degradation of ERAD-L substrates (Carvalho, Stanley, and Rapoport 2010; R. G. Gardner et al. 2000). The continued necessity of downstream components, including the ubiquitination machinery and the Cdc48 ATPase complex, was observed. The presence of a Hrd1 channel was further corroborated by photo-crosslinking experiments, which demonstrated the proximity of the substrate to Hrd1 during the process of retro-translocation (Carvalho, Stanley, and Rapoport 2010). It is noteworthy that the N-terminal of the substrate establish interactions with both Hrd3 and Der1, whereas the C-terminal establishes interactions with only Hrd1. This suggests that the substrate is transferred from Hrd3 to Der1 and from Der1 to Hrd1 in a sequential manner (Carvalho, Stanley, and Rapoport 2010).

Subsequent in vitro experiments utilizing purified proteins reconstituted in LUVs demonstrated the binding capacity of Hrd1 to soluble ERAD-L substrate CPY* and autoubiquitination of Hrd1 which leads to the recruitment of Cdc48 AAA-ATPase. The autoubiquitination of Hrd1 was further shown to polyubiquitinate CPY* resulting in the release of ubiquitinated CPY* from Hrd1 (Stein et al. 2014). In this study, it was observed that the substrate underwent complete cleavage by external proteases following reconstitution indicating the substrate was only present outside of the vesicles. As a result, it was not possible to definitively establish the occurrence of retrotranslocation (Stein et al. 2014). Nonetheless, the experimental findings could indicate that Hrd1 is responsible for the formation of the ERAD translocon. This was confirmed by one of the pivotal studies relevant to this thesis that involves an in vitro experimental setup wherein ubiquitinated Hrd1 reconstituted into proteoliposomes fuses to planar lipid bilayers (PLBs) and the subsequent formation of a translocon can lead to small conductance events. The observed effect was reversible, as the channel was inactivated upon deubiquitination of Hrd1. Significantly, the addition of CPY* resulted in increased channel conductance events suggesting the substrate mediated expansion or activation of the translocon (Vasic et al. 2020). The process of retrotranslocation was also replicated in vitro using proteoliposomes comprising both Hrd1 and a single-spanning transmembrane substrate Pdr5 fused to CPY* (CPY*-TM) leading to a membrane bound misfolded fusion protein. Hrd1 polyubiquitinated a segment in the substrate that was inside the lumen of the vesicles when the ubiquitination machinery was added, indicating that it migrated across the membrane of the liposomes. Hrd1 exhibited proficient autoubiquitination at the lysine residues located within its RING finger domain. This process

was proposed to constitute retrotranslocation in vitro and promote the degradation of ERAD-L substrates in in vivo conditions (Baldridge and Rapoport 2016).

Multiple cryo-electron microscopy (cryo-EM) investigations have been conducted to examine the structural characteristics of Hrd1, along with its associated subunits. In one structural study, Hrd1 was found to exist as a heterodimer together with Hrd3. Hrd1 is observed to bind to the luminal domain of Hrd3, resulting in the formation of an arch by Hrd3 on the luminal side of the ER. Furthermore, out of the eight TMs present in Hrd1, five TMs (TMs 3, 4, and 6-8 of a single Hrd1 molecule) contribute to the formation of a large cavity that extends from the cytosol to the membrane's luminal side. Notably, TM 1 of Hrd1 acts as a seal for the neighboring Hrd1 molecule's funnel on the cytosolic side representing probably closed conformation of a translocon (Schoebel et al. 2017). This structure suggested that existence of a water filled pore. In another structural investigation, Hrd1 was identified as existing in a monomeric conformation alongside Hrd3, Der1, and Usa1. Hrd1 and Der1 are connected through Usa1 on the cytosolic side, with the lateral gates of Hrd1 and Der1 positioned in close proximity to each other. Both luminal and cytosolic cavities are present for the insertion of substrates (Wu et al. 2020). This structure implied the presence of Hrd1 as a half channel structure which can impart membrane thinning. In summary, a substantial body of evidence strongly suggests that Hrd1 is responsible for the formation of the retrotranslocon. Nevertheless, despite the plethora of evidence that has been presented thus far, inquiries regarding the involvement of other components of the HRD ligase in the process of retrotranslocation persist.

2.2 Aims

Electrophysiological studies have provided insights into the functional role of Hrd1 as a channel. These studies have directly measured the channel activity of Hrd1 and have revealed that its characteristics deviate from that of other known protein translocation channels. Within the complete HRD complex all subunits, Hrd1, Hrd3, Usa1 and Der1, most likely play their respective parts for the functionality of ERAD-L. As section 2.1.9.2 and 2.1.9.3 mention in detail, the direct contribution of Der1 and Hrd1, and the effect of substrate retrotranslocation on ERAD-L was shown but the specific impact of these subunits on the gating mechanism of Hrd1 remains uncertain. Therefore, in this thesis we aim to investigate how gating dynamics are changed when Hrd1 is integrated in the HRD complex as opposed to isolated Hrd1 characteristics. We especially want to determine how the presence of Der1, which was never included in electrophysiology experiments before, influences Hrd1 gating.

We had the wonderful opportunity to team up with the talented researchers at Dr. Alexander Stein's lab (Max Planck Institute of Multidisciplinary Sciences). Together with Benjamin Gnoth, a dedicated PhD student from their group, we obtained purified protein complexes isolated from yeast. This collaboration allowed us to tap into their expertise in ubiquitination assays, and it provided invaluable insights that have greatly enriched the overall project.

Our main objective was to evaluate the activity of Hrd1 and the HRD complex using high-resolution single channel electrophysiology also commonly known as the planar lipid bilayer (PLB) electrophysiology technique, as described by Harsman et al. 2011. This approach offers an alternative to patch clamp means of measuring the activity of ion channels and, if suitable, protein translocases. The method exploits the observation that numerous protein translocases exhibit the formation of aqueous pores during substrate translocation. This phenomenon gives rise to a voltage-dependent conductance, which can be quantitatively assessed as an indicator of channel functionality (Harsman et al. 2011). The measurement of the conductance can be utilized for the determination of the channel's pore size and also facilitates the real-time assessment of channel opening and closing and dwell time at the individual molecule scale. Importantly, this approach facilitates the manipulation of both sides of the channel, a capability that is not easily achievable with liposomes. In addition, we conducted an analysis to characterize the interactions between the model substrate CPY* and the HRD complex channel.

2.3 Materials and Methods

2.3.1 Materials

Table 2.1 Lipids used in this investigation

Name	**Company**
1-palmitoyl-2-oleoyl-glycero-3-Phosphocholine (POPC)	**Avanti Polar Lipids**
1,2-dioleoyl-sn-glycero-3-Phosphoethanolamine (DOPE)	Avanti Polar Lipids
1,2-dioleoyl-sn-glycero-3-phospho-L-serine (DOPS)	Avanti Polar Lipids
Cholesterol (ovine wool, >98%)	Avanti Polar Lipids
L-a-Phosphatidylcholine (soybean, Type IV-S) (SIV-PC)	Sigma Aldrich

Table 2.2 Special consumables

Chemical	**Supplier**
Acetone >99.8% p.a.	Carl Roth GmbH & Co KG
Ethanol >99.8% p.a.	Carl Roth GmbH & Co KG
Methanol >99.9% p.a.	Carl Roth GmbH & Co KG
Trichloromethane/Chloroform	Carl Roth GmbH & Co KG
n-Decyl ß-maltoside (DM-C)	GLYCON Biochemicals
Pierce detergent removal spin 0.5ml	Life Technologies GmbH
Adenosine triphosphate (ATP)	Sigma Aldrich
HEPES	Carl Roth GmbH & Co KG
Potassium chloride (KCl)	Carl Roth GmbH & Co KG
Magnesium chloride ($MgCl_2$)	Carl Roth GmbH & Co KG
Chloroform	Merck, DE
Nuclepore Track etched polcarbonate membrane	Whatman
Filter supports	Avanti Polar Lipids

Materials used for electrophysiological measurements are described in Chapter 1 Table 1.2.

2.3.2 Methods

All the proteins used in this study has been kindly provided by Lab of Dr. Alexander Stein (Max Planck Institute for Multidisciplinary Sciences) and isolated from *Saccharomyces cerevisiae*. The proteins utilized in this study are Hrd1, HRD complex, Uba1, Ubc7, Cue1, Usp2 and CPY*.

2.3.2.1 Preparation of liposomes with membrane composition of ER

The methodology outlined in Hernandez et al. 2012 was employed to determine the composition and concentration of lipids. Stock solutions of POPC, DOPE, DOPS, and cholesterol were prepared with lyophilized powders using chloroform (Avanti Polar Lipids) as the solvent. To generate liposomes, lipids were combined in the specified molar ratios (as outlined in Table 2.3) within glass test tubes. The lipid mixtures were subjected to a drying process using a stream of nitrogen gas in the presence of chloroform. Subsequently, the samples were incubated in a desiccator for a duration of 3 hours to ensure thorough drying. The lipids that had been dried were rehydrated by adding the liposome buffer, which consisted of 150 Mm KCl, 10 mM MOPOS, pH 7 to achieve a final concentration of 20 mM. To produce unilamellar vesicles, the lipid mixture underwent seven cycles of freezing in liquid nitrogen followed by thawing at room temperature. To obtain liposomes with a desired size, such as large unilamellar vesicles (LUVs), the mixture underwent 11 rounds of extrusion through 400 nm polycarbonate membranes (Whatman). Subsequently, the mixture was further extruded 21 times through a 400 nm polycarbonate membrane using a mini-extruder manufactured by Avanti Polar Lipids.

Table 2.3 Composition of lipids for the endoplasmic reticulum liposomes

% Lipid	**Lipid**	**µM**
60	POPC	12.00
20	DOPE	4.00
10	DOPS	2.00
10	Cholesterol (5mg/ml)	2.00
100	Total	20

2.3.2.2 Reconstitution of Hrd1 or HRD complex into liposomes and ubiquitination

The protocol for reconstituting Hrd1 or HRD complex into liposomes was kindly provided by Benjamin Gnoth, AG Alexander Stein (Max Planck Institute for Multidisciplinary Sciences). To reconstitute Hrd1 or Hrd1 holocomplex into liposomes along with adapter protein Cue1, n-Decyl ß-maltoside (DM) was used as the solubilization detergent. According to Hernandez et al. 2012 the process of protein insertion is highly dependent on the ratio of lipids and detergents, denoted as the R-value, which can be calculated by the equation below by Rigaud and Lévy 2003.

$$R = \frac{[D_{total}] - [D_{CMC}]}{[lipid]} \quad (7)$$

where $[D_{total}]$ and $[D_{CMC}]$ represents the total and critical micelle concentration (CMC) of the detergent, respectively; and [lipid] denote the lipid concentration. For Hrd1 or HRD complex reconstitution with Cue1, 4 mM of the ER liposomes were mixed with the detergent DM at an R value of 1.5, along with 0.8 µM Hrd1, 3.2 µM full length Cue1 in 150 Mm KCl, 10 mM MOPOS, pH 7 buffer. The sample mixture was incubated for 1 hr at RT and detergent was removed by incubating the solution three times through detergent removal spin columns, each for 20 minutes at RT. Then liposomes were eluted by centrifugation at 5000 rpm for 5 mins. The Hrd1 or HRD complex proteoliposomes were incubated with components of ubiquitination machinery to ubiquitinate the Hrd1 or Hrd1 holocomplex. Ubiquitination machinery consist of 0.02 µM Uba1, 0.4 µM Ubc7 and 20 µM ubiquitin. The reaction was initiated by adding 2.5 mM ATP and incubated for 1 hr at RT.

2.3.2.3 Electrophysiological characterization

A general protocol to perform electrophysiological characterization and fusion of proteoliposomes to bilayer is described in detail in last chapter in section 1.3.2.5.

2.3.2.4 In situ ubiquitination

For in situ ubiquitination experiments, Hrd1 or HRD complex proteoliposomes were only ubiquinated once they were fused to the PLB in asymmetrical buffer conditions. One additional drawback of the experimental arrangement is the inability to visually observe the fusion of proteoliposomes with the bilayer. To address this limitation, the buffer was agitated following the addition of proteoliposomes and subsequently incubated for a duration of approximately 15-30 minutes. Then the ubiquitination

machinery consisting of 0.02 µM Uba1, 0.4 µM Ubc7, 20 µM ubiquitin along with 2.5 mM ATP was directly added to the cis or both chamber of the PLB setup. The buffer used in *in situ* ubiquitination experiments consisted of 250 Mm KCl or 20 Mm KCl, 10 mM MOPOS, 5 mM $Mgcl_2$ pH 7. $Mgcl_2$ was used to activate ATP and start the ubiquitination reaction.

2.3.2.5 Deubiquitination and Substrate Specificity of Channels

In order to investigate the interactions between substrate and enzyme within the bilayer, proteins were introduced to the designated side of the bilayer at the prescribed concentration, while maintaining symmetrical buffer conditions after fusion of proteoliposomes into the PLB. In the present study, two distinct substrates were used. The first component under consideration is Usp2, an enzyme classified as a deubiquitinase. The second component is CPY*, a misfolded substrate associated with the ERAD-L pathway. Usp2 was introduced into either the cis chamber or both chambers, with a final concentration of 1 µM. Similarly, CPY* was introduced into either the trans chamber or both chambers, with a final concentration of 100 nM, as previously described (Vasic et al. 2020). The buffer solution in both chambers was subsequently subjected to 2-5 minutes of mixing using magnetic stirrers, followed by a 2-minute resting period before the recordings were recommenced.

2.4 Results

The initial step in investigating the molecular processes of HRD complex involved the establishment of a comprehensive baseline for the channel behaviour of single Hrd1. In addition to investigating potential differences in behaviour between the Hrd1 and the HRD complex channel characteristics described in previous studies, it was necessary to surpass the degree of information provided in these prior studies. We believe that by doing so we may attain a more profound comprehension of the behaviour of the HRD complex in the cell. Since, integral membrane proteins are inherently insoluble in polar solvents, it necessitated their reconstitution into liposomes mimicking ER membrane composition. In order to achieve this objective, large unilamellar vesicles (LUV) measuring 100 nm in diameter were generated from a phospholipid mixture consisting of POPC:DOPE:DOPS:Cholesterol with a composition ratio of 60:20:10:10 (mol%). The phospholipid mixture was incubated with the detergent DM followed by the addition of the protein purified in detergent. Subsequently, the detergent was gradually removed using detergent removal resins, which led to reconstitution of the protein within the lipid membrane. In this study, we used Hrd1 and the HRD complex, which consists of Hrd1, Hrd3, Usa1, and Der1 containing liposomes together with Cue1 which is an adapter protein for Ubc7 (E2 enzyme), as depicted in Figure 2.6 for electrophysiological characterization.

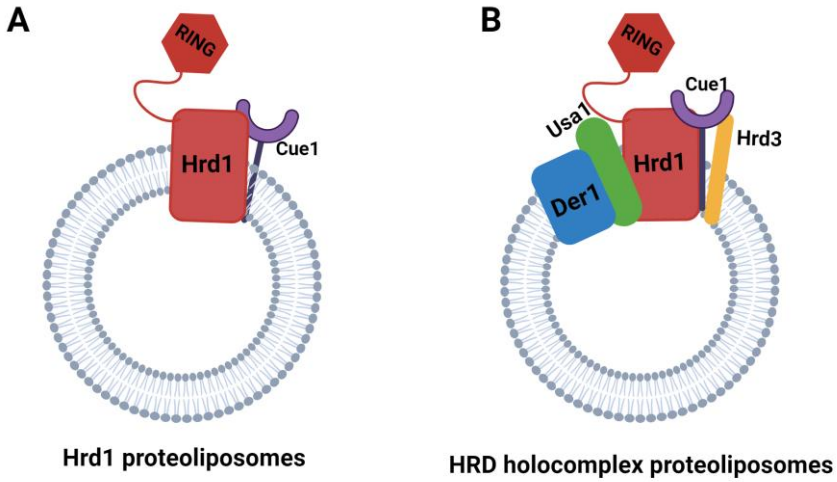

Figure 2.6: Proteoliposomes used for PLB experiments. (A) single Hrd1 (B) HRD complex along with the adapter protein Cue1. Created with BioRender.com

2.4.1 Gating dynamics of Hrd1

In order to initiate our experiment, we used the Hrd1 protein reconstituted into LUVs. This was done to conduct single channel electrophysiological characterisation measurements, with the aim of optimizing the experimental approach and to replicate previously observed results. Upon the addition of ubiquitinated Hrd1 proteoliposomes, we observed a consistent and stable fusion of the Hrd1 channels into the bilayer, which aligns with the previous findings (Vasic et al. 2020). To observe the general gating behaviour of the Hrd1 channel, constant holding potentials ranging from −60 mV to 60 mV were applied to the bilayer containing Hrd1 channels, in 20 mV steps for 60 s each. The present experimental observations, conducted under symmetrical buffer conditions and at constant voltages, primarily indicate the occurrence of smaller gating events mostly 50-70 pS (Figure 2.7A). However, sporadic gating events at a higher conductance state, reaching up to 850 pS-1000 pS, were also seen compared to previous maximum conductance of 620 pS observed in (Vasic et al. 2020) (Figure 2.7B and C). This conductance corresponds to a pore size of 3.42 nm. Then we derived current changes, ΔI from the recorded data utilizing the reconstruction technique algorithm based on stepR (Hotz et al. 2013) and subsequently divided by the applied voltage U in order to obtain the conductance change, ΔG. From conductance state histograms as shown in Figure 2.7C main- and sub-conductance states were determined. The main conductance state was observed to be 50 pS, but also rare gating events at higher conductance changes occured. As a control for this experiment, non-ubiquitinated Hrd1 liposomes were added to the PLBs. No fusion events were observed, nor did the addition induced any current flow confirming that only ubiquitinated single Hrd1 form a water filled pore.

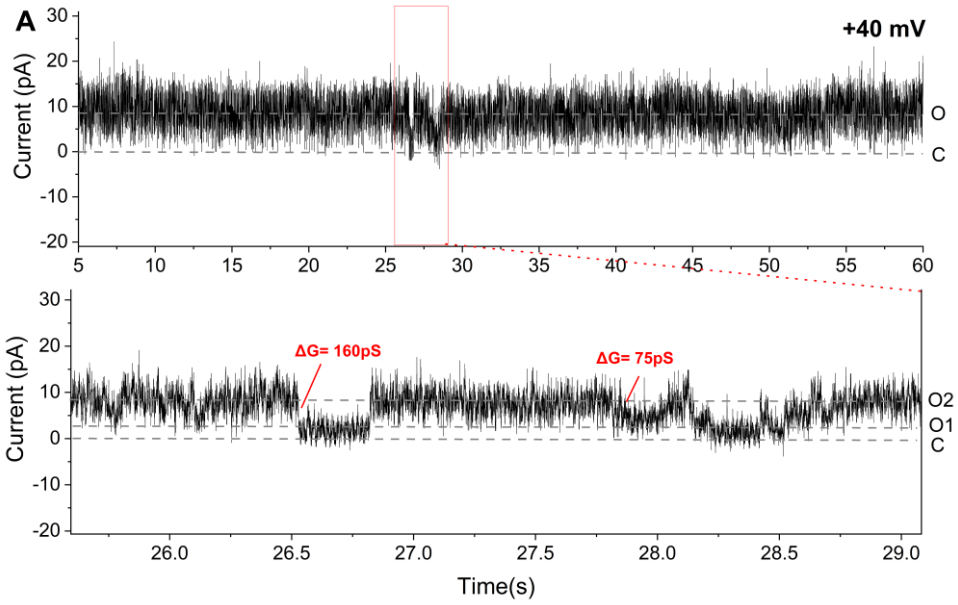

Figure 2.7 continued on next page

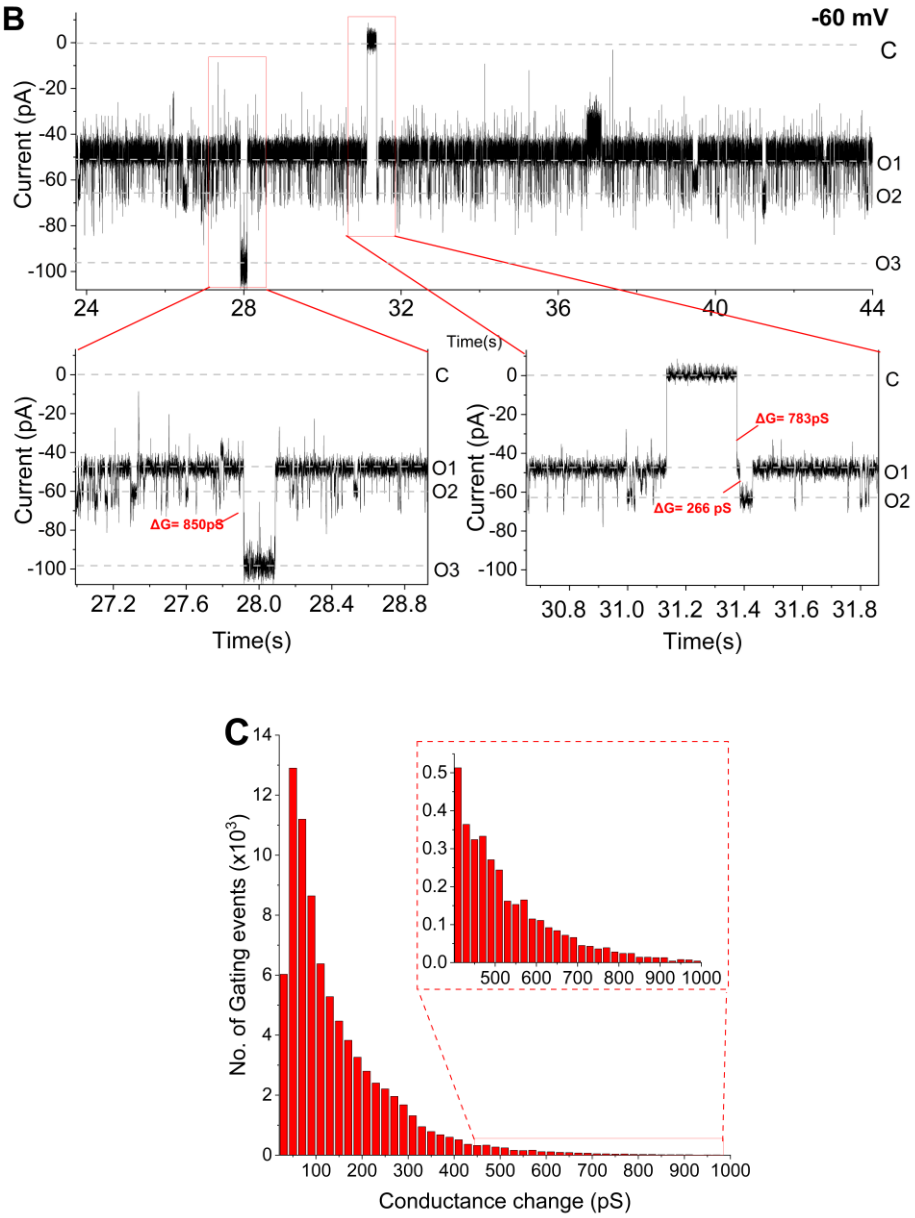

Figure 2.7: Gating dynamics of the single Hrd1. (A) Representative example of a current trace of the single Hrd1 at +40 mV. Buffer: 250 mM KCl, 10 mM MOPS/Tris, pH 7 (cis/trans), (B) Schematic representation of a current trace of the single Hrd1 at constant voltage of -60 mV. Buffer: 250 mM KCl, 10 mM MOPS/Tris, pH 7 (cis/trans), C and O represent the closed and open state respectively. Conductance changes are marked as ΔG. (C) Conductance-state histogram of the single Hrd1 channel calculated from the gating events at varying holding potentials (combined n= 3 independent experiments). The zoomed-in plot illustrates various gating events observed at higher conductance changes.

2.4.2 Current voltage relationship of Hrd1

In order to further evaluate the overall gating behaviour, we recorded the current flow through the channel while it was subjected to a varying voltage range. We measured voltage ramps from -50 mV to +50 mV in both symmetrical and asymmetrical conditions. Under asymmetrical salt conditions (250 mM KCl, cis; 20 mM KCl, trans), ubiquitinated Hrd1 proteoliposomes displayed slightly positive reversal potentials. In single-channel voltage ramp recordings, mean reversal potential obtained for the Hrd1 channel from yeast (n = 3 bilayers) is U_{rev}= +7.4 ± 0.08 mV (Figure 2.8A). These values both correspond to marginal cationic selectivities of $P_{K^+} : P_{Cl^-}$ = 1.4: 1. Interestingly the Sec61 translocon in yeast shows a reversal potential of -7.6 ± 2.4 mV and anion selectivity of $P_{Cl^-} : P_{K^+}$ = 1.42 (F. Erdmann et al. 2010). Under symmetrical conditions, Hrd1 showed a linear current voltage relationship with no rectification (Figure 2.8B). I also observed that the Hrd1 translocon was not stable and led to bilayer instabilities at high voltages above ± 60 mV.

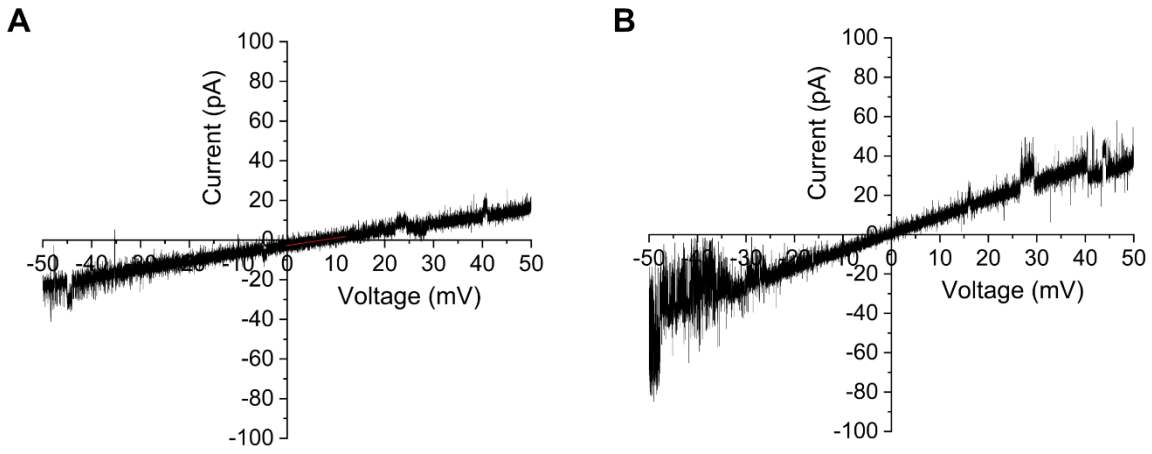

Figure 2.8: Voltage ramp recording of a bilayer containing the single Hrd1 from -50 mV to +50 mV. Representative of n=3 bilayers. Buffer conditions for experiments A: 250 mM KCl, 10 mM MOPS/Tris, pH 7 (cis), 20 mM KCl, 10 mM MOPS/Tris, pH 7 (trans) B: 250 mM KCl, 10 mM MOPS/Tris, pH 7 (cis/trans)

2.4.3 Ubiquitinated HRD complex fuses to the PLBs

Subsequently, we proceeded with the characterization of the HRD complex, in order to determine whether it forms a water-filled pore similar to that of the single Hrd1. Additionally, we aimed to investigate whether the presence of Hrd3, Der1, and Usa1 has any impact on the channel properties

of the HRD ligase. No channel activity was seen when the non-ubiquitinated HRD complex reconstituted in liposomes was added to the bilayer, as such showing the same behaviour of non-ubiquitinated Hrd1. Based on this observation, it may be inferred that the absence of vesicle fusion with the bilayer can be attributed to the closed state of the HRD complex channel, rendering it impermeable to the osmolyte. In contrast, we observed channel activity in the presence of ubiquitinated HRD complexes. To observe the general gating behaviour of the HRD complex channel, constant holding potentials ranging from −40 mV to 40 mV were applied to the HRD complex containing bilayer in 20 mV steps for 60 s each. Higher holding potential couldn't be achieved as the bilayer was instable at elevated voltages. Most of the gating events observed are smaller, in range of 50-70 pS as seen with the single Hrd1 (Figure 2.9A). Unlike for Hrd1, not many high conductance state gating events were seen in a range above 400 pS. The conductance state histogram of the HRD complex shows that the maximum conductance state reached was 600 pS (Figure 2.9B). This conductance corresponds to the pore size of 2.4 nm.

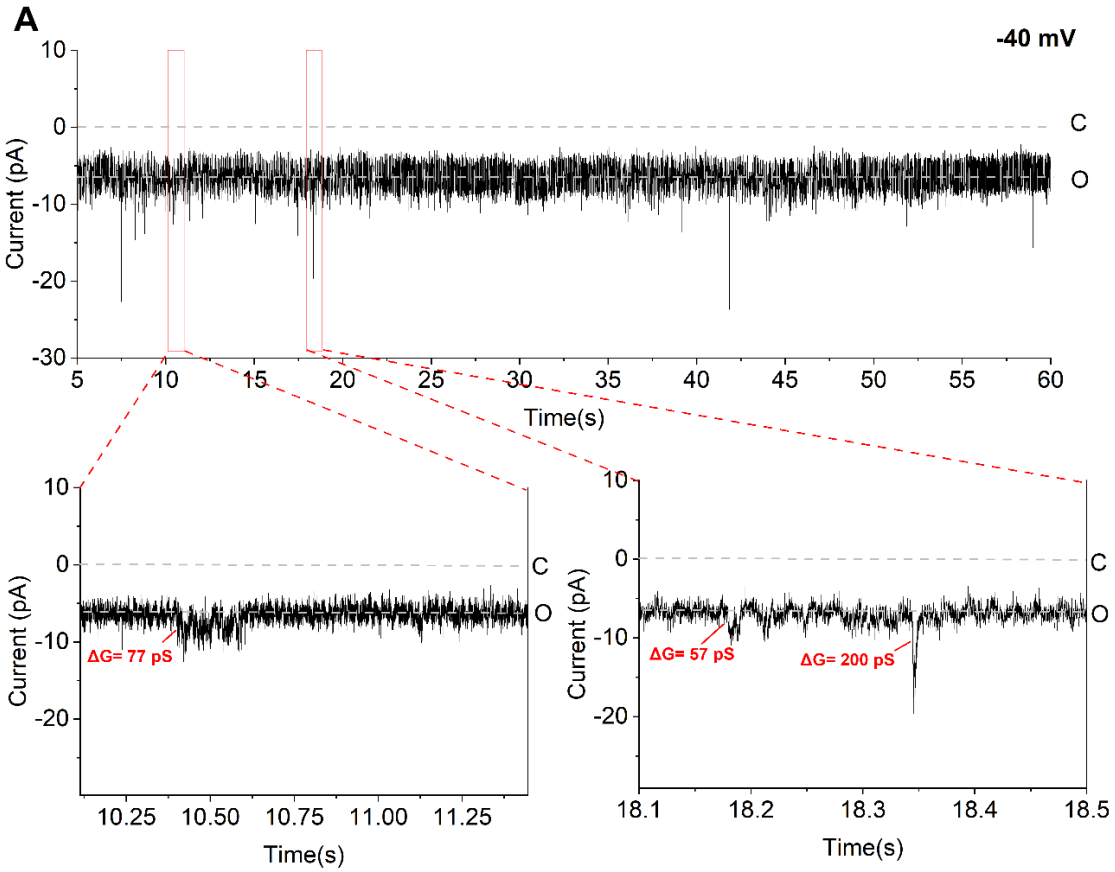

Figure 2.9 continued on next page

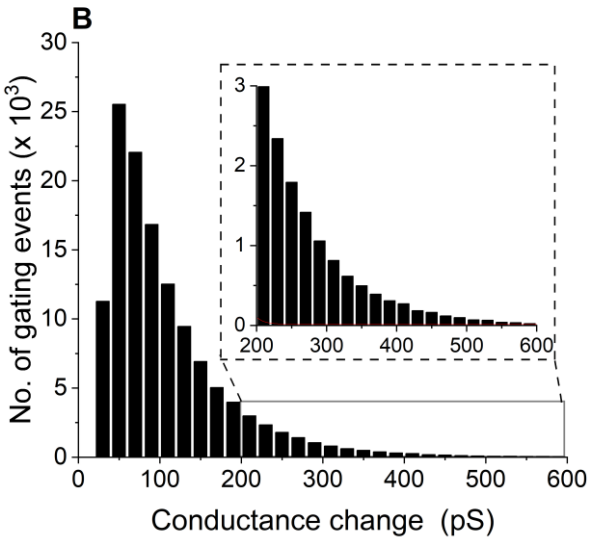

Figure 2.9: Gating dynamics of the HRD complex. (A) Representative example of a current trace of the HRD complex at constant voltage of -40 mV. Buffer: 250 mM KCl, 10 mM MOPS/Tris, pH 7 (cis/trans). C and O represent the closed and open state respectively. Conductance changes are marked as ΔG. (B) Conductance-state histogram of the HRD complex channel calculated from the gating events at varying holding potentials (combined n= 6 independent experiments). The zoomed-in plot illustrates various gating events observed at higher conductance changes.

2.4.4 In situ ubiquitination

Extremely low fusion rates, which led to a limited number of measurements, were also observed as a major experimental limitation during the HRD complex measurements, similar to what was observed for Hrd1. The low fusion rate may be attributed to the presence of long polyubiquitin chains on the ubiquitinated HRD complex, potentially causing steric hindrance during proteoliposome fusion with the bilayer. In order to overcome that, Hrd1 or HRD complex was ubiquitinated after it potentially fused to the bilayer. This counteracts the theory of osmotic gradient dependent fusion of open channels with the bilayer (Section 1.3.2.5.4), but we proceeded to test it anyway. The system was simplified by utilizing single Hrd1 proteoliposomes, which were added to the bilayer under asymmetrical buffer conditions and incubated for 15-30 minutes to allow for proteoliposomes fusion with the bilayer. Subsequently, the ubiquitination process was initiated by adding the ubiquitination machinery, including Uba1, Ubc7, ubiquitin and ATP to both sides of the bilayer. We observed current flows probably coming from rapid opening events and subsequent breakage of the bilayer. This might be due to an excessive amount of ubiquitination occurring on the Hrd1 proteoliposomes which could lead to opening of multiple Hrd1 channels in the bilayer. When the bilayer was reformed, fusion events reoccurred ~ every 30 sec-1 min but measurements were not possible using this system as the bilayer

was consistently unstable and breaking every few seconds (Figure 2.10). Figure 2.10 shows a current trace of such a scenario: following the fusion of single Hrd1 proteoliposomes to PLBs, the bilayer breaks as the current goes to -1000 pA; then after reforming the bilayer, the current goes back to 0 pA until more Hrd1 proteoliposomes fuse to the bilayer. We also decreased the concentration of Hrd1 in proteoliposomes which made the system slightly more stable indicating that the excessive amount of ubiquitination occurring on the Hrd1 proteoliposomes may be a contributing factor to bilayer instability. In addition, we conducted an experiment to decelerate the ubiquitination process. This was achieved by employing soluble Cue1 as an alternative to the whole membrane-bound Cue1. Furthermore, we utilized a ubiquitin mutant, K48R, which exclusively facilitates the monoubiquitination of Hrd1. Similar approach was also used to measure the HRD complex. Nevertheless, these approaches did not effectively address the instabilities present in the bilayer. Consequently, we opted to measure the preubiquitinated Hrd1 or the HRD complex in our bilayer, rather than pursuing in situ ubiquitination.

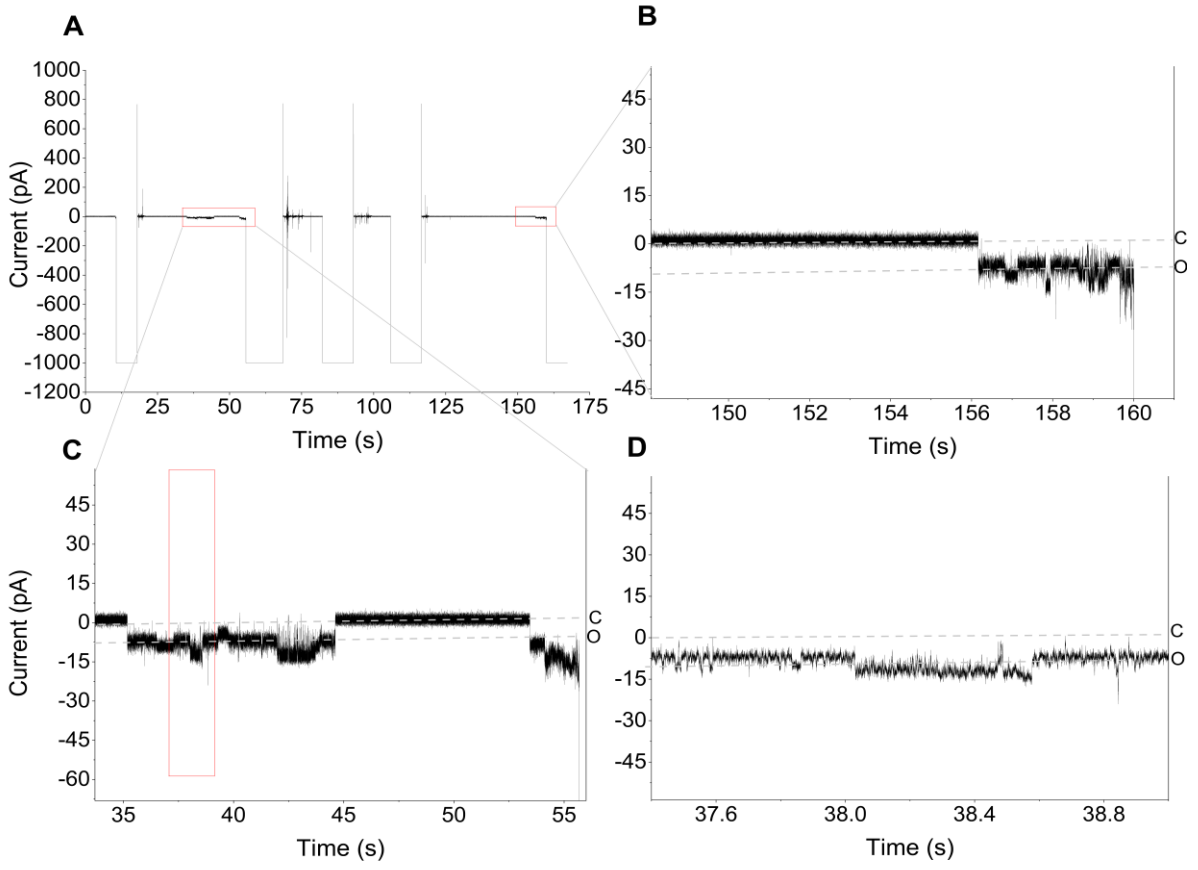

Figure 2.10: In situ ubiquitination. Representative example of a current trace of a bilayer containing the single Hrd1 followed by addition of 0.02 µM Uba1, 0.4 µM Ubc7, 20 µM ubiquitin and 2.5 µM ATP in absence of a voltage. (A) Current trace showing fusion of Hrd1 proteoliposomes to the bilayer after ubiquitination, unstable bilayer followed by rupture in bilayer and subsequent reformation. (B) and

(C) represent zoom plot from the current trace shown in (A), and (D) represents a zoom plot from the red box shown in current trace in (C); Buffer: 250 mM KCl, 10 mM MOPS/Tris, 5mM $MgCl_2$ pH 7 (cis), 20 mM KCl, 10 mM MOPS/Tris, 5mM $MgCl_2$ pH 7 (trans). C and O represent the closed and open state respectively.

2.4.5 Inconsistencies with reversal potential in HRD complex

The reversal potential for the single Hrd1 exhibited a consistent range. However, when measuring the HRD complex, a wide diversity in reverse potential was observed, ranging from +12 mV to +55 mV. Bilayer instabilities posed a significant challenge in the setup of our experimental procedure. As observed in the voltages ramp recordings (Figure 2.11), the bilayer was instable even at lower voltages of ±40 mV. There were few fusion events observed with the HRD complex proteoliposomes and only few were stable enough for the duration to finish a complete recording. In this thesis, only complete recordings are used for analysis to ensure accurate interpretation of the data. This kind of diversity in reversal potential along with the destabilizing effect on the membrane indicates an interaction between the translocon in question and with the membrane. Different complex composition can also lead to different reversal potential. Residual detergent could also potentially make the bilayer instable, however additional detergent removal step for the HRD complex proteoliposomes didn't make any difference.

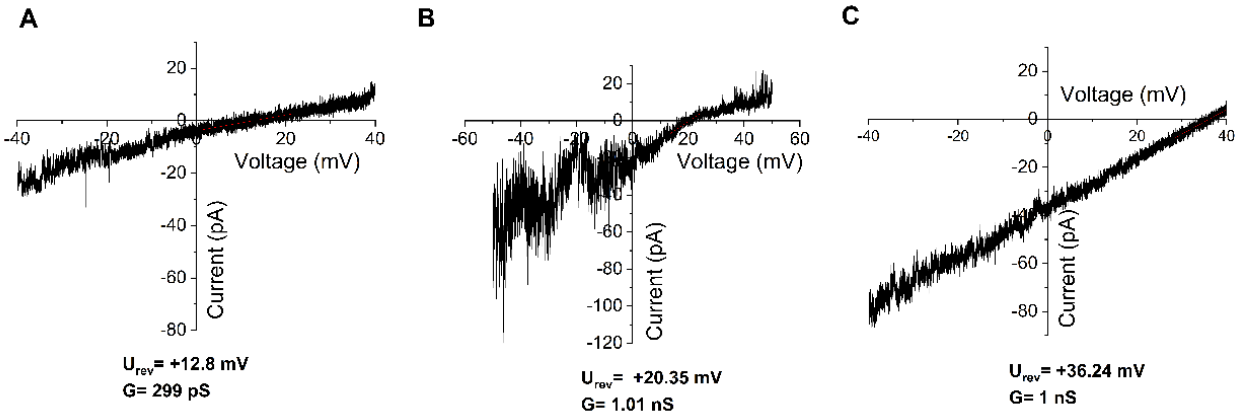

Figure 2.11 continued on next page

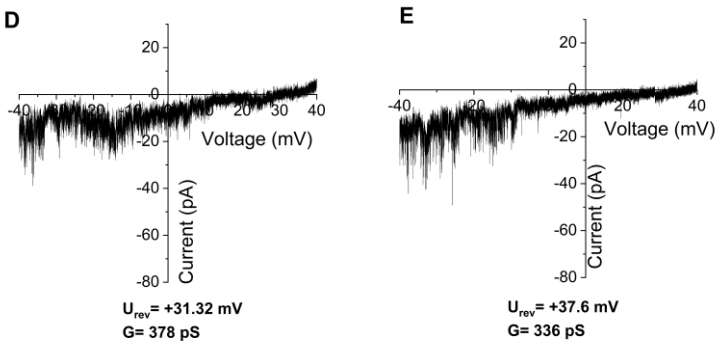

Figure 2.11: Voltage ramp recording of a bilayer containing the HRD complex. (A) to (E) represents voltage ramps from independent measurements. Buffer: 250 mM KCl, 10 mM MOPS/Tris, pH 7 (cis/trans)

2.4.6 Response of the HRD complex to deubiquitinase enzyme Usp2

Previous experimental findings have demonstrated that Hrd1 reconstituted into planar bilayers with the cytosolic RING domain located on the cis side and the substrate connecting with the luminal domain on the trans side. The PLBs experiment demonstrated that the addition of the DUB enzyme, Usp2, to the cytosolic RING domain-containing side resulted in the closure of the ubiquitinated Hrd1 open channel (Vasic et al. 2020). In this study, we applied the same methodology to the HRD complex proteoliposomes for identification of the HRD complex E3 ligase activity. Ubiquitinated HRD complex channel was fused to the bilayer and the buffer was perfused to the symmetric conditions. Subsequently, the Usp2 enzyme was added on the cis side of the chamber facing the cytosolic RING domain. Addition of 1 µM Usp2 to the cis side of the PLB setup which corresponds to the cytosolic side in cells, led to closing of an open ubiquitinated HRD complex channel most likely by deubiquitinating it. Voltage ramp recording from -40 mV to +40 mV showed a decrease in voltage dependent response to the current after addition of 1 µM Usp2 (n=7 bilayers) (Figure 2.12).

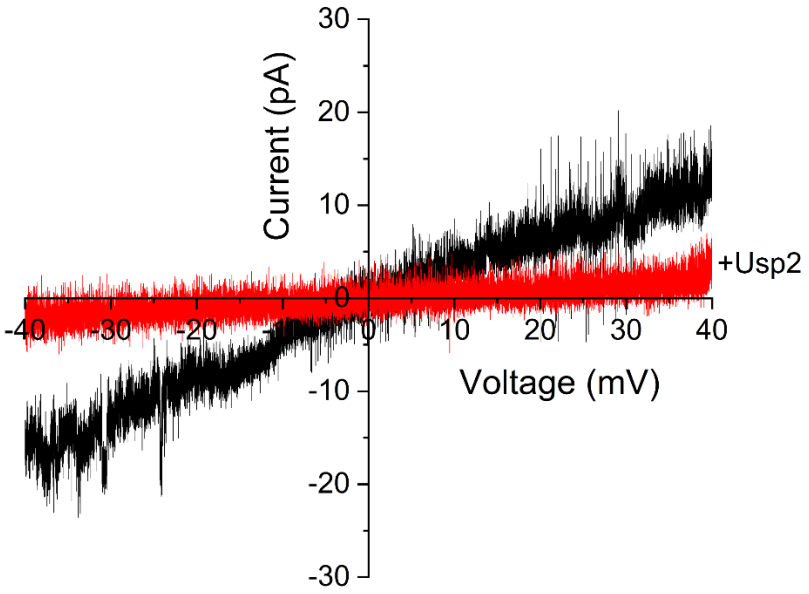

Figure 2.12: Voltage ramp recording of a bilayer containing the HRD complex from -40 mV to +40 mV before and after the addition of Usp2. Representative of n=7 bilayers. Red colour indicates addition of 1 µM Usp2 on cis side. Buffer: 250 mM KCl, 10 mM MOPS/Tris, pH 7 (cis/trans)

Current traces at indicated voltages also show a decrease in conductivity after Usp2 addition (Figure 2.13). Of note current traces from the HRD complex after deubiquitination don't show stable gating events as seen in the single Hrd1 channel implicating structural changes in the HRD complex due to involvement of other components of the HRD complex most likely Hrd1 and Der1.

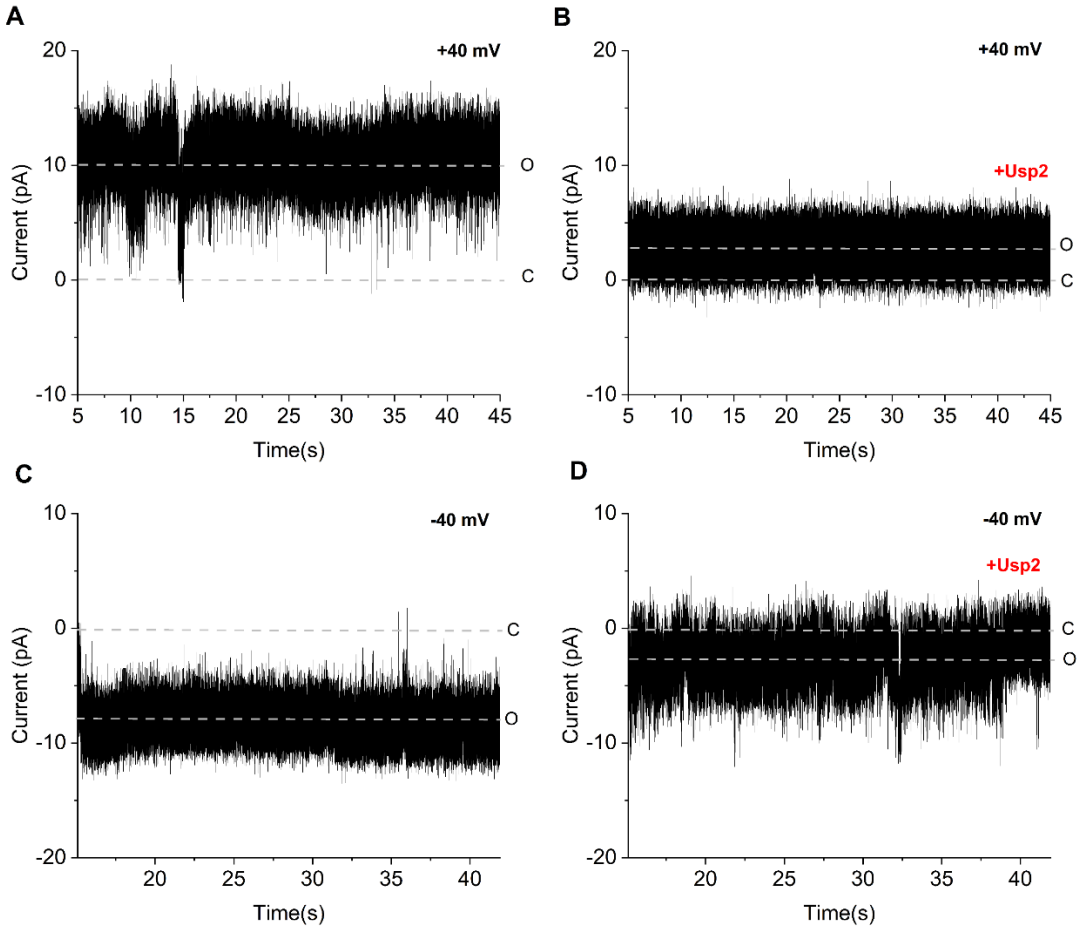

Figure 2.13: Representative example of current traces of the HRD complex at constant voltage before and after the addition of Usp2. (A) and (C) represent current trace in absence of Usp2 at +40 mV and -40 mV respectively and (B) and (D) represent current trace at +40 mV and -40 mV respectively with 1 µM Usp2. Buffer: 250 mM KCl, 10 mM MOPS/Tris, pH 7 (cis/trans). C and O represent closed and open state respectively.

Next, as described above, the conductance states, ΔG, were plotted against their frequency in a conductance state histogram (Figure 2.14). The histogram illustrates that the addition of Usp2 results in a reduction of gating events occurring at all but specifically higher conductance changes, in comparison to the conditions prior to Usp2 addition. The computation of open probability ($Po = I_{mean}/I_{max}$) indicates a chance of approximately 35% that the channel is in an open state in ubiquitinated condition. Furthermore, when the holding potential is increased to positive and negative voltages above ±40 mV, the open probability of the channel exhibits a gradual decline but it further decreases to around 12% upon the addition of Usp2 (Figure 2.14C). This suggests that the deubiquitination by Usp2 results in the removal of ubiquitin molecules, leading to the closure of the channel.

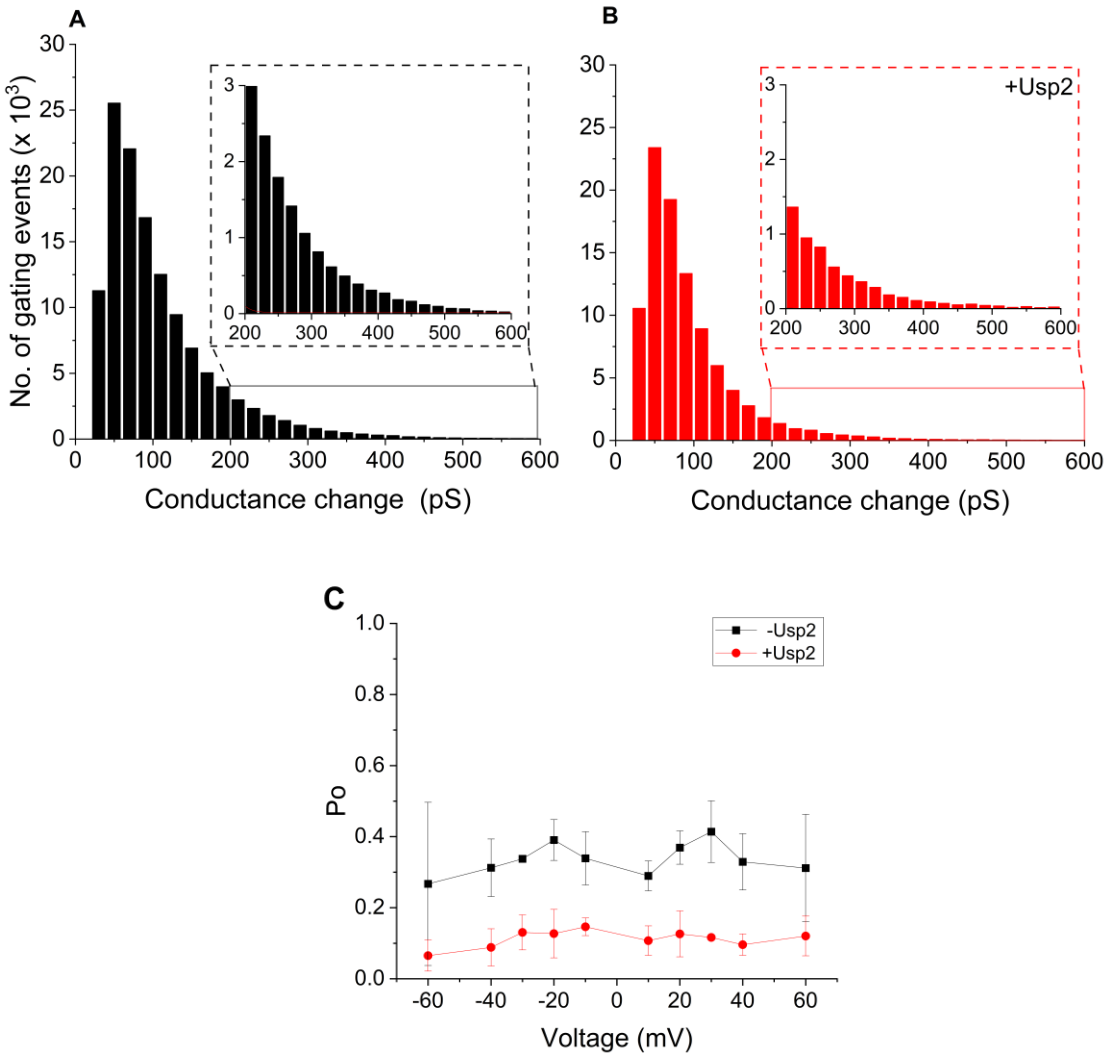

Figure 2.14: Usp2 induced decreased gating activity in the reconstituted HRD complex channels. Conductance-state histogram of the HRD complex channels. (A) before (black) and (B) after (red) in situ incubation with 1 µM Usp2, calculated from gating events at varying holding potentials (n= 6 independent experiments). The zoomed-in plot illustrates the decrease in gating events, after Usp2 addition. (C)Voltage dependence of the HRD complex channels opening probability (Po) before and after addition of 1 µM Usp2. For voltages ±20 mV and ±40 mV, n= 5 independent experiments and for ±10 mV, ±30 mV and ±60 mV, n= 3 independent experiments. Data are expressed as mean ± SD.

2.4.7 Response of the HRD complex to the model substrate CPY*

The model substrate CPY* has been widely studied in ERAD-L retrotranslocation. Vasic et al. 2020 showed that the addition of CPY* to the trans side of the bilayer which corresponds to the ER lumen activates the single Hrd1 channel and leads to flickering, large gating events and increase in pore size, indicating that the substrate interacts with the single Hrd1 in situ. We used the same approach to see substrate engagement with the HRD complex. The current flow through the channel was measured while subjecting it to a range of voltages spanning from -40 mV to +40 mV under symmetrical conditions. When we added CPY* to the bilayer containing an open ubiquitinated HRD complex channel, we saw the same effect of flickering and increase in large gating events in comparison to the conditions without CPY* addition (Figure 2.15). One of the major challenges during measurements with CPY* was the instability caused probably by this activation which led to high current spikes and disrupted bilayers within seconds.

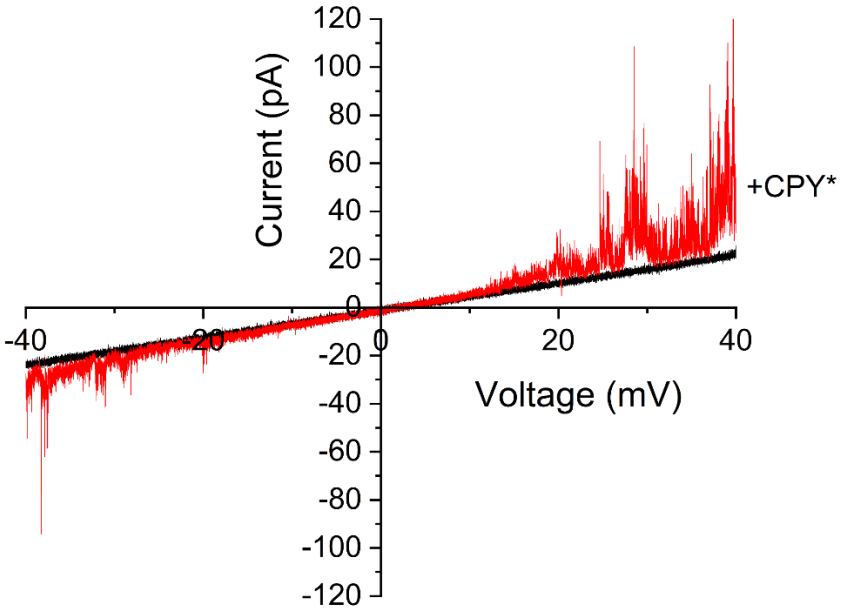

Figure 2.15: Voltage ramp recording of a bilayer containing the HRD complex before and after addition of the model substrate CPY* (n=4). Red colour indicates addition of 100 nm CPY* on trans side. Buffer: 250 mM KCl, 10 mM MOPS/Tris, pH 7 (cis/trans)

Current traces at a holding potential of -20 mV already shows an increase in conductance and large gating events after the addition of CPY* indicating the substrates still interacts with the components of the HRD complex (Figure 2.16B). However, at holding potential of just +40mV, the bilayer was hardly stable for a few minutes and had a tendency to show conductance spikes and rupturing. This indicates that the integrity of other components in the HRD complex might be compromised or somehow the ubiquitinated HRD complex which represents the open state of the channel itself made the bilayer instable. This was supported by the control experiments where only the addition of CPY* or ubiquitination machinery, or the non-ubiquitinated HRD complex alone to the bilayer did not result in any disruption of the bilayer. It is noteworthy that in PLBs the substrate couldn't retrotranslocate to the other side completely as Cdc48 ATPase is not integrated in the liposomes. But we also expected that the substrate blocks the channel completely rather than leading to an increase in the pore size of the channel formed by the HRD complex.

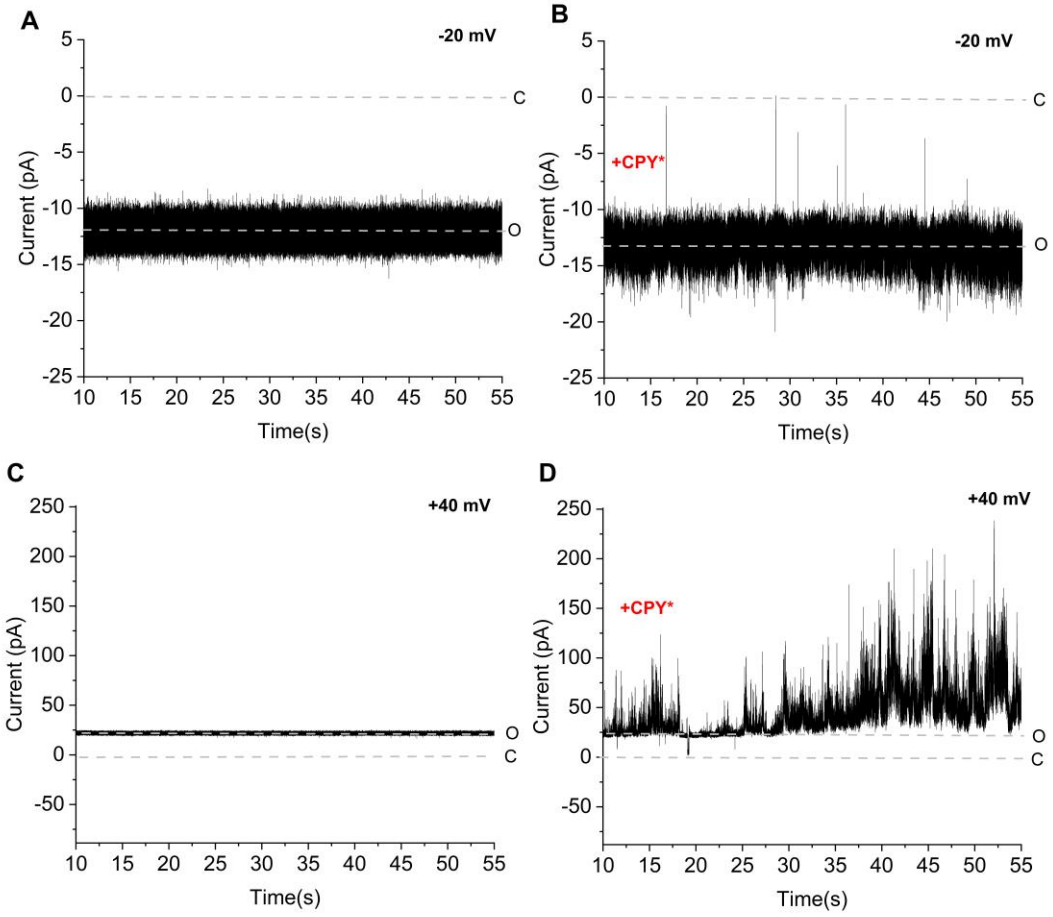

Figure 2.16: Representative example of current trace of the HRD complex at constant voltage before and after addition of the model substrate CPY*. (A) and (C) represent current trace at +40 mV and -40 mV respectively and (B) and (D) represent current trace at +40 mV and -40 mV respectively with 100 nm CPY*. Buffer: 250 mM KCl, 10 mM MOPS/Tris, pH 7 (cis/trans). C and O represent closed and open state respectively.

We then again calculated conductance states and the results are summarised in a histogram in Figure 2.17. we observed more gating events without the presence of CPY* especially at lower conductance state. At 70 pS, there were 7,916 gating events compared to 4,012 gating events after addition of CPY* (from raw data of histogram in Figure 2.17A and B). But the addition of 100 nm CPY* results in an increase of gating events occurring at higher conductance changes above 250 pS (Figure 2.17C and D), in comparison to the conditions prior to CPY* addition (Figure 2.17A and C). The increase in gating events at large conductance (Figure 2.17B and D, Figure 2.18B) up to 1000-1200 pS also indicates expansion of the pore to a size of 3.4- 3.9 nm. Altogether, this increase in number of gating events at higher conductance changes indicates expansion of the channel forming component in HRD complex after addition of the model substrate, CPY*.

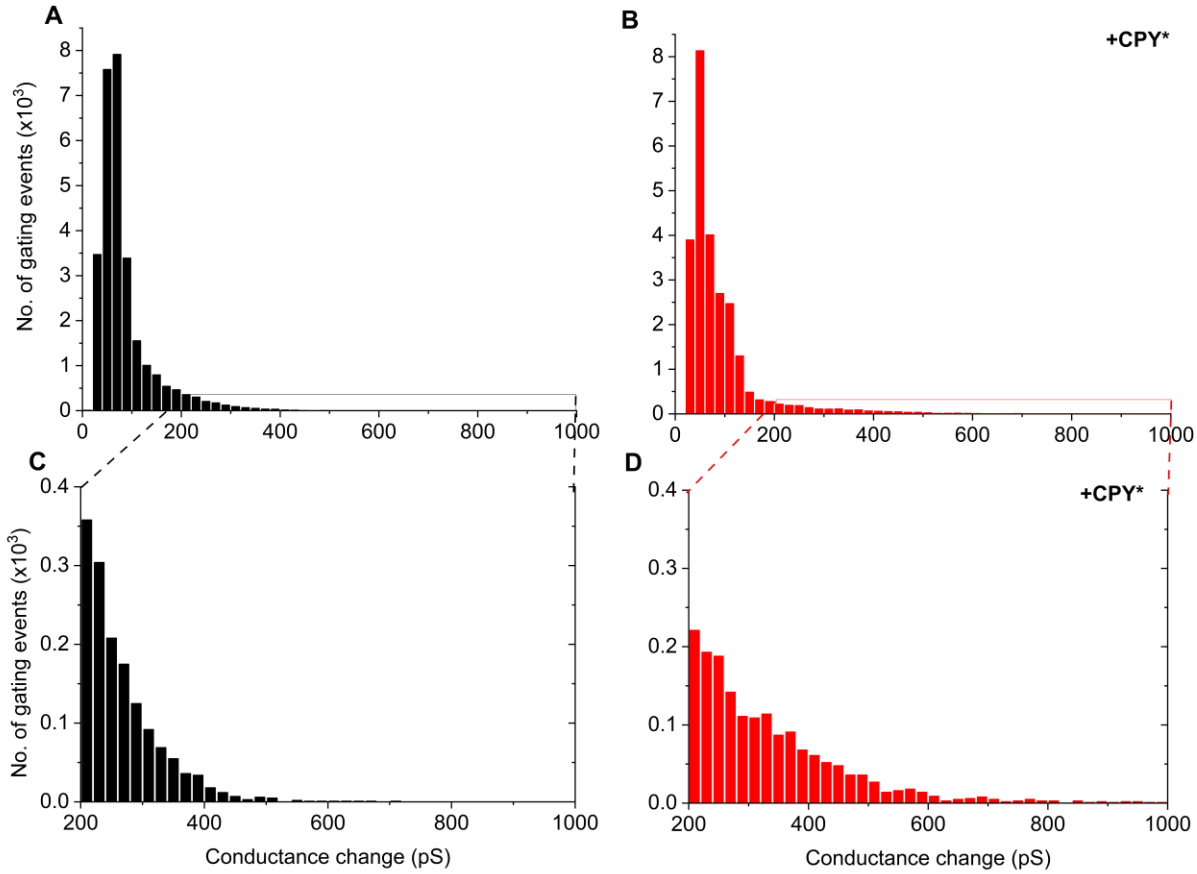

Figure 2.17: Conductance-state histogram of the HRD complex channels before and after addition of the model substrate CPY*. (A and C) before and (B and D) after in situ incubation with 100 nm CPY*, calculated from gating events at varying holding potentials (n= 5 independent experiments). (C) and (D) are zoomed-in plot which illustrates the increase in gating events at high conductance changes, after CPY* addition.

The investigation of the temporal dimension of the HRD complex gating has the potential to provide valuable understanding of the dynamics of the channel. The analysis presented in Figure 2.18 focused on the dwell time periods, which refer to the residency times of the channel at a distinct conductance. This analysis was conducted both before and after the addition of CPY*. The majority of the gating events occur between 0-0.75 seconds both before and after the addition of CPY* and show no significant difference. But addition of CPY* leads to gating events at higher conductance states of ~ 500 pS show a longer dwell time of 0-0.5 s (blue circle in Figure 2.18) in comparison to the conductance states prior to the addition of CPY*. Surprisingly, there is also a significant decrease in gating events at higher dwell times from 0.75 seconds after addition of CPY* (Figure 2.18C), which could be due to the inability of the HRD channel to stay in open states as it was observed before that the addition of CPY* leads to instability of the bilayer.

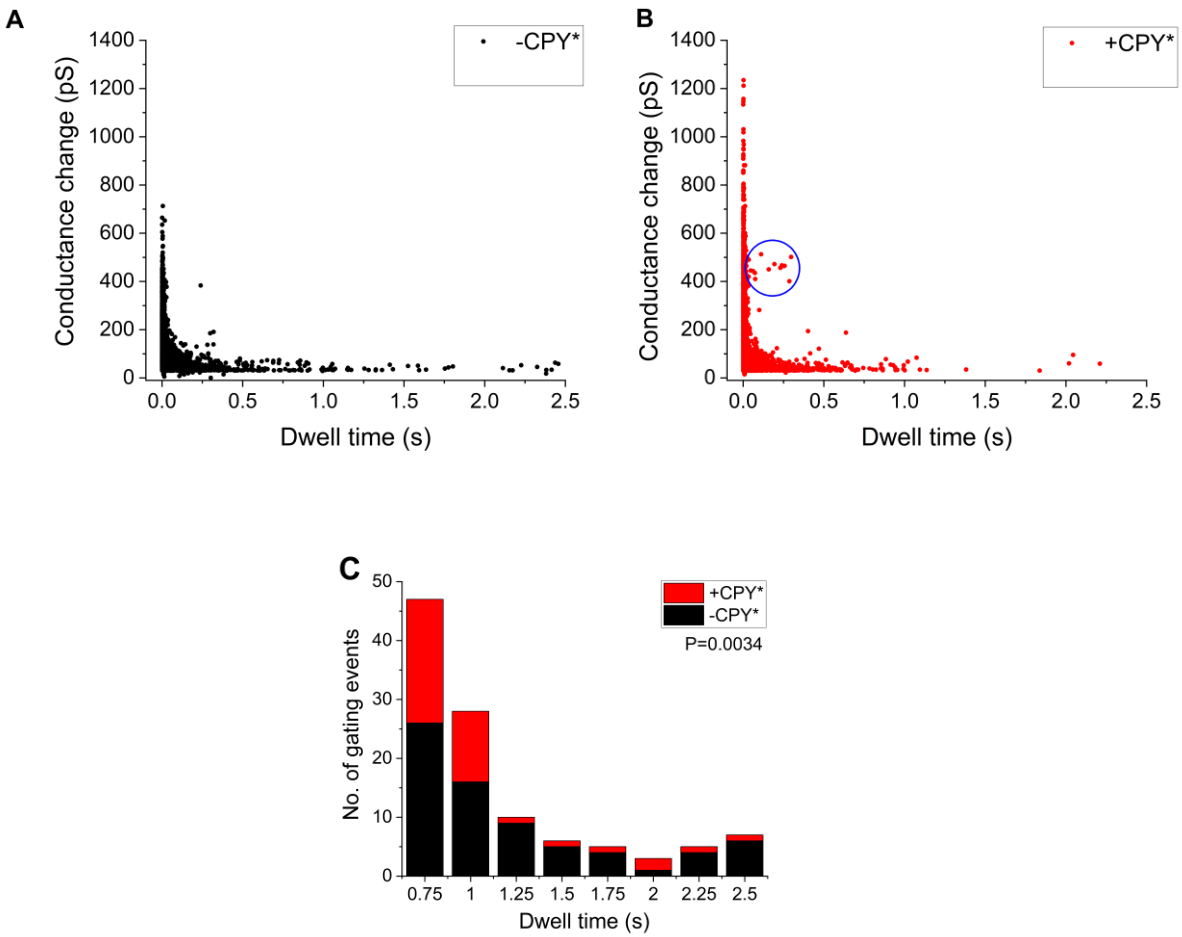

Figure 2.18: Dwell time data of the HRD complex at different conductance changes. Dwell time plotted against conductance change before (A) and after addition of 100 nm CPY* of a bilayer containing the HRD complex channel. (C) Comparison of number of gating events at higher dwell times from 0.75-2.5 seconds before (black) and after (red) the addition of CPY*. P value indicates value obtained from paired test. n=5 independent experiments.

2.5 Discussion

The HRD complex is the primary complex responsible for facilitating the ERAD-L pathway, which is involved in the retrotranslocation of misfolded substrates from the ER lumen. The HRD complex involved in ERAD-L comprises four fundamental components, namely Hrd1, Hrd3, Usa1, and Der1. Within the HRD complex, each individual component plays a crucial function, and the collective effort of all components is necessary for the retrotranslocation of ERAD-L substrates. Recently, the mechanism underlying retrotranslocation of misfolded substrates has been elucidated through the examination of the electrophysiological properties of the Hrd1 protein. These investigations have revealed that Hrd1 is the first known water-filled pore that is regulated by ubiquitination (Vasic et al. 2020). In the cellular system, it would exist as a complex within the ER membrane and there are numerous in vivo studies describing the importance of different subunits of the HRD complex. In this study, we were interested to see how electrophysiological properties of Hrd1 change in the context of the HRD complex. We indeed observed channel activity through the measurements of the HRD complex reconstituted in proteoliposomes.

2.5.1 The HRD complex forms an ion channel regulated by ubiquitination

We used high resolution single channel electrophysiology to study the functional properties of the HRD complex. The HRD complex was purified from yeast and reconstituted into LUVs mimicking the ER lipid composition which was performed and optimized by our collaborators (Section 2.3.2.2). When the non-ubiquitinated HRD complex was added to the bilayer, no ion flux was observed. However, when the ubiquitinated HRD complex was added to the proteoliposomes, ion flux was observed along with gating events, which indicated the presence of a pore in the bilayer (Figure 2.9A). The process of auto-ubiquitination in the RING domain of Hrd1 is necessary for the formation of a retrotranslocation pore (Vasic et al. 2020). This finding is consistent with the previously reported ubiquitination dependent opening and closing of a channel observed in Hrd1 measurements and also retrotranslocation shown in vitro by Hrd1 alone (Vasic et al. 2020; Baldridge and Rapoport 2016). There is evidence of ion channels regulated by ubiquitination previously as well. Some classic examples are regulation of the voltage-gated KCNQ1 potassium channel and epithelial Na^+ channels (ENaC) by an E3 ligase NEDD4/NEDD4-like-dependent ubiquitination (Jespersen et al. 2007; Lamothe and Zhang 2016). But NEDD4 ligases mainly regulate activity of ion channels by recycling them after ubiquitination rather than the ion conductance as it is for Hrd1. Recently it was found that the N-terminal ubiquitination of a TRP channel TRPV4 led to decreased calcium influx without increasing the number of channels on the cell surface and vice versa. This suggests that ubiquitination negatively

modulates TRPV4 channel activity regardless of its cell membrane location (Aisenberg et al. 2022). But Hrd1 was the first instance where an E3 ligase was shown to form a channel regulated by autoubiquitination, leading to removal of misfolded substrates from the ER (Vasic et al. 2020).

2.5.2 Current voltage relationship of single Hrd1 and HRD complex

The determination of the reversal potential for a channel that exhibits a selectivity towards a specific type of ion can be readily approximated by employing the Goldman-Hodgkin-Katz equation (Goldman 1943; Hodgkin and Katz 1949). The study conducted by Vasic et al. 2020 demonstrates the existence of several reversal potentials during electrophysiological characterization of Hrd1, ranging from 250 mM to 20 mM KCl with a low preference for cations. In this study, a single reversal potential was seen with high accuracy when going through a voltage range in a salt gradient from 250 mM to 20 mM KCl. The obtained reversal potential was determined to be U_{rev}= +7.4 ± 0.08 mV (Figure 2.8A) which corresponds to a marginal cationic selectivity of $P_{K^+} : P_{Cl^-}$ = 1.4. Interestingly the Sec61 translocon in yeast which imports protein from the cytosol to the ER shows an anion selectivity of -7.6 ± 2.4 mV and anion selectivity of $P_{Cl^-} : P_{K^+}$ = 1.42 (F. Erdmann et al. 2010). This raises the question of how the export and import of proteins might change the membrane potential of the ER. It is anticipated that the resting TM potential of the ER is either neutral or slightly negative, with a negative lumen compared to the cytosol (Burdakov, Petersen, and Verkhratsky 2005; Lam and Galione 2013). The ER is also involved in Ca^{2+} signalling which is regulated by various receptors and channels. The prevailing concept posits that, despite the substantial efflux of calcium from the ER lumen during calcium release, the membrane potential of the ER remains rather constant. This is attributed to a simultaneous influx of potassium ions that counterbalances the outward movement of calcium ions (Klier, Roo, and Miller 2022). Nonetheless, obtaining precise measurements of the membrane potential of the ER and especially focussing on how it changes during import and export of proteins in intact cells is a technically challenging task.

The HRD complex on the contrary to Hrd1 shows a very different and diverse range of reversal potentials, from +12 mV to +55 mV. Normally the reversal potential of a channel for one specific type of an ion in a particular salt gradient is somewhat similar. However, this diversity in reversal potential and ion selectivities we see in HRD complex can have various explanations. The components of HRD complex, Hrd1, Hrd3, Der1 and Usa1 are all purified from the yeast membrane as a single complex. One can expect theoretically that the complex remains intact, but due to the use of harsh detergent and purification conditions, it might be possible that they disintegrate, leading to different complex composition or change in membrane stability. Sometimes contaminants or residual detergents in the

complex from purification or from liposome reconstitution can solubilize the lipid membrane causing instability.

2.5.3 Gating dynamics of the HRD complex and it's response to model substrate

To compare gating dynamics of Hrd1 and the HRD complex, electrophysiological characterization of single Hrd1 was also performed (Figure 2.7). Both ubiquitinated Hrd1 and the HRD holocomplex channel exhibited a state of inactivity and limited size due to the infrequent occurrence of large gating events and the conductance states falling within the 50-70 pS range which corresponds to a pore size of 0.5-0.6 nm (Figure 2.7A, Figure 2.9). The conductance state was reported previously electrophysiological characterization of single Hrd1 were between 10-50 pS (Vasic et al. 2020). We observed a different range because the filter cut off was set at 30 pS to calculate the gating events and filter out the noise which can be calculated as gating events by the automated reconstruction process implemented in the R-package "stepR" (Hotz et al. 2013). But the main conductance observed in this thesis for Hrd1 and HRD complex, as well as in the previous results of Hrd1 by Vasic et al. 2020, remained similar at 50 pS. The observed gating events in the Hrd1 protein exhibited distinct and well-defined gating characteristics, spanning a range of up to 1000 pS, which corresponds to a maximal pore size of 3.42 nm (Figure 2.7C). In contrast to single Hrd1, the gating events observed in the HRD complex were less well defined, with the maximum gating events reaching only 600 pS, corresponding to a maximal pore size of 2.4 nm (Figure 2.14A, Figure 2.17A and C). If Hrd1 was the sole constituent responsible for channel formation inside the HRD complex, it could be inferred that the anticipated pore size remained consistent. However, the gating behaviour underwent alterations, suggesting that the components of the HRD complex influenced the dynamics of the pore. Single Hrd1 formed a pore without any other subunits of the HRD complex, as it was found that overexpression of Hrd1 could compensate for the absence of any other subunit within the HRD complex (Carvalho, Stanley, and Rapoport 2010).

Next we studied the interaction of the HRD complex with the model substrate CPY*. Vasic et al. 2020 had previously shown that the addition of 100 nm CPY* to the trans side of the bilayer, which corresponded to the luminal side of the ER and showed flickering in ion currents and increased gating events. This approach of addition of substrates and antibodies to the translocon in question is not uncommon in PLB experiments. When substrate interaction was studied by single channel electrophysiology for mitochondrial protein importer channels Tom40, Tim23 and Tim22, each of the importers exhibited a response to corresponding substrate presequences at low concentrations characterized by flickering, whereas at high concentrations, closure of the channel was induced (Hill

et al. 1998; Truscott et al. 2001; Kovermann et al. 2002). We had expected that, depending on how the misfolded substrate CPY* interacted with the HRD complex, it would either block the pore, resulting in no ion flux, or lead to an expansion of pore size, accompanied by an increase in ion flux and conductance. The addition of 100 nm CPY* to the trans side of the bilayer, increased the number of gating events, which led to high-frequency flickering of the channel (Figure 2.15, Figure 2.16). Overall channel closure was not observed with 100 nm CPY*. Different concentration of CPY* should be tested in PLB experiments to see how the HRD complex would respond. Another important finding is that proteins consistently insert in the same direction, as the addition of substrate to only one side i.e. trans is sufficient to observe the flickering effect caused by substrate-mediated interaction as observed previously by Vasic et al. 2020. Vasic et al. 2020 also showed that Hrd1 responds to Usp2 by decreasing the ion flux and ultimately closing the channel. The catalytic core of the Usp2 which consist of Cys, His, Asp/Asn in sequence, binds to the ubiquitinated Hrd1 and removes the ubiquitin molecule (Renatus et al. 2006). It was also observed that the cytosolic RING domain always inserted on the cis side of the bilayer. In our experimental approach we observed the same results: the addition of Usp2 to the cis side of the bilayer led to a decrease in ion flux and decreased the conductance of the HRD channel (Figure 2.13 and Figure 13).

We saw that the ubiquitinated HRD complex channels exhibit a maximal pore size of around 2.4 nm but the pore size according to the main conductance state is ~ 0.5 nm. This observation suggests that the non-stimulated channel (without the substrate) possesses the capacity to expand to bigger pore sizes. The diameter of an α-helix is 1.2 nm (Sinden 1994) which means that two α-helices can pass through the HRD complex side by side when the channel is at maximal pore size. In the cell, chaperones help misfolded proteins to stay in a soluble state, but these misfolded proteins are not in a completely unfolded state and still retain regions of folded polypeptide. It is now known that Cdc48 unfolds the misfolded polypeptide once the polypeptide chain moves to the cytosol (Twomey et al. 2019). Therefore, misfolded substrates might require a much bigger pore size to be accommodated and it is plausible that substrate binding may lower the energy barrier for this additional expansion. In agreement with this, the measured maximal conductance states following the addition of CPY* were found to be higher and within the range of 1200 pS which correspond to a pore size of 3.92 nm, which is much bigger than the maximal pore size in the absence of CPY*. The continual open state of a translocon can have detrimental effects on the ER luminal homeostasis due to the potential movement of ions, which can disrupt the membrane potential. To avoid such leak currents under non-translocation activity would explain why only substrate addition leads to further expansion of the pore.

The pore size of the substrate-activated HRD complex channel correlates with other channels that are involved in the translocation of folded proteins. Peroxisomes also have the capability to internalize substantial folded proteins with diameters ranging from 4-9 nm due to the oligomerization of pore forming components, Pex5 and Pex14 (Walton, Hill, and Subramani 1995; Meinecke et al. 2010b). The expansion of pore size up to ~4.7 nm in the peroxisomes import mechanism was seen when incubated with its cargo components, which includes folded proteins containing the PTS2 signal (Montilla-Martinez et al. 2015). We also found that human PEX5L complexes forms a maximal pore size of 3.3 nm with the substrates (Ghosh et al. 2023). Protein import into chloroplasts by TOC/TIC which are also known to import folded substrates, forms a maximal pore size of 3–3.5 nm (Ganesan and Theg 2019). On the contrary, the translocation systems of bacterial Sec and mitochondrial TOM/TIM exhibit a dependence on unfolded substrates and possess relatively small pores in comparison to the TOC/TIC translocon (Ganesan et al. 2018). So far, Hrd1 channels have only be activated with CPY*, but it would be interesting to see how different substrates stimulate the pore size and other characteristics of the channel. Yeast peroxisomal PTS1 specific pores also expand more in presence of large cargo molecules (Meinecke et al. 2010b). Similar effects might be observed with single Hrd1 or HRD complex channel as well. On a different note, a recent discovery has identified a degradation signal called degron, which plays a crucial role in the identification and degradation of substrates targeted for Hrd1-centric ERAD and for further degradation by the cytosolic proteasome (Sharninghausen et al. 2023). In future, for substrate interaction studies, peptides with degrons can be utilized to characterize the channel properties.

2.5.4 Regulation of protein translocon pores

The regulation of protein translocation pores is governed by a variety of gating mechanisms. One of the well-known mechanisms is dynamic modulation of the TM segment of the pore providing the ability to open or enlarge by a conformational shift and/or the assembly of several pore-forming units (Ganesan and Theg 2019). In Hrd1, the main mechanism of open and closing is regulated by ubiquitination and deubiquitination respectively, of the cytosolic RING domain (Vasic et al. 2020; Peterson et al. 2019). One main feature associated with expansion of pore size has been the flexibility in the TM region. In Hrd1 dimeric structure, the cytosolic cavity shows hydrophilic and charged residues. The residues have a relatively lower density of side chains when compared to those engaged in helix interactions which suggests that these residues possess a greater degree of flexibility. The cryo-EM structure does not exhibit a discernible electron density for the RING domain, suggesting flexibility in this region (Schoebel et al. 2017). The process of dimerization between two Hrd1 molecules is facilitated by the interaction surfaces formed by TM domains 1 and 2 of one Hrd1

molecule with TM domains 8 and 3 of the other molecule, as well as the interaction between TM domain 3 of both Hrd1 molecules (Schoebel et al. 2017). The RING domain is located few amino acids away from TM 8 and the cryo EM structure suggests the involvement of possibly only the RING domain from one Hrd1 molecule for dimerization. Autoubiquitination of the Hrd1 molecule on the RING domain might also induce a conformational change. But structural models described so far don't consider the RING domain activity. How Der1's conformation might play a role in this retrotranslocation is also mysterious.

One of the initial observations about the enlargement of pores during the process of protein translocation was made in relation to the ER Sec61 translocon. It was observed that the Sec61 translocon exhibited varying channel widths while in the presence or absence of ribosomes (Hamman et al. 1997). The TolC protein, which belongs to the type I outer membrane component, is characterized by its b-barrel transmembrane domains and helical coiled coil periplasmic domains. These structural features enable TolC to regulate the pore by undergoing twisting motions that result in its opening and closing, resembling the movement of an iris (Pei et al. 2011). In the above examples, the flexibility in TM region was the mechanism for expansion of the pore. The Tom40 protein, which forms a pore in the outer membrane of mitochondria and consists of a 19-stranded beta-barrel structure, does not seem to undergo expansion due to absence of such flexible regions but it did show gating (Bausewein et al. 2017; M. P. Schwartz and Matouschek 1999; Hill et al. 1998). There is no biochemical or structural evidence that suggests that monomeric Hrd1 can form a pore alone. Either oligomerization of Hrd1 or engagement of Hrd1 with Der1, which are both essential for ERAD-L might be key to how the ERAD retrotranslocon is regulated. This is further discussed in the section 2.5.6.

2.5.5 Membrane thinning as a mechanism for retrotranslocation

Instability of the bilayer upon addition of ubiquitinated HRD complex posed the main technical challenge for electrophysiological characterizations. The reason for this might be hidden in the cryo-EM structures of Hrd1 and Der1 which reveal that the lateral gates of Hrd1 and Der1 are oriented towards each other. These proteins interact on the luminal side of the membrane, primarily through specific amino acid residues located in TM2 of Der1 and TM3 of Hrd1. This interaction results in the formation of two hydrophilic "half-channels" (Wu et al. 2020). The cytosolic side of the region between these two proteins has a significant depression, characterized by a membrane thickness of around 2.4 nm, which contrasts with the average thickness of approximately 4 nm observed in other regions. The thinning of the membrane was verified by MD simulations. Additionally, experimental testing demonstrated that Hrd1, when present alone, is sufficient to produce membrane thinning on the

cytosolic side, likely due to the presence of hydrophilic residues (Wu et al. 2020). Along the same lines, it is worth noting that Der1 exhibits a cytosolic cavity that is characterized by the presence of many hydrophilic residues, hence resulting in a region of membrane thinning and mutation of these amino acids to hydrophobic residues increased membrane thickness and greatly impeded ERAD-L (Wu et al. 2020; Kreutzberger et al. 2019). The presence of these hydrophilic residues is a distinctive characteristic of active rhomboid proteases, as evidenced by prior structural observations (Y. Wang, Zhang, and Ha 2006; Z. Wu et al. 2006). This membrane thinning supposedly reduces the energy barrier for translocation of the hydrophilic substrate peptide which would likely happen on the interface between translocases and the membrane. Several other translocases are proposed to adopt the same translocation mechanism. In the bacterial membrane insertase YidC, there are 5 TMs which form a cytosolic cavity and a lipid-facing aperture. Short helices of TMs 3–5 were shown to cause local membrane thinning in MD stimulations. The data presented in this study indicate that TM segments of substrates are able to penetrate the cavity, and furthermore, the region of the membrane that has been thinned, enhances the translocation of hydrophilic segments to the opposite side of the membrane. The mitochondrial carrier protein Tim22, responsible for protein insertion into the inner membrane, is comprised of four TMs. It has a curved surface with pronounced invaginations on both sides of the inner membrane. However, it does not possess a conventional hydrophilic cavity. Similarly, to the aforementioned instances, it is seen that the lipid-interacting region of the protein is considerably shorter than the typical bilayer thickness (Yutong Zhang et al. 2021). Consequently, it is suggested that the membrane thinning induced by Tim22 aids in the insertion of membrane proteins (Wu and Rapoport 2021). One of the more well studied examples is the bacterial Eco-MscL channel which thins the membrane around it but does not lead to spontaneous gating of channels. Membrane thining made them easier to gate, suggesting it may modulate gating but was not the primary stimulus. Later it was found to be gated by the lipids in the pore (Perozo et al. 2002; Iscla and Blount 2012; X. C. Zhang, Liu, and Li 2016; Yixiao Zhang et al. 2021). This indicates that membrane thinning does exists in different translocon but this factor is not necessarily the transport mechanism in all cases. When we introduced the ubiquitinated Hrd1/Hrd3/Usa1 complex, which had been reconstituted in liposomes, to PLBs, it was seen that fusion occurred; nevertheless, the bilayer promptly underwent subsequent rupture indicating no channel formation without Der1. The potential source of the bilayer instability seen during the measurement of the HRD complex could be attributed to the membrane thinning effect induced by Hrd1 and Der1 proteins.

2.5.6 Unravelling the oligomeric states of Hrd1 and Der1 during retrotranslocation

The process of oligomerization is believed to play a crucial role in the adaptation of E3 ligase activity to meet the specific demands of the cell (Balaji and Hoppe 2020; Hu and Fearon 1999; Plechanovová et al. 2011; Hoppe et al. 2004). Previous studies have also demonstrated the occurrence of dimerization in cytoplasmic RING-finger and U-box type ubiquitin-ligases (Knipscheer and Sixma 2007). Nonetheless, certain RING E3 ligases have demonstrated the ability to undergo dimerization or create oligomers via regions that exhibit different structural characteristics and are physically distant from the RING domain (Metzger et al. 2014; Fiorentini, Esposito, and Rittinger 2020). The oligomerization of Hrd1 is a necessary process for the degradation of ERAD-L substrates (Carvalho, Stanley, and Rapoport 2010). The N- and C- terminal domains of the Hrd1 are responsible for inducing oligomerization and binding to Der1, respectively which is facilitated by Usa1 (Horn et al. 2009; Thibault and Ng 2012). The oligomeric state of functional Hrd1 in the HRD complex remains elusive. There are different cryo-EM structures available displaying different oligomeric states of Hrd1 and Der1 during retrotranslocation. The limitation of these structures is that the retrotranslocation complex, as observed in both the Hrd1 homodimer model (Schoebel et al. 2017) and the Hrd1-Der1 heterodimer model (Wu et al. 2020), does not exhibit the formation of a substrate conducting pore. Schoebel et al. 2017 showed a dimeric structure of Hrd1-Hrd3 in which Hrd1 exists as a dimer and forms a cytosolic cavity by its TM3- TM8. The cytosolic cavity within the dimeric Hrd1 structure needs a significant conformational shift or helix rearrangements for the passage of substrate peptide chains as this model suggest the cavity is in the closed conformation by TM1 of a neighboring Hrd1. This is consistent with the in vivo experiments that show that ERAD-L substrate efficiently crosslinks to Hrd1 without Usa1, which is necessary for oligomerization (Carvalho, Stanley, and Rapoport 2010). In the heterodimer model, Hrd1 exist as monomer together with Hrd3, Der1 and Usa1. The cytosolic cavity in this model is not restricted by TM domains indicating substrates can pass through but this model too lacks a typical channel like structure. It shows membrane thinning as the mechanism to reduce the energy barrier to move the substrate polypeptide chains (Wu et al. 2020).

A recent study which used single-molecule total internal reflection fluorescence (TIRF) approach to count Hrd1 reconstituted into liposomes found that Hrd1 assembles in diverse oligomeric configurations in LUVs, with predominantly monomers and dimers at low protein-to-lipid ratios (Hrd1: lipid 1:5 and 1:20) and mostly oligomers at high ratios. Even when the ratios were extremely low, the proportion of dimers to monomers was maintained (Assainar, Ragunathan, and Baldridge 2023). In the in vitro ubiquitination assay, which was necessary for retrotranslocation, it was shown that dimers

assembled polyubiquitin chains, while Hrd1 monomers could not autoubiquitinate (Assainar, Ragunathan, and Baldridge 2023). In our experiments we used a 1:5000 Hrd1 protein to lipid ratio implying that most of our liposomes were either empty or in monomer/dimer configuration. This might explain the low fusion rate we observed, as only ubiquitinated Hrd1 is supposed to form a water filled pore. I also propose that Hrd1 might exist in dimers in vitro and retrotranslocate substrates upon autoubiquitination. In line with this Hrd1 is essential for HRD complex stability, forms a channel only upon ubiquitination and structural data also support a dimeric state. However, in the cell, Hrd1 is part of a multi subunit complex and probably forms a pore in conjunction with Der1. This could explain why our bilayer experiments exhibit ion flux when a ubiquitinated HRD complex is present. Dimerization or oligomerization can be also linked to pore formation in mitochondrial translocase Tom40 in cryo EM structure from both yeast and humans (Tucker and Park 2019; Guan et al. 2021). On the contrary, for other mitochondrial translocase Tim23, it was suggested that it typically exists in a dimeric form, but it undergoes dissociation upon binding to a presequences, resulting in the formation of an active monomeric channel or hetero-oligomeric channels with other TIM23 subunits (Bauer et al. 1996).

The cryo-EM structure of the HRD ligase, demonstrates the presence of only a single Der1 molecule within the complex (Wu et al. 2020). Der1 is an essential subunit within the HRD complex, as any deletions or mutations occurring in the TM region of Der1 hinder the translocation of soluble proteins across the ER membrane (Knop et al. 1996; Mehnert, Sommer, and Jarosch 2014). According to a study conducted by Wu et al. 2020, the trajectory of the polypeptide through the membrane encompasses the luminal and cytosolic compartments of Der1 and Hrd1. In another study, it was demonstrated that the Der1 homolog Dfm1, which plays a role in the retrotranslocation of ERAD-M substrates, employs rhomboid-like signature motifs to facilitate the retrotranslocation of folded luminal domains. Only the monomeric, but not the oligomeric, form of Dfm1 exhibited retrotranslocation of substrates. It is worth noting that rhomboid proteases typically operate as monomers but exist as dimers when they are physiologically inactive (Kreutzberger and Urban 2018). However, structure of human Derlin-1 (human homolog of Der1) adopts a homotetrameric configuration, encircling a tunnel that spans the ER membrane (B. Rao et al. 2021). The tunnel possesses a diameter ranging from around 1.2 to 1.5 nm, hence exhibiting sufficient size to accommodate the passage of an α helix. The membrane structure exhibits a lateral gate, which could facilitate the entry of transmembrane proteins into the tunnel and consequently functions as a protein translocon that enables the retrotranslocation of misfolded proteins (B. Rao et al. 2021). However, the pore size of 1.2 nm may not be sufficient for the translocation of folded proteins, although it is likely to expand in the presence of a substrate. Mammalian Derlin-1 is more similar to Dfm1 than Der1 due to presence of a small heterodimer partner

(SHP) box at the C-terminal which serves as a Cdc48p/ Valosin-containing protein (VCP)–binding motif (B. Rao et al. 2021). Hence, it is plausible that the translocation process facilitated by Der1 exhibits dissimilarities. Altogether, it can also be suggested that Hrd1 forms a translocation pore together with Der1 and they act as half channels. Moreover, the oligomeric conformation of both Hrd1 and Der1 seems quite crucial for retrotranslocation of misfolded substrates and should be explored further to elucidate the mechanistic details.

2.5.7 Mechanism of retrotranslocation by HRD complex

Based on the previous in vitro experimental results and structural analyses (Carvalho, Stanley, and Rapoport 2010; Stein et al. 2014; Vashistha et al. 2016; Wu et al. 2020) and electrophysiological data of the HRD complex presented in this thesis, as well as considering the observed membrane thinning effects mediated by Hrd1 and Der1 (Wu et al. 2020), it is possible to draw conclusions on the retrotranslocation mechanism. The initial step involves the recognition of a misfolded luminal substrate to Hrd3, followed by its subsequent binding to Hrd1 within the HRD complex (Figure 2.19A). Then Hrd1 autoubiquitinates on distinct lysine residues located inside its cytosolic RING domain. The substrate exhibits binding affinity towards both Hrd1 and Der1, forming a loop structure that is oriented towards the cytosolic region (Figure 2.19B). The process of autoubiquitination results in the activation of the translocon, which is accompanied by the presence of a thinned membrane region that aids in reducing the energy barrier. It is still debatable if membrane thinning and pore formation are mutually exclusive for retrotranslocation of the substrate. But both the proteins Hrd1 and Der1 in the HRD complex play a role in the process of channel formation and stabilization, hence aiding in the efficient transit of the substrate as there is no pore formation observed without Der1. Afterwards, Hrd1 polyubiquitinates the substrate on the cytosolic side of the ER membrane. Polyubiquitination serves as a molecular modification that designates the substrate for subsequent extraction and degradation processes. Concurrently, the process of Hrd1 autoubiquitination facilitates the recruitment of the Cdc48 complex to the specific area where substrate retrotranslocation occurs (Figure 2.19C). The Cdc48 complex utilizes ATP hydrolysis to generate mechanical force, enabling it to remove the substrate from the ER membrane. This extraction process occurs through the retrotranslocation channel, wherein the Cdc48 complex unfolds the ubiquitin chains once the substrate is on the cytosolic side (Twomey et al. 2019). Both Hrd1 and Der1 play a role in stabilizing the channel throughout the extraction process, thereby facilitating the effective translocation of the substrate. Following successful extraction, DUB enzymes effectively remove the ubiquitin chains from both Hrd1 and the substrate (Figure 2.19D). This closes the retrotranslocation channel, resetting the HRD complex for future rounds of retrotranslocation.

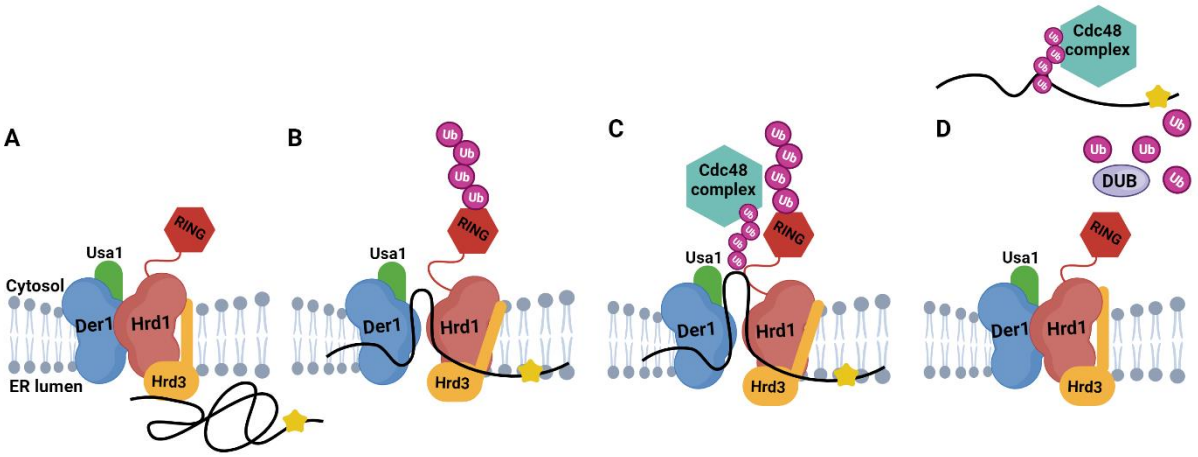

Figure 2.19 Schematic representation of retrotranslocation by the HRD complex. (A)Recognition of substrate by Hrd3 (B)Binding of substrate to both Hrd1 and Der1 in a loop like configuration, autoubiquitination of Hrd1 and opening of the HRD complex (C)Polyubiquitination of the substrate by Hrd1 and recruitment of Cdc48 complex (D)Removal of polyubiquitinated substrate by Cdc48 complex, deubiquitination of Hrd1 RING domain by DUB and closure of the HRD complex.

2.6 Bibliography

Agarraberes, Fernando A, and J. Fred Dice. 2001. 'Protein Translocation across Membranes'. *Biochimica et Biophysica Acta (BBA) - Biomembranes* 1513 (1): 1–24. https://doi.org/10.1016/S0304-4157(01)00005-3.

Aisenberg, William H., Brett A. McCray, Jeremy M. Sullivan, Erika Diehl, Lauren R. DeVine, Jonathan Alevy, Anna M. Bagnell, et al. 2022. 'Multiubiquitination of TRPV4 Reduces Channel Activity Independent of Surface Localization'. *Journal of Biological Chemistry* 298 (4). https://doi.org/10.1016/j.jbc.2022.101826.

Akutsu, Masato, Ivan Dikic, and Anja Bremm. 2016. 'Ubiquitin Chain Diversity at a Glance'. *Journal of Cell Science* 129 (5): 875–80. https://doi.org/10.1242/jcs.183954.

Allen, Simon, Hassan Y. Naim, and Neil J. Bulleid. 1995. 'Intracellular Folding of Tissue-Type Plasminogen Activator: EFFECTS OF DISULFIDE BOND FORMATION ON N-LINKED GLYCOSYLATION AND SECRETION (∗)'. *Journal of Biological Chemistry* 270 (9): 4797–4804. https://doi.org/10.1074/jbc.270.9.4797.

Assainar, Basila Moochickal, Kaushik Ragunathan, and Ryan D. Baldridge. 2023. 'Direct Observation of Autoubiquitination for an Integral Membrane Ubiquitin Ligase in ERAD'. bioRxiv. https://doi.org/10.1101/2023.06.20.545802.

Bachiller, Sara, Isabel M. Alonso-Bellido, Luis Miguel Real, Eva María Pérez-Villegas, José Luis Venero, Tomas Deierborg, José Ángel Armengol, and Rocío Ruiz. 2020. 'The Ubiquitin Proteasome System in Neuromuscular Disorders: Moving Beyond Movement'. *International Journal of Molecular Sciences* 21 (17): 6429. https://doi.org/10.3390/ijms21176429.

Bagola, Katrin, Maximilian von Delbrück, Gunnar Dittmar, Martin Scheffner, Inbal Ziv, Michael H. Glickman, Aaron Ciechanover, and Thomas Sommer. 2013. 'Ubiquitin Binding by a CUE Domain Regulates Ubiquitin Chain Formation by ERAD E3 Ligases'. *Molecular Cell* 50 (4): 528–39. https://doi.org/10.1016/j.molcel.2013.04.005.

Bakshi, Tania, David Pham, Raminderjeet Kaur, and Bingyun Sun. 2022. 'Hidden Relationships between N-Glycosylation and Disulfide Bonds in Individual Proteins'. *International Journal of Molecular Sciences* 23 (7): 3742. https://doi.org/10.3390/ijms23073742.

Balaji, Vishnu, and Thorsten Hoppe. 2020. 'Regulation of E3 Ubiquitin Ligases by Homotypic and Heterotypic Assembly'. *F1000Research* 9 (February): F1000 Faculty Rev-88. https://doi.org/10.12688/f1000research.21253.1.

Balchin, David, Manajit Hayer-Hartl, and F. Ulrich Hartl. 2016. 'In Vivo Aspects of Protein Folding and Quality Control'. *Science* 353 (6294): aac4354. https://doi.org/10.1126/science.aac4354.

Baldridge, Ryan D., and Tom A. Rapoport. 2016. 'Autoubiquitination of the Hrd1 Ligase Triggers Protein Retrotranslocation in ERAD'. *Cell* 166 (2): 394–407. https://doi.org/10.1016/j.cell.2016.05.048.

Bauer, Matthias F., Christian Sirrenberg, Walter Neupert, and Michael Brunner. 1996. 'Role of Tim23 as Voltage Sensor and Presequence Receptor in Protein Import into Mitochondria'. *Cell* 87 (1): 33–41. https://doi.org/10.1016/S0092-8674(00)81320-3.

Bausewein, Thomas, Deryck J. Mills, Julian D. Langer, Beate Nitschke, Stephan Nussberger, and Werner Kühlbrandt. 2017. 'Cryo-EM Structure of the TOM Core Complex from Neurospora Crassa'. *Cell* 170 (4): 693-700.e7. https://doi.org/10.1016/j.cell.2017.07.012.

Bays, Nathan W., Richard G. Gardner, Linda P. Seelig, Claudio A. Joazeiro, and Randolph Y. Hampton. 2001. 'Hrd1p/Der3p Is a Membrane-Anchored Ubiquitin Ligase Required for ER-Associated Degradation'. *Nature Cell Biology* 3 (1): 24–29. https://doi.org/10.1038/35050524.

Bazirgan, Omar A., and Randolph Y. Hampton. 2008. 'Cue1p Is an Activator of Ubc7p E2 Activity in Vitro and in Vivo*'. *Journal of Biological Chemistry* 283 (19): 12797–810. https://doi.org/10.1074/jbc.M801122200.

Bernardi, Kaleena M., Jeffrey M. Williams, Marjolein Kikkert, Sjaak van Voorden, Emmanuel J. Wiertz, Yihong Ye, and Billy Tsai. 2010. 'The E3 Ubiquitin Ligases Hrd1 and Gp78 Bind to and Promote Cholera Toxin Retro-Translocation'. *Molecular Biology of the Cell* 21 (1): 140–51. https://doi.org/10.1091/mbc.E09-07-0586.

Bodnar, Nicholas O., and Tom A. Rapoport. 2017. 'Molecular Mechanism of Substrate Processing by the Cdc48 ATPase Complex'. *Cell* 169 (4): 722-735.e9. https://doi.org/10.1016/j.cell.2017.04.020.

Bordallo, Javier, Richard K. Plemper, Andreas Finger, and Dieter H. Wolf. 1998. 'Der3p/Hrd1p Is Required for Endoplasmic Reticulum-Associated Degradation of Misfolded Lumenal and Integral Membrane Proteins'. *Molecular Biology of the Cell* 9 (1): 209–22. https://doi.org/10.1091/mbc.9.1.209.

Breitling, Jörg, and Markus Aebi. 2013. 'N-Linked Protein Glycosylation in the Endoplasmic Reticulum'. *Cold Spring Harbor Perspectives in Biology* 5 (8): a013359. https://doi.org/10.1101/cshperspect.a013359.

Brodsky, Jeffrey L. 2012. 'Cleaning Up: ER-Associated Degradation to the Rescue'. *Cell* 151 (6): 1163–67. https://doi.org/10.1016/j.cell.2012.11.012.

Burdakov, Denis, Ole H. Petersen, and Alexei Verkhratsky. 2005. 'Intraluminal Calcium as a Primary Regulator of Endoplasmic Reticulum Function'. *Cell Calcium*, Frontiers in calcium signalling, 38 (3): 303–10. https://doi.org/10.1016/j.ceca.2005.06.010.

Byun, Hyewon, Yongqiang Gou, Adam Zook, Mary M. Lozano, and Jaquelin P. Dudley. 2014. 'ERAD and How Viruses Exploit It'. *Frontiers in Microbiology* 5. https://www.frontiersin.org/articles/10.3389/fmicb.2014.00330.

Cabana, Valérie C., and Marc P. Lussier. 2022. 'From Drosophila to Human: Biological Function of E3 Ligase Godzilla and Its Role in Disease'. *Cells* 11 (3): 380. https://doi.org/10.3390/cells11030380.

Carroll, Sarah M., and Randolph Y. Hampton. 2010. 'Usa1p Is Required for Optimal Function and Regulation of the Hrd1p Endoplasmic Reticulum-Associated Degradation Ubiquitin Ligase'. *The Journal of Biological Chemistry* 285 (8): 5146–56. https://doi.org/10.1074/jbc.M109.067876.

Carvalho, Pedro, Veit Goder, and Tom A. Rapoport. 2006. 'Distinct Ubiquitin-Ligase Complexes Define Convergent Pathways for the Degradation of ER Proteins'. *Cell* 126 (2): 361–73. https://doi.org/10.1016/j.cell.2006.05.043.

Carvalho, Pedro, Ann Marie Stanley, and Tom A. Rapoport. 2010. 'Retrotranslocation of a Misfolded Luminal ER Protein by the Ubiquitin-Ligase Hrd1p'. *Cell* 143 (4): 579–91. https://doi.org/10.1016/j.cell.2010.10.028.

Chavan, Manasi, and William Lennarz. 2006. 'The Molecular Basis of Coupling of Translocation and N-Glycosylation'. *Trends in Biochemical Sciences* 31 (1): 17–20. https://doi.org/10.1016/j.tibs.2005.11.010.

Chen, Xiang, Zaw Min Htet, Erika López-Alfonzo, Andreas Martin, and Kylie J. Walters. 2021. 'Proteasome Interaction with Ubiquitinated Substrates: From Mechanisms to Therapies'. *The FEBS Journal* 288 (18): 5231–51. https://doi.org/10.1111/febs.15638.

Christianson, John C., and Yihong Ye. 2014. 'Cleaning up in the Endoplasmic Reticulum: Ubiquitin in Charge'. *Nature Structural & Molecular Biology* 21 (4): 325–35. https://doi.org/10.1038/nsmb.2793.

Clerc, Simone, Christian Hirsch, Daniela Maria Oggier, Paola Deprez, Claude Jakob, Thomas Sommer, and Markus Aebi. 2009. 'Htm1 Protein Generates the N-Glycan Signal for Glycoprotein Degradation in the Endoplasmic Reticulum'. *The Journal of Cell Biology* 184 (1): 159–72. https://doi.org/10.1083/jcb.200809198.

Denic, Vladimir, Erin M. Quan, and Jonathan S. Weissman. 2006. 'A Luminal Surveillance Complex That Selects Misfolded Glycoproteins for ER-Associated Degradation'. *Cell* 126 (2): 349–59. https://doi.org/10.1016/j.cell.2006.05.045.

Dong, Mei, James P. Bridges, Karen Apsley, Yan Xu, and Timothy E. Weaver. 2008. 'ERdj4 and ERdj5 Are Required for Endoplasmic Reticulum-Associated Protein Degradation of Misfolded Surfactant Protein C'. *Molecular Biology of the Cell* 19 (6): 2620–30. https://doi.org/10.1091/mbc.e07-07-0674.

Elia, Francesco, Lalitha Yadhanapudi, Thomas Tretter, and Karin Römisch. 2019. 'The N-Terminus of Sec61p Plays Key Roles in ER Protein Import and ERAD'. *PLOS ONE* 14 (4): e0215950. https://doi.org/10.1371/journal.pone.0215950.

Ellgaard, Lars, and Ari Helenius. 2003. 'Quality Control in the Endoplasmic Reticulum'. *Nature Reviews Molecular Cell Biology* 4 (3): 181–91. https://doi.org/10.1038/nrm1052.

Elsasser, Suzanne, Devin Chandler-Militello, Britta Müller, John Hanna, and Daniel Finley. 2004. 'Rad23 and Rpn10 Serve as Alternative Ubiquitin Receptors for the Proteasome *'. *Journal of Biological Chemistry* 279 (26): 26817–22. https://doi.org/10.1074/jbc.M404020200.

Elsasser, Suzanne, Rayappa R. Gali, Martin Schwickart, Christopher N. Larsen, David S. Leggett, Britta Müller, Matthew T. Feng, Fabian Tübing, Gunnar A. G. Dittmar, and Daniel Finley. 2002. 'Proteasome Subunit Rpn1 Binds Ubiquitin-like Protein Domains'. *Nature Cell Biology* 4 (9): 725–30. https://doi.org/10.1038/ncb845.

Erdmann, Frank, Martin Jung, Patrick Maurer, Anke Harsman, Richard Zimmermann, and Richard Wagner. 2010. 'The Mammalian and Yeast Translocon Complexes Comprise a Characteristic Sec61 Channel'. *Biochemical and Biophysical Research Communications* 396 (3): 714–20. https://doi.org/10.1016/j.bbrc.2010.04.168.

Fewell, Sheara W., and Jeffrey L. Brodsky. 2013. 'Entry into the Endoplasmic Reticulum: Protein Translocation, Folding and Quality Control'. In *Madame Curie Bioscience Database [Internet]*. Landes Bioscience. https://www.ncbi.nlm.nih.gov/books/NBK6210/.

Finger, Andreas, Michael Knop, and Dieter H. Wolf. 1993. 'Analysis of Two Mutated Vacuolar Proteins Reveals a Degradation Pathway in the Endoplasmic Reticulum or a Related Compartment of Yeast'. *European Journal of Biochemistry* 218 (2): 565–74. https://doi.org/10.1111/j.1432-1033.1993.tb18410.x.

Fiorentini, Filippo, Diego Esposito, and Katrin Rittinger. 2020. 'Does It Take Two to Tango? RING Domain Self-Association and Activity in TRIM E3 Ubiquitin Ligases'. *Biochemical Society Transactions* 48 (6): 2615–24. https://doi.org/10.1042/BST20200383.

Foresti, Ombretta, Annamaria Ruggiano, Hans K Hannibal-Bach, Christer S Ejsing, and Pedro Carvalho. 2013. 'Sterol Homeostasis Requires Regulated Degradation of Squalene Monooxygenase by the Ubiquitin Ligase Doa10/Teb4'. Edited by Michael S Brown. *eLife* 2 (July): e00953. https://doi.org/10.7554/eLife.00953.

Ganesan, Iniyan, Lan-Xin Shi, Mathias Labs, and Steven M. Theg. 2018. 'Evaluating the Functional Pore Size of Chloroplast TOC and TIC Protein Translocons: Import of Folded Proteins'. *The Plant Cell* 30 (9): 2161–73. https://doi.org/10.1105/tpc.18.00427.

Ganesan, Iniyan, and Steven M. Theg. 2019. 'Structural Considerations of Folded Protein Import through the Chloroplast TOC/TIC Translocons'. *FEBS Letters* 593 (6): 565–72. https://doi.org/10.1002/1873-3468.13342.

Gardner, Richard G., Gwendolyn M. Swarbrick, Nathan W. Bays, Stephen R. Cronin, Sharon Wilhovsky, Linda Seelig, Christine Kim, and Randolph Y. Hampton. 2000. 'Endoplasmic Reticulum Degradation Requires Lumen to Cytosol Signaling'. *The Journal of Cell Biology* 151 (1): 69–82.

Gauss, Robert, Kazue Kanehara, Pedro Carvalho, Davis T. W. Ng, and Markus Aebi. 2011. 'A Complex of Pdi1p and the Mannosidase Htm1p Initiates Clearance of Unfolded Glycoproteins from the Endoplasmic Reticulum'. *Molecular Cell* 42 (6): 782–93. https://doi.org/10.1016/j.molcel.2011.04.027.

Gauss, Robert, Thomas Sommer, and Ernst Jarosch. 2006. 'The Hrd1p Ligase Complex Forms a Linchpin between ER-Lumenal Substrate Selection and Cdc48p Recruitment'. *The EMBO Journal* 25 (9): 1827–35. https://doi.org/10.1038/sj.emboj.7601088.

Gavin, Anne-Claude, Patrick Aloy, Paola Grandi, Roland Krause, Markus Boesche, Martina Marzioch, Christina Rau, et al. 2006. 'Proteome Survey Reveals Modularity of the Yeast Cell Machinery'. *Nature* 440 (7084): 631–36. https://doi.org/10.1038/nature04532.

George, Arlene J., Yarely C. Hoffiz, Antoinette J. Charles, Ying Zhu, and Angela M. Mabb. 2018. 'A Comprehensive Atlas of E3 Ubiquitin Ligase Mutations in Neurological Disorders'. *Frontiers in Genetics* 9. https://www.frontiersin.org/articles/10.3389/fgene.2018.00029.

Gillece, P., M. Pilon, and K. Römisch. 2000. 'The Protein Translocation Channel Mediates Glycopeptide Export across the Endoplasmic Reticulum Membrane'. *Proceedings of the National Academy of Sciences of the United States of America* 97 (9): 4609–14. https://doi.org/10.1073/pnas.090083497.

Gillece, Pauline, José Manuel Luz, William J. Lennarz, Francisco Javier De La Cruz, and Karin Römisch. 1999. 'Export of a Cysteine-Free Misfolded Secretory Protein from the Endoplasmic Reticulum for Degradation Requires Interaction with Protein Disulfide Isomerase'. *The Journal of Cell Biology* 147 (7): 1443–56. https://doi.org/10.1083/jcb.147.7.1443.

Goldman, David E. 1943. 'POTENTIAL, IMPEDANCE, AND RECTIFICATION IN MEMBRANES'. *Journal of General Physiology* 27 (1): 37–60. https://doi.org/10.1085/jgp.27.1.37.

Gong, Bing, Miroslav Radulovic, Maria E. Figueiredo-Pereira, and Christopher Cardozo. 2016. 'The Ubiquitin-Proteasome System: Potential Therapeutic Targets for Alzheimer's Disease and Spinal Cord Injury'. *Frontiers in Molecular Neuroscience* 9. https://www.frontiersin.org/articles/10.3389/fnmol.2016.00004.

Goot, Annemieke T. van der, Margaret M. P. Pearce, Dara E. Leto, Thomas A. Shaler, and Ron R. Kopito. 2018. 'Redundant and Antagonistic Roles of XTP3B and OS9 in Decoding Glycan and Non-Glycan Degrons in ER-Associated Degradation'. *Molecular Cell* 70 (3): 516-530.e6. https://doi.org/10.1016/j.molcel.2018.03.026.

Graner, Michael W., Kevin O. Lillehei, and Emmanuel Katsanis. 2015. 'Endoplasmic Reticulum Chaperones and Their Roles in the Immunogenicity of Cancer Vaccines'. *Frontiers in Oncology* 4 (January): 379. https://doi.org/10.3389/fonc.2014.00379.

Greenblatt, Ethan J., James A. Olzmann, and Ron R. Kopito. 2011. 'Derlin-1 Is a Rhomboid Pseudoprotease Required for the Dislocation of Mutant α-1 Antitrypsin from the Endoplasmic Reticulum'. *Nature Structural & Molecular Biology* 18 (10): 1147–52. https://doi.org/10.1038/nsmb.2111.

Guan, Zeyuan, Ling Yan, Qiang Wang, Liangbo Qi, Sixing Hong, Zhou Gong, Chuangye Yan, and Ping Yin. 2021. 'Structural Insights into Assembly of Human Mitochondrial Translocase TOM Complex'. *Cell Discovery* 7 (1): 1–5. https://doi.org/10.1038/s41421-021-00252-7.

Hamman, B. D., J. C. Chen, E. E. Johnson, and A. E. Johnson. 1997. 'The Aqueous Pore through the Translocon Has a Diameter of 40-60 A during Cotranslational Protein Translocation at the ER Membrane'. *Cell* 89 (4): 535–44. https://doi.org/10.1016/s0092-8674(00)80235-4.

Hampton, Randolph Y, and Thomas Sommer. 2012. 'Finding the Will and the Way of ERAD Substrate Retrotranslocation'. *Current Opinion in Cell Biology*, Membranes and organelles, 24 (4): 460–66. https://doi.org/10.1016/j.ceb.2012.05.010.

Harsman, Anke, Philipp Bartsch, Birgit Hemmis, Vivien Krüger, and Richard Wagner. 2011. 'Exploring Protein Import Pores of Cellular Organelles at the Single Molecule Level Using the Planar Lipid Bilayer Technique'. *European Journal of Cell Biology* 90 (9): 721–30. https://doi.org/10.1016/j.ejcb.2011.04.012.

Hartl, F. Ulrich. 2017. 'Protein Misfolding Diseases'. *Annual Review of Biochemistry* 86 (1): 21–26. https://doi.org/10.1146/annurev-biochem-061516-044518.

Helenius, Ari, and Markus Aebi. 2004. 'Roles of N-Linked Glycans in the Endoplasmic Reticulum'. *Annual Review of Biochemistry* 73 (1): 1019–49. https://doi.org/10.1146/annurev.biochem.73.011303.073752.

Hernandez, Javier M., Alexander Stein, Elmar Behrmann, Dietmar Riedel, Anna Cypionka, Zohreh Farsi, Peter J. Walla, Stefan Raunser, and Reinhard Jahn. 2012. 'Membrane Fusion Intermediates via

Directional and Full Assembly of the SNARE Complex'. *Science (New York, N.Y.)* 336 (6088): 1581–84. https://doi.org/10.1126/science.1221976.

Hershko, Avram, and Aaron Ciechanover. 1998. 'The Ubiquitin System'. *Annual Review of Biochemistry* 67 (1): 425–79. https://doi.org/10.1146/annurev.biochem.67.1.425.

Hill, Kerstin, Kirstin Model, Michael T. Ryan, Klaus Dietmeier, Falk Martin, Richard Wagner, and Nikolaus Pfanner. 1998. 'Tom40 Forms the Hydrophilic Channel of the Mitochondrial Import Pore for Preproteins'. *Nature* 395 (6701): 516–21. https://doi.org/10.1038/26780.

Hitt, Reiner, and Dieter H. Wolf. 2004. 'Der1p, a Protein Required for Degradation of Malfolded Soluble Proteins of the Endoplasmic Reticulum: Topology and Der1-like Proteins'. *FEMS Yeast Research* 4 (7): 721–29. https://doi.org/10.1016/j.femsyr.2004.02.003.

Hodgkin, A. L., and B. Katz. 1949. 'The Effect of Sodium Ions on the Electrical Activity of Giant Axon of the Squid'. *The Journal of Physiology* 108 (1): 37–77. https://doi.org/10.1113/jphysiol.1949.sp004310.

Hoppe, Thorsten, Giuseppe Cassata, José M. Barral, Wolfdieter Springer, Alex H. Hutagalung, Henry F. Epstein, and Ralf Baumeister. 2004. 'Regulation of the Myosin-Directed Chaperone UNC-45 by a Novel E3/E4-Multiubiquitylation Complex in C. Elegans'. *Cell* 118 (3): 337–49. https://doi.org/10.1016/j.cell.2004.07.014.

Horn, Sabine C., Jennifer Hanna, Christian Hirsch, Corinna Volkwein, Anja Schütz, Udo Heinemann, Thomas Sommer, and Ernst Jarosch. 2009. 'Usa1 Functions as a Scaffold of the HRD-Ubiquitin Ligase'. *Molecular Cell* 36 (5): 782–93. https://doi.org/10.1016/j.molcel.2009.10.015.

Hotz, Thomas, Ole M. Schütte, Hannes Sieling, Tatjana Polupanow, Ulf Diederichsen, Claudia Steinem, and Axel Munk. 2013. 'Idealizing Ion Channel Recordings by a Jump Segmentation Multiresolution Filter'. *IEEE Transactions on NanoBioscience* 12 (4): 376–86. https://doi.org/10.1109/TNB.2013.2284063.

Hu, G., and E. R. Fearon. 1999. 'Siah-1 N-Terminal RING Domain Is Required for Proteolysis Function, and C-Terminal Sequences Regulate Oligomerization and Binding to Target Proteins'. *Molecular and Cellular Biology* 19 (1): 724–32. https://doi.org/10.1128/MCB.19.1.724.

Humphreys, Luke M., Paul Smith, Zhuoyao Chen, Shahd Fouad, and Vincenzo D'Angiolella. 2021. 'The Role of E3 Ubiquitin Ligases in the Development and Progression of Glioblastoma'. *Cell Death & Differentiation* 28 (2): 522–37. https://doi.org/10.1038/s41418-020-00696-6.

Husnjak, Koraljka, Suzanne Elsasser, Naixia Zhang, Xiang Chen, Leah Randles, Yuan Shi, Kay Hofmann, Kylie J. Walters, Daniel Finley, and Ivan Dikic. 2008. 'Proteasome Subunit Rpn13 Is a Novel Ubiquitin Receptor'. *Nature* 453 (7194): 481–88. https://doi.org/10.1038/nature06926.

Huyer, Gregory, Wachirapon F. Piluek, Zoya Fansler, Stefan G. Kreft, Mark Hochstrasser, Jeffrey L. Brodsky, and Susan Michaelis. 2004. 'Distinct Machinery Is Required in Saccharomyces Cerevisiae for the Endoplasmic Reticulum-Associated Degradation of a Multispanning Membrane Protein and a Soluble Luminal Protein *'. *Journal of Biological Chemistry* 279 (37): 38369–78. https://doi.org/10.1074/jbc.M402468200.

Hwang, Jiwon, and Ling Qi. 2018. 'Quality Control in the Endoplasmic Reticulum: Crosstalk between ERAD and UPR Pathways'. *Trends in Biochemical Sciences* 43 (8): 593–605. https://doi.org/10.1016/j.tibs.2018.06.005.

Iscla, Irene, and Paul Blount. 2012. 'Sensing and Responding to Membrane Tension: The Bacterial MscL Channel as a Model System'. *Biophysical Journal* 103 (2): 169–74. https://doi.org/10.1016/j.bpj.2012.06.021.

Izawa, Toshiaki, Hiroyuki Nagai, Toshiya Endo, and Shuh-ichi Nishikawa. 2012. 'Yos9p and Hrd1p Mediate ER Retention of Misfolded Proteins for ER-Associated Degradation'. *Molecular Biology of the Cell* 23 (7): 1283–93. https://doi.org/10.1091/mbc.E11-08-0722.

Jakob, Claude A., Patricie Burda, Jürgen Roth, and Markus Aebi. 1998. 'Degradation of Misfolded Endoplasmic Reticulum Glycoproteins in *Saccharomyces Cerevisiae* Is Determined by a Specific Oligosaccharide Structure'. *The Journal of Cell Biology* 142 (5): 1223–33. https://doi.org/10.1083/jcb.142.5.1223.

Jarosch, Ernst, Christof Taxis, Corinna Volkwein, Javier Bordallo, Daniel Finley, Dieter H. Wolf, and Thomas Sommer. 2002. 'Protein Dislocation from the ER Requires Polyubiquitination and the AAA-ATPase Cdc48'. *Nature Cell Biology* 4 (2): 134–39. https://doi.org/10.1038/ncb746.

Jespersen, Thomas, Mathieu Membrez, Céline S. Nicolas, Bruno Pitard, Olivier Staub, Søren-Peter Olesen, Isabelle Baró, and Hugues Abriel. 2007. 'The KCNQ1 Potassium Channel Is Down-Regulated by Ubiquitylating Enzymes of the Nedd4/Nedd4-like Family'. *Cardiovascular Research* 74 (1): 64–74. https://doi.org/10.1016/j.cardiores.2007.01.008.

Kalies, Kai-Uwe, Susanne Allan, Tatiana Sergeyenko, Heike Kröger, and Karin Römisch. 2005. 'The Protein Translocation Channel Binds Proteasomes to the Endoplasmic Reticulum Membrane'. *The EMBO Journal* 24 (13): 2284–93. https://doi.org/10.1038/sj.emboj.7600731.

Kalies, Kai-Uwe, and Enno Hartmann. 1998. 'Protein Translocation into the Endoplasmic Reticulum (ER)'. *European Journal of Biochemistry* 254 (1): 1–5. https://doi.org/10.1046/j.1432-1327.1998.2540001.x.

Kim, Ikjin, Kaixia Mi, and Hai Rao. 2004. 'Multiple Interactions of Rad23 Suggest a Mechanism for Ubiquitylated Substrate Delivery Important in Proteolysis'. *Molecular Biology of the Cell* 15 (7): 3357–65. https://doi.org/10.1091/mbc.e03-11-0835.

Kim, Woong, Eric D. Spear, and Davis T.W. Ng. 2005. 'Yos9p Detects and Targets Misfolded Glycoproteins for ER-Associated Degradation'. *Molecular Cell* 19 (6): 753–64. https://doi.org/10.1016/j.molcel.2005.08.010.

Klier, Pavel E. Z., Ryan Roo, and Evan W. Miller. 2022. 'Fluorescent Indicators for Imaging Membrane Potential of Organelles'. *Current Opinion in Chemical Biology* 71 (December): 102203. https://doi.org/10.1016/j.cbpa.2022.102203.

Knipscheer, Puck, and Titia K Sixma. 2007. 'Protein–Protein Interactions Regulate Ubl Conjugation'. *Current Opinion in Structural Biology*, Catalysis and regulation / Proteins, 17 (6): 665–73. https://doi.org/10.1016/j.sbi.2007.09.001.

Knop, M., A. Finger, T. Braun, K. Hellmuth, and D. H. Wolf. 1996. 'Der1, a Novel Protein Specifically Required for Endoplasmic Reticulum Degradation in Yeast'. *The EMBO Journal* 15 (4): 753–63.

Kovermann, Peter, Kaye N Truscott, Bernard Guiard, Peter Rehling, Naresh B Sepuri, Hanne Müller, Robert E Jensen, Richard Wagner, and Nikolaus Pfanner. 2002. 'Tim22, the Essential Core of the Mitochondrial Protein Insertion Complex, Forms a Voltage-Activated and Signal-Gated Channel'. *Molecular Cell* 9 (2): 363–73. https://doi.org/10.1016/S1097-2765(02)00446-X.

Kreutzberger, Alex J. B., Ming Ji, Jesse Aaron, Ljubica Mihaljević, and Siniša Urban. 2019. 'Rhomboid Distorts Lipids to Break the Viscosity-Imposed Speed Limit of Membrane Diffusion'. *Science* 363 (6426): eaao0076. https://doi.org/10.1126/science.aao0076.

Kreutzberger, Alex J. B., and Siniša Urban. 2018. 'Single-Molecule Analyses Reveal Rhomboid Proteins Are Strict and Functional Monomers in the Membrane'. *Biophysical Journal* 115 (9): 1755–61. https://doi.org/10.1016/j.bpj.2018.09.024.

Lam, Andy K. M., and Antony Galione. 2013. 'The Endoplasmic Reticulum and Junctional Membrane Communication during Calcium Signaling'. *Biochimica et Biophysica Acta (BBA) - Molecular Cell Research*, Functional and structural diversity of the endoplasmic reticulum, 1833 (11): 2542–59. https://doi.org/10.1016/j.bbamcr.2013.06.004.

Lamothe, S. M., and S. Zhang. 2016. 'Chapter Five - Ubiquitination of Ion Channels and Transporters'. In *Progress in Molecular Biology and Translational Science*, edited by Sudha K. Shenoy, 141:161–223. Ubiquitination and Transmembrane Signaling. Academic Press. https://doi.org/10.1016/bs.pmbts.2016.02.005.

Larburu, Natacha, Christopher J. Adams, Chao-Sheng Chen, Piotr R. Nowak, and Maruf M. U. Ali. 2020. 'Mechanism of Hsp70 Specialized Interactions in Protein Translocation and the Unfolded Protein Response'. *Open Biology* 10 (8): 200089. https://doi.org/10.1098/rsob.200089.

Lederkremer, Gerardo Z. 2009. 'Glycoprotein Folding, Quality Control and ER-Associated Degradation'. *Current Opinion in Structural Biology*, Carbohydradtes and glycoconjugates / Biophysical methods, 19 (5): 515–23. https://doi.org/10.1016/j.sbi.2009.06.004.

Li, Wei, Daqi Tu, Axel T. Brunger, and Yihong Ye. 2007. 'A Ubiquitin Ligase Transfers Preformed Polyubiquitin Chains from a Conjugating Enzyme to a Substrate'. *Nature* 446 (7133): 333–37. https://doi.org/10.1038/nature05542.

Liu, Chao, Weixiao Liu, Yihong Ye, and Wei Li. 2017. 'Ufd2p Synthesizes Branched Ubiquitin Chains to Promote the Degradation of Substrates Modified with Atypical Chains'. *Nature Communications* 8 (1): 14274. https://doi.org/10.1038/ncomms14274.

Lopata, Anna, Andreas Kniss, Frank Löhr, Vladimir V. Rogov, and Volker Dötsch. 2020. 'Ubiquitination in the ERAD Process'. *International Journal of Molecular Sciences* 21 (15): 5369. https://doi.org/10.3390/ijms21155369.

Medicherla, Balasubrahmanyam, Zlatka Kostova, Antje Schaefer, and Dieter H Wolf. 2004. 'A Genomic Screen Identifies Dsk2p and Rad23p as Essential Components of ER-Associated Degradation'. *EMBO Reports* 5 (7): 692–97. https://doi.org/10.1038/sj.embor.7400164.

Mehnert, Martin, Thomas Sommer, and Ernst Jarosch. 2014. 'Der1 Promotes Movement of Misfolded Proteins through the Endoplasmic Reticulum Membrane'. *Nature Cell Biology* 16 (1): 77–86. https://doi.org/10.1038/ncb2882.

Mehnert, Martin, Franziska Sommermeyer, Maren Berger, Sathish Kumar Lakshmipathy, Robert Gauss, Markus Aebi, Ernst Jarosch, and Thomas Sommer. 2015. 'The Interplay of Hrd3 and the Molecular Chaperone System Ensures Efficient Degradation of Malfolded Secretory Proteins'. *Molecular Biology of the Cell* 26 (2): 185–94. https://doi.org/10.1091/mbc.E14-07-1202.

Meinecke, Michael, Christian Cizmowski, Wolfgang Schliebs, Vivien Krüger, Sabrina Beck, Richard Wagner, and Ralf Erdmann. 2010. 'The Peroxisomal Importomer Constitutes a Large and Highly Dynamic Pore'. *Nature Cell Biology* 12 (3): 273–77. https://doi.org/10.1038/ncb2027.

Metzger, Meredith B., Jonathan N. Pruneda, Rachel E. Klevit, and Allan M. Weissman. 2014. 'RING-Type E3 Ligases: Master Manipulators of E2 Ubiquitin-Conjugating Enzymes and Ubiquitination'. *Biochimica et Biophysica Acta (BBA) - Molecular Cell Research*, Ubiquitin-Proteasome System, 1843 (1): 47–60. https://doi.org/10.1016/j.bbamcr.2013.05.026.

Montilla-Martinez, Malayko, Sabrina Beck, Jessica Klümper, Michael Meinecke, Wolfgang Schliebs, Richard Wagner, and Ralf Erdmann. 2015. 'Distinct Pores for Peroxisomal Import of PTS1 and PTS2 Proteins'. *Cell Reports* 13 (10): 2126–34. https://doi.org/10.1016/j.celrep.2015.11.016.

Nakatsukasa, Kunio, Sylvia Wigge, Yuki Takano, Tomoyuki Kawarasaki, Takumi Kamura, and Jeffrey L. Brodsky. 2022. 'A Positive Genetic Selection for Transmembrane Domain Mutations in HRD1 Underscores the Importance of Hrd1 Complex Integrity during ERAD'. *Current Genetics* 68 (2): 227–42. https://doi.org/10.1007/s00294-022-01227-1.

Nejatfard, Anahita, Nicholas Wauer, Satarupa Bhaduri, Adam Conn, Saroj Gourkanti, Narinderbir Singh, Tiffany Kuo, Rachel Kandel, Rommie E. Amaro, and Sonya E. Neal. 2021. 'Derlin Rhomboid Pseudoproteases Employ Substrate Engagement and Lipid Distortion to Enable the Retrotranslocation of ERAD Membrane Substrates'. *Cell Reports* 37 (3): 109840. https://doi.org/10.1016/j.celrep.2021.109840.

Ng, Davis T.W., Eric D. Spear, and Peter Walter. 2000. 'The Unfolded Protein Response Regulates Multiple Aspects of Secretory and Membrane Protein Biogenesis and Endoplasmic Reticulum Quality Control'. *Journal of Cell Biology* 150 (1): 77–88. https://doi.org/10.1083/jcb.150.1.77.

Ninagawa, Satoshi, Ginto George, and Kazutoshi Mori. 2021. 'Mechanisms of Productive Folding and Endoplasmic Reticulum-Associated Degradation of Glycoproteins and Non-Glycoproteins'. *Biochimica et Biophysica Acta (BBA) - General Subjects* 1865 (3): 129812. https://doi.org/10.1016/j.bbagen.2020.129812.

Nishikawa, Shuh-ichi, Sheara W. Fewell, Yoshihito Kato, Jeffrey L. Brodsky, and Toshiya Endo. 2001. 'Molecular Chaperones in the Yeast Endoplasmic Reticulum Maintain the Solubility of Proteins for Retrotranslocation and Degradation'. *Journal of Cell Biology* 153 (5): 1061–70. https://doi.org/10.1083/jcb.153.5.1061.

Olszewski, Michal M., Cameron Williams, Ken C. Dong, and Andreas Martin. 2019. 'The Cdc48 Unfoldase Prepares Well-Folded Protein Substrates for Degradation by the 26S Proteasome'. *Communications Biology* 2 (1): 1–8. https://doi.org/10.1038/s42003-019-0283-z.

Pei, Xue-Yuan, Philip Hinchliffe, Martyn F. Symmons, Eva Koronakis, Roland Benz, Colin Hughes, and Vassilis Koronakis. 2011. 'Structures of Sequential Open States in a Symmetrical Opening Transition of the TolC Exit Duct'. *Proceedings of the National Academy of Sciences of the United States of America* 108 (5): 2112–17. https://doi.org/10.1073/pnas.1012588108.

Pereira, Fabio, Mandy Rettel, Frank Stein, Mikhail M. Savitski, Ian Collinson, and Karin Römisch. 2019. 'Effect of Sec61 Interaction with Mpd1 on Endoplasmic Reticulum-Associated Degradation'. *PLOS ONE* 14 (1): e0211180. https://doi.org/10.1371/journal.pone.0211180.

Perozo, Eduardo, Anna Kloda, D. Marien Cortes, and Boris Martinac. 2002. 'Physical Principles Underlying the Transduction of Bilayer Deformation Forces during Mechanosensitive Channel Gating'. *Nature Structural Biology* 9 (9): 696–703. https://doi.org/10.1038/nsb827.

Peterson, Brian G, Morgan L Glaser, Tom A Rapoport, and Ryan D Baldridge. 2019. 'Cycles of Autoubiquitination and Deubiquitination Regulate the ERAD Ubiquitin Ligase Hrd1'. Edited by Ramanujan S Hegde and David Ron. *eLife* 8 (November): e50903. https://doi.org/10.7554/eLife.50903.

Pfeiffer, Anett, Heike Stephanowitz, Eberhard Krause, Corinna Volkwein, Christian Hirsch, Ernst Jarosch, and Thomas Sommer. 2016. 'A Complex of Htm1 and the Oxidoreductase Pdi1 Accelerates Degradation of Misfolded Glycoproteins'. *Journal of Biological Chemistry* 291 (23): 12195–207. https://doi.org/10.1074/jbc.M115.703256.

Pickart, Cecile M., and Michael J. Eddins. 2004. 'Ubiquitin: Structures, Functions, Mechanisms'. *Biochimica et Biophysica Acta (BBA) - Molecular Cell Research*, The Ubiquitin-Proteasome System, 1695 (1): 55–72. https://doi.org/10.1016/j.bbamcr.2004.09.019.

Pilon, Marinus, Karin Römisch, Dong Quach, and Randy Schekman. 1998. 'Sec61p Serves Multiple Roles in Secretory Precursor Binding and Translocation into the Endoplasmic Reticulum Membrane'. *Molecular Biology of the Cell* 9 (12): 3455–73. https://doi.org/10.1091/mbc.9.12.3455.

Pilon, Marinus, Randy Schekman, and Karin Römisch. 1997. 'Sec61p Mediates Export of a Misfolded Secretory Protein from the Endoplasmic Reticulum to the Cytosol for Degradation'. *The EMBO Journal* 16 (15): 4540–48. https://doi.org/10.1093/emboj/16.15.4540.

Pisa, Rudolf, and Tom A. Rapoport. 2022. 'Disulfide-Crosslink Analysis of the Ubiquitin Ligase Hrd1 Complex during Endoplasmic Reticulum-Associated Protein Degradation'. *Journal of Biological Chemistry* 298 (9): 102373. https://doi.org/10.1016/j.jbc.2022.102373.

Plechanovová, Anna, Ellis G. Jaffray, Stephen A. McMahon, Kenneth A. Johnson, Iva Navrátilová, James H. Naismith, and Ronald T. Hay. 2011. 'Mechanism of Ubiquitylation by Dimeric RING Ligase RNF4'. *Nature Structural & Molecular Biology* 18 (9): 1052–59. https://doi.org/10.1038/nsmb.2108.

Quan, Erin M., Yukiko Kamiya, Daiki Kamiya, Vladimir Denic, Jimena Weibezahn, Koichi Kato, and Jonathan S. Weissman. 2008. 'Defining the Glycan Destruction Signal for Endoplasmic Reticulum-Associated Degradation'. *Molecular Cell* 32 (6): 870–77. https://doi.org/10.1016/j.molcel.2008.11.017.

Rabinovich, Efrat, Anat Kerem, Kai-Uwe Fröhlich, Noam Diamant, and Shoshana Bar-Nun. 2002. 'AAA-ATPase P97/Cdc48p, a Cytosolic Chaperone Required for Endoplasmic Reticulum-Associated Protein Degradation'. *Molecular and Cellular Biology* 22 (2): 626–34. https://doi.org/10.1128/MCB.22.2.626-634.2002.

Rao, Bing, Shaobai Li, Deqiang Yao, Qian Wang, Ying Xia, Yi Jia, Yafeng Shen, and Yu Cao. 2021. 'The Cryo-EM Structure of an ERAD Protein Channel Formed by Tetrameric Human Derlin-1'. *Science Advances* 7 (10): eabe8591. https://doi.org/10.1126/sciadv.abe8591.

Rao, Rammohan V, and Dale E Bredesen. 2004. 'Misfolded Proteins, Endoplasmic Reticulum Stress and Neurodegeneration'. *Current Opinion in Cell Biology* 16 (6): 653–62. https://doi.org/10.1016/j.ceb.2004.09.012.

Rapoport, Tom A. 2007. 'Protein Translocation across the Eukaryotic Endoplasmic Reticulum and Bacterial Plasma Membranes'. *Nature* 450 (7170): 663–69. https://doi.org/10.1038/nature06384.

Rapoport, Tom A., Long Li, and Eunyong Park. 2017. 'Structural and Mechanistic Insights into Protein Translocation'. *Annual Review of Cell and Developmental Biology* 33 (1): 369–90. https://doi.org/10.1146/annurev-cellbio-100616-060439.

Ravid, Tommer, and Mark Hochstrasser. 2007. 'Autoregulation of an E2 Enzyme by Ubiquitin-Chain Assembly on Its Catalytic Residue'. *Nature Cell Biology* 9 (4): 422–27. https://doi.org/10.1038/ncb1558.

Read, Adam, and Martin Schröder. 2021. 'The Unfolded Protein Response: An Overview'. *Biology* 10 (5): 384. https://doi.org/10.3390/biology10050384.

Renatus, Martin, Shirley Gil Parrado, Allan D'Arcy, Ulf Eidhoff, Bernd Gerhartz, Ulrich Hassiepen, Benoit Pierrat, et al. 2006. 'Structural Basis of Ubiquitin Recognition by the Deubiquitinating Protease USP2'. *Structure* 14 (8): 1293–1302. https://doi.org/10.1016/j.str.2006.06.012.

Rigaud, Jean-Louis, and Daniel Lévy. 2003. 'Reconstitution of Membrane Proteins into Liposomes'. In *Methods in Enzymology*, 372:65–86. Liposomes, Part B. Academic Press. https://doi.org/10.1016/S0076-6879(03)72004-7.

Riley, B.E., J.C. Lougheed, K. Callaway, M. Velasquez, E. Brecht, L. Nguyen, T. Shaler, et al. 2013. 'Structure and Function of Parkin E3 Ubiquitin Ligase Reveals Aspects of RING and HECT Ligases'. *Nature Communications* 4 (1): 1982. https://doi.org/10.1038/ncomms2982.

Schäfer, Antje, and Dieter H Wolf. 2009. 'Sec61p Is Part of the Endoplasmic Reticulum-Associated Degradation Machinery'. *The EMBO Journal* 28 (19): 2874–84. https://doi.org/10.1038/emboj.2009.231.

Schoebel, Stefan, Wei Mi, Alexander Stein, Sergey Ovchinnikov, Ryan Pavlovicz, Frank DiMaio, David Baker, et al. 2017. 'Cryo-EM Structure of the Protein-Conducting ERAD Channel Hrd1 in Complex with Hrd3'. *Nature* 548 (7667): 352–55. https://doi.org/10.1038/nature23314.

Schulz, Jasmin, Dönem Avci, Markus A. Queisser, Aljona Gutschmidt, Lena-Sophie Dreher, Emma J. Fenech, Norbert Volkmar, Yuki Hayashi, Thorsten Hoppe, and John C. Christianson. 2017. 'Conserved Cytoplasmic Domains Promote Hrd1 Ubiquitin Ligase Complex Formation for ER-Associated Degradation (ERAD)'. *Journal of Cell Science* 130 (19): 3322–35. https://doi.org/10.1242/jcs.206847.

Schwartz, Alan L., and Aaron Ciechanover. 2009. 'Targeting Proteins for Destruction by the Ubiquitin System: Implications for Human Pathobiology'. *Annual Review of Pharmacology and Toxicology* 49 (1): 73–96. https://doi.org/10.1146/annurev.pharmtox.051208.165340.

Schwartz, Michael P., and Andreas Matouschek. 1999. 'The Dimensions of the Protein Import Channels in the Outer and Inner Mitochondrial Membranes'. *Proceedings of the National Academy of Sciences* 96 (23): 13086–90. https://doi.org/10.1073/pnas.96.23.13086.

Sharninghausen, Rachel, Jiwon Hwang, Devon Dennison, and Ryan D. Baldridge. 2023. 'Identification of ERAD-Dependent Degrons for the Endoplasmic Reticulum Lumen'. bioRxiv. https://doi.org/10.1101/2023.06.21.546000.

Sinden, Richard R. 1994. 'DNA–Protein Interactions'. In *DNA Structure and Function*, 287–325. Elsevier. https://doi.org/10.1016/B978-0-08-057173-7.50013-4.

Snyder, Nathan A., and Gustavo M. Silva. 2021. 'Deubiquitinating Enzymes (DUBs): Regulation, Homeostasis, and Oxidative Stress Response'. *The Journal of Biological Chemistry* 297 (3): 101077. https://doi.org/10.1016/j.jbc.2021.101077.

Stanley, Ann Marie, Pedro Carvalho, and Tom Rapoport. 2011. 'Recognition of an ERAD-L Substrate Analyzed by Site-Specific in Vivo Photocrosslinking'. *FEBS Letters* 585 (9): 1281–86. https://doi.org/10.1016/j.febslet.2011.04.009.

Stein, Alexander, Annamaria Ruggiano, Pedro Carvalho, and Tom A. Rapoport. 2014. 'Key Steps in ERAD of Luminal ER Proteins Reconstituted with Purified Components'. *Cell* 158 (6): 1375–88. https://doi.org/10.1016/j.cell.2014.07.050.

Stewart, Mikaela D., Tobias Ritterhoff, Rachel E. Klevit, and Peter S. Brzovic. 2016. 'E2 Enzymes: More than Just Middle Men'. *Cell Research* 26 (4): 423–40. https://doi.org/10.1038/cr.2016.35.

Stolz, Alexandra, Wolfgang Hilt, Alexander Buchberger, and Dieter H. Wolf. 2011. 'Cdc48: A Power Machine in Protein Degradation'. *Trends in Biochemical Sciences* 36 (10): 515–23. https://doi.org/10.1016/j.tibs.2011.06.001.

Sun, Zhihao, and Jeffrey L. Brodsky. 2019. 'Protein Quality Control in the Secretory Pathway'. *Journal of Cell Biology* 218 (10): 3171–87. https://doi.org/10.1083/jcb.201906047.

Szathmary, Reka, Regula Bielmann, Mihai Nita-Lazar, Patricie Burda, and Claude A. Jakob. 2005. 'Yos9 Protein Is Essential for Degradation of Misfolded Glycoproteins and May Function as Lectin in ERAD'. *Molecular Cell* 19 (6): 765–75. https://doi.org/10.1016/j.molcel.2005.08.015.

Thibault, Guillaume, and Davis T.W. Ng. 2012. 'The Endoplasmic Reticulum-Associated Degradation Pathways of Budding Yeast'. *Cold Spring Harbor Perspectives in Biology* 4 (12): a013193. https://doi.org/10.1101/cshperspect.a013193.

Truscott, K. N., P. Kovermann, A. Geissler, A. Merlin, M. Meijer, A. J. Driessen, J. Rassow, N. Pfanner, and R. Wagner. 2001. 'A Presequence- and Voltage-Sensitive Channel of the Mitochondrial Preprotein Translocase Formed by Tim23'. *Nature Structural Biology* 8 (12): 1074–82. https://doi.org/10.1038/nsb726.

Tsai, Yien Che, and Allan M. Weissman. 2010. 'The Unfolded Protein Response, Degradation from the Endoplasmic Reticulum, and Cancer'. *Genes & Cancer* 1 (7): 764–78. https://doi.org/10.1177/1947601910383011.

Tucker, Kyle, and Eunyong Park. 2019. 'Cryo-EM Structure of the Mitochondrial Protein-Import Channel TOM Complex at near-Atomic Resolution'. *Nature Structural & Molecular Biology* 26 (12): 1158–66. https://doi.org/10.1038/s41594-019-0339-2.

Twomey, Edward C., Zhejian Ji, Thomas E. Wales, Nicholas O. Bodnar, Scott B. Ficarro, Jarrod A. Marto, John R. Engen, and Tom A. Rapoport. 2019. 'Substrate Processing by the Cdc48 ATPase Complex Is Initiated by Ubiquitin Unfolding'. *Science (New York, N.Y.)* 365 (6452): eaax1033. https://doi.org/10.1126/science.aax1033.

Vashistha, Nidhi, Sonya E. Neal, Amanjot Singh, Sarah M. Carroll, and Randolph Y. Hampton. 2016. 'Direct and Essential Function for Hrd3 in ER-Associated Degradation'. *Proceedings of the National Academy of Sciences* 113 (21): 5934–39. https://doi.org/10.1073/pnas.1603079113.

Vasic, Vedran, Niels Denkert, Claudia C. Schmidt, Dietmar Riedel, Alexander Stein, and Michael Meinecke. 2020. 'Hrd1 Forms the Retrotranslocation Pore Regulated by Auto-Ubiquitination and Binding of Misfolded Proteins'. *Nature Cell Biology* 22 (3): 274–81. https://doi.org/10.1038/s41556-020-0473-4.

Vembar, Shruthi S., and Jeffrey L. Brodsky. 2008. 'One Step at a Time: Endoplasmic Reticulum-Associated Degradation'. *Nature Reviews Molecular Cell Biology* 9 (12): 944–57. https://doi.org/10.1038/nrm2546.

Wahlman, Judit, George N. DeMartino, William R. Skach, Neil J. Bulleid, Jeffrey L. Brodsky, and Arthur E. Johnson. 2007. 'Real-Time Fluorescence Detection of ERAD Substrate Retrotranslocation in a Mammalian In Vitro System'. *Cell* 129 (5): 943–55. https://doi.org/10.1016/j.cell.2007.03.046.

Walton, P. A., P. E. Hill, and S. Subramani. 1995. 'Import of Stably Folded Proteins into Peroxisomes'. *Molecular Biology of the Cell* 6 (6): 675–83. https://doi.org/10.1091/mbc.6.6.675.

Wang, Miao, and Randal J. Kaufman. 2016. 'Protein Misfolding in the Endoplasmic Reticulum as a Conduit to Human Disease'. *Nature* 529 (7586): 326–35. https://doi.org/10.1038/nature17041.

Wang, Xiaoli, Y. Y. Lawrence Yu, Nancy Myers, and Ted H. Hansen. 2013. 'Decoupling the Role of Ubiquitination for the Dislocation versus Degradation of Major Histocompatibility Complex (MHC) Class I Proteins during Endoplasmic Reticulum-Associated Degradation (ERAD)'. *The Journal of Biological Chemistry* 288 (32): 23295–306. https://doi.org/10.1074/jbc.M113.482018.

Wang, Yongcheng, Yingjiu Zhang, and Ya Ha. 2006. 'Crystal Structure of a Rhomboid Family Intramembrane Protease'. *Nature* 444 (7116): 179–80. https://doi.org/10.1038/nature05255.

Wu, Pan, Huani Gao, Jing Liu, Dylan K. Kosma, Shiyou Lü, and Huayan Zhao. 2021. 'Insight into the Roles of the ER-Associated Degradation E3 Ubiquitin Ligase HRD1 in Plant Cuticular Lipid Biosynthesis'. *Plant Physiology and Biochemistry* 167 (October): 358–65. https://doi.org/10.1016/j.plaphy.2021.08.021.

Wu, Xudong, and Tom A. Rapoport. 2021. 'Translocation of Proteins through a Distorted Lipid Bilayer'. *Trends in Cell Biology* 31 (6): 473–84. https://doi.org/10.1016/j.tcb.2021.01.002.

Wu, Xudong, Marc Siggel, Sergey Ovchinnikov, Wei Mi, Vladimir Svetlov, Evgeny Nudler, Maofu Liao, Gerhard Hummer, and Tom A. Rapoport. 2020. 'Structural Basis of ER-Associated Protein Degradation Mediated by the Hrd1 Ubiquitin Ligase Complex'. *Science* 368 (6489): eaaz2449. https://doi.org/10.1126/science.aaz2449.

Wu, Zhuoru, Nieng Yan, Liang Feng, Adam Oberstein, Hanchi Yan, Rosanna P. Baker, Lichuan Gu, Philip D. Jeffrey, Sinisa Urban, and Yigong Shi. 2006. 'Structural Analysis of a Rhomboid Family Intramembrane Protease Reveals a Gating Mechanism for Substrate Entry'. *Nature Structural & Molecular Biology* 13 (12): 1084–91. https://doi.org/10.1038/nsmb1179.

Xie, Wei, and Davis T. W. Ng. 2010. 'ERAD Substrate Recognition in Budding Yeast'. *Seminars in Cell & Developmental Biology*, Quality control in the endoplasmic reticulum, 21 (5): 533–39. https://doi.org/10.1016/j.semcdb.2010.02.007.

Xu, Ping, Duc M. Duong, Nicholas T. Seyfried, Dongmei Cheng, Yang Xie, Jessica Robert, John Rush, Mark Hochstrasser, Daniel Finley, and Junmin Peng. 2009. 'Quantitative Proteomics Reveals the Function of Unconventional Ubiquitin Chains in Proteasomal Degradation'. *Cell* 137 (1): 133–45. https://doi.org/10.1016/j.cell.2009.01.041.

Ye, Yihong, Hemmo H. Meyer, and Tom A. Rapoport. 2001. 'The AAA ATPase Cdc48/P97 and Its Partners Transport Proteins from the ER into the Cytosol'. *Nature* 414 (6864): 652–56. https://doi.org/10.1038/414652a.

Zattas, Dimitrios, and Mark Hochstrasser. 2015. 'Ubiquitin-Dependent Protein Degradation at the Yeast Endoplasmic Reticulum and Nuclear Envelope'. *Critical Reviews in Biochemistry and Molecular Biology* 50 (1): 1–17. https://doi.org/10.3109/10409238.2014.959889.

Zehner, Matthias, Andrea L. Marschall, Erik Bos, Jan-Gero Schloetel, Christoph Kreer, Dagmar Fehrenschild, Andreas Limmer, et al. 2015. 'The Translocon Protein Sec61 Mediates Antigen Transport from Endosomes in the Cytosol for Cross-Presentation to CD8+ T Cells'. *Immunity* 42 (5): 850–63. https://doi.org/10.1016/j.immuni.2015.04.008.

Zhang, Xuejun C., Zhenfeng Liu, and Jie Li. 2016. 'From Membrane Tension to Channel Gating: A Principal Energy Transfer Mechanism for Mechanosensitive Channels'. *Protein Science : A Publication of the Protein Society* 25 (11): 1954–64. https://doi.org/10.1002/pro.3017.

Zhang, Yixiao, Csaba Daday, Ruo-Xu Gu, Charles D. Cox, Boris Martinac, Bert L. de Groot, and Thomas Walz. 2021. 'Visualization of the Mechanosensitive Ion Channel MscS under Membrane Tension'. *Nature* 590 (7846): 509–14. https://doi.org/10.1038/s41586-021-03196-w.

Zhang, Yutong, Xiaomin Ou, Xuezheng Wang, Dongjie Sun, Xueyin Zhou, Xiaofei Wu, Qing Li, and Long Li. 2021. 'Structure of the Mitochondrial TIM22 Complex from Yeast'. *Cell Research* 31 (3): 366–68. https://doi.org/10.1038/s41422-020-00399-0.

Zheng, Ning, and Nitzan Shabek. 2017. 'Ubiquitin Ligases: Structure, Function, and Regulation'. *Annual Review of Biochemistry* 86 (1): 129–57. https://doi.org/10.1146/annurev-biochem-060815-014922.

Zimmermann, Richard, Susanne Eyrisch, Mazen Ahmad, and Volkhard Helms. 2011. 'Protein Translocation across the ER Membrane'. *Biochimica et Biophysica Acta (BBA) - Biomembranes*, Including the Special Section: Protein translocation across or insertion into membranes, 1808 (3): 912–24. https://doi.org/10.1016/j.bbamem.2010.06.015.